frontiers | Research Topics

Epileptic seizure disorders in animal models: Advances in translational approaches

Edited by
Evgenia Sitnikova, Gilles van Luijtelaar and Filiz Onat

Published in
Frontiers in Neurology
Frontiers in Neuroscience

ISSN 1664-8714
ISBN 978-2-8325-4854-7
DOI 10.3389/978-2-8325-4854-7

About Frontiers

Frontiers is more than just an open access publisher of scholarly articles: it is a pioneering approach to the world of academia, radically improving the way scholarly research is managed. The grand vision of Frontiers is a world where all people have an equal opportunity to seek, share and generate knowledge. Frontiers provides immediate and permanent online open access to all its publications, but this alone is not enough to realize our grand goals.

Frontiers journal series

The Frontiers journal series is a multi-tier and interdisciplinary set of open-access, online journals, promising a paradigm shift from the current review, selection and dissemination processes in academic publishing. All Frontiers journals are driven by researchers for researchers; therefore, they constitute a service to the scholarly community. At the same time, the *Frontiers journal series* operates on a revolutionary invention, the tiered publishing system, initially addressing specific communities of scholars, and gradually climbing up to broader public understanding, thus serving the interests of the lay society, too.

Dedication to quality

Each Frontiers article is a landmark of the highest quality, thanks to genuinely collaborative interactions between authors and review editors, who include some of the world's best academicians. Research must be certified by peers before entering a stream of knowledge that may eventually reach the public - and shape society; therefore, Frontiers only applies the most rigorous and unbiased reviews. Frontiers revolutionizes research publishing by freely delivering the most outstanding research, evaluated with no bias from both the academic and social point of view. By applying the most advanced information technologies, Frontiers is catapulting scholarly publishing into a new generation.

What are Frontiers Research Topics?

Frontiers Research Topics are very popular trademarks of the *Frontiers journals series*: they are collections of at least ten articles, all centered on a particular subject. With their unique mix of varied contributions from Original Research to Review Articles, Frontiers Research Topics unify the most influential researchers, the latest key findings and historical advances in a hot research area.

Find out more on how to host your own Frontiers Research Topic or contribute to one as an author by contacting the Frontiers editorial office: frontiersin.org/about/contact

Epileptic seizure disorders in animal models: Advances in translational approaches

Topic editors

Evgenia Sitnikova — Institute of Higher Nervous Activity and Neurophysiology (RAS), Russia

Gilles van Luijtelaar — Radboud University, Netherlands

Filiz Onat — Acıbadem University, Türkiye

Citation

Sitnikova, E., van Luijtelaar, G., Onat, F., eds. (2024). *Epileptic seizure disorders in animal models: Advances in translational approaches*. Lausanne: Frontiers Media SA. doi: 10.3389/978-2-8325-4854-7

Table of contents

frontiers | Frontiers in Neurology

TYPE Editorial
PUBLISHED 22 April 2024
DOI 10.3389/fneur.2024.1414940

OPEN ACCESS

EDITED AND REVIEWED BY
Fernando Cendes,
State University of Campinas, Brazil

*CORRESPONDENCE
Evgenia Sitnikova
✉ eu.sitnikova@ihna.ru

RECEIVED 09 April 2024
ACCEPTED 11 April 2024
PUBLISHED 22 April 2024

CITATION
Sitnikova E, Onat F and van Luijtelaar G (2024) Editorial: Epileptic seizure disorders in animal models: advances in translational approaches. *Front. Neurol.* 15:1414940. doi: 10.3389/fneur.2024.1414940

Editorial: Epileptic seizure disorders in animal models: advances in translational approaches

Evgenia Sitnikova[1]*, Filiz Onat[2] and Gilles van Luijtelaar[3]

[1]Institute of Higher Nervous Activity and Neurophysiology of Russian Academy of Sciences, Moscow, Russia, [2]Department of Neuroscience, Institute of Health Sciences, Acıbadem University Istanbul, Istanbul, Türkiye, [3]Donders Centre for Cognition, Radboud University, Nijmegen, Netherlands

KEYWORDS

translational neuroscience, rodent models, genetic models, genetic predisposition, epileptogenesis

Editorial on the Research Topic
Epileptic seizure disorders in animal models: advances in translational approaches

Epilepsy is the fourth most common neurological disorder worldwide. Many etiologically relevant animal models of epilepsy have been developed in small rodents (mice and rats) that may help to overcome these challenges. Our Research Topic aims to gain fundamental knowledge from animal models of epilepsy to improve our understanding of the neurobiological etiology of seizures, genetic correlates, and related comorbidities of different types of epilepsy. This is a collection of studies that aim to bridge the translational gap between animal data and clinical trials (Figure 1).

Topics of interest include the following:

- How can the translational value of animal models be improved?

The review paper by Bosco et al. has focused on sudden unexpected death in epilepsy (SUDEP) as the leading cause of seizure-related premature death, most prevalent in young adults with drug-resistant epilepsy. The authors considered the translational value of animal models and brought together the evidence that dilute brown agouti coat color (DBA/2) mice, which are genetically susceptible to audiogenic generalized seizures, could be regarded as a relevant animal model of SUDEP with a sufficient amount of face validity and perhaps also predictive validity.

Zhang et al. conducted an experimental study in a rat model of focal cortical dysplasia induced by *in utero* X-ray-radiation and compared expression profiles with those obtained in surgical specimens from patients. The study proposes that the epileptogenesis of focal cortical dysplasia type IIb and tuberous sclerosis complex is caused by changes in the expression of α-synuclein, a member of the synuclein family that plays a crucial role in modulating synaptic transmission in the central nervous system, which is associated with an impairment of N-methyl-D-aspartate (NMDA)-ergic mechanisms. Further studies on the modulatory effects of α-synuclein on seizure activity are warranted.

The review paper by Sibarov et al. considered the product of the immediate early gene encoding the activity-regulated cytoskeleton-associated (Arc) protein in the pathogenesis of epilepsy. Arc protein modulates the excitatory-inhibitory balance in mammalian neuronal networks. In active neurons, Arc protein forms retrovirus-like capsids within synapses. After seizures, released Arc particles can accumulate in astrocytes. In their translational approach, the authors focused on rodent models of convulsive and non-convulsive seizures and on genetic models of epilepsy to elucidate the intricate role of Arc in epilepsy. It is proposed that changes in Arc-protein-mediated activity can potentially affect the excitatory-inhibitory balance of the involved neuronal network, either by lowering the seizure threshold and promoting stability or by inducing lability.

- The knowledge gained from rat/mouse strains with a genetic predisposition to epilepsy.

Yavuz et al. conducted an experimental study in the genetic absence epilepsy rat from Strasbourg (GAERS). The authors examined the pro-absence effect of the alpha 2A adrenoreceptor (AR) agonist dexmedetomidine, which was administered systemically in GAERS during the first postnatal month. Their study indicates that the alpha 2A-AR mechanism is involved in the unilateral onset of absence-like seizures in the left cortex in close to 50% of the animals. The unilateral onset does fit with recent theories of the focal onset of an archetypal type of generalized epilepsy.

Toplu et al. used GAERS to investigate the orexin-type 2 receptor (OX2R) signaling pathway in absence epilepsy. The authors discovered that the OX2R agonist had a suppressive effect on spike-wave discharges, as demonstrated by significantly reduced OX2R expression in the cortex and thalamus. This effect may be attributed to the agonist's regulation of the wake/sleep state. The therapeutic potential of targeting OX2R in the treatment of various types of epilepsy, and especially absence epilepsy awaits further research.

- The knowledge gained from knockout and genetically modified rats/mice.

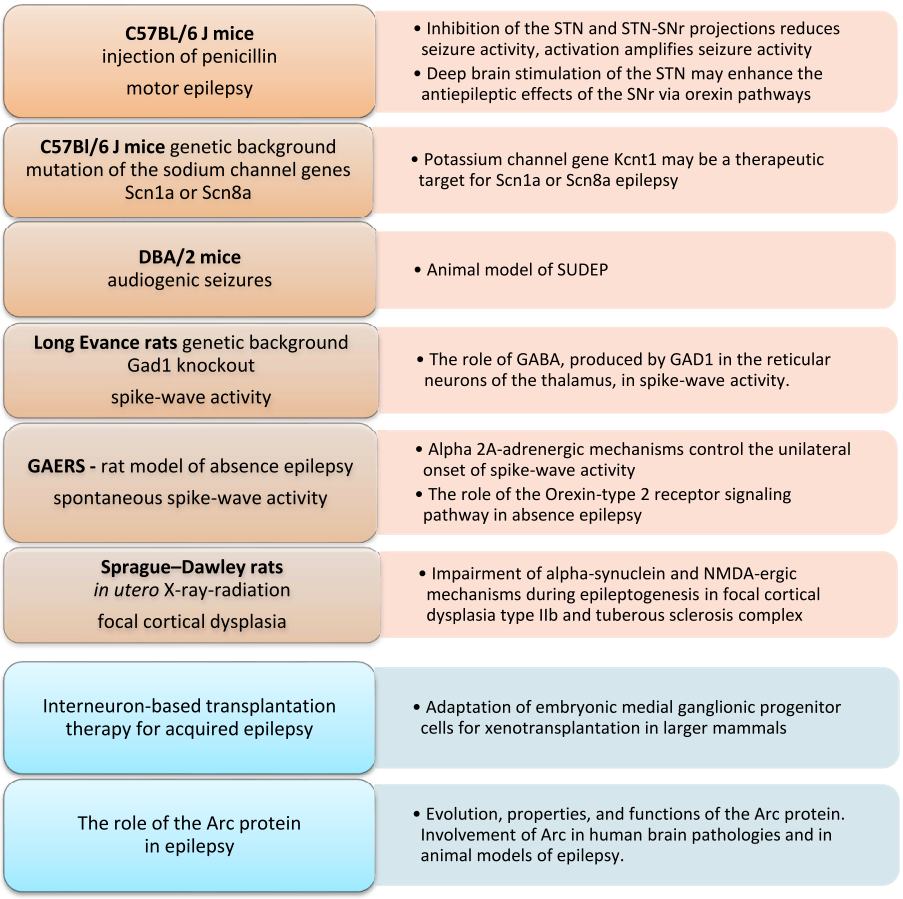

FIGURE 1
Animal models and approaches to understanding epilepsy as covered in this Research Topic ("*Epileptic seizure disorders in animal models: advances in translational approaches*"). Arc protein, activity-regulated cytoskeleton-associated protein; DBA/2, dilute brown agouti coat color mice; GABA, gamma-aminobutyric acid; GAD1, glutamate decarboxylase 1; GAERS, genetic absence epilepsy rats from Strasbourg; NMDA, N-methyl-D-aspartate; SUDEP, sudden unexpected death in epilepsy.

Liu et al. investigated the gamma-aminobutyric acid (GABA)-ergic mechanisms of epileptic activity. They targeted Glutamate decarboxylase 1 (GAD1)- an enzyme involved in the synthesis of GABA and obtained Gad1 knockout rats from the Long-Evans background. The authors propose a functional model in which GABA produced by GAD1 in the reticular thalamic neurons is released outside the synapses and causes inhibition within the reticular thalamic nucleus. Of note, these thalamic neurons are a major source of inhibition of the thalamic-cortical relay cells.

- New genetic technologies to model epilepsy in rats/mice.

The study by Hill et al. was conducted in mice with mutations in the sodium channel genes Scn1a or Scn8a. Mutations in these genes can lead to dysfunction of sodium channels, resulting in increased neuronal excitability and predisposing individuals to seizures, such as in Dravet syndrome and febrile seizures. Both genes are also involved in developmental and epileptic encephalopathies, which represent severe seizure disorders with inadequate treatment options. Their study indicates that a reduction of *Kcnt1* expression is protective in mouse models of *Scn1a* and *Scn8a* epilepsy, suggesting that patients with *SCN1A* and *SCN8A* mutations may benefit from treatment with a *KCNT1* ASO or KCNT1-specific channel blocker.

- Novel treatment options for patients with therapy-resistant epilepsy.

Xue et al. used a penicillin-induced model of motor epilepsy in adult male C57BL/6 J mice and employed optogenetic and chemogenetic approaches to study the involvement of the subthalamic nucleus (STN) and the substantia nigra pars reticulata (SNr) in motor seizures. Inhibition of excitatory neurons in the STN and the projections from the STN to the SNr reduced seizure activity, but activation of these neurons and pathways amplified seizure activity. The authors also concluded that deep brain stimulation of the STN may be a potential treatment for motor epilepsy and may enhance the SNr's antiepileptic effects through orexin pathways.

The review by Righes Marafiga and Baraban discusses interneuron-based transplantation therapy in acquired epilepsy models, such as the well-known pilocarpine model of Temporal Lobe epilepsy. These authors consider a novel strategy that used embryonic medial ganglionic (MGE) progenitor cells to target parvalbumin-expressing and somatostatin-expressing cells in epileptic networks. Most importantly, this represents a true disease-modifying therapy in the form of the selective addition of new inhibitory interneurons to these circuits.

Author contributions

ES: Writing – review & editing, Writing – original draft, Visualization, Conceptualization. FO: Writing – review & editing. GL: Writing – review & editing.

Funding

The author(s) declare financial support was received for the research, authorship, and/or publication of this article. ES received a research grant from the Russian Science Foundation (Grant No. 23-25-00166).

Conflict of interest

The authors declare that the research was conducted in the absence of any commercial or financial relationships that could be construed as a potential conflict of interest.

The author(s) declared that they were an editorial board member of Frontiers, at the time of submission. This had no impact on the peer review process and the final decision.

Publisher's note

frontiers | Frontiers in Neuroscience

TYPE Mini Review
PUBLISHED 14 April 2023
DOI 10.3389/fnins.2023.1177678

OPEN ACCESS

EDITED BY
Evgenia Sitnikova,
Institute of Higher Nervous Activity and Neurophysiology (RAS),
Russia

REVIEWED BY
Ramachandran Prakasam,
Washington University in St. Louis,
United States

*CORRESPONDENCE
Scott C. Baraban
✉ scott.baraban@ucsf.edu

SPECIALTY SECTION
This article was submitted to Translational Neuroscience, a section of the journal Frontiers in Neuroscience

RECEIVED 01 March 2023
ACCEPTED 28 March 2023
PUBLISHED 14 April 2023

CITATION
Righes Marafiga J and Baraban SC (2023) Cell therapy for neurological disorders: Progress towards an embryonic medial ganglionic eminence progenitor-based treatment. *Front. Neurosci.* 17:1177678. doi: 10.3389/fnins.2023.1177678

Cell therapy for neurological disorders: Progress towards an embryonic medial ganglionic eminence progenitor-based treatment

Joseane Righes Marafiga[1] and Scott C. Baraban[1,2]*

[1]Department of Neurological Surgery, University of California San Francisco, San Francisco, CA, United States, [2]Helen Wills Institute for Neuroscience, University of California Berkeley, Berkeley, CA, United States

Impairment of development, migration, or function of inhibitory interneurons are key features of numerous circuit-based neurological disorders, such as epilepsy. From a therapeutic perspective, symptomatic treatment of these disorders often relies upon drugs or deep brain stimulation approaches to provide a general enhancement of GABA-mediated inhibition. A more effective strategy to target these pathological circuits and potentially provide true disease-modifying therapy, would be to selectively add new inhibitory interneurons into these circuits. One such strategy, using embryonic medial ganglionic (MGE) progenitor cells as a source of a unique sub-population of interneurons, has already proven effective as a cell transplantation therapy in a variety of preclinical models of neurological disorders, especially in mouse models of acquired epilepsy. Here we will discuss the evolution of this interneuron-based transplantation therapy in acquired epilepsy models, with an emphasis on the recent adaptation of MGE progenitor cells for xenotransplantation into larger mammals.

KEYWORDS

interneuron, GABA, porcine, progenitor cells, epilepsy

Introduction

Interneurons mediate inhibitory synaptic transmission, brain oscillations and cortical processing (Isaacson and Scanziani, 2011). Alteration of GABAergic transmission, following interneuron loss or dysfunction, can disrupt synaptic inhibition within neuronal networks and facilitate development of epilepsy (Kumar and Buckmaster, 2006; Knopp et al., 2008; Katsarou et al., 2017), autism spectrum disorders (Paterno et al., 2021; Fontes-Dutra et al., 2023), schizophrenia (Nakazawa et al., 2012) and other neurological conditions (Calcagnotto et al., 2005; Marín, 2012). Among these, epilepsy is a common and devastating condition, affecting more than 70 million people worldwide and approximately 3.4 million people in the United States (Ngugi et al., 2011; Zack and Kobau, 2017). As a first line treatment, antiseizure medications (ASMs) potentiating GABAergic inhibition are routinely used to control seizures (Löscher and Klein, 2021). However, alternative treatments are needed for drug-resistant epilepsy patients comprising nearly 30% of this patient population (Kwan and Brodie, 2000). In a select group of these patients, surgical removal of seizure foci is considered the best available treatment (Wiebe et al., 2001, Spencer and Huh, 2008, Jobst and Cascino, 2015). While a well-established

procedure, invasive surgical resection carries significant risk for cognitive and psychological impact (Sherman et al., 2011); and its success is directly correlated with identification of seizure foci, which cannot always be defined or safely removed (Rosenow and Lüders, 2001). Deep brain stimulation (DBS) also provides a degree of seizure control in some patients by targeting propagation points within the epileptic network but is also invasive and not selective to inhibitory or excitatory pathways (Piper et al., 2022). In recent years, a promising alternative therapy using GABAergic progenitor cell-based transplantation has emerged with potential to selectively add new functional inhibitory neurons into the epileptic network (Baraban et al., 2009; Hunt et al., 2013; Casalia et al., 2017).

Preclinical transplantation studies using murine embryonic progenitors from medial ganglionic eminence (MGE) consistently demonstrate robust abilities to (i) migrate, differentiate and integrate into host circuits as inhibitory interneurons (Alvarez-Dolado et al., 2006; Calcagnotto et al., 2010), (ii) make synaptic inhibitory connections onto host brain excitatory neurons (Howard and Baraban, 2016; Hsieh and Baraban, 2017), (iii) enhance synaptic inhibition (Alvarez-Dolado et al., 2006; Calcagnotto et al., 2010; Howard et al., 2014) and (iv) abolish spontaneous seizures and epilepsy-related comorbidities in mouse models of acquired epilepsy (Baraban et al., 2009; Hunt et al., 2013; Casalia et al., 2017). Based on these investigations, transplanted MGE-derived interneurons are therapeutic because they increase surround inhibition in host brain by forming new inhibitory synapses within the epileptic network while other proposed mechanisms such as secretion of unidentified "trophic factors" or "reorganization of host circuitry" (Southwell et al., 2010, 2014; Priya et al., 2019) are not supported by experimental evidence. While these proof-of-principle studies involved embryonic donor cells from mice transplanted into recipient mice, moving to a larger mammal requires a cross-species xenotransplantation strategy. In our efforts to translate this promising therapy to larger mammals, we focused our attention on porcine donors as there is significant translational clinical precedent for using tissue or organs derived from pigs for xenotransplantation. In this mini-review, we discuss our earlier MGE transplantation work using mice and more recent studies highlighting the potential for porcine MGE xenotransplantation as a therapy for intractable epilepsies.

Embryonic MGE progenitors transplantation therapy

During development, MGE is a primary source of inhibitory interneuron progenitors, generating primarily parvalbumin-expressing (PV) and somatostatin-expressing (SOM) cells (Wonders and Anderson, 2006). Over the past 20 years, studies utilizing embryonic murine MGE progenitors were extremely successful in demonstrating that MGE-derived cells are valuable candidates for interneuron transplantation therapies (Alvarez-Dolado et al., 2006; Martínez-Cerdeño et al., 2010; Zipancic et al., 2010; Bráz et al., 2012; Hunt et al., 2013; Hunt and Baraban, 2015; Casalia et al., 2017; Zhu et al., 2019; Paterno et al., 2020). Transplanted MGE progenitors offer widespread therapeutic coverage in a dysfunctional brain as embryonic MGE-derived progenitors survive (up to 22%) and migrate (up to 5 mm from injection site) extensively within cortical and hippocampal regions following transplantation (Alvarez-Dolado et al., 2006; Baraban et al., 2009; Hunt et al., 2013). In nearly two decades of investigation, embryonic MGE-derived cells have never been shown to proliferate in the host brain, but consistently share morphological features of native interneurons, with elaborated dendritic trees, and typical interneuron morphologies: bipolar cells, multipolar cells, basket cells, neurons with small body or chandelier cells (Alvarez-Dolado et al., 2006; Calcagnotto et al., 2010; Hunt et al., 2013). Most importantly, interneurons derived from embryonic murine MGE progenitors express the primary inhibitory neurotransmitter GABA and differentiate into a specific sub-population of PV-and SOM-positive GABAergic interneurons (Table 1). MGE-derived interneurons maintain electrophysiological properties of mature interneurons *in vitro*, such as fast-spiking and regular-spiking firing properties in current-clamp recordings (Alvarez-Dolado et al., 2006; Hunt et al., 2013; Howard and Baraban, 2016), and receive both inhibitory and excitatory synaptic input from host brain neurons as measured by voltage-clamp recordings of postsynaptic current (Martínez-Cerdeño et al., 2010; Sebe and Baraban, 2010; Howard and Baraban, 2016). Importantly, murine MGE-derived interneurons do not enhance GABA-mediated synaptic inhibition to endogenous interneurons which would suggest a caudal ganglionic eminence (CGE) interneuron lineage (Baraban et al., 2009; Larimer et al., 2016; Hsieh and Baraban, 2017). Enhancement of GABA-mediated inhibition following transplantation of MGE progenitors is also 'self-limiting' in that increased inhibition observed in host circuits does not scale with injection size but reaches a plateau (Sebe et al., 2014; Southwell et al., 2014). As expected for these interneuron sub-populations, MGE-derived interneurons integrate in hosts brain to mediate synaptic inhibition onto somatic and dendritic postsynaptic neuronal compartments of principal excitatory neurons as shown in dual patch-clamp recordings (Howard and Baraban, 2016) and optogenetic stimulation of transplant-derived interneurons (Hsieh and Baraban, 2017). Moreover, as a basis for therapeutic application in conditions where synaptic inhibition may be compromised (e.g., epilepsy, autism or schizophrenia), MGE-derived interneurons consistently enhance miniature and spontaneous inhibitory postsynaptic currents onto excitatory (but not inhibitory) pyramidal neurons in host brain (Alvarez-Dolado et al., 2006; Hunt et al., 2013; Howard and Baraban, 2016; Casalia et al., 2017; Hsieh and Baraban, 2017). The consistency of these findings across time and different investigators sets a standard for how any transplantation protocol purporting to utilize MGE progenitor cells should be judged.

Mice provide unique advantages for development of MGE-derived transplantation protocols as a potential disease modifying therapy for epilepsy. First, our understanding of interneuron origins, sub-populations and functions derive from a wealth of rodent publications. Second, a variety of rodent epilepsy models are already available and easily accessible. As discussed, anatomical, immunohistochemical and functional properties of transplanted murine MGE-derived interneurons are now established (Alvarez-Dolado et al., 2006; Howard et al., 2014; Howard and Baraban, 2016; Hsieh and Baraban, 2017). As are studies (replicated over several publications) that transplanted murine MGE progenitors offer a potential cure in mouse models of epilepsy. One of the most studied rodent epilepsy models representing temporal lobe epilepsy (TLE), is the pilocarpine model (Turski et al., 1983; Cavalheiro et al., 1991; Cavalheiro, 1995; Sanabria et al., 2002). Using this model we demonstrated that at 60 days following transplantation, adult

TABLE 1 Medial ganglionic eminence.

Cell source	Author, year	Recipient, age	Interneuron markers	Additional properties
Murine embryonic progenitor cells	Alvarez-Dolado et al. (2006)	CD-1 mice, P3-4	CTX: GABA (68.6%) PV (38.3%); SOM (43.2%); CR (1.9%); NPY (7.8%). HP: GABA (42.8%); PV (33.7%); SOM (33.8%); CR (10.3%); NPY (13.1%).	• Migration >5 mm from injection site • Regular-spiking non-pyramidal, burst-onset regular-spiking non-pyramidal and fast-spiking firing properties
	Calcagnotto et al. (2010)	CD-1 mice, P60	HP: GABA (54.6%); PV (34.6%); SOM (34.3%); CR (3.5%); NPY (18.8%)	• Fully mature morphology
	Hunt et al. (2013)	CD-1 mice, P60	HP: GAD67 (63%); PV (7.7%); SOM (41.3%); nNOS (21.6%); CR (6.4%); NPY (7.5%); Reelin (12.5%); VIP (0%).	• Migration >1.5 mm from injection site • Regular-spiking non-pyramidal, burst-spiking, late-spiking and fast-spiking firing properties
	Howard and Baraban (2016)	CD-1 mice, P1-3	HP: GAD67 (61.2%); PV (22.5%); SOM (36.2%); CR (6.98%); NPY (3.56%)	• Regular-spiking non-pyramidal and fast-spiking firing properties
	Hsieh and Baraban (2017)	CD-1 mice, P2	HP: PV (28.8%); SOM (36.3%); nNOS (9.4%); CR (5.4%); Reelin (10.7%); VIP (0.25%).	• Functional inhibitory connections with native pyramidal neurons
Human embryonic stem cells	Maroof et al. (2013)	NOD-SCID IL2RG$^{-/-}$ mice, P2	CTX: GABA (90.2%) no PV or SOM cells	• "Physiologically active neurons" • Undifferentiated bipolar or unipolar morphologies
	Nicholas et al. (2013)	SCID mice, P2	CTX: GABA (50.9%); PV (not reported); SOM (50.1%); CB (60.9%); CR (72.5%).	• "A fraction of human cells migrated more than 1 mm" • Significant delay to spike at threshold and little adaptation (Type I) and rapid adaptation (Type II) firing properties

P: postnatal day; CTX: cortex; HP: hippocampus; GABA: gamma-aminobutyric acid; PV: parvalbumin; SOM: somatostatin; CR: calretinin; VIP: vasoactive intestinal peptide; NPY: neuropeptide Y; nNOS: neuronal nitric oxide synthase; CB: calbindin.

epileptic mice receiving MGE progenitor cells (after the emergence of documented epileptic phenotypes) exhibit a 92% reduction in spontaneous seizure frequency as measured by video-EEG monitoring and rescue of epilepsy-related comorbid behaviors in a variety of established assays including open field and Morris-Water maze deficits (Hunt et al., 2013). Despite some initial unfounded concerns following this report questioning "whether transplanted interneurons can integrate into neural circuits affected by long-standing epilepsy, or whether they exert a long-lasting effect on seizure phenotypes" (Henderson et al., 2014; Southwell et al., 2014), these effects were robust. Indeed in 2017, again using the pilocarpine model, we reported that embryonic MGE transplantation into adult epileptic mice produced an 84 to 88% reduction in spontaneous seizure frequency, again rescued open field and handling comorbid behaviors, and functionally restored GABA-mediated inhibition to levels similar to age-matched naïve controls. These effects, noted at 60 to 240 days after transplantation, demonstrate a clear functional restoration of synaptic inhibition in a hippocampal network affected by seizures and a persistent rescue of epilepsy phenotypes (Casalia et al., 2017).

Potential physiological incompatibility and ethical issues that come with murine progenitor cells limit the translation of this approach to a larger mammal. While some would argue that human induced pluripotent stem cells (hiPSC) could solve these issues, published hiPSC protocols do not convincingly report data for PV-and SOM-expressing neurons with the ability to migrate widely and functionally integrate as mature interneurons following transplantation. Despite Waldau et al. (2010) claims that the "majority" of hiPSC-derived cells become GABAergic cells, only 10% of these cells co-labeled with an antibody recognizing GABA while, inconsistent with an MGE lineage, 57% of these cells co-labeled with an antibody recognizing S-100B (Waldau et al., 2010). In Nicholas et al. (2013), following transplantation into immune-deficient mice only a very small fraction of hiPSC-derived putative "MGE-like" cells survive (3–9%), PV-positive neurons were not identified and 73% of cells expressed calretinin (e.g., an interneuron marker for cells originating in CGE) (Nicholas et al., 2013). Additionally, Maroof et al. (2013) demonstrated that hiPSC-derived neurons did not differentiate morphologically into interneurons, nor express SOM or PV (Maroof et al., 2013). Putative human iPSC-derived "MGE" cells in Upadhya et al. (2019) expanded by ~129% following intra-hippocampal grafting suggesting that these stem cells continued to proliferate in the host brain and could result in teratoma formation (Upadhya et al., 2019). Functional integration and enhancement of synaptic inhibition in host brain receiving these hiPSC-derived cells was not demonstrated in any of these studies. Finally, a recent single-nuclei and single-cell transcriptomic analysis of these published hiPSC-derived interneuron protocols (Allison et al., 2021) concluded that "none of these methods produced mature, postnatal-like interneurons as defined functionally

(electrophysiology) or transcriptionally." Therefore, current human iPSC protocols do not faithfully recapitulate crucial properties of embryonic MGE progenitors, and should be interpreted with a note of caution before being used as a strategy for interneuron-based transplant therapy in patients with epilepsy, and other neurological disorders, such as ASD, Alzheimer's disease and schizophrenia.

Porcine MGE progenitor cells

Porcine xenotransplantation studies raise the possibility of developing safe and effective human therapies for several neurological disorders (Fink et al., 2000; Cooper et al., 2002; Hryhorowicz et al., 2017; Sykes and Sachs, 2019; Casalia et al., 2021; Simeone et al., 2022). As such, our laboratory recently turned our attention to using porcine embryonic tissue as an MGE progenitor source for xenotransplantation. In Casalia et al. (2021), we demonstrated that porcine MGE-derived cells recapitulate molecular, morphological and immunohistochemical profiles similar to those established for murine MGE-derived cells (Casalia et al., 2021). First, embryonic porcine MGE express transcription factors, such as *Nkx2.1*, *Lhx6*, and Dlx2, indicative of an MGE lineage (Cobos et al., 2005, 2006, 2007; Vogt et al., 2014). Second, *in vitro* and *in vivo* protocols show that porcine MGE progenitors exhibit a robust migratory capacity similar to murine MGE progenitors (Wichterle et al., 1999, 2001; Alvarez-Dolado et al., 2006; Hunt and Baraban, 2015). Third, under appropriate *in vitro* induction protocols, porcine MGE progenitors differentiate into cortical or hippocampal GABAergic with mature interneuron-like morphologies and expression of GABA, SOM and the vesicular GABA transporter (vGAT) (Casalia et al., 2021). Fourth, following xenotransplantation into adult rat hippocampus, porcine MGE-derived neurons migrate, display morphological similarities similar to mature native interneurons (e.g., basket cells, multipolar neurons, bipolar cells) and express both GABA and SOM (Alvarez-Dolado et al., 2006; Hunt et al., 2013; Casalia et al., 2021). Note, commercially available antibodies recognizing porcine PV-expressing neurons were not selective enough to evaluate this sub-population in these studies. Further, porcine MGE-derived neurons did not exhibit morphologic features of mature cortical pyramidal neurons and tumors were not observed in any host animal receiving porcine MGE progenitors. Together, these findings confirm that MGE-derived interneuron development is conserved across species. Future studies should evaluate the intrinsic electrophysiological properties and functional enhancement of synaptic inhibition for these porcine MGE-derived interneurons following xenotransplantation.

While additional characterization of porcine MGE progenitors awaits, a highly successful N-of-1 trial was recently reported for a refractory, domoic-acid poisoned epileptic California sea-lion playfully named Cronutt (Simeone et al., 2022). Domoic-acid poisoned sea lions consistently present with spontaneous convulsive seizures, hippocampal atrophy including loss of hippocampal PV-and SOM-expressing interneurons, and cognitive/behavioral deficits, similar to patients with TLE (de Lanerolle et al., 2003; Buckmaster et al., 2014; Cendes et al., 2014; Ives-Deliperi and Butler, 2021). Cronutt, rescued initially by the Marine Mammal Center and eventually adopted by Six Flags Discovery Kingdome presented with uncontrollable convulsive seizures (up to 10 per day), hippocampal atrophy (Cook et al., 2021), lethargy and severe weight loss. After considering euthanasia, we developed a protocol for

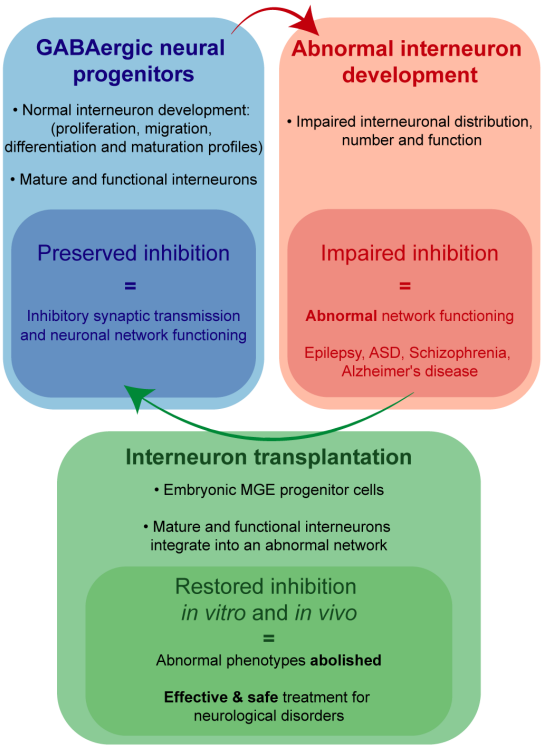

FIGURE 1
Interneuron-based cell transplantation therapy.

stereotaxic-guided xenotransplantation of embryonic porcine MGE progenitors in a sea lion. In the initial case report at 12 months following xenotransplantation, handlers at the Six Flags pinniped facility reported Cronutt's complete absence of convulsive seizures, with significant improvements in appetite, weight gain, and general behaviors (Simeone et al., 2022). Anecdotal observations now stretching beyond 28 months post xenotransplantation continue to report a seizure-free outcome and significant improvements in behavior and cognition.

Conclusion

While precise mechanism(s) by which interneuron dysfunction contributes to epilepsy (and related neurological disorders) remains an active area of investigation, an aspirational treatment goal is a "no seizures, no side effects" outcome. Although this goal remains elusive, patient and animal model data converge on a hypothesis that such a treatment could involve enhancement of GABA-mediated synaptic inhibition. Transplanted embryonic MGE progenitors have consistently been shown to migrate and functionally integrate in host circuits to enhance synaptic inhibition in a manner resembling that possible with native interneurons. Properties of interneurons derived from murine and porcine MGE progenitors make them ideal candidates for a cell transplantation treatment (Figure 1). Indeed, MGE transplantation drastically reduced seizures, abolished epilepsy-related comorbidities and failed to show any adverse side effects in experimental rodent models of acquired epilepsy and the case of a naturally occurring large mammal with TLE. Therefore, we are optimistic embryonic MGE progenitors offer a safe and effective

means toward developing a disease-modifying (no seizures, no side effects) treatment for intractable epilepsies.

Author contributions

JR wrote the first draft of the manuscript. SB wrote and reviewed the final version of the manuscript. All authors contributed to the article and approved the submitted version.

Funding

This work was supported by NIH/NINDS grant R01 NS-071785–13 to SB.

Conflict of interest

The authors declare that the research was conducted in the absence of any commercial or financial relationships that could be construed as a potential conflict of interest.

Publisher's note

All claims expressed in this article are solely those of the authors and do not necessarily represent those of their affiliated organizations, or those of the publisher, the editors and the reviewers. Any product that may be evaluated in this article, or claim that may be made by its manufacturer, is not guaranteed or endorsed by the publisher.

References

Allison, T., Langerman, J., Sabri, S., Otero-Garcia, M., Lund, A., Huang, J., et al. (2021). Defining the nature of human pluripotent stem cell-derived interneurons via single-cell analysis. *Stem Cell Rep.* 16, 2548–2564. doi: 10.1016/j.stemcr.2021.08.006

Alvarez-Dolado, M., Calcagnotto, M. E., Karkar, K. M., Southwell, D. G., Jones-Davis, D. M., Estrada, R. C., et al. (2006). Cortical inhibition modified by embryonic neural precursors grafted into the postnatal brain. *J. Neurosci.* 26, 7380–7389. doi: 10.1523/JNEUROSCI.1540-06.2006

Baraban, S. C., Southwell, D. G., Estrada, R. C., Jones, D. L., Sebe, J. Y., Alfaro-Cervello, C., et al. (2009). Reduction of seizures by transplantation of cortical GABAergic interneuron precursors into Kv1.1 mutant mice. *Proc. Natl. Acad. Sci. U. S. A.* 106, 15472–15477. doi: 10.1073/pnas.0900141106

Bráz, J. M., Sharif-Naeini, R., Vogt, D., Kriegstein, A., Alvarez-Buylla, A., Rubenstein, J. L., et al. (2012). Forebrain GABAergic neuron precursors integrate into adult spinal cord and reduce injury-induced neuropathic pain. *Neuron* 74, 663–675. doi: 10.1016/j.neuron.2012.02.033

Buckmaster, P. S., Wen, X., Toyoda, I., Gulland, F. M., and van Bonn, W. (2014). Hippocampal neuropathology of domoic acid-induced epilepsy in California Sea lions (*Zalophus californianus*). *J. Comp. Neurol.* 522, 1691–1706. doi: 10.1002/cne.23509

Calcagnotto, M. E., Paredes, M. F., Tihan, T., Barbaro, N. M., and Baraban, S. C. (2005). Dysfunction of synaptic inhibition in epilepsy associated with focal cortical dysplasia. *J. Neurosci.* 25, 9649–9657. doi: 10.1523/JNEUROSCI.2687-05.2005

Calcagnotto, M. E., Zipancic, I., Piquer-Gil, M., Mello, L. E., and Alvarez-Dolado, M. (2010). Grafting of GABAergic precursors rescues deficits in hippocampal inhibition. *Epilepsia* 51, 66–70. doi: 10.1111/j.1528-1167.2010.02613.x

Casalia, M. L., Howard, M. A., and Baraban, S. C. (2017). Persistent seizure control in epileptic mice transplanted with gamma-aminobutyric acid progenitors. *Ann. Neurol.* 82, 530–542. doi: 10.1002/ana.25021

Casalia, M. L., Li, T., Ramsay, H., Ross, P. J., Paredes, M. F., and Baraban, S. C. (2021). Interneuron origins in the embryonic porcine medial ganglionic Eminence. *J. Neurosci.* 41, 3105–3119. doi: 10.1523/JNEUROSCI.2738-20.2021

Cavalheiro, E. A. (1995). The pilocarpine model of epilepsy. *Ital. J. Neurol. Sci.* 16, 33–37. doi: 10.1007/BF02229072

Cavalheiro, E. A., Leite, J. P., Bortolotto, Z. A., Turski, W. A., Ikonomidou, C., and Turski, L. (1991). Long-term effects of pilocarpine in rats: structural damage of the brain triggers kindling and spontaneous recurrent seizures. *Epilepsia* 32, 778–782. doi: 10.1111/j.1528-1157.1991.tb05533.x

Cendes, F., Sakamoto, A. C., Spreafico, R., Bingaman, W., and Becker, A. J. (2014). Epilepsies associated with hippocampal sclerosis. *Acta Neuropathol.* 128, 21–37. doi: 10.1007/s00401-014-1292-0

Cobos, I., Borello, U., and Rubenstein, J. L. (2007). Dlx transcription factors promote migration through repression of axon and dendrite growth. *Neuron* 54, 873–888. doi: 10.1016/j.neuron.2007.05.024

Cobos, I., Calcagnotto, M. E., Vilaythong, A. J., Thwin, M. T., Noebels, J. L., Baraban, S. C., et al. (2005). Mice lacking Dlx1 show subtype-specific loss of interneurons, reduced inhibition and epilepsy. *Nat. Neurosci.* 8, 1059–1068. doi: 10.1038/nn1499

Cobos, I., Long, J. E., Thwin, M. T., and Rubenstein, J. L. (2006). Cellular patterns of transcription factor expression in developing cortical interneurons. *Cereb. Cortex* 16, i82–i88. doi: 10.1093/cercor/bhk003

Cook, P. F., Hoard, V. A., Dolui, S., Frederick, B. D., Redfern, R., Dennison, S. E., et al. (2021). An MRI protocol for anatomical and functional evaluation of the California Sea lion brain. *J. Neurosci. Methods* 353:109097. doi: 10.1016/j.jneumeth.2021.109097

Cooper, D. K., Gollackner, B., Knosalla, C., and Teranishi, K. (2002). Xenotransplantation--how far have we come? *Transpl. Immunol.* 9, 251–256. doi: 10.1016/S0966-3274(02)00010-2

De Lanerolle, N. C., Kim, J. H., Williamson, A., Spencer, S. S., Zaveri, H. P., Eid, T., et al. (2003). A retrospective analysis of hippocampal pathology in human temporal lobe epilepsy: evidence for distinctive patient subcategories. *Epilepsia* 44, 677–687. doi: 10.1046/j.1528-1157.2003.32701.x

Fink, J. S., Schumacher, J. M., Ellias, S. L., Palmer, E. P., Saint-Hilaire, M., Shannon, K., et al. (2000). Porcine xenografts in Parkinson's disease and Huntington's disease patients: preliminary results. *Cell Transplant.* 9, 273–278. doi: 10.1177/096368970000900212

Fontes-Dutra, M., Righes Marafiga, J., Santos-Terra, J., Deckmann, I., Brum Schwingel, G., Rabelo, B., et al. (2023). GABAergic synaptic transmission and cortical oscillation patterns in the primary somatosensory area of a valproic acid rat model of autism spectrum disorder. *Eur. J. Neurosci.* 57, 527–546. doi: 10.1111/ejn.15893

Henderson, K. W., Gupta, J., Tagliatela, S., Litvina, E., Zheng, X., Van Zandt, M. A., et al. (2014). Long-term seizure suppression and optogenetic analyses of synaptic connectivity in epileptic mice with hippocampal grafts of GABAergic interneurons. *J. Neurosci.* 34, 13492–13504. doi: 10.1523/JNEUROSCI.0005-14.2014

Howard, M. A., and Baraban, S. C. (2016). Synaptic integration of transplanted interneuron progenitor cells into native cortical networks. *J. Neurophysiol.* 116, 472–478. doi: 10.1152/jn.00321.2016

Howard, M. A., Rubenstein, J. L., and Baraban, S. C. (2014). Bidirectional homeostatic plasticity induced by interneuron cell death and transplantation *in vivo*. *Proc. Natl. Acad. Sci. U. S. A.* 111, 492–497. doi: 10.1073/pnas.1307784111

Hryhorowicz, M., Zeyland, J., Słomski, R., and Lipiński, D. (2017). Genetically modified pigs as organ donors for xenotransplantation. *Mol. Biotechnol.* 59, 435–444. doi: 10.1007/s12033-017-0024-9

Hsieh, J. Y., and Baraban, S. C. (2017). Medial ganglionic Eminence progenitors transplanted into hippocampus integrate in a functional and subtype-appropriate manner. *eNeuro*:4:359. doi: 10.1523/ENEURO.0359-16.2017

Hunt, R. F., and Baraban, S. C. (2015). Interneuron transplantation as a treatment for epilepsy. *Cold Spring Harb. Perspect. Med.*:a022376:5. doi: 10.1101/cshperspect.a022376

Hunt, R. F., Girskis, K. M., Rubenstein, J. L., Alvarez-Buylla, A., and Baraban, S. C. (2013). GABA progenitors grafted into the adult epileptic brain control seizures and abnormal behavior. *Nat. Neurosci.* 16, 692–697. doi: 10.1038/nn.3392

Isaacson, J. S., and Scanziani, M. (2011). How inhibition shapes cortical activity. *Neuron* 72, 231–243. doi: 10.1016/j.neuron.2011.09.027

Ives-Deliperi, V., and Butler, J. T. (2021). Mechanisms of cognitive impairment in temporal lobe epilepsy: a systematic review of resting-state functional connectivity studies. *Epilepsy Behav.* 115:107686. doi: 10.1016/j.yebeh.2020.107686

Jobst, B. C., and Cascino, G. D. (2015). Resective epilepsy surgery for drug-resistant focal epilepsy: a review. *JAMA* 313, 285–293. doi: 10.1001/jama.2014.17426

Katsarou, A. M., Moshé, S. L., and Galanopoulou, A. S. (2017). Interneuronopathies and their role in early life epilepsies and neurodevelopmental disorders. *Epilepsia Open* 2, 284–306. doi: 10.1002/epi4.12062

Knopp, A., Frahm, C., Fidzinski, P., Witte, O. W., and Behr, J. (2008). Loss of GABAergic neurons in the subiculum and its functional implications in temporal lobe epilepsy. *Brain* 131, 1516–1527. doi: 10.1093/brain/awn095

Kumar, S. S., and Buckmaster, P. S. (2006). Hyperexcitability, interneurons, and loss of GABAergic synapses in entorhinal cortex in a model of temporal lobe epilepsy. *J. Neurosci.* 26, 4613–4623. doi: 10.1523/JNEUROSCI.0064-06.2006

Kwan, P., and Brodie, M. J. (2000). Early identification of refractory epilepsy. *N. Engl. J. Med.* 342, 314–319. doi: 10.1056/NEJM200002033420503

Larimer, P., Spatazza, J., Espinosa, J. S., Tang, Y., Kaneko, M., Hasenstaub, A. R., et al. (2016). Caudal ganglionic Eminence precursor transplants disperse and integrate as lineage-specific interneurons but do not induce cortical plasticity. *Cell Rep.* 16, 1391–1404. doi: 10.1016/j.celrep.2016.06.071

Löscher, W., and Klein, P. (2021). The pharmacology and clinical efficacy of Antiseizure medications: from bromide salts to Cenobamate and beyond. *CNS Drugs* 35, 935–963. doi: 10.1007/s40263-021-00827-8

Marín, O. (2012). Interneuron dysfunction in psychiatric disorders. *Nat. Rev. Neurosci.* 13, 107–120. doi: 10.1038/nrn3155

Maroof, A. M., Keros, S., Tyson, J. A., Ying, S. W., Ganat, Y. M., Merkle, F. T., et al. (2013). Directed differentiation and functional maturation of cortical interneurons from human embryonic stem cells. *Cell Stem Cell* 12, 559–572. doi: 10.1016/j.stem.2013.04.008

Martínez-Cerdeño, V., Noctor, S. C., Espinosa, A., Ariza, J., Parker, P., Orasji, S., et al. (2010). Embryonic MGE precursor cells grafted into adult rat striatum integrate and ameliorate motor symptoms in 6-OHDA-lesioned rats. *Cell Stem Cell* 6, 238–250. doi: 10.1016/j.stem.2010.01.004

Nakazawa, K., Zsiros, V., Jiang, Z., Nakao, K., Kolata, S., Zhang, S., et al. (2012). GABAergic interneuron origin of schizophrenia pathophysiology. *Neuropharmacology* 62, 1574–1583. doi: 10.1016/j.neuropharm.2011.01.022

Ngugi, A. K., Kariuki, S. M., Bottomley, C., Kleinschmidt, I., Sander, J. W., and Newton, C. R. (2011). Incidence of epilepsy: a systematic review and meta-analysis. *Neurology* 77, 1005–1012. doi: 10.1212/WNL.0b013e31822cfc90

Nicholas, C. R., Chen, J., Tang, Y., Southwell, D. G., Chalmers, N., Vogt, D., et al. (2013). Functional maturation of hPSC-derived forebrain interneurons requires an extended timeline and mimics human neural development. *Cell Stem Cell* 12, 573–586. doi: 10.1016/j.stem.2013.04.005

Paterno, R., Casalia, M., and Baraban, S. C. (2020). Interneuron deficits in neurodevelopmental disorders: implications for disease pathology and interneuron-based therapies. *Eur. J. Paediatr. Neurol.* 24, 81–88. doi: 10.1016/j.ejpn.2019.12.015

Paterno, R., Marafiga, J. R., Ramsay, H., Li, T., Salvati, K. A., and Baraban, S. C. (2021). Hippocampal gamma and sharp-wave ripple oscillations are altered in a Cntnap2 mouse model of autism spectrum disorder. *Cell Rep.* 37:109970. doi: 10.1016/j.celrep.2021.109970

Piper, R. J., Richardson, R. M., Worrell, G., Carmichael, D. W., Baldeweg, T., Litt, B., et al. (2022). Towards network-guided neuromodulation for epilepsy. *Brain* 145, 3347–3362. doi: 10.1093/brain/awac234

Priya, R., Rakela, B., Kaneko, M., Spatazza, J., Larimer, P., Hoseini, M. S., et al. (2019). Vesicular GABA transporter is necessary for transplant-induced critical period plasticity in mouse visual cortex. *J. Neurosci.* 39, 2635–2648. doi: 10.1523/JNEUROSCI.1253-18.2019

Rosenow, F., and Lüders, H. (2001). Presurgical evaluation of epilepsy. *Brain* 124, 1683–1700. doi: 10.1093/brain/124.9.1683

Sanabria, E. R., da Silva, A. V., Spreafico, R., and Cavalheiro, E. A. (2002). Damage, reorganization, and abnormal neocortical hyperexcitability in the pilocarpine model of temporal lobe epilepsy. *Epilepsia* 43, 96–106. doi: 10.1046/j.1528-1157.43.s.5.31.x

Sebe, J. Y., and Baraban, S. C. (2010). The promise of an interneuron-based cell therapy for epilepsy. *Dev. Neurobiol.* 71, 107–117. doi: 10.1002/dneu.20813

Sebe, J. Y., Looke-Stewart, E., and Baraban, S. C. (2014). GABAB receptors in maintenance of neocortical circuit function. *Exp. Neurol.* 261, 163–170. doi: 10.1016/j.expneurol.2014.05.018

Sherman, E. M., Wiebe, S., Fay-Mcclymont, T. B., Tellez-Zenteno, J., Metcalfe, A., Hernandez-Ronquillo, L., et al. (2011). Neuropsychological outcomes after epilepsy surgery: systematic review and pooled estimates. *Epilepsia* 52, 857–869. doi: 10.1111/j.1528-1167.2011.03022.x

Simeone, C. A., Andrews, J. P., Johnson, S. P., Casalia, M., Kochanski, R., Chang, E. F., et al. (2022). Xenotransplantation of porcine progenitor cells in an epileptic California Sea lion (Zalophus californianus): illustrative case. *J Neurosurg Case Lessons* 3:1474. doi: 10.3171/CASE21417

Southwell, D. G., Froemke, R. C., Alvarez-Buylla, A., Stryker, M. P., and Gandhi, S. P. (2010). Cortical plasticity induced by inhibitory neuron transplantation. *Science* 327, 1145–1148. doi: 10.1126/science.1183962

Southwell, D. G., Nicholas, C. R., Basbaum, A. I., Stryker, M. P., Kriegstein, A. R., Rubenstein, J. L., et al. (2014). Interneurons from embryonic development to cell-based therapy. *Science* 344:1240622. doi: 10.1126/science.1240622

Spencer, S., and Huh, L. (2008). Outcomes of epilepsy surgery in adults and children. *Lancet Neurol.* 7, 525–537. doi: 10.1016/S1474-4422(08)70109-1

Sykes, M., and Sachs, D. H. (2019). Transplanting organs from pigs to humans. *Sci. Immunol.* 4:6298. doi: 10.1126/sciimmunol.aau6298

Turski, W. A., Cavalheiro, E. A., Schwarz, M., Czuczwar, S. J., Kleinrok, Z., and Turski, L. T. (1983). Limbic seizures produced by pilocarpine in rats: behavioural, electroencephalographic and neuropathological study. *Behav. Brain Res.* 9, 315–335. doi: 10.1016/0166-4328(83)90136-5

Upadhya, D., Hattiangady, B., Castro, O. W., Shuai, B., Kodali, M., Attaluri, S., et al. (2019). Human induced pluripotent stem cell-derived MGE cell grafting after status epilepticus attenuates chronic epilepsy and comorbidities via synaptic integration. *Proc. Natl. Acad. Sci. U. S. A.* 116, 287–296. doi: 10.1073/pnas.1814185115

Vogt, D., Hunt, R. F., Mandal, S., Sandberg, M., Silberberg, S. N., Nagasawa, T., et al. (2014). Lhx6 directly regulates Arx and CXCR7 to determine cortical interneuron fate and laminar position. *Neuron* 82, 350–364. doi: 10.1016/j.neuron.2014.02.030

Waldau, B., Hattiangady, B., Kuruba, R., and Shetty, A. K. (2010). Medial ganglionic eminence-derived neural stem cell grafts ease spontaneous seizures and restore GDNF expression in a rat model of chronic temporal lobe epilepsy. *Stem Cells* 28, 1153–1164. doi: 10.1002/stem.446

Wichterle, H., Garcia-Verdugo, J. M., Herrera, D. G., and Alvarez-Buylla, A. (1999). Young neurons from medial ganglionic eminence disperse in adult and embryonic brain. *Nat. Neurosci.* 2, 461–466. doi: 10.1038/8131

Wichterle, H., Turnbull, D. H., Nery, S., Fishell, G., and Alvarez-Buylla, A. (2001). In utero fate mapping reveals distinct migratory pathways and fates of neurons born in the mammalian basal forebrain. *Development* 128, 3759–3771. doi: 10.1242/dev.128.19.3759

Wiebe, S., Blume, W. T., Girvin, J. P., and Eliasziw, M.Effectiveness and Efficiency of Surgery for Temporal Lobe Epilepsy Study Group (2001). A randomized, controlled trial of surgery for temporal-lobe epilepsy. *N. Engl. J. Med.* 345, 311–318. doi: 10.1056/NEJM200108023450501

Wonders, C. P., and Anderson, S. A. (2006). The origin and specification of cortical interneurons. *Nat. Rev. Neurosci.* 7, 687–696. doi: 10.1038/nrn1954

Zack, M. M., and Kobau, R. (2017). National and state estimates of the numbers of adults and children with active epilepsy–United States, 2015. *MMWR Morb. Mortal. Wkly Rep.* 66, 821–825. doi: 10.15585/mmwr.mm6631a1

Zhu, B., Eom, J., and Hunt, R. F. (2019). Transplanted interneurons improve memory precision after traumatic brain injury. *Nat. Commun.* 10:5156. doi: 10.1038/s41467-019-13170-w

Zipancic, I., Calcagnotto, M. E., Piquer-Gil, M., Mello, L. E., and Alvarez-Dolado, M. (2010). Transplant of GABAergic precursors restores hippocampal inhibitory function in a mouse model of seizure susceptibility. *Cell Transplant.* 19, 549–564. doi: 10.3727/096368910X491383

frontiers | Frontiers in Neuroscience

TYPE Original Research
PUBLISHED 05 May 2023
DOI 10.3389/fnins.2023.1157060

OPEN ACCESS

EDITED BY
Gilles van Luijtelaar,
Radboud University, Netherlands

REVIEWED BY
Claire-Anne Gutekunst,
Emory University, United States
John Michael Power,
University of New South Wales, Australia

*CORRESPONDENCE
Tao Xue
✉ 2992326676@qq.com
Chunlei Han
✉ hanchunlei622@163.com
Jianguo Zhang
✉ zjguo73@126.com

†These authors have contributed equally to this work

RECEIVED 02 February 2023
ACCEPTED 17 April 2023
PUBLISHED 05 May 2023

CITATION
Xue T, Wang S, Chen S, Wang H, Liu C, Shi L, Bai Y, Zhang C, Han C and Zhang J (2023) Subthalamic nucleus stimulation attenuates motor seizures via modulating the nigral orexin pathway.
Front. Neurosci. 17:1157060.
doi: 10.3389/fnins.2023.1157060

Subthalamic nucleus stimulation attenuates motor seizures via modulating the nigral orexin pathway

Tao Xue[1*†], Shu Wang[1†], Shujun Chen[2], Huizhi Wang[3], Chong Liu[3], Lin Shi[1], Yutong Bai[1], Chunkui Zhang[4], Chunlei Han[1*] and Jianguo Zhang[1,3*]

[1]Department of Neurosurgery, Beijing Tiantan Hospital, Capital Medical University, Beijing, China, [2]Department of Neurology, Beijing Tiantan Hospital, Capital Medical University, Beijing, China, [3]Beijing Neurosurgical Institute, Capital Medical University, Beijing, China, [4]Beijing Institute of Basic Medical Sciences, Beijing, China

Background: Focal motor seizures that originate in the motor region are a considerable challenge because of the high risk of permanent motor deficits after resection. Deep brain stimulation of the subthalamic nucleus (STN-DBS) is a potential treatment for motor epilepsy that may enhance the antiepileptic actions of the substantia nigra pars reticulata (SNr). Orexin and its receptors have a relationship with both STN-DBS and epilepsy. We aimed to investigate whether and how STN inputs to the SNr regulate seizures and the role of the orexin pathway in this process.

Methods: A penicillin-induced motor epileptic model in adult male C57BL/6J mice was established to evaluate the efficacy of STN-DBS in modulating seizure activities. Optogenetic and chemogenetic approaches were employed to regulate STN-SNr circuits. Selective orexin receptor type 1 and 2 antagonists were used to inhibit the orexin pathway.

Results: First, we found that high-frequency ipsilateral or bilateral STN-DBS was effective in reducing seizure activity in the penicillin-induced motor epilepsy model. Second, inhibition of STN excitatory neurons and STN-SNr projections alleviates seizure activities, whereas their activation amplifies seizure activities. In addition, activation of the STN-SNr circuits also reversed the protective effect of STN-DBS on motor epilepsy. Finally, we observed that STN-DBS reduced the elevated expression of orexin and its receptors in the SNr during seizures and that using a combination of selective orexin receptor antagonists also reduced seizure activity.

Conclusion: STN-DBS helps reduce motor seizure activity by inhibiting the STN-SNr circuit. Additionally, orexin receptor antagonists show potential in suppressing motor seizure activity and may be a promising therapeutic option in the future.

KEYWORDS

subthalamic nucleus, substantia nigra pars reticulata, deep brain stimulation, motor seizure, orexin

Introduction

Epilepsy, one of the most prevalent neurological disorders, affects around 1% of the population (Devinsky et al., 2018). The pathological condition known as epilepsy is a circuit-level disease with hypersynchronous or excessive discharges and increased neuronal excitability as a result of an excitatory-inhibitory imbalance (Paz and Huguenard, 2015). Surgical resection is an effective therapeutic option for roughly 30% of individuals who continue to experience seizures despite receiving appropriate antiepileptic medications (Gomez-Alonso and Bellas-Lamas, 2015; Vakharia et al., 2018). Nonetheless, focal motor seizures originating in the motor region, particularly the primary motor cortex (M1), represent a considerable challenge due to the high risk of permanent motor deficits caused by ablation of the epileptic foci (Rosenow and Luders, 2001; Jobst and Cascino, 2015). As a result, the investigation of alternate therapy options for such individuals remains an active research area. Neuromodulatory approaches, such as deep brain stimulation (DBS), are hypothesized to normalize the abnormal brain activity and have been developed as an alternative treatment over the past several decades (Xue et al., 2022). The anterior nucleus of the thalamus (ANT), an important node in the Papez circuit, is currently the most commonly used stimulus target in the treatment of epilepsy (Fisher et al., 2010; Salanova et al., 2015). ANT-DBS demonstrated satisfactory control of temporal lobe seizures but less control of seizures arising from other regions (Fasano et al., 2021). Thus, for epileptic patients with motor seizures, especially for seizures originating from motor areas, it is necessary to explore new stimulation targets.

The subthalamic nucleus (STN), which plays an important role in the basal ganglia pathway, projects directly to the substantia nigra pars reticulata (SNr), which is a part of the well-known nigral regulatory system involved in epilepsy (Gale, 1992). In frontal lobe motor seizures, animal experiments have verified the activation of the indirect pathway, including STN, SNr, and their upstream and downstream nuclei (Brodovskaya et al., 2021). STN-DBS has already been widely used in movement disorders, such as Parkinson's disease (Weaver et al., 2009), and is thought to enhance the antiepileptic actions of SNr (Salanova, 2018). Despite several clinical case reports and pilot studies that have identified its potential role in the treatment of motor seizures (Benabid et al., 2002; Chabardes et al., 2002; Handforth et al., 2006; Lee et al., 2006; Ren et al., 2020), the exact neural circuit mechanism of STN-DBS in controlling seizures remains unclear. The excitatory hypothalamic peptide orexin (also known as hypocretin), which has two subtypes named orexin A (OA) and orexin B (OB), is secreted by a group of neurons located in the hypothalamus close to the STN that project to both STN and SNr (Peyron et al., 1998). Furthermore, STN and SNr have two types of orexin receptors, OX1R and OX2R, which are co-localized in these two regions (Korotkova et al., 2002; Li et al., 2019). Endogenous orexin A/B maintains the physiological discharge of STN glutamatergic neurons and SNr GABAergic neurons (Korotkova et al., 2002; Sheng et al., 2018). In addition, exogenous extra orexin A/B was found to increase penicillin-induced epileptic activity (Kortunay et al., 2012), and orexin receptor antagonisms were observed to reduce seizures in multiple epilepsy models (Zhu et al., 2015; Roundtree et al., 2016; Kordi Jaz et al., 2017). Meanwhile, DBS can affect the expression of orexin receptors (Dong et al., 2021). Therefore, we systematically investigated whether and how STN inputs to SNr regulate seizures and the role that the orexin pathway plays in this process using a mouse model in which epilepsy originated from M1. Identifying the neural circuitry and molecular mechanism responsible for motor seizures could result in the development of more precise therapeutic approaches to control seizures.

Abbreviations: AAV, adeno-associated virus; ANT, anterior nucleus of the thalamus; DBS, deep brain stimulation; FS, focal seizure; GS, generalized seizure; M1, primary motor cortex; OA, Orexin A; OB, Orexin B; OX1R, orexin receptor type 1; OX2R, orexin receptor type 2; PBS, phosphate buffer solution; PFA, paraformaldehyde; STN, subthalamic nucleus; SNR, substantia nigra pars reticulata.

Materials and methods

Animals

In the study, 238 male C57BL/6 J mice, aged 6–8 weeks, were used. The mice were group-housed in cages containing 4–6 mice and were kept in a controlled environment with a 12-h light/dark cycle and a temperature of 20–23°C. The mice had free access to food and water and were cared for in accordance with the National Institute of Health Guide for the Care and Use of Laboratory Animals. All procedures involving the mice were approved by the Animal Advisory Committee of the Beijing Tiantan Hospital and conformed to the Animal Research: Reporting *In Vivo* Experiments (ARRIVE) guidelines. Information about mice mortality and exclusion can be found in Supplementary Table 1.

Stereotactic surgery

Mice were anesthetized using sodium pentobarbital (50 mg/kg, i.p., Sigma-Aldrich) and had their heads fixed in a stereotaxic apparatus (68,044, RWD Instruments). To ensure that the mice remained pain-free during the procedure, additional doses of sodium pentobarbital were administered if a pain response was observed upon paw pinch. The body temperature of the anesthetized mice was maintained at 37°C using a heating pad. An incision was made on the head to expose the skull, and burr holes were stereotactically made on the skull after removing the pericranium.

Microinjections were administered using a gauge needle and an Ultra Micro Pump (R-480, RWD Instruments) for viral delivery, with the coordinates for the left STN, left SNr, and left M1 being −2.0 mm AP, +1.6 mm ML, −4.6 mm V; −3.4 mm AP, +1.5 mm ML, −4.4 mm V; and + 2.1 mm AP, +2 mm ML, −1.7 mm V from Bregma, respectively, based on the mouse brain atlas (Paxinos and Franklin, 2004). The viruses were infused over a period of 5–10 min, and the syringe was left in place until 10 min after the end of the infusion to allow for diffusion. Adeno-associated viruses (AAVs) were injected at a total volume of 0.1–0.5 µl, based on the size of the brain region, and approximately 3 weeks were allowed for maximal viral expression.

After 3 weeks of viral delivery, bipolar stimulation electrodes (CBBRF50, FHC), optical fibers (ULC-589-200-0.73-4.0, Newdoon Inc), or single-guide cannulas (62,001, RWD Instruments) were implanted 300 µm above the center of the M1, STN, or SNr, based on the specific experiment, using stereotaxic coordinates. These were

fixed to the skull using dental cement, and three anchoring skull screws (diameter of 1 mm) were placed in the skull also for EEG recording, two of which were placed over the left neocortex (first electrode, −1.00 mm AP, +1.5 mm ML; second electrode, +3.00 mm AP, +1.5 mm ML), one of which was placed over the cerebellum to serve as the reference electrode. The implantation site and viral expression in the mice were verified after behavioral testing, and only mice with correct implantation location and viral expression were included in the analysis. Throughout the surgical procedures, the mice were kept on a heating pad and were returned to their home cages after post-surgery recovery.

Seizure induction

After 1 week of recovery from stereotactic surgery, penicillin was administered to freely moving mice through a guide cannula implanted in the M1 region using an Ultra Micro Pump (KDS LEGATO 130, RWD Instruments). The infusion rate was set at 0.1 μl/min, with a total injection of 1 μl of penicillin (200 IU/μL, P105489, Aladdin). EEG recordings were obtained beginning 10 min prior to the penicillin injection and continued for 180 min. Thirty minutes before the penicillin injection, the mice in the different groups received either a saline injection (i.p.) or CNO (1 mg/kg, i.p.), depending on the specific experiment being conducted. The severity of behavioral seizures was evaluated using Racine's criteria (Racine, 1972), which included the following: (1) facial movement, (2) head nodding, (3) unilateral forelimb clonus, (4) bilateral forelimb clonus and rearing, and (5) rearing and falling. Seizure stages 1–3 was classified as focal seizures (FSs), and stages 4–5 were classified as general seizures (GSs). The number of FSs and GSs were recorded by an investigator who was unaware of the group assignments during a 3-h observation period.

DBS and photostimulation

The DBS electrodes were connected to a stimulator (Master-8 Programmable Stimulator, AMPI, Jerusalem, Israel), which delivered electrical pulses (pulse width = 60 μs, intensity = 100 μA) at specific frequencies based on the experimental design. The electrodes of the sham group were not connected to the stimulator, and therefore, the animals in this group did not receive any stimulation.

Blue (465 nm, 30 Hz, 10 ms, 10 mW) or yellow (589 nm, continuous, 10 mW) laser light was delivered using an optical stimulation system (IOS-465/589, RWD Instruments). For the negative control group, the parameters of the laser were adjusted to be the same as those used in the experimental group. The power of the laser was adjusted to approximately 10 mW, as measured using a power meter (Thorlabs).

EEG recordings and fiber photometry

EEG activity was recorded using a data acquisition system (PowerLab, AD Instruments). The biological signals from the electrodes were amplified and filtered (bandpass of 0.1–50 Hz) using BioAmp amplifiers (AD Instruments). The EEG signal was digitized at a sampling rate of 1,024 Hz and displayed and stored on a personal computer. The frequency and amplitude of epileptiform EEG activity were analyzed offline using LabChart software (AD Instruments) (Yildirim et al., 2010). Only spikes with amplitudes greater than three times the baseline activity were included in the analysis. The EEG power spectrum was analyzed offline using the basal activity recorded prior to the penicillin injection. Only the 0.5–50 Hz range of all spectra was used for further analysis, with faster frequency bands being cropped. EEG power was calculated in the following frequency bands: delta (0.5–4 Hz), theta (4–8 Hz), alpha (8–13 Hz), beta (13–30 Hz), and gamma (30–50 Hz). Examples of EEG recordings for different periods of epileptic activity can be found in Supplementary Figure S1A.

Fiber photometry of calcium signals was initiated 1 week after the implantation surgery. GCaMP fluorescence was collected using a fiber photometry system (inper) and analyzed using a supporting data processing software (Inper Data Process, inper). The data were segmented according to individual trials, and the values of fluorescence change (ΔF/F) were calculated as (F − F0)/F0. Heatmaps or average plots were used to present the ΔF/F values. Examples of calcium signals after triple injection of AAVs in three brain regions: M1, STN and SNr during seizures can be found in Supplementary Figure S1B.

Immunofluorescence labeling

Mice were anesthetized and transcardially perfused with 0.9% NaCl and then with 4% paraformaldehyde (PFA) in phosphate buffer solution (PBS). Their brains were dissected, fixed in 4% PFA for 6 h at 4°C, and transferred to solutions of 20 and 30% sucrose in PBS for 36–48 h. The brains were coronally sectioned into 40-μm slices using a freezing microtome (Leica, CM1950), and the slices were collected for immunostaining. The slices were pre-incubated in a solution of 3% bovine serum albumin (w/v) and 0.5% Triton X-100 (v/v) for 2 h at room temperature, followed by overnight incubation at 4°C with the appropriate primary antibodies (listed in Supplementary Table S2). Among them, the antibody of c-Fos was used to determine the enhancement neural activity induced by penicillin and the antibodies of OX1R, OX2R were used to detect the expression and colocalization in SNr. They were then incubated with fluorescent secondary antibodies (Alexa fluor 488-conjugated goat anti-rabbit [A11008]; Alexa fluor 546-conjugated donkey anti-rabbit [A10040]; Invitrogen; all 1:2000) for 2 h at room temperature. The primary and secondary antibodies were diluted in PBS containing 3% bovine serum albumin (w/v) and 0.3% Triton X-100. The fluorescent signals were examined and photographed using an A1R laser-scanning confocal microscope (Nikon A1R, Japan) with magnification = 10× and numerical aperture = 0.45. The relative fluorescence intensity was analyzed using ImageJ software by observers who were blinded to the experimental groups.

Western blot analysis

Briefly, brain tissues containing SNr were homogenized in 1% sodium dodecyl sulfate (SDS). Protein aliquots of 20 μl from each sample were separated by 8% SDS-polyacrylamide gel electrophoresis

and transferred to a polyvinylidene fluoride membrane. The membrane was blocked with 3% non-fat milk in PBS at room temperature for 2 h and then incubated with the primary antibodies [rabbit-anti-OX1R or rabbit-anti-OX2R (details in Supplementary Table S2) or mouse-anti-GAPDH (Invitrogen, PA1-988, 1:1000)] overnight at 4°C. After being washed three times, the membrane was incubated with HRP (anti-mouse: sc-2004; anti-rabbit: sc-2005, Santa Cruz Biotechnology) at room temperature, and the protein bands were visualized using the ECL system (Tanon Inc., 5,200). The gray scale of the bands was quantified using ImageJ software.

Elisa

The acquired supernatants of SNr were collected and stored at −80°C until use. All operations of ELISA for OA (EM0453, Wuhan Fine Biotech Co.) and OB (CX4453, Shanghai Chuangxiang Co.) were conducted according to the manufacturer's instructions.

Viral vectors and drugs

rAAV-CaMKIIα-mCherry (titre: 1.2×10^{13} v.g.ml^{-1}), rAAV/retro-hSyn-eYFP (titre: 1.3×10^{13} v.g.ml^{-1}), rAAV-CaMKIIa-GCaMp6m (titre: 1.1×10^{13} v.g.ml^{-1}), rAAV-CaMKIIα-hChR2 (H134R)-eYFP (titre: 5.8×10^{12} v.g.ml^{-1}), rAAV-CaMKIIα-eNpHR-eYFP (titre: 5.2×10^{12} v.g.ml^{-1}), rAAV-EF1α-DIO-hM3D (Gq)-mCherry (titre: 1.7×10^{13} v.g.ml^{-1}), rAAV-EF1α-DIO-hM4D(Gi)-mCherry (titre: 2.2×10^{13} v.g.ml^{-1}), and rAAV/retro-hSyn-CRE (titre: 1.8×10^{13} v.g.ml^{-1}) were purchased from BrainVTA Co., Ltd. (Wuhan, China). All viral vectors were aliquoted and stored at −80°C until use.

The selective antagonists for OX1R and OX2R, named SB-334867 (10 μM, item no. 19145) and JNJ-10397049 (10 μM, item no. 14139), were purchased from Cayman Chemical Co. (Ann Arbor, MI, United States) and stored at −20°C until use.

Statistics

Data are presented as means ± SD. The number of experimental replicates (n) is indicated in the figures and refers to the number of experimental subjects that were independently treated in each experimental condition. Statistical comparisons were conducted using Prism (version 8.0) with the appropriate methods. No statistical methods were applied to pre-determine the sample size or to randomize the groups. All analyses were two-tailed, and a value of p <0.05 was considered statistically significant. A detailed statistical description of all figures can be found in Supplementary Table S3.

Results

Ipsilateral/bilateral high-frequency (130Hz) STN-DBS alleviates seizures in motor epilepsy

To examine the effects of different frequencies of STN-DBS on seizure control in motor epilepsy, we recorded the calcium signals of M1 excitatory neurons using fiber photometry in freely moving epileptic mice with STN-DBS (ipsilateral stimulation, 10/60/130 Hz, 100 μA, 60 μs, 30-s on–off cycle; Figures 1A,B). Following stereotaxic infusion of the AAVs into M1, the calcium indicator GCaMP6m was efficiently expressed in M1 neurons (Figure 1C). Then, we implanted an optical fiber into the M1 for recordings of GCaMP fluorescence changes and an electrode into the STN to induce electrical stimulation (Figure 1C; Supplementary Figure S1C). We observed an increased calcium response in ipsilateral M1 after injection of penicillin and sham. Low-frequency (10 Hz) and moderate-frequency (60 Hz) stimulation of STN did not attenuate the calcium signal of seizures, while high-frequency (130 Hz) STN-DBS alleviated the seizures (Figure 1D). Therefore, the frequency setting of 130 Hz was used for subsequent experiments.

Next, we aimed to assess whether ipsilateral and bilateral high-frequency STN-DBS had different effects on seizure improvement. Continuous 130-Hz stimulation was used to identify the efficacy of ipsilateral/bilateral STN-DBS for motor seizure control (Figures 1E,F). A typical EEG and the corresponding power spectrum are shown in Figure 1G. EEG analysis demonstrated that both ipsilateral and bilateral stimulation significantly decreased the spike frequency (Figure 1H), amplitude (Figure 1I), and power spectral density (Figure 1J) of motor seizures. In addition, ipsilateral STN-DBS significantly prolonged the latency to GS, whereas bilateral stimulation significantly prolonged the onset of both FS and GS (Figures 1K,L). Meanwhile, ipsilateral/bilateral STN-DBS distinctly reduced the number of FSs and GSs (Figures 1M,N; Supplementary Figure S1D) but failed to prevent the development of the seizure stages (Figure 1O). Furthermore, the neurons in M1, STN, and SNr were activated after penicillin injection with c-Fos expression (Supplementary Figure S1E). Ipsilateral/bilateral STN-DBS significantly reduced the fluorescent intensity of c-Fos (Figures 1P,Q), suggesting that STN-DBS reversed the hyperexcitability of multiple brain regions affected by the motor epilepsy network. The above results suggest that both ipsilateral and bilateral high-frequency STN-DBS have similar effects in improving seizures in the mouse motor epilepsy model. Therefore, after various considerations of efficacy, cost, and convenience, ipsilateral 130-Hz STN-DBS was considered to be effective and was used in subsequent relevant experiments.

Activation of STN excitatory neurons amplifies seizure activities

To investigate the role of STN excitatory neurons (most of them being glutamatergic neurons) in seizures of motor epilepsy, we used an optogenetic approach to selectively stimulate Channelrhodopsin 2 (ChR2)-expressing excitatory neurons in the STN of CamKIIα-ChR2-eYFP mice (Figures 2A,B). Histological data confirmed the presence of eYFP-expressing neurons and an inserted optical fiber in the STN (Figure 2C). Representative EEG and power spectrum confirmed that blue-light stimulation (465 nm, 30 Hz, 10 ms, 10 mW, 180-s on–off cycle) amplified seizure activities in six mice, suggesting that activation of STN excitatory neurons can deteriorate seizures originating from M1. Yellow-light stimulation (589 nm, 30 Hz, 10 ms, 10 mW, 180-s on–off cycle), serving as the control stimulation, was associated with similar seizure activities as no-light stimulation (Figure 2D). Statistics analysis of EEG also revealed that

10.3389/fnins.2023.1157060

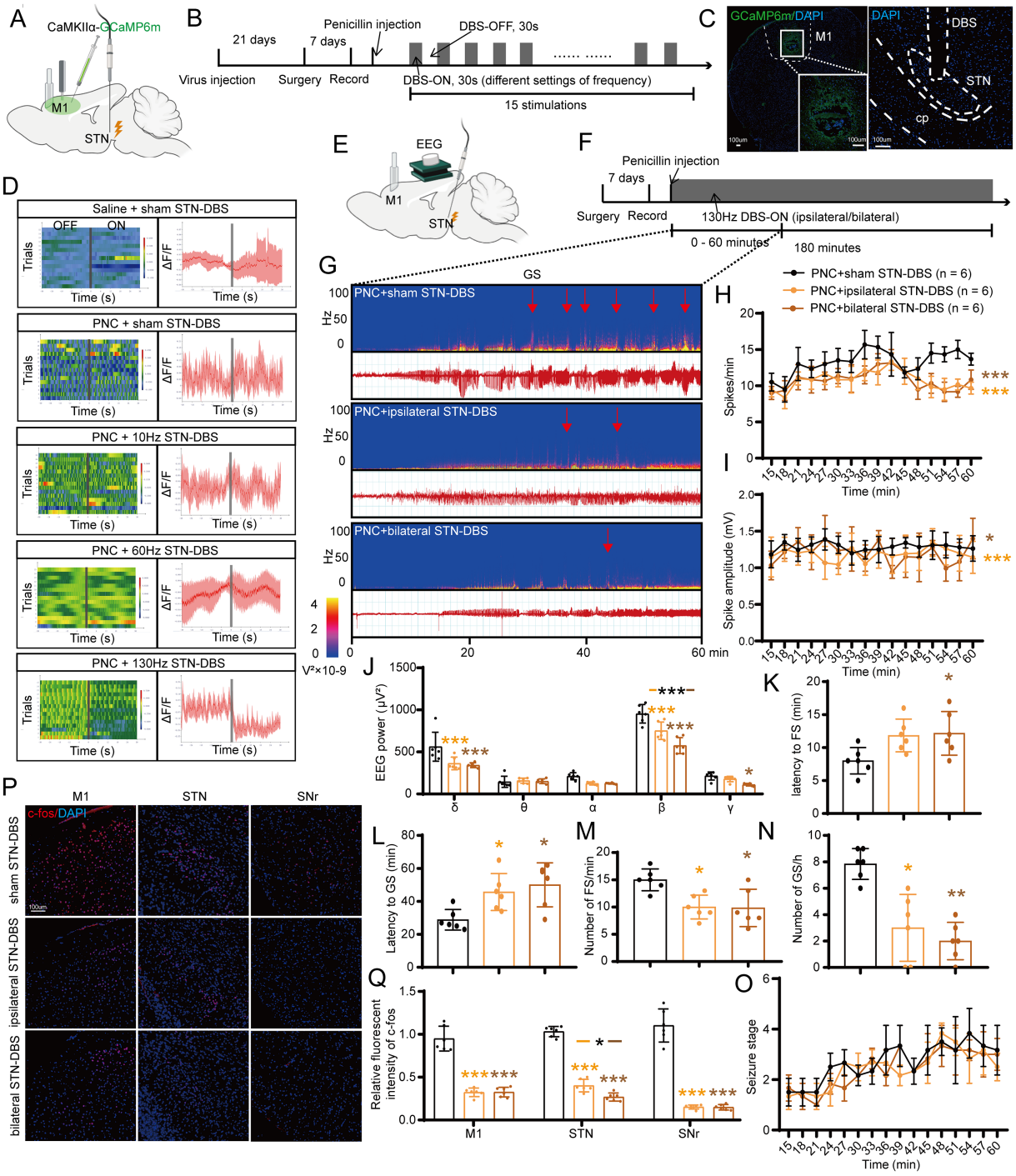

FIGURE 1
Effects of deep brain stimulation of the subthalamic nucleus (STN-DBS) on motor epilepsy. **(A,B)** Scheme and time course of the experiment for the efficacy of different frequencies of STN-DBS in motor epileptic mice. **(C)** Representative images of the primary motor cortex (M1) and STN, confirming the expression of CaMKIIα-GCaMP6m and location of the electrode. Scale bar=100μm. Left, M1; Right, STN. **(D)** Fiber photometry of M1 excitatory neural dynamics during motor seizures in CaMKIIα-GCaMP6m^{M1} mice according to different groups. Left column, heatmap illustration of calcium signals. Color scale indicates ΔF/F, and warmer colors indicate higher fluorescence signals; Right column, peri-event plots of the average calcium signals corresponding to the heatmaps. Red lines indicate mean, and shaded areas indicate SD. The gray lines represent electrical stimulation. **(E,F)** Scheme and time course of the experiment for the efficacy of ipsilateral and bilateral high-frequency (130Hz) STN-DBS in motor epileptic mice. **(G)** Representative EEG spectra power and raw EEG; red arrowheads indicate generalized seizure (GS) onset. Effects of ipsilateral and bilateral high-frequency (130Hz) STN-DBS on **(H)** spike frequency, **(I)** spike amplitude, **(J)** spectral power density, **(K)** latency to FS, **(L)** latency to GS, **(M)** number of FS, **(N)** number of GS, and **(O)** development of seizure stage. **(P)** Immunofluorescence analysis was performed using antibodies against c-Fos (red) in brain sections of M1, STN, and substantia nigra pars reticulata (SNr). Nuclei were fluorescently labeled with DAPI (blue). Scale bar=100μm. **(Q)** Relative fluorescence intensity of c-Fos in M1, STN, and SNr. *p<0.05, **p<0.01, ***p<0.001. Colored asterisk indicates the comparison of the corresponding group and the penicillin + sham STN-DBS group; black asterisk with two different colored horizontal lines to the left and right represents comparison of the corresponding two groups. Data are presented as means ± SD. Detailed statistical methods and data are provided in Supplementary materials.

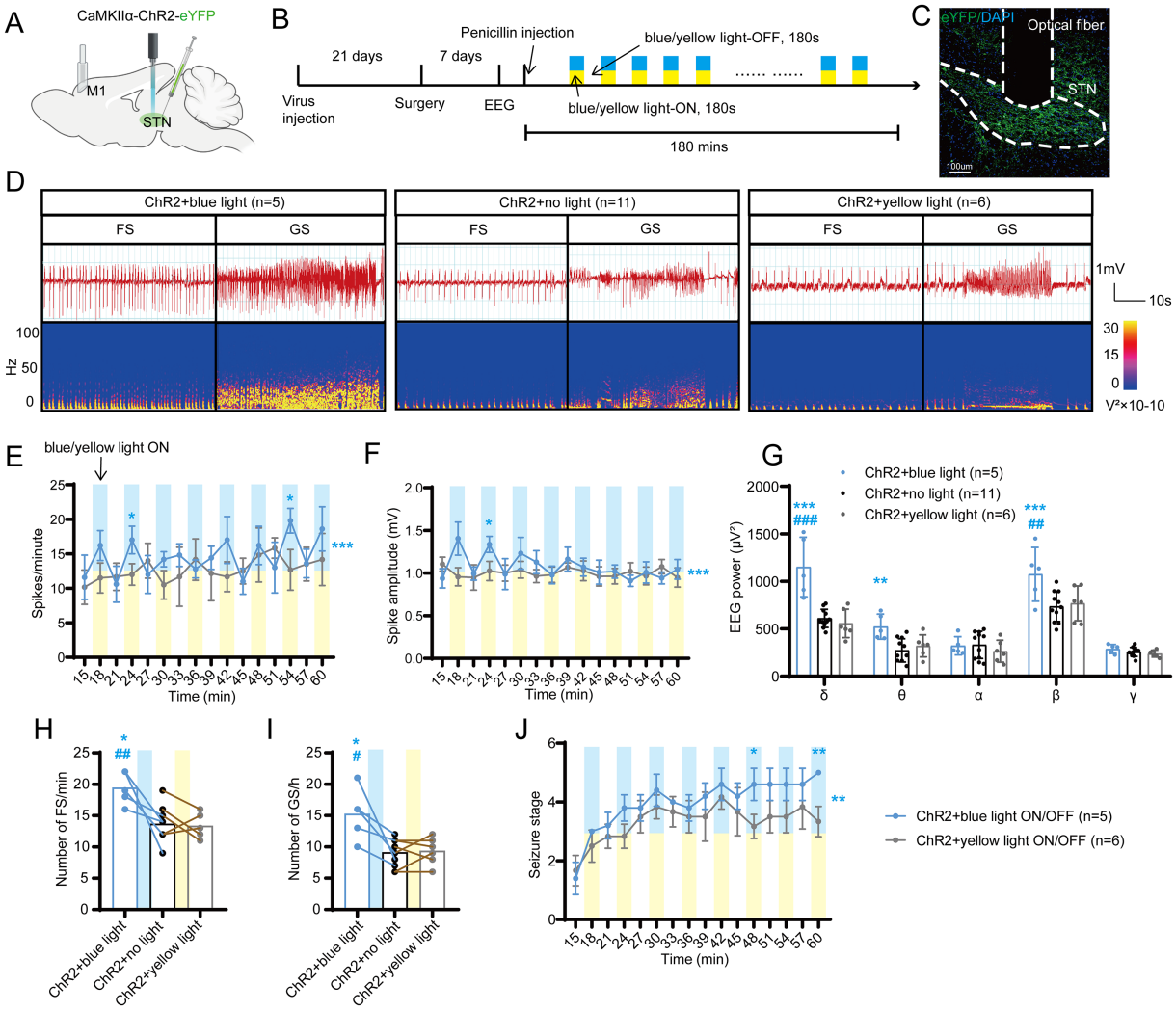

FIGURE 2
Optogenetic activation of the subthalamic nucleus (STN) excitatory neurons amplifies seizure activities in motor epilepsy. **(A,B)** Scheme and time course of the experiment for viral injection and photostimulation of motor epileptic mice. **(C)** Representative images of the STN, confirming the expression of CaMKIIα-ChR2-eYFP and location of the optic fiber. Scale bar=100μm. **(D)** Representative EEGs and corresponding EEG spectra power for focal seizure (FS) and generalized seizure (GS). Effects of optogenetic activation of the STN excitatory neurons on **(E)** spike frequency, **(F)** spike amplitude, **(G)** spectral power density, **(H)** number of FS, **(I)** number of GS, and **(J)** development of seizure stage. For panels **(E,F,J)**, *p<0.05, **p<0.01, ***p<0.001. Colored asterisk located at the right side of the curve indicates comparison through the entire period; colored asterisk located above the curve indicates comparison at the specific time point. The half-blue and half-yellow rectangles indicate photostimulation according to the groups. For panels **(G–I)**, */#p<0.05, **/##p<0.01, ***/###p<0.001. Asterisk indicates comparison with the ChR2+no light group; pound symbol indicates comparison with the ChR2+yellow light group. Data are presented as means ± SD. Detailed statistical methods and data are provided in Supplementary materials.

mice in the ChR2 + blue light ON/OFF group ($n = 5$) had higher spike frequency (Figure 2E) and amplitude (Figure 2F) than those in the ChR2 + yellow light ON/OFF group; the effect was more pronounced especially during the initial few stimulations (within 30 min after injection). In addition, blue-light stimulation enhanced the spectral density and increased the number of FSs and GSs, while yellow-light stimulation had no effect, compared to no light (Figures 2G–I). Finally, the 180-s ON/OFF stimulation with blue light could significantly accelerate the seizure stages compared to yellow light (Figure 2J). Thus, the above results illustrate that driving STN excitatory neurons amplify seizure activities in the penicillin motor epilepsy model.

Inhibition of STN excitatory neurons attenuates seizure activities

To further test whether STN excitatory neurons are required for seizures of motor epilepsy, we introduced eNpHR into the STN of mice to selectively photo-inhibit STN excitatory neurons (Figures 3A,B). Histological data confirmed the expression of eNpHR-eYFP and the location of the fiber in the STN (Figure 3C). Figure 3D shows the typical EEG and power spectrum, indicating that yellow-light stimulation (589 nm, continuous, 10 mW, 180-s on–off cycle) attenuated seizure activities and blue-light stimulation (465 nm, continuous, 10 mW, 180-s on–off cycle) exerted similar effects as no

10.3389/fnins.2023.1157060

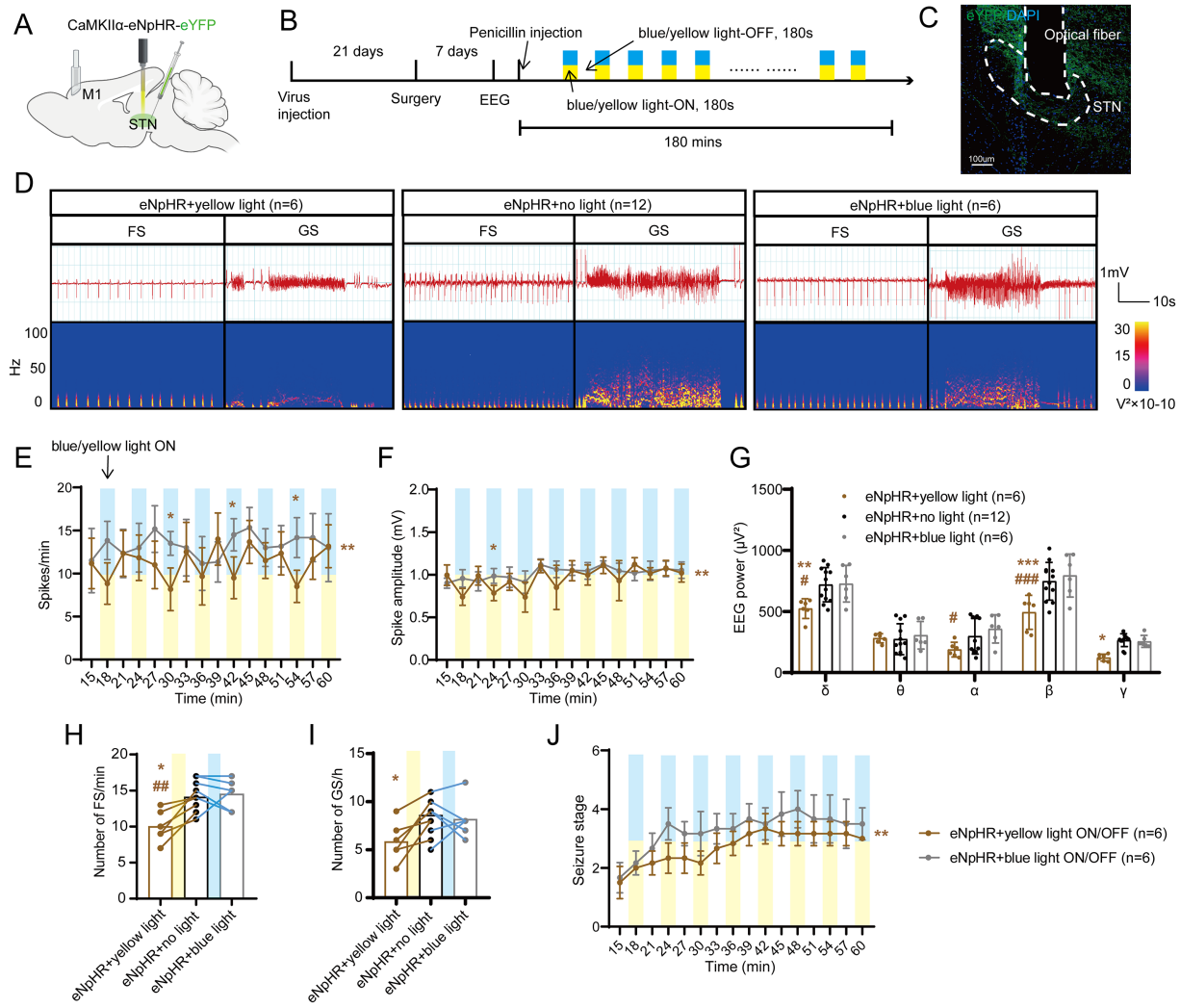

FIGURE 3
Optogenetic inhibition of the subthalamic nucleus (STN) excitatory neurons amplifies seizure activities in motor epilepsy. **(A,B)** Scheme and time course of the experiment for viral injection and photostimulation of motor epileptic mice. **(C)** Representative images of the STN, confirming the expression of CaMKIIα-eNpHR-eYFP and location of the optic fiber. Scale bar=100μm. **(D)** Representative EEGs and corresponding EEG spectra power for focal seizure (FS) and generalized seizure (GS). Effects of optogenetic inhibition of the STN excitatory neurons on **(E)** spike frequency, **(F)** spike amplitude, **(G)** spectral power density, **(H)** number of FS, **(I)** number of GS, and **(J)** development of seizure stage. For panels **(E,F,J),** *p<0.05, **p<0.01. Colored asterisk located at the right side of curve indicates comparison with the entire period; colored asterisk located above the curve indicates comparison at the specific time point. The half-blue and half-yellow rectangles represent photostimulation according to the group. For panels **(G–I),** */#p<0.05, **/##p<0.01, ***/###p<0.001. Asterisk indicates comparison with the eNpHR + no light group; pound symbol indicates comparison with the eNpHR + blue light group. Data are presented as means ± SD. Detailed statistical methods and data are provided in Supplementary materials.

light. Meanwhile, EEG analysis demonstrated that mice in the eNpHR + yellow light ON/OFF group (n = 6) had fewer spikes (Figure 3E) and lower spike amplitudes (Figure 3F) than those in the eNpHR + blue light ON/OFF group; yellow light significantly reduced the EEG power compared to blue light and no light in δ and β bands (Figure 3G). In addition, yellow light significantly reduced the numbers of FSs compared to no light and blue light, and significantly decreased the numbers of GSs compared to no light (Figures 3H,I). Finally, yellow light ON/OFF circulation slowed down the development of the seizure stages compared to blue light (Figure 3J). According to the evidence presented above, STN excitatory neurons bidirectionally regulate the magnitude of seizures in the motor epilepsy model. Activation of STN neurons amplifies seizures, while inhibition of STN neurons alleviates seizures.

STN-SNr circuit bidirectionally regulates seizures

Next, we aimed to test how STN neurons are involved in seizure regulation of motor epilepsy. Previous studies have found that frontal epilepsy originating from the supplementary motor area is more likely to activate dopamine D2 receptor-expressing neurons in the indirect pathway (Brodovskaya et al., 2021). Moreover, in the basal ganglia

10.3389/fnins.2023.1157060

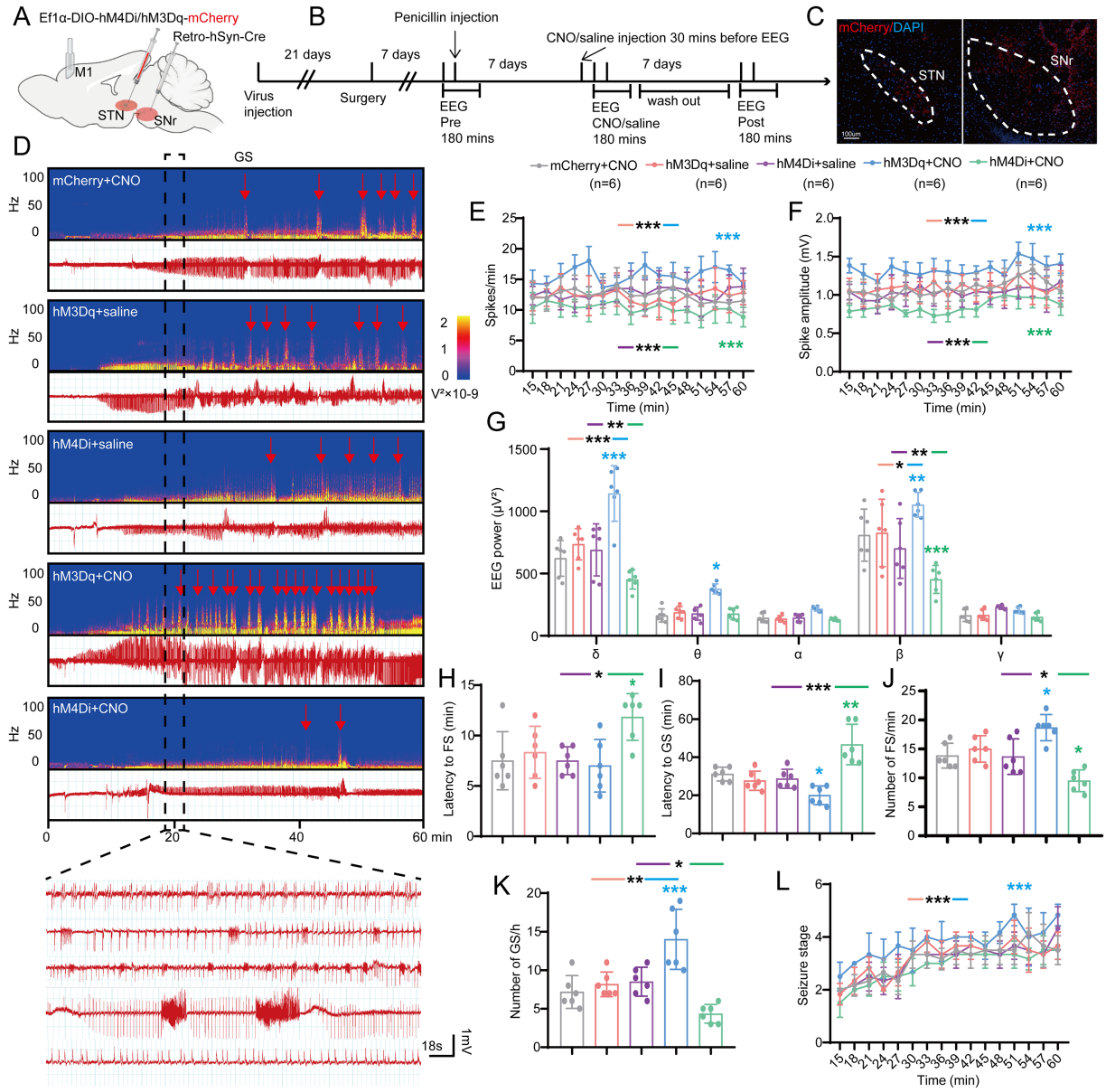

FIGURE 4
Effects of chemogenetic regulation of the subthalamic nucleus-substantia nigra pars reticulata (STN-SNr) circuit on motor epilepsy. **(A,B)** Scheme and time course of experiment. **(C)** Representative images of the STN and SNr, confirming the expression of virus. Scale bar=100μm. Left, STN; Right, SNr. **(D)** Representative EEG spectra power and raw EEG; below are enlarged raw EEG segments corresponding to the dotted boxes; red arrowheads indicate generalized seizure (GS) onset. Effects of chemogenetic regulation of the STN-SNr circuit on **(E)** spike frequency, **(F)** spike amplitude, **(G)** spectral power density, **(H)** latency to FS, **(I)** latency to GS, **(J)** number of FS, **(K)** number of FS, and **(L)** development of seizure stage. *p<0.05, **p<0.01, ***p<0.001. Colored asterisk indicates comparison of the corresponding group and the mCherry + CNO group; black asterisk with two different colored horizontal lines to the left and right indicates comparison of the corresponding two groups. Data are presented as means ± SD. Detailed statistical methods and data are provided in Supplementary materials.

circuit, the downstream nuclear outputs of the STN are mainly through SNr and globus pallidus internus (GPi). Additionally, SNr, instead of GPi, has also been found to be closely related to a type of epilepsy. Therefore, we mainly explored whether the STN-SNr circuit plays an important role in motor epilepsy. The classic STN-SNr projections were briefly verified by anterograde and retrograde tracer AAVs (Supplementary Figures S1F,G).

Initially, we adopted a chemogenetic method to observe whether enhancing or suppressing the activity of STN-SNr projections can alleviate motor seizures. AAV-Ef1α-DIO-hM4Di/hM3Dq/(empty)-mCherry and AAV2-retro-hSyn-Cre were injected into the STN and SNr, respectively (Figures 4A,B). The first virus expressed hM4Di/hM3Dq, two designed G-protein-coupled receptors sensitive to the metabolite of clozapine, clozapine-N-oxide (CNO), and was usually employed to suppress/enhance neuronal activity (Urban and Roth, 2015). Histological data confirmed the mCherry-expressing neurons in the STN and SNr (Figure 4C). STN-SNr hM4Di/hM3Dq-mCherry mice received CNO (i.p. 1 mg/kg in saline vehicle) half an hour before penicillin injection (200 IU/μL, 1.0 μl) *via* the implanted cannula guide into the M1. STN-SNr hM4Di/hM3Dq-mCherry mice

treated with saline or STN-SNr mCherry mice treated with CNO served as controls. The representative graphs of EEG and power spectrum are shown in Figure 4D. Chemogenetic suppression of STN-SNr projections substantially reduced spike frequency (Figure 4E), spike amplitude (Figure 4F), and EEG density (Figure 4G), prolonged latency to FSs (Figure 4H) and GSs (Figure 4I), lowered the number of FSs and GSs (Figures 4J,K) but failed to retard seizure progression (Figure 4L). Conversely, activation of the STN-SNr circuit significantly increased spike frequency (Figure 4E), spike amplitude (Figure 4F), and EEG density (Figure 4G) and shortened the latency to GSs (Figure 4I) but not FSs (Figure 4H). It also increased the number of FSs, GSs (Figures 4J,K; Supplementary Figure S3A) and accelerated the development of the seizure stages (Figure 4L). In addition, on the 7th day before and after the use of CNO/saline, tests without any drugs were conducted to further confirm the effect of chemogenetic inhibition/activation on motor seizure activities *via* self-comparison of the data before, at, and after the administration of CNO in each group. The results showed that mice in the mCherry + CNO group had similar seizure numbers and latency to FS at pre, CNO, and post time points (Supplementary Figures S2A–D). STN-SNr hM3Dq mice had more frequent seizures and shorter latency to FSs and GSs at the time of injection of CNO (Supplementary Figures S2E–H). Moreover, two mice died after CNO injection (Supplementary Table 1). HM4Di exhibited the opposite effects (Supplementary Figures S2I–L).

Second, to further verify whether photo-activation or photo-inhibition of STN-SNr projections can regulate seizure activity of motor epilepsy, we injected CamKIIα-ChR2/eNpHR/(empty)-eYFP into the STN and implanted an optic fiber into the SNr delivering intermittent blue/yellow-light stimulation to activate or inhibit the STN inputs to SNr (Figures 5A,B). Histological data confirmed the expression of eYFP in the STN and the location of the fiber in the SNr (Figure 5C). STN-SNr eYFP mice treated with blue/yellow-light or STN-SNr ChR2/eNpHR mice treated with no light served as controls. The typical EEG with power spectra found that ChR2 + blue-light stimulation (465 nm, 30 Hz, 10 ms, 10 mW, 180-s on–off cycle) deteriorated seizure activities, while eNpHR+ yellow-light stimulation (589 nm, continuous, 10 mW, 180-s on–off cycle) improved seizure activities (Figure 5D). Photo-activation of STN-SNr circuit increased spike frequency (Figure 5E), spike amplitude (Figure 5F), power spectral density (Figure 5G), and number of FSs (Figure 5H) and GSs (Figure 5I) and accelerated seizure progression (Figure 5J). Photo-inhibition exerted opposite effects, except that it did not significantly lower spike amplitude (Figures 5K–P). The aforementioned data show that STN-SNr projections modulate seizure severity in a bidirectional manner in motor epilepsy models, indicating that the anti−/pro-epileptic action was mediated by STN-SNr direct projections and not by the passing fibers.

STN-DBS alleviates seizures by inhibiting the STN-SNr circuit

According to the above-mentioned results, we found that high-frequency STN electrical stimulation can exert a similar effect on the inhibition of STN excitatory neurons or STN-SNr circuit. Therefore, we speculated that STN-DBS can improve epileptic activity in mice by inhibiting STN-SNr projections. To understand how STN-DBS alleviates seizures in motor epilepsy mice, we implanted ipsilateral electrodes into the STN and simultaneously employed chemogenetic AAV with CNO to selectively activate the STN-SNr projections (Figures 6A,B). Histological data confirmed the DBS location and the mCherry-expressing neurons in the STN and SNr (Figure 6C). The representative EEG and the corresponding power spectrum are shown in Figure 6D. The EEG analysis demonstrated that, compared to sham-DBS, STN-DBS significantly decreased the spike frequency, amplitude, and power spectral density of motor seizures. In addition, similar to STN-DBS, STN-DBS + mCherry served as a vehicle control and showed a decrease in seizure activities, while mice in the STN-DBS + hM3Dq group showed almost no rescue effects and had significantly higher spike frequency (Figure 6E), amplitude (Figure 6F), and EEG density (Figure 6G) compared to those in the STN-DBS and STN-DBS + mCherry groups. In addition, STN-DBS significantly prolonged the latency to GSs, reduced the numbers of FSs and GSs, and delayed the development of behavioral seizure stages, with STN-DBS + mCherry exhibiting similar results. Conversely, mice in the STN-DBS + hM3Dq group had distinctly short latency to FSs (Figure 6H) and GSs (Figure 6I), higher numbers of FSs (Figure 6J) and GSs (Figure 6K; Supplementary Figure S3B), and more rapid development of seizure stages (Figure 6L) compared to those in the STN-DBS and STN-DBS + mCherry groups, except that there was no significant difference in the number of FSs between the STN-DBS + hM3Dq and STN-DBS + mCherry groups. Overall, we found that activation of the STN-SNr circuit can eliminate the benefits of high-frequency STN-DBS, suggesting that STN-DBS may improve seizure activity by inhibiting the STN-SNr circuit.

Targeting SNr orexin receptors attenuates seizure activities

Since STN-DBS and optogenetic/chemogenetic inhibition of STN-SNr projections were sufficient for seizure rescue in motor epileptic mice, we examined whether a similar effect might be achieved using a molecular target. Orexin and its receptors are expressed in SNr (Korotkova et al., 2002; Li et al., 2019), and several studies found their important role in epilepsy (Zhu et al., 2015; Roundtree et al., 2016; Kordi Jaz et al., 2017). First, we reconfirmed the expression and co-localization of OX1R and OX2R in the SNr (Figure 7A). Next, to further explore the expression change of orexin and its receptors in the SNr following penicillin injection and STN-DBS, ELISA was used to detect the expression of OA and OB, considering their small molecular weight of 15kD. Western blot (WB) was used to evaluate the expressions of OX1R and OX2R. The results showed that the concentrations of OA and OB in the SNr were significantly increased after penicillin injection. STN-DBS reversed the enhancement of OA and OB in motor epilepsy mice, whereas sham-DBS had no effect (Figures 7B,C). Representative WB plot is shown in Figure 7D. Meanwhile, quantitative analysis found a similar expression change of OX1R and OX2R (Figures 7E,F). These data indicated that the expressions of orexin and its receptors are enhanced during seizures, and STN-DBS can reduce the expression of orexin and its receptors, which may cause reduced binding of orexin and its receptors. Next, we aimed to test whether the OX1R antagonist, SB-334867, and the OX2R antagonist, JNJ-10397049, could attenuate seizure activities in the motor

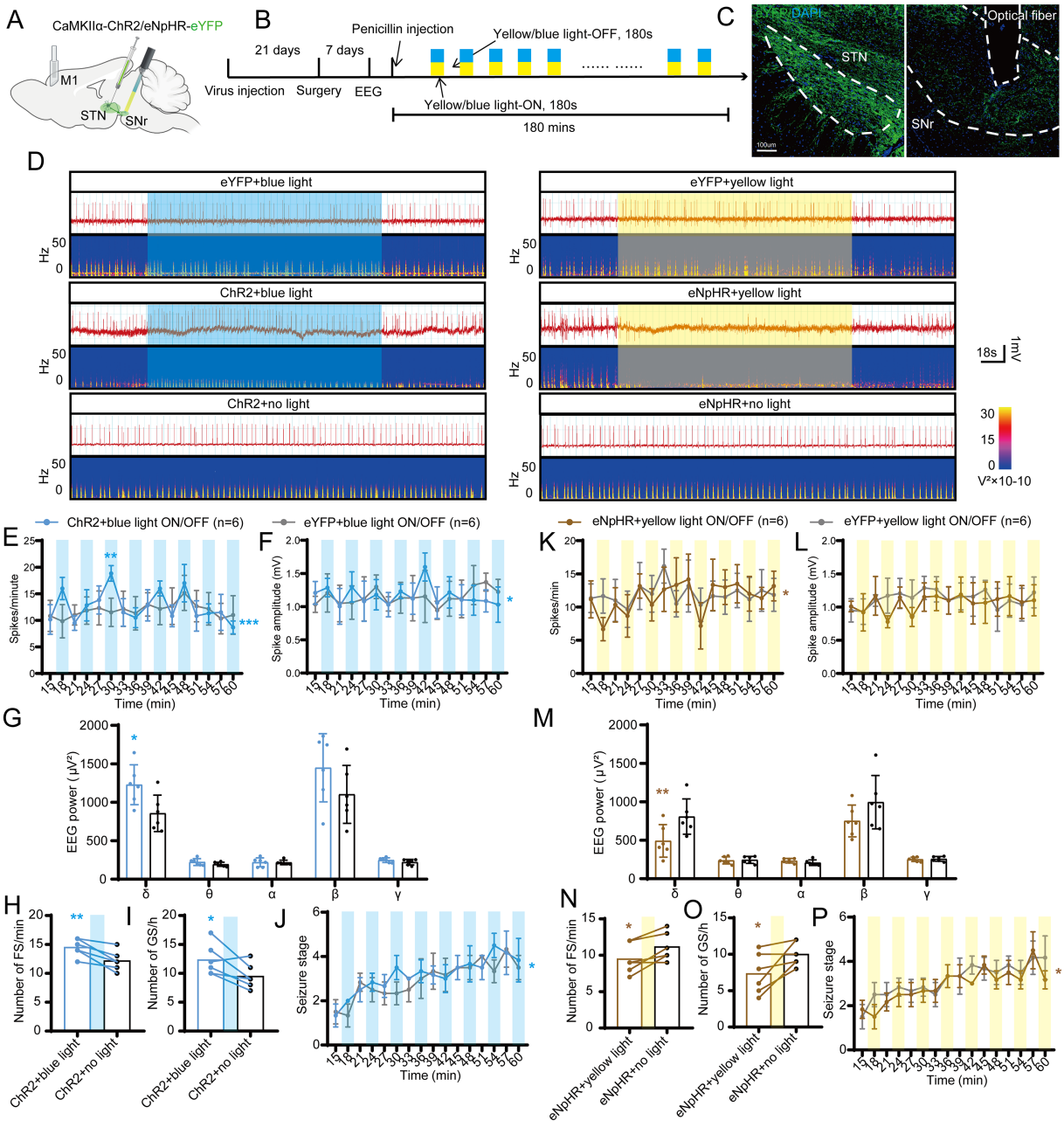

FIGURE 5
Effects of optogenetic regulation of the subthalamic nucleus-substantia nigra pars reticulata (STN-SNr) circuit on motor epilepsy. **(A,B)** Scheme and time course of experiment. **(C)** Representative images of the STN and SNr, confirming the expression of virus and location of the optic fiber. Scale bar=100μm. Left, STN; Right, SNr. **(D)** Representative EEGs and corresponding EEG spectra power for focal seizure (FS). Effects of optogenetic activation of the STN-SNr circuit on **(E)** spike frequency, **(F)** spike amplitude, **(G)** spectral power density, **(H)** number of FS, **(I)** number of generalized seizure (GS), and **(J)** development of seizure stage. Effects of optogenetic inhibition of the STN-SNr circuit on **(K)** spike frequency, **(L)** spike amplitude, **(M)** spectral power density, **(N)** number of FS, **(O)** number of generalized seizure (GS), and **(P)** development of seizure stage. *p<0.05, **p<0.01, ***p<0.001. Colored rectangles represent photostimulation. Data are presented as means ± SD. Detailed statistical methods and data are provided in Supplementary materials.

epilepsy model (Figures 7G,H). A typical EEG and the corresponding power spectrum are shown in Figure 7I. EEG analysis demonstrated that selective inhibition of OX1R and dual inhibition of orexin receptors significantly decreased the spike frequency (Figure 7J), amplitude (Figure 7K), and EEG power (Figure 7L), while inhibition of OX2R failed to reduce spike frequency but lowered the spike amplitude and EEG power. In addition, for the behaviors, only dual inhibition substantially prolonged the latency to FSs (Figure 7M) and GSs (Figure 7N), decreased the numbers of FSs (Figure 7O) and GSs (Figure 7P; Supplementary Figure S3C), and delayed the seizure progression (Figure 7Q), while there was no statistically significant difference between OX1R antagonist or OX2R antagonist and vehicle. Together, these data indicate that targeting orexin receptors in SNr circuits may offer a potential therapeutic approach to alleviate seizure activities in motor epilepsy.

10.3389/fnins.2023.1157060

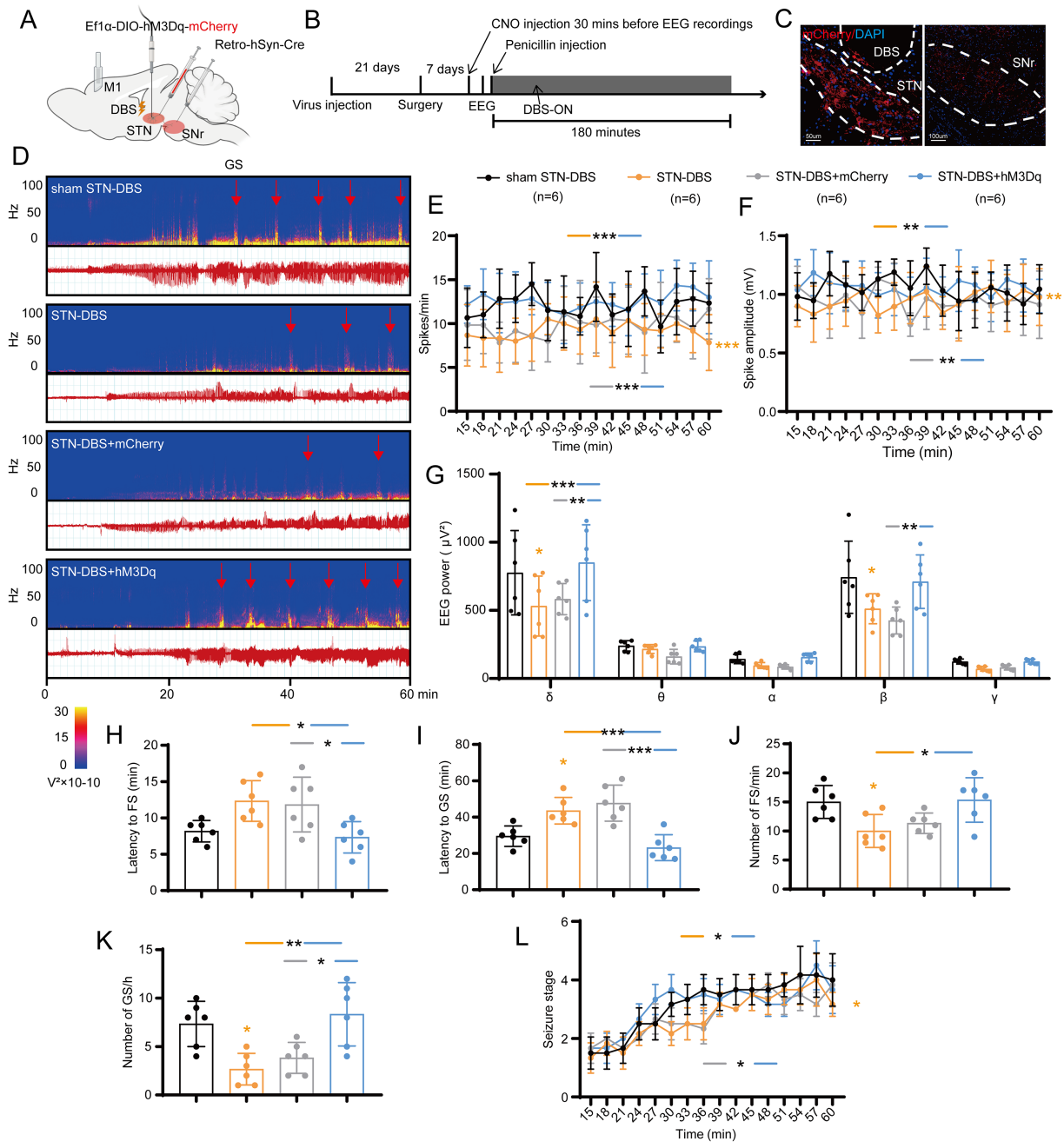

FIGURE 6
Deep brain stimulation of the subthalamic nucleus (STN-DBS) alleviates seizures by inhibiting the STN-substantia nigra pars reticulata (STN-SNr) circuit. **(A,B)** Scheme and time course of experiment. **(C)** Representative images of the STN and SNr, confirming the expression of the virus and the location of the electrode. Left, STN, Scale bar=50μm; Right, SNr, Scale bar=100μm. **(D)** Representative EEG spectra power and raw EEG; red arrowheads indicate generalized seizure (GS) onset. Effects of ipsilateral high-frequency (130Hz) STN-DBS with chemogenetic activation of the STN-SNr circuit on **(E)** spike frequency, **(F)** spike amplitude, **(G)** spectral power density, **(H)** latency to FS, **(I)** latency to GS, **(J)** number of focal seizure (FS), **(K)** number of GS, and **(L)** development of seizure stage. *p<0.05, **p<0.01, ***p<0.001. Colored asterisk indicates comparison of the corresponding group and the sham STN-DBS group; black asterisk with two different colored horizontal lines to the left and right indicates comparison of the corresponding two groups. Data are presented as means ± SD. Detailed statistical methods and data are provided in Supplementary materials.

Discussion

Seizures that emerge from the motor cortex networks are associated with considerable impairment. Regrettably, the implicated brain areas and causative processes underpinning the neural circuits have not been adequately studied. We found that STN, a specific site within the interconnected cortico-subcortical network in sensory-motor integration and motor control, is involved in the propagation network of focal motor seizures. Furthermore, high-frequency electrical stimulation of the STN can profoundly alleviate the motor cortex epileptic activity, implying that the STN may be a preferable target of DBS for motor seizures. Additionally, by utilizing

10.3389/fnins.2023.1157060

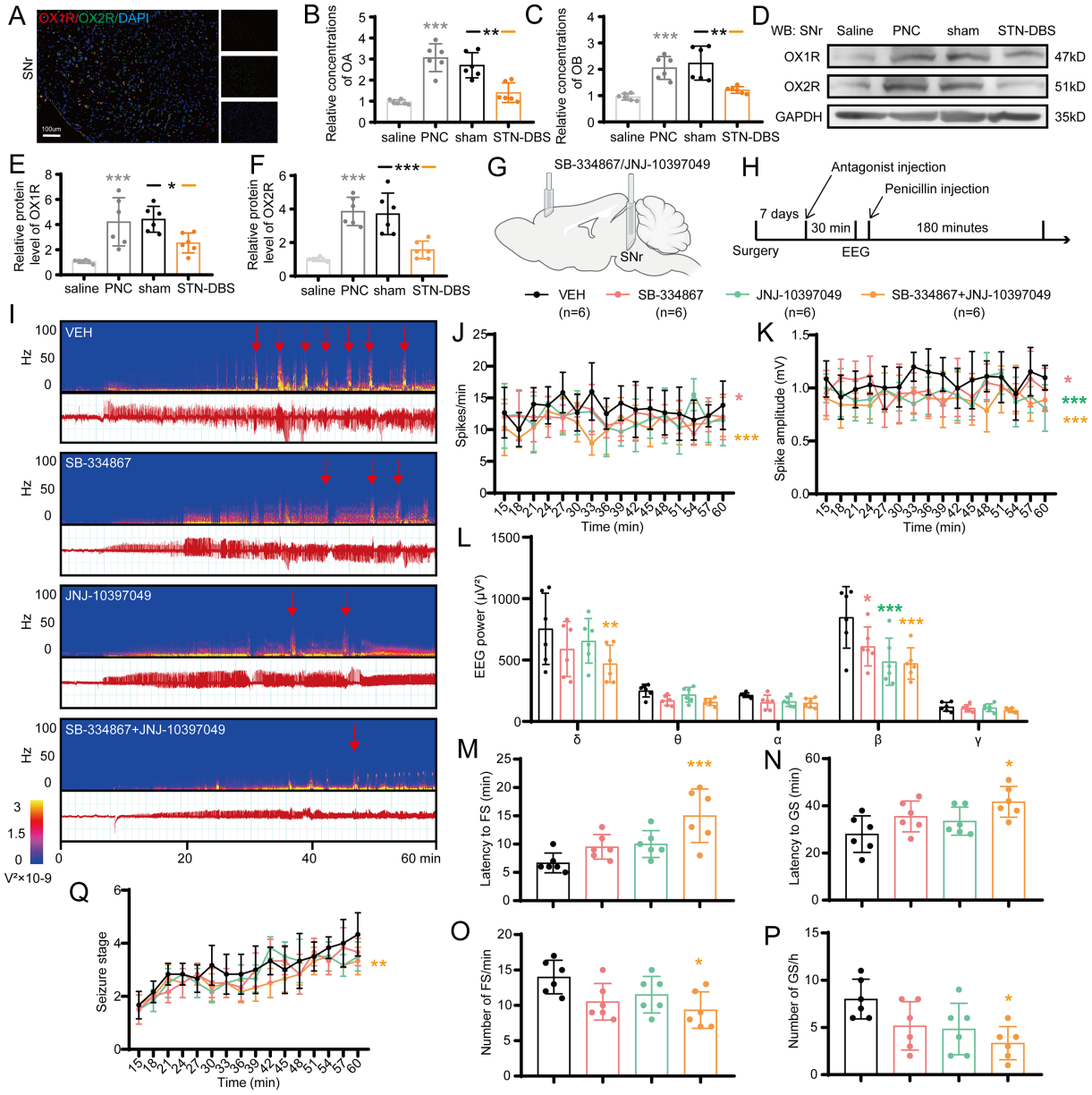

FIGURE 7
Modulating orexin receptors type 1 (OX1R) and 2 (OX2R) in substantia nigra pars reticulata (SNr) alleviates seizures. **(A)** Immunofluorescence analysis was performed using antibodies against OX1R (red) and OX2R (green) in brain sections of the SNr. Nuclei were fluorescently labeled with DAPI (blue). Representative image confirms the expression and co-localization of OX1R and OX2R in the SNr. Scale bar=100μm. Relative concentrations of **(B)** orexin A (OA) and **(C)** orexin B (OB) in the SNr, as detected by ELISA. Western blot analysis with **(D)** representative image and quantification of **(E)** OX1R and **(F)** OX2R levels in the SNr. *p<0.05, **p<0.01, ***p<0.001. Gray asterisk indicates comparison of penicillin (PNC) and saline groups; black asterisk with black and orange horizontal lines to the left and right indicates comparison of the PNC+sham STN-DBS and PNC+real STN-DBS (ipsilateral, 130Hz) groups. **(G,H)** Scheme and time course of the experiment for the efficacy of orexin receptor antagonists in motor epileptic mice. **(I)** Representative EEG spectra power and raw EEG; red arrowheads indicate generalized seizure (GS) onset. Effects of orexin receptor antagonist injection in the SNr on **(J)** spike frequency, **(K)** spike amplitude, **(L)** spectral power density, **(M)** latency to FS, **(N)** latency to GS, **(O)** number of focal seizure (FS), **(P)** number of GS, and **(Q)** development of seizure stage. *p<0.05, **p<0.01, ***p<0.001. Colored asterisk indicates comparison of the corresponding group and the vehicle group. Data are presented as means ± SD. Detailed statistical methods and data are provided in Supplementary materials.

optogenetics and chemogenetics, we showed that selectively suppressing the excitatory neurons in the STN may be advantageous for seizure management, and the STN-SNr circuit-specific mechanism contributes to the causal underpinnings of motor seizures. This suggests that STN-SNr circuits play a crucial role in reducing seizures in motor epilepsy and that STN-DBS may lower motor seizure activity by inhibition of the STN-SNr projections (Figure 8). Finally, we discovered molecular targets capable of influencing the STN-SNr circuits and showed that orexin receptor antagonists that target SNr neurons rescue seizure activity (Figure 8). Taken together, we not only

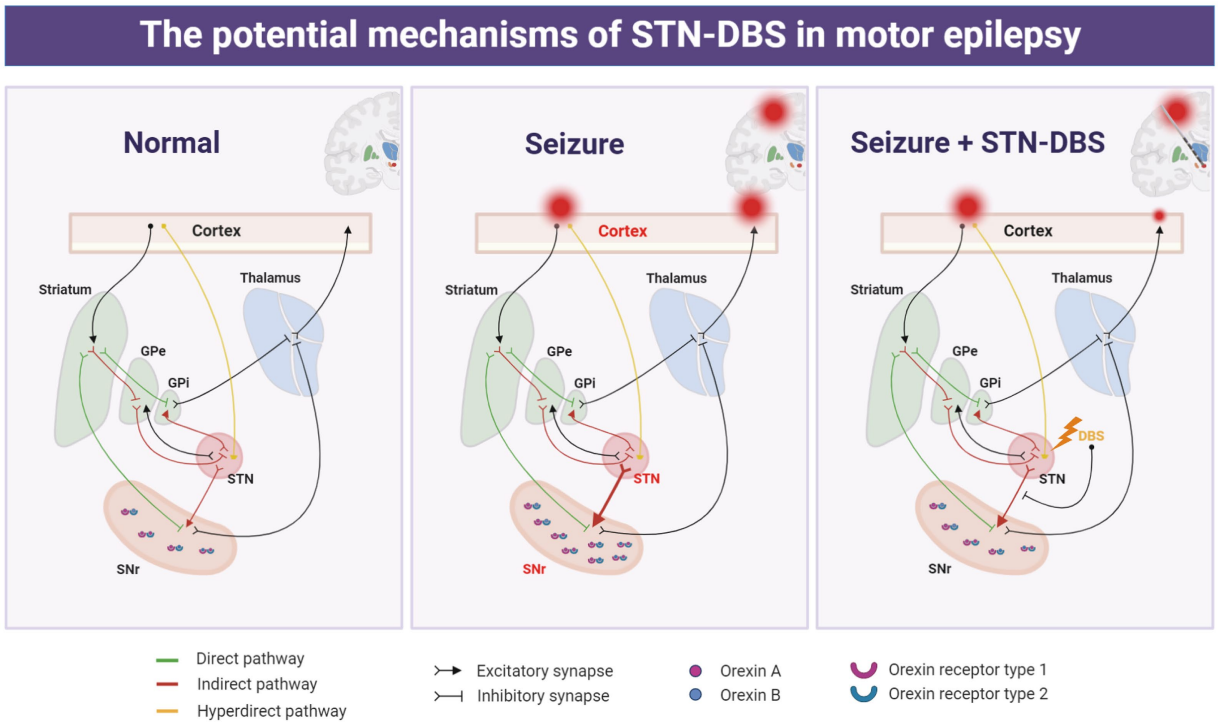

FIGURE 8
Schematic representation of the potential mechanism of action of deep brain stimulation of the subthalamic nucleus (STN-DBS) in motor epilepsy.

discovered the circuit pathways responsible for seizure activity in motor epileptic mice but also proposed that employing STN-DBS or orexin receptor antagonists capable of modulating STN-SNr circuits offers an attractive treatment for epilepsy originating from the motor cortex.

STN is a well-known clinical target for therapeutic neurostimulation in movement disorders, including Parkinson's disease and dystonia (Benabid et al., 2001; Weaver et al., 2009; Ryvlin and Jehi, 2022; Xue et al., 2022). Because of its surgical accessibility, this structure might be a viable option for targeted epilepsy treatment. Although the significance of the STN in epilepsy has received less attention, there is still evidence for it. On the one hand, some small-scale pilot clinical investigations have found it to be effective in the treatment of seizures, particularly focal motor seizures. Benabid et al. initially reported a case of a 5-year-old girl with drug-resistant epilepsy who underwent unilateral high-frequency STN-DBS, which was associated with an 80% reduction in seizure frequency as well as improvement in motor and cognitive function over a 2.5-year follow-up (Benabid et al., 2002). Other minor, uncontrolled investigations have also revealed a > 50% decrease of seizures (Chabardes et al., 2002; Handforth et al., 2006; Lee et al., 2006). Ren et al. investigated the modulatory effects of STN-DBS at various stimulation frequencies in seven patients with refractory focal motor seizures. In particular, low-frequency (20 Hz) or high-frequency (100/130 Hz) stimulation increased or decreased epileptic activity produced from motor regions (Ren et al., 2020). On the other hand, some experimental studies based on rodent epileptic models also found that STN is a promising therapeutic target of electrical stimulation for suppressing seizures. Vercueil et al. observed that 130-Hz, 60-μs STN-DBS suppressed seizures in a rat model of genetic absence epilepsy but only with bilateral stimulation (Vercueil et al., 1998). In addition, Lado et al. demonstrated that 130-Hz stimulation of the STN increased seizure threshold in a flurothyl-induced epileptic model, while a higher frequency of 260 or 800 Hz had no effect or even lowered the threshold (Lado et al., 2003). Additionally, STN-DBS was found to be effective in blocking seizures in some other models, such as those developed using kainic acid injection (Usui et al., 2005) or amygdaloid kindling (Shi et al., 2006). In summary, consistent with previous studies, our study also found that high-frequency stimulation was effective for motor epilepsy, while low-and medium-frequency stimulation did not improve or alleviate seizure control. High-frequency stimulation parameters were not studied because most studies also focused on high-frequency stimulation at around 130 Hz. There is also some controversy regarding the effects of unilateral and bilateral stimulation. There were many inconsistencies in previous studies, with some reporting that both unilateral and bilateral stimulation are effective and others suggesting that only bilateral stimulation is effective. Our study found that unilateral (ipsilateral) STN-DBS could effectively reduce epileptic activity, and bilateral stimulation showed similar or even better efficacy, but there was no statistically significant advantage compared to unilateral STN-DBS. Accordingly, the current and previous studies have consistently proven the effectiveness of STN-DBS for the treatment of motor epilepsy. Although previous studies have only identified this phenomenon, the underlying mechanism of the

effects of STN-DBS on epilepsy remains unclear. This was the focus of our study. This study is the first to illustrate the circuit and molecular mechanism of STN-DBS for the treatment of motor epilepsy.

With regard to the circuit, STN-SNr projections are part of the classical basal ganglia pathways. SNr is composed of approximately 90% GABAergic neurons and receives a monosynaptic glutamatergic input from the STN (Shen and Johnson, 2006; Deniau et al., 2007). SNr is a well-established nigral inhibitory system, and it has been identified to have a seizure gating function (Gale, 1988). There is adequate evidence that direct inhibition of the SNr, *via* GABAergic drugs, GABAergic cell transplant, electrical stimulation, or optogenetic silencing or lesioning, can suppress various seizure types in animals (Garant and Gale, 1983; Thompson and Suchomelova, 2004; Shi et al., 2006; Castillo et al., 2008; Tollner et al., 2011; Gey et al., 2016; Wicker et al., 2019). Meanwhile, some previous studies have found that inhibition of the STN and its monosynaptic glutamatergic input to SNr can attenuate seizure susceptibility (Dybdal and Gale, 2000; Usui et al., 2005; Backofen-Wehrhahn et al., 2018). In line with previous research, our study demonstrated that photo-inhibition of STN or photo−/chemo-inhibition of the STN-SNr circuit can satisfactorily attenuate motor FSs and secondary GSs in models with epilepsy arising from M1. Moreover, we found that when high-frequency STN-DBS plus chemogenetic activation of the STN-SNr pathway was used, the original improvement of electrical stimulation was canceled out, suggesting that STN-DBS may ameliorate seizures by regulating the excitability of the STN-SNr loop. This study revealed the partly circuit-related mechanism of improvement by STN-DBS in motor epilepsy. However, considering that this study only focused on STN-SNr projections, it is not known whether other projections of the STN are also involved in the improvement of epileptic activity by STN-DBS. In addition, it is necessary to further explore the downstream nucleus that is regulated by SNr and how it ultimately affects epilepsy.

In addition, orexin, another focus of this study, is secreted by a group of neurons in the hypothalamus that are located closest to the STN and project to the STN and SNr (Peyron et al., 1998). Several studies have found that the orexin pathway plays a vital role in various seizures (Samzadeh et al., 2020; Celli and Luijtelaar, 2022; Konduru et al., 2022). Previous studies have observed the expression and co-localization of OX1R and OX2R in the STN and SNr (Korotkova et al., 2002; Li et al., 2019). Therefore, we were naturally aware of whether the decrease of seizure activity by STN-DBS in motor epilepsy is related to the regulation of the orexin pathway. Our results show that STN-DBS can restore (downregulate) the elevated levels of OA, OB, OX1R, and OX2R associated with seizures in the SNr. Furthermore, antagonizing both OX1R and OX2R simultaneously can play a similar role as high-frequency STN-DBS and attenuate motor epilepsy. We identified the molecular targets that modulate the seizure activity in the STN-SNr circuit, which has the potential to be a drug target for the treatment of motor epilepsy.

Overall, our results demonstrate that high-frequency STN-DBS attenuates motor seizures *via* inhibition of the STN-SNr circuits. The orexin system plays a vital role during electrical stimulation, and orexin receptor antagonists have a therapeutic potential in suppressing motor seizure activities. This study contributes to a better understanding of the current network theory of epilepsy and the mechanism of STN-DBS.

Data availability statement

The original contributions presented in the study are included in the article/Supplementary material, further inquiries can be directed to the corresponding authors.

Ethics statement

The animal study was reviewed and approved by the Animal Advisory Committee of the Beijing Tiantan Hospital.

Author contributions

TX: conceptualization, investigation, methodology, and wrote the original draft. SW: investigation, methodology, and wrote the revised draft. SC: data curation and investigation. HW: formal analysis and software. CL: investigation and validation. LS: visualization. YB: data curation. CZ: methodology and data curation. CH: conceptualization, funding acquisition, wrote the original draft, and supervision. JZ: conceptualization, funding acquisition, project administration, and supervision. All authors contributed to the article and approved the submitted version.

Funding

This work was supported by the National Natural Science Foundation of China [grant numbers 82171442 and 81901314].

Conflict of interest

The authors declare that the research was conducted in the absence of any commercial or financial relationships that could be construed as a potential conflict of interest.

Publisher's note

All claims expressed in this article are solely those of the authors and do not necessarily represent those of their affiliated organizations, or those of the publisher, the editors and the reviewers. Any product that may be evaluated in this article, or claim that may be made by its manufacturer, is not guaranteed or endorsed by the publisher.

Supplementary material

The Supplementary material for this article can be found online at: https://www.frontiersin.org/articles/10.3389/fnins.2023.1157060/full#supplementary-material

References

Backofen-Wehrhahn, B., Gey, L., Broer, S., Petersen, B., Schiff, M., Handreck, A., et al. (2018). Anticonvulsant effects after grafting of rat, porcine, and human mesencephalic neural progenitor cells into the rat subthalamic nucleus. *Exp. Neurol.* 310, 70–83. doi: 10.1016/j.expneurol.2018.09.004

Benabid, A. L., Koudsie, A., Benazzouz, A., Vercueil, L., Fraix, V., Chabardes, S., et al. (2001). Deep brain stimulation of the corpus luysi (subthalamic nucleus) and other targets in Parkinson's disease. Extension to new indications such as dystonia and epilepsy. *J. Neurol.* 248:37. doi: 10.1007/pl00007825

Benabid, A. L., Minotti, L., Koudsie, A., de Saint, M. A., and Hirsch, E. (2002). Antiepileptic effect of high-frequency stimulation of the subthalamic nucleus (corpus luysi) in a case of medically intractable epilepsy caused by focal dysplasia: a 30-month follow-up: technical case report. *Neurosurgery* 50, 1385–1391. doi: 10.1097/00006123-200206000-00037

Brodovskaya, A., Shiono, S., and Kapur, J. (2021). Activation of the basal ganglia and indirect pathway neurons during frontal lobe seizures. *Brain* 144, 2074–2091. doi: 10.1093/brain/awab119

Castillo, C. G., Mendoza-Trejo, S., Aguilar, M. B., Freed, W. J., and Giordano, M. (2008). Intranigral transplants of a GABAergic cell line produce long-term alleviation of established motor seizures. *Behav. Brain Res.* 193, 17–27. doi: 10.1016/j.bbr.2008.04.023

Celli, R., and Luijtelaar, G. V. (2022). The orexin system: a potential player in the pathophysiology of absence epilepsy. *Curr. Neuropharmacol.* 20, 1254–1260. doi: 10.2174/1570159X19666211215122833

Chabardes, S., Kahane, P., Minotti, L., Koudsie, A., Hirsch, E., and Benabid, A. L. (2002). Deep brain stimulation in epilepsy with particular reference to the subthalamic nucleus. *Epileptic Disord.* 4, S83–S93.

Deniau, J. M., Mailly, P., Maurice, N., and Charpier, S. (2007). The pars reticulata of the substantia nigra: a window to basal ganglia output. *Prog. Brain Res.* 160, 151–172. doi: 10.1016/S0079-6123(06)60009-5

Devinsky, O., Vezzani, A., O'Brien, T. J., Jette, N., Scheffer, I. E., de Curtis, M., et al. (2018). Epilepsy. *Nat. Rev. Dis. Primers.* 4:18024. doi: 10.1038/nrdp.2018.24

Dong, X., Ye, W., Tang, Y., Wang, J., Zhong, L., Xiong, J., et al. (2021). Wakefulness-promoting effects of lateral hypothalamic area-deep brain stimulation in traumatic brain injury-induced comatose rats: upregulation of alpha1-adrenoceptor subtypes and downregulation of gamma-aminobutyric acid beta receptor expression via the orexins pathway. *World Neurosurg.* 152, e321–e331. doi: 10.1016/j.wneu.2021.05.089

Dybdal, D., and Gale, K. (2000). Postural and anticonvulsant effects of inhibition of the rat subthalamic nucleus. *J. Neurosci.* 20, 6728–6733. doi: 10.1523/JNEUROSCI.20-17-06728.2000

Fasano, A., Eliashiv, D., Herman, S. T., Lundstrom, B. N., Polnerow, D., Henderson, J. M., et al. (2021). Experience and consensus on stimulation of the anterior nucleus of thalamus for epilepsy. *Epilepsia* 62, 2883–2898. doi: 10.1111/epi.17094

Fisher, R., Salanova, V., Witt, T., Worth, R., Henry, T., Gross, R., et al. (2010). Electrical stimulation of the anterior nucleus of thalamus for treatment of refractory epilepsy. *Epilepsia* 51, 899–908. doi: 10.1111/j.1528-1167.2010.02536.x

Gale, K. (1988). Progression and generalization of seizure discharge: anatomical and neurochemical substrates. *Epilepsia* 29, S15–S34. doi: 10.1111/j.1528-1157.1988.tb05795.x

Gale, K. (1992). Subcortical structures and pathways involved in convulsive seizure generation. *J. Clin. Neurophysiol.* 9, 264–277. doi: 10.1097/00004691-199204010-00007

Garant, D. S., and Gale, K. (1983). Lesions of substantia nigra protect against experimentally induced seizures. *Brain Res.* 273, 156–161. doi: 10.1016/0006-8993(83)91105-8

Gey, L., Gernert, M., and Loscher, W. (2016). Continuous bilateral infusion of vigabatrin into the subthalamic nucleus: effects on seizure threshold and GABA metabolism in two rat models. *Neurobiol. Dis.* 91, 194–208. doi: 10.1016/j.nbd.2016.03.012

Gomez-Alonso, J., and Bellas-Lamas, P. (2015). Surgical treatment for drug-resistant epilepsy. *JAMA* 313:1572. doi: 10.1001/jama.2015.2883

Handforth, A., DeSalles, A. A., and Krahl, S. E. (2006). Deep brain stimulation of the subthalamic nucleus as adjunct treatment for refractory epilepsy. *Epilepsia* 47, 1239–1241. doi: 10.1111/j.1528-1167.2006.00563.x

Jobst, B. C., and Cascino, G. D. (2015). Resective epilepsy surgery for drug-resistant focal epilepsy: a review. *JAMA* 313, 285–293. doi: 10.1001/jama.2014.17426

Konduru, S. R., Isaacson, J. R., Lasky, D. J., Zhou, Z., Rao, R. K., Vattem, S. S., et al. (2022). Dual orexin antagonist normalized sleep homeostatic drive, enhanced GABAergic inhibition, and suppressed seizures after traumatic brain injury. *Sleep* 45:zsac238. doi: 10.1093/sleep/zsac238

Kordi Jaz, E., Moghimi, A., Fereidoni, M., Asadi, S., Shamsizadeh, A., and Roohbakhsh, A. (2017). SB-334867, an orexin receptor 1 antagonist, decreased seizure and anxiety in pentylenetetrazol-kindled rats. *Fundam. Clin. Pharmacol.* 31, 201–207. doi: 10.1111/fcp.12249

Korotkova, T. M., Eriksson, K. S., Haas, H. L., and Brown, R. E. (2002). Selective excitation of GABAergic neurons in the substantia nigra of the rat by orexin/hypocretin in vitro. *Regul. Pept.* 104, 83–89. doi: 10.1016/s0167-0115(01)00323-8

Kortunay, S., Erken, H. A., Erken, G., Genç, O., Şahiner, M., Turgut, S., et al. (2012). Orexins increase penicillin-induced epileptic activity. *Peptides* 34, 419–422. doi: 10.1016/j.peptides.2012.02.013

Lado, F. A., Velisek, L., and Moshe, S. L. (2003). The effect of electrical stimulation of the subthalamic nucleus on seizures is frequency dependent. *Epilepsia* 44, 157–164. doi: 10.1046/j.1528-1157.2003.33802.x

Lee, K. J., Jang, K. S., and Shon, Y. M. (2006). Chronic deep brain stimulation of subthalamic and anterior thalamic nuclei for controlling refractory partial epilepsy. *Acta Neurochir. Suppl.* 99, 87–91. doi: 10.1007/978-3-211-35205-2_17

Li, G. Y., Zhuang, Q. X., Zhang, X. Y., Wang, J. J., and Zhu, J. N. (2019). Ionic mechanisms underlying the excitatory effect of orexin on rat subthalamic nucleus neurons. *Front. Cell. Neurosci.* 13:153. doi: 10.3389/fncel.2019.00153

Paxinos, G, and Franklin, KBJ. *The mouse brain in stereotaxic coordinates. Compact 2nd ed.* Boston, MA Elsevier Academic Press (2004)

Paz, J. T., and Huguenard, J. R. (2015). Microcircuits and their interactions in epilepsy: is the focus out of focus? *Nat. Neurosci.* 18, 351–359. doi: 10.1038/nn.3950

Peyron, C., Tighe, D. K., van den Pol, A. N., de Lecea, L., Heller, H. C., Sutcliffe, J. G., et al. (1998). Neurons containing hypocretin (orexin) project to multiple neuronal systems. *J. Neurosci.* 18, 9996–10015. doi: 10.1523/JNEUROSCI.18-23-09996.1998

Racine, R. J. (1972). Modification of seizure activity by electrical stimulation. II. Motor seizure. *Electroencephalogr. Clin. Neurophysiol.* 32, 281–294. doi: 10.1016/0013-4694(72)90177-0

Ren, L., Yu, T., Wang, D., Wang, X., Ni, D., Zhang, G., et al. (2020). Subthalamic nucleus stimulation modulates motor epileptic activity in humans. *Ann. Neurol.* 88, 283–296. doi: 10.1002/ana.25776

Rosenow, F., and Luders, H. (2001). Presurgical evaluation of epilepsy. *Brain* 124, 1683–1700. doi: 10.1093/brain/124.9.1683

Roundtree, H. M., Simeone, T. A., Johnson, C., Matthews, S. A., Samson, K. K., and Simeone, K. A. (2016). Orexin receptor antagonism improves sleep and reduces seizures in Kcna 1-null mice. *Sleep* 39, 357–368. doi: 10.5665/sleep.5444

Ryvlin, P., and Jehi, L. E. (2022). Neuromodulation for refractory epilepsy. *Epilepsy Curr.* 22, 11–17. doi: 10.1177/15357597211065587

Salanova, V. (2018). Deep brain stimulation for epilepsy. *Epilepsy Behav.* 88, 21–24. doi: 10.1016/j.yebeh.2018.06.041

Salanova, V., Witt, T., Worth, R., Henry, T. R., Gross, R. E., Nazzaro, J. M., et al. (2015). Long-term efficacy and safety of thalamic stimulation for drug-resistant partial epilepsy. *Neurology* 84, 1017–1025. doi: 10.1212/WNL.0000000000001334

Samzadeh, M., Papuc, E., Furtak-Niczyporuk, M., and Rejdak, K. (2020). Decreased cerebrospinal fluid orexin-a (Hypocretin-1) concentrations in patients after generalized convulsive status epilepticus. *J. Clin. Med.* 9:3354. doi: 10.3390/jcm9103354

Shen, K. Z., and Johnson, S. W. (2006). Subthalamic stimulation evokes complex EPSCs in the rat substantia nigra pars reticulata in vitro. *J. Physiol.* 573, 697–709. doi: 10.1113/jphysiol.2006.110031

Sheng, Q., Xue, Y., Wang, Y., Chen, A. Q., Liu, C., Liu, Y. H., et al. (2018). The subthalamic neurons are activated by both orexin-a and orexin-B. *Neuroscience* 369, 97–108. doi: 10.1016/j.neuroscience.2017.11.008

Shi, L. H., Luo, F., Woodward, D. J., and Chang, J. Y. (2006). Basal ganglia neural responses during behaviorally effective deep brain stimulation of the subthalamic nucleus in rats performing a treadmill locomotion test. *Synapse* 59, 445–457. doi: 10.1002/syn.20261

Shi, L. H., Luo, F., Woodward, D., and Chang, J. Y. (2006). Deep brain stimulation of the substantia nigra pars reticulata exerts long lasting suppression of amygdala-kindled seizures. *Brain Res.* 1090, 202–207. doi: 10.1016/j.brainres.2006.03.050

Thompson, K. W., and Suchomelova, L. M. (2004). Transplants of cells engineered to produce GABA suppress spontaneous seizures. *Epilepsia* 45, 4–12. doi: 10.1111/j.0013-9580.2004.29503.x

Tollner, K., Wolf, S., Loscher, W., and Gernert, M. (2011). The anticonvulsant response to valproate in kindled rats is correlated with its effect on neuronal firing in the substantia nigra pars reticulata: a new mechanism of pharmacoresistance. *J. Neurosci.* 31, 16423–16434. doi: 10.1523/JNEUROSCI.2506-11.2011

Urban, D. J., and Roth, B. L. (2015). DREADDs (designer receptors exclusively activated by designer drugs): chemogenetic tools with therapeutic utility. *Annu. Rev. Pharmacol. Toxicol.* 55, 399–417. doi: 10.1146/annurev-pharmtox-010814-124803

Usui, N., Maesawa, S., Kajita, Y., Endo, O., Takebayashi, S., and Yoshida, J. (2005). Suppression of secondary generalization of limbic seizures by stimulation of subthalamic nucleus in rats. *J. Neurosurg.* 102, 1122–1129. doi: 10.3171/jns.2005.102.6.1122

Vakharia, V. N., Duncan, J. S., Witt, J. A., Elger, C. E., Staba, R., and Engel, J. Jr. (2018). Getting the best outcomes from epilepsy surgery. *Ann. Neurol.* 83, 676–690. doi: 10.1002/ana.25205

Vercueil, L., Benazzouz, A., Deransart, C., Bressand, K., Marescaux, C., Depaulis, A., et al. (1998). High-frequency stimulation of the subthalamic nucleus suppresses absence seizures in the rat: comparison with neurotoxic lesions. *Epilepsy Res.* 31, 39–46. doi: 10.1016/s0920-1211(98)00011-4

Weaver, F. M., Follett, K., Stern, M., Hur, K., Harris, C., Marks, W. J. J., et al. (2009). Bilateral deep brain stimulation vs best medical therapy for patients with advanced Parkinson disease: a randomized controlled trial. *JAMA* 301, 63–73. doi: 10.1001/jama.2008.929

Wicker, E., Beck, V. C., Kulick-Soper, C., Kulick-Soper, C. V., Hyder, S. K., Campos-Rodriguez, C., et al. (2019). Descending projections from the substantia nigra pars reticulata differentially control seizures. *Proc. Natl. Acad. Sci.* 116, 27084–27094. doi: 10.1073/pnas.1908176117

Xue, T., Chen, S., Bai, Y., Han, C., Yang, A., and Zhang, J. (2022). Neuromodulation in drug-resistant epilepsy: a review of current knowledge. *Acta Neurol. Scand.* 146, 786–797. doi: 10.1111/ane.13696

Yildirim, M., Ayyildiz, M., and Agar, E. (2010). Endothelial nitric oxide synthase activity involves in the protective effect of ascorbic acid against penicillin-induced epileptiform activity. *Seizure* 19, 102–108. doi: 10.1016/j.seizure.2009.12.005

Zhu, F., Wang, X. Q., Chen, Y. N., Yang, N., Lang, S. Y., Zuo, P. P., et al. (2015). Changes and overlapping distribution in the expression of CB1/OX1-GPCRs in rat hippocampus by kainic acid-induced status epilepticus. *Brain Res.* 1597, 14–27. doi: 10.1016/j.brainres.2014.11.002

frontiers | Frontiers in Neurology

TYPE Review
PUBLISHED 07 July 2023
DOI 10.3389/fneur.2023.1201104

OPEN ACCESS

EDITED BY
Evgenia Sitnikova,
Institute of Higher Nervous Activity and Neurophysiology (RAS), Russia

REVIEWED BY
Ramachandran Prakasam,
Washington University in St. Louis, United States
Igor Meglinski,
Aston University, United Kingdom

*CORRESPONDENCE
Vassiliy Tsytsarev
✉ tsytsarev@umaryland.edu

RECEIVED 06 April 2023
ACCEPTED 02 June 2023
PUBLISHED 07 July 2023

CITATION
Sibarov DA, Tsytsarev V, Volnova A, Vaganova AN, Alves J, Rojas L, Sanabria P, Ignashchenkova A, Savage ED and Inyushin M (2023) Arc protein, a remnant of ancient retrovirus, forms virus-like particles, which are abundantly generated by neurons during epileptic seizures, and affects epileptic susceptibility in rodent models.
Front. Neurol. 14:1201104.
doi: 10.3389/fneur.2023.1201104

Arc protein, a remnant of ancient retrovirus, forms virus-like particles, which are abundantly generated by neurons during epileptic seizures, and affects epileptic susceptibility in rodent models

Dmitry A. Sibarov[1], Vassiliy Tsytsarev[2]*, Anna Volnova[3], Anastasia N. Vaganova[3], Janaina Alves[4], Legier Rojas[4], Priscila Sanabria[4], Alla Ignashchenkova[5], Elton D. Savage[6] and Mikhail Inyushin[4]

[1]Sechenov Institute of Evolutionary Physiology and Biochemistry of the Russian Academy of Sciences, Saint Petersburg, Russia, [2]Department of Anatomy and Neurobiology, University of Maryland School of Medicine, Baltimore, MD, United States, [3]Institute of Translational Biomedicine, Saint Petersburg State University, Saint Petersburg, Russia, [4]School of Medicine, Universidad Central del Caribe, Bayamón, PR, United States, [5]Nevsky Center of Scientific Collaboration, Saint Petersburg, Russia, [6]Böblingen Dental, Böblingen, Germany

A product of the immediate early gene Arc (Activity-regulated cytoskeleton-associated protein or Arc protein) of retroviral ancestry resides in the genome of all tetrapods for millions of years and is expressed endogenously in neurons. It is a well-known protein, very important for synaptic plasticity and memory consolidation. Activity-dependent Arc expression concentrated in glutamatergic synapses affects the long-time synaptic strength of those excitatory synapses. Because it modulates excitatory-inhibitory balance in a neuronal network, the Arc gene itself was found to be related to the pathogenesis of epilepsy. General Arc knockout rodent models develop a susceptibility to epileptic seizures. Because of activity dependence, synaptic Arc protein synthesis also is affected by seizures. Interestingly, it was found that Arc protein in synapses of active neurons self-assemble in capsids of retrovirus-like particles, which can transfer genetic information between neurons, at least across neuronal synaptic boutons. Released Arc particles can be accumulated in astrocytes after seizures. It is still not known how capsid assembling and transmission timescale is affected by seizures. This scientific field is relatively novel and is experiencing swift transformation as it grapples with difficult concepts in light of evolving experimental findings. We summarize the emergent literature on the subject and also discuss the specific rodent models for studying Arc effects in epilepsy. We summarized both to clarify the possible role of Arc-related pseudo-viral particles in epileptic disorders, which may be helpful to researchers interested in this growing area of investigation.

KEYWORDS

Arc/Arg3.1, epilepsy, learning, memory, retrovirus, seizures, capsid

1. Introduction

It is known that a significant part (about 8%) of the cell genome in mammals is represented by endogenous retroviruses (ERVs), thus inheriting the ancient germ-line cell infections by retroviruses and the transmission of their genome to the descendants (1–3). While most ERVs are not replication-competent due to broken or tightly controlled viral genes, weakened control can activate ancient retroviral genes and their coded proteins in cancers and senescent cells (4, 5). Besides that, some also retain activity and are important biochemical players in everyday life. For example, ancient viral envelope proteins in the outer cellular layer of the placenta help fusion of the trophoblast cells and became a crucial element in allowing normal pregnancy (6, 7) others determine the fusion of muscle cells and muscle sexual dimorphism (8, 9). Unfortunately, many ERV-related proteins are also implicated in different neurological diseases (10, 11). However, there is not much information regarding their possible role in the pathogenesis of epilepsy.

Actively regulated cytoskeletal-associated (ARC) protein, a protein encoded by the ARC- gene, was characterized in the end of the last century (12, 13). ARC–protein is localized at the synaptic contacts of neurons, and its synthesis depends on the NMDA receptor. This protein plays a critical role in the molecular processes associated with learning and memory and may also serve as a marker of plastic changes in the brain (14, 15).

It is known that the epileptic activity of neurons depends on excitatory-inhibitory synaptic balance (16, 17). Some proteins are well-known regulators of excitatory gain: Pyk2 and Src kinase proteins are the part of NMDA receptor complex (18). PYk2/Src are direct effectors, triggered in active neurons, directly modulating hippocampal excitatory synapses (19). On the other hand, it was determined also that synaptic modulation depends on Arc protein (Activity-regulated cytoskeleton-associated protein, product of endogenous retroviral Arc gene) with recognized activity-dependent expression in neuronal synapses and its expression level is regulated by N-methyl-D-aspartate (NMDA) receptor activation (12). Recently, it was found that Arc protein forms full retrovirus-like capsid in synapses, and may transfer short RNAs from one cell to a post synaptic cell in this way later affecting synaptic morphology (20–22). Interestingly, Arc protein expression changes drastically during epileptic seizures (21, 23).

The study of Arc protein and its synaptic effects is a novel rapidly changing field, but this knowledge is of utmost importance to the understanding of epilepsy because it determines the balance of excitatory and inhibitory synaptic inputs to seizure-prone neurons and the stability of a neuronal network at whole. Here we summarize the emergent literature on this last subject, representing in bullet points Arc's known effects and properties, and then briefly reviewing Arc involvement in epilepsy and relevant experiments in rodent models.

1.1. Arc known properties

Mammalian Activity-Regulated Cytoskeleton-Associated protein (Arc, and its variants, products of immediate early Arc gene) is known for its exquisite importance for synapse maturation, synaptic plasticity, learning, and memory, while the dysregulation of Arc expression can have vast consequences for normal brain function, triggering aberrant wiring of neuronal circuits (24, 25). Arc/Arg3.1 mediates activity-dependent elimination of redundant climbing fiber to Purkinje cell synapses in the developing cerebellum (26). In glutamate neurons, following activation of the NMDA receptor, Arc mRNA became significantly upregulated in the nucleus before being transported to the dendrites for translation (12, 27). At postsynaptic sites Arc mRNA localizes in the PSD-95-NMDAR complexes and binds to inactive CaMKIIβ (not bound to calmodulin) (28, 29). Activation of calcium entry via ionotropic glutamate receptors, especially the NMDA subtype, during normal synaptic transmission and in seizures results in calmodulin-dependent dissociation of Arc mRNA from CaMKIIβ and PKA-dependent induction of Arc protein expression (29, 30). Later it happens that spines on dendrites, where Arc was produced, change their morphology increasing the spine density and proportion of thin spines, together with the endocytosis of AMPA receptors leading to decreased synaptic efficacy (21). Arc hyperexpression facilitates not only AMPA endocytosis but also downregulates transcription of the GluA1 subunit of the AMPA receptor which favors synaptic downscaling (31, 32). In this way, Arc participates in synaptic long-term potentiation and the consolidation of long-term memory (33). Interestingly, Arc transcription exhibited distinct temporal kinetics depending on the activation of excitatory inputs that convey functionally distinct information (34).

1.2. The mechanism of Arc protein function

Upon hyperexpression, in local dendritic compartments, Arc protein assembles into retrovirus-like capsids packing predominantly Arc mRNA. These capsids leave neurons wrapped in extracellular vesicles and can transmit mRNA to nearby cells (20, 22). Curiously, activation of metabotropic glutamate receptors (mGluR) facilitates Arc mRNA translation in capsid "infected" neurons (20, 22). Arc capsid-mediated transfection was not yet observed in the mammalian brain, but in mice, Arc expression in DRG neurons results in capsid formation modulating skin vasodilation (35). Arc mRNA transfer between cells can probably explain why after hyperactivity Arc accumulates not only in neurons but also in astrocytes, while it is originated from nearby neurons (27, 36, 37). Mammalian Arc protein lacks zinc fingers but has positively charged motifs binding polyanionic mRNA (38–40). This probably allows nonspecific packing of neuronal host mRNAs other than Arc mRNAs, because half of the RNAs encapsidated by retroviruses are host-derived RNAs (41). Extracellular vesicles are supposed to participate in the spread of different neurodegenerative pathologies over time in an activity-dependent manner via synaptic connections (42, 43). Generally, it looks probable that Arc capsids may mediate activity-dependent intercellular paracrine transfer of genetic information, which may alter neighboring cell response to network activity.

1.3. Arc protein forms virus-like particles and their history

Recently it became clear that Arc protein is not only some important regulatory synaptic protein but turns out to be repurposed retrotransposon protein that mediates intercellular mRNA transfer (22, 44, 45). This mechanism involves formation (mainly by glutamatergic neurons) and expression in their synapses of pseudo-viral, retrovirus-like particles (of about 60 nm diameter) made by Arc protein multimers, which encapsulates specific neuronal mRNA and then are trafficked across synaptic boutons (20, 46). The median part of the Arc protein sequence has similarity to modern retroviruses (for example HIV) Group-specific antigen (Gag). Like HIV Gag, Arc forms capsomeres (Figure 1) which self-assemble into capsids of about 30 nM in diameter, while the multimerization of Arc is mediated by its N-terminal helical coil motif (48–50). Arc protein ensembles form multiple capsomeres with symmetric pentameric structures (Figure 1), resembling some viral ion channels (48). Arc variants are found in both birds and humans, but not fish. It is hypothesized that Arc was inserted into the ancestral genome of all tetrapods (amphibians, reptiles, birds, mammals) around 350–400 million years ago. In humans, Arc is found in the greatest amount in brain structures associated with memory, which may be associated with synaptic plasticity and consolidation of memories (44, 51).

Of course, virus-like transport of mRNA can be employed not only in long-term memory, and Arc can be presented better as a multifunctional signaling hub (52). For example, it was shown that Arc can transport mRNAs from mutated genes related to schizophrenia (53). Arc may also play a role in the immunity and activity-dependent β-amyloid generation (30, 54).

1.4. Evolution of Arc proteins

Evolutionary analysis shows that Arc is derived from a lineage of Ty3/gypsy retrotransposons, which are also ancestors to retroviruses, that have been repurposed during the evolution to mediate intercellular communication in the nervous system (20, 22). Thus, animals before tetrapods most probably use Ty3/gypsy variants for memory consolidation. On the other hand, the tetrapod Arc protein structure is similar to the one which has been found in Schizophora (true) flies (Dipteros), thus it may have been transferred to a common ancestor of these insects independently (22, 48). At least two Arc homologs (dArc1 and dArc2) are found in flies, which arose by genomic duplication of an ancestral dArc gene but were not detected in any other dipteran (e.g., mosquitoes) or protostome species (20, 22). In Drosophila Arc1 protein forms capsid-like structures that bind mRNA in neurons and are loaded into extracellular vesicles. These vesicles pass from motor neurons to muscles. The disruption of the transfer, in turn, blocks synaptic plasticity (20). Thus, the transsynaptic mechanism of mRNA transport involving retrovirus-like Arc- capsids and extracellular vesicles can be considered proven (55).

While Arc genes originated independently, they still share significant homology in the retroviral Gag domain, and thus the ability to form capsids. Interestingly, the protein participating in memory consolidation in fish retains some immunoreactivity to Arc (56). This domestication of proteins using transposable elements is a well-known phenomenon known as lateral gene transfer that can enrich the recipient and provide a mechanism for evolutionary flexibility (57, 58). About one-half of the mammalian genome consists of DNA with viral or transposon origin and about 8% belong to ancient retroviruses (2, 59). According to the Gene Expression Omnibus (GEO) database for gene expression profiling, the Arc gene was identified as a candidate gene involved in the pathogenesis of various neurological diseases, including epilepsy and a number of others, such as depression.

2. Possible involvement of Arc in the mechanisms of neuropsychic disorders

2.1. Human brain pathologies associated with ARC-protein

Actively regulated cytoskeletal-associated (ARC) protein, encoded by the ARC gene, was characterized at the end of the last century (12, 13). This protein is localized in the synaptic contacts of neurons, and its synthesis is dependent on the NMDA receptor's activity. This protein plays a critical role in the molecular processes associated with learning and memory and may also serve as a marker of plastic changes in the brain (15).

Impaired Arc protein synthesis is associated with various brain pathologies, including memory disorders, Alzheimer's disease, autism spectrum disorders, schizophrenia, and epilepsy (60–62). Arc cellular pathways have emerged as key regulators of synaptic plasticity, and are becoming known for being central players in genetic risk for many neural disorders (20).

Thus, in a study on a large sample of patients, it was shown that both rare mutations and epigenetic regulation of ARC contribute to the pathogenesis of schizophrenia, at least in some patients (20, 63). It has also been shown that small mutations affecting one or more nucleotides are extremely widespread among glutamatergic postsynaptic proteins, including proteins associated with ARC and NMDAR, regulated by synaptic activity. At the same time, genes affected by mutations in schizophrenia overlap with genes affected by mutations in autism spectrum disorders and some other brain pathologies (64).

Patients with epilepsy have an increased likelihood of experiencing psychotic symptoms, many of which are similar to those of depression. However, many psychiatric comorbidities, not just the symptoms of depression, are more common in patients with epilepsy (65). It remains an open question whether depression is a risk factor for the development of epilepsy.

Interesting results were obtained by measuring the level of Arc/Arg3.1 in the blood plasma of children with a diagnosed autism spectrum disorder (ASDs) (66). The average level of Arc/Arg3.1 protein in blood plasma in autism was significantly higher than in the control (healthy) group. However, no significant association was found between plasma Arc/Arg3.1 protein levels and measures of autism severity (66). This suggests that Arc/Arg3.1 can be used as an early biomarker for diagnosing autism (66).

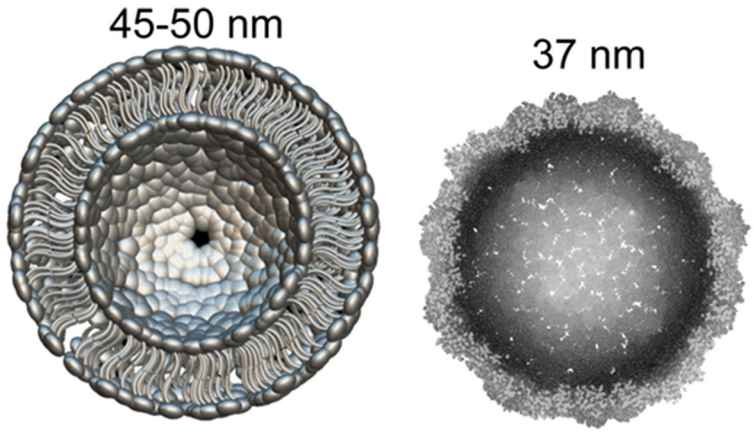

FIGURE 1
What can be found in synapse: the diameter of glutamatergic synaptic vesicle **(Left)** is approximately 45–50 nM [model drawn according to cryo-EM data by Du et al. (47)]. dArc1 capsid **(Right)**—a viral-like particle made by polymerization of 240 Arc-protein formed capsomeres (47, 48).

Autism and Angelman syndrome (AS) share many common characteristics, although Angelman syndrome is not usually included in ASD (67, 68). Angelman Syndrome is a neurological disorder caused by a mutation of the E3 ubiquitin ligase UBE3A, a gene whose mutation is associated with autism spectrum disorders. In childhood, seizures are observed in approximately 80–90% of patients with AS (69). Arc is one of the target proteins of the UBE3A gene. Since Arc is involved in learning and memory, its expression directly affects the manifestation of AS, including the epileptic seizures, typical of this syndrome. But the function of UBE3A during nervous system development and how UBE3A mutations give rise to cognitive impairment in individuals with AS and ASDs remains unclear. Nevertheless, we know that experience-driven neuronal activity induces UBE3A transcription. UBE3A then regulates excitatory synapse development by controlling the degradation of Arc (67). Disruption of UBE3A function in neurons leads to an increase in Arc expression and a concomitant decrease in the number of AMPA receptors at excitatory synapses. This deregulation of AMPA receptor expression at synapses may contribute to the brain pathologies that occur in AS and possibly other ASDs (67). Most researchers agree that the genesis of epileptic seizures in AS has a complex genesis (17). It is known that in patients with AS, there is a global decrease in the volume of a number of subcortical structures and an increase in the volume of gray matter. The degree of the abnormality correlates with the severity of seizures, suggesting that the occurrence of seizures may be directly related to morphological changes in the brain (17).

Fragile X Syndrome (FXS) is one of the most common inherited forms of developmental delay (70). Epilepsy is reported in up to 20% of individuals with fragile X syndrome (71). It was shown that the FMR1 gene, which produces the FMRP protein is responsible for FXS. One of the biological manifestations of FXS is elevated levels of metabotropic glutamate receptor (mGluR)-dependent long-term depression (LTD), (mGluR-LTD) a type of synaptic plasticity which is characterized by a reduction in the synaptic response at the excitatory synapses and overexpression of several proteins including Arc (72, 73). This abnormal overexpression of Arc leads to increased endocytosis of AMPARs and increased mGluR-LTD. In addition, altered dendritic spine morphology was observed not only in animal models of FXS but also in humans with this disorder (70, 74).

Epilepsy does not have a clearly identifiable cause in about half of patients. Also, this disease can be associated with various factors, including various genetic abnormalities. Some types of epilepsy are linked to certain genes, but generally, genetic factors can make a person more sensitive to the mechanisms that cause seizures. In addition, epilepsy has a wide comorbidity with other brain pathologies. Thus, we most likely cannot speak about the direct responsibility of the genetic pathologies of Arc for the formation of one form or another of epilepsy in humans, but Arc can certainly be associated with epilepsy.

2.2. Expression of Arc protein in neurons activated by epileptic seizures

Arc depletion may affect memory loss in the post-ictal state. It is known that memory problems experienced by people with epilepsy are characterized by difficulty in retrieving episodes or events that happened before a seizure and even general semantic information (43). Genetic interference of activity-dependent Arc protein expression in the rat hippocampus impairs the maintenance of long-term potentiation and blocks the consolidation of long-term memory (33, 75). Can it be associated with the dysregulation of Arc protein expression during a seizure? It can be assumed that new methods of *in vivo* molecular imaging can help answer this question to some extent (76, 77).

Arc is an activity-dependent immediate early gene, its mRNA is translocated only to dendritic spines of active neurons where it is translated to Arc protein, which then multimerizes in capsids forming viral-like particles implanted with mRNA. Then in the form of viral-like particles, Arc-mRNA is loaded into extracellular vesicles and trafficked to postsynaptic boutons, participating in

regulating dendritic spine morphology and the receptor content of glutamatergic synapses controlling synaptic plasticity changes and memory (20, 21, 31, 47, 78, 79). Notably Arc expression is augmented in synapses of recently activated neurons of the epileptic seizure focal zone but rapidly declines, probably due to dysregulation during aberrant neuronal overexcitation (80). For example, temporal lobe epilepsy originates from the mesolimbic network and provokes damage to the hippocampus including the dentate gyrus, which is very vulnerable to status epilepticus (81–83).

It is generally accepted that hippocampal sclerosis provokes the hippocampus to generate seizures resulting from the loss of interneurons and pyramids accompany the formation of recurrent synaptic circuits by dentate gyrus cells (DGC) (84, 85). Arc upregulation in DGC between seizures accompanies increased spine density which enhances excitatory input from the entorhinal cortex, which precedes the formation of recurrent mossy fiber synapses (80, 86). Conversely, hippocampal regions not affected by seizures preserve normal Arc expression (80).

Many authors studied the association between Arc expression and epileptogenesis. It is known that spine loss and other dendritic abnormalities occur in epilepsy which to some extent may be also associated with Arc (87). Of course, the Arc gene affects a whole galaxy of genes, and therefore the phenotypic consequences of its mutations are very diverse (21, 37, 88). Also, some genes and their products are necessary for Arc functioning and transport, and the disruption of these genes lead also to changes in neural net excitation (74).

2.3. Genetic studies of Arc expression during epileptogenesis

As part of the analysis of the role of Arc in epileptogenesis on clinical material, we analyzed the transcriptomic data from the National Center of Biotechnology Information (NCBI) public repository Gene Expression Omnibus (GEO) to evaluate the ARC expression in brain areas that are damaged in epilepsy (89). The RNA sequencing data were searched in the GEO Browser for the terms "epilepsy", "epileptic", and "seizure". Afterward, we searched the GEO database for the terms "kainate", "electroconvulsive", and "pentylenetetrazol" to receive the data for the most common models of epilepsy. Each GEO dataset included in the analysis should meet the following criteria: (1) expression data in raw counts, fragments per kilobase per million mapped fragments (FPKM), or transcripts per million (TPM); (2) a clear explanation of sample origin (the datasets which comprise samples described like a "brain sample," when the brain structure was not specified, were excluded); (3) at least three samples per study group; (4) the expression patterns were studied in brain structures, data for other tissues were excluded.

Four relevant datasets for the ARC expression pattern in human brain parts were mined (Table 1). In all datasets, only patients with temporal lobe epilepsy were included, and hippocampal structures were studied, except 17 neocortical temporal lobe samples in GSE134697. Further, no healthy or non-epileptic controls were included in the studies in the appropriate number ($n \geq 3$) that did not allow for comparison of damaged tissues with normal tissues from healthy subjects.

No differences in ARC expression levels in mesial temporal lobe epilepsy patients with or without concomitant hippocampal sclerosis were identified in GSE71058 by an edgeR likelihood ratio test (Padj > 0.05) (93). Likewise, there were no significant differences in ARC expression levels between patients with low and high seizure frequencies in GSE127871. All data were count per million (CPM) normalized by edgeR package CPM function and demonstrated the congruent ARC expression levels (93). Applying the Expression Atlas recommendations, the expression levels may be interpreted as low expression (i.e. CPM between 0.5 and 10) or medium (CPM between 10 and 1,000) in all studied structures (94).

In mice, transcriptome modifications were studied in the hippocampus, neocortical structures, and cerebellum in genetic models of epilepsy (Table 2). No differences in Arc expression levels between control and study groups were identified in any study when likelihood ratio test (for raw counts) or empirical Bayes statistics *eBayes* function in limma package (for log 2 FPKM-normalized data) were applied (99). The only exception is the dramatic loss of Arc in the hippocampal transcriptome of mice lacking miR-22 during the epileptogenesis after kainate injection compared to the identically treated wild-type animals (Padj $<$ 0.05). miR-22 loss results in an exacerbated epilepsy phenotype in kainate-induced epilepsy and is associated with the reduction of an inflammatory response at the transcriptional level (96).

In contrast, the significant downregulation of Arc expression was identified in CA1 superficial layer in response to kainate treatment (Padj $<$ 0.0019) in rats (Table 3). As well, Arc expression was downregulated in the dorsal subiculum (Padj $<$ 0.0024) in response to the induction of acute seizures in rats by electric stimulation. No differences in Arc expression were identified between control and epileptic model rats when the whole hippocampus or *corpora quadrigemina* were studied. So, the demonstrated discrepancy between results revealed in mouse and rat models may be caused by expression examination in the whole hippocampus instead of the separated parts of this complex structure.

Genetic studies of Arc expression during epileptogenesis in humans and animals are still rare to provide non-contradictory conclusions on Arc's role in seizure-related pathologies. According to available datasets for the Arc expression, only in mice and rats, but not in humans, the downregulation of Arc expression was revealed in response to seizures. Further accumulation of more detailed data on Arc expression in specific regions of the brain is likely to allow more specific conclusions to be drawn in the future.

3. Animal epilepsy model

3.1. Arc gene expression in rodent epilepsy models

Practically all rodent epilepsy seizure induction models affect Arc expression. In rodent models, Arc gene expression can be stimulated by practically any method which induces seizure activity in the brain, at least in the hippocampus and cortex, but Arc

TABLE 1 ARC expression in the temporal lobe samples of epileptic patients.

Gene set ID	Title	Structure	Study group(s)	Expression levels (in CPM)
GSE71058 (90)	Gene expression profiling in dentate granule cells from patients with mesial temporal lobe epilepsy with or without hippocampal sclerosis	*Gyrus dentatus*	12 patients with mesial temporal lobe epilepsy, including 5 samples from patients with hippocampal sclerosis and 7 without hippocampal sclerosis.	0–84.45
GSE94744 (91)	Microglia and the immune response to a human temporal lobe seizure	*CA1*	7 patients with mesial temporal lobe epilepsy and hippocampal sclerosis	1.01–28.62
		CA3		5.16–33.61
		Gyrus dentatus		3.20–18.02
		Subiculum		5.36–55.77
GSE127871	Altered expression of signaling pathways regulating neuronal excitability in hippocampal tissue of temporal lobe epilepsy patients with low and high seizure frequency	*Hippo- campus*	Investigation of alterations in hippocampal gene expression in temporal lobe epilepsy (<4 seizure episodes per month vs. >4 seizures per month, 5 and 7 patients per group, respectively)	2.34–66.01
GSE134697 (92)	Hippocampal and neocortex transcriptome sequencing data from 17 mesial temporal lobe epilepsy patients and 2 neocortex samples from neurologically healthy controls	*Temporal neocortex*	17 mesial temporal lobe epilepsy patients	6.34–31.63
		Hippocampus		2.58–98.75

TABLE 2 Arc expression in genetic models of epilepsy in mice.

Gene set ID	Title	Structure	Study group(s)	Expression levels*	Differential expression	Measure units
GSE138370 (95)	Changes in calcium homeostasis and gene expression implicated in epilepsy in hippocampi of mice overexpressing ORAI1	*Hippocampus*	ORAI1 overexpressing group ($n = 3$) *vs.* WT** ($n = 3$)	49.38–90.56	NS	CPM
GSE147466 (96)	Genetic deletion of microRNA-22 blunts the inflammatory transcriptional response to status epilepticus and exacerbates epilepsy in mice	*Hippocampus*	miR-22-/- ($n = 4$) *vs.* WT ($n = 4$); status epilepticus in both groups	44.47–75.63	Loss of Arc expression in miR-22-/– group (Pagj < 0.023)	FPKM
GSE151742 (97)	Expression of the neuronal tRNA n-Tr20 regulates synaptic transmission and seizure susceptibility	*Hippocampus*	B6N-n-Tr20-/- ($n = 3$) *vs.* B6N WT ($n = 3$)	66.48–161.59 (ribosomal), 66.58–128.52 (total)	NS	CPM
GSE169481 (98)	Deletion of a non-canonical regulatory sequence causes loss of Scn1a expression and epileptic phenotypes in mice	*Hippocampus*	heterozygous Scn1a KO (n=3) *vs.* WT (n = 4)	114.12–209.22	NS	CPM
GSE215425	WWOX P47T loss-of-function mutation induces epilepsy, progressive neuroinflammation, and cerebellar degeneration	*Prefrontal cortex*	WWOX P47T (loss-of-function mutation induces epilepsy, $n = 5$) *vs.* WT (n = 5)	43.70–698.65	NS	CPM
		Parietal cortex		34.47–496.00	NS	CPM
		Hippocampus		34.21–231.61	NS	CPM
		Cerebellum	WWOX P47T ($n = 3$) *vs.* WT ($n = 4$)	18.57–29.26	NS	CPM

*In control animals.
**NS, non-significant.

expression is time-dependent and the stimulation later turns to depression (80, 103, 104).

Initial hyperproduction of Arc can be seen in epilepsy models with kainate, D1-receptor agonists, 4-Aminopyridine (4AP), Bicuculline (Bic), and Forskolin, pilocarpine, pentylenetetrazole, kindling, activation of mGluR, electroconvulsive stimulation (Also Arc mRNA and proteins are rapidly induced in the striatum after acute cocaine administration (80, 105–111). Details on epileptic models inducing Arc expression are presented in Table 4.

Arc expression demonstrates complex behavior in seizure generation. The threshold of stimulation intensity (depolarization threshold) required for induction of Arc expression varies between brain regions (23). Particularly in the case of most intensive electroconvulsive stimulation, the proportion of Arc-positive neurons following seizures was highest in the dentate gyrus, intermediate in the CA3 region of the hippocampus, and lowest in the perirhinal cortex (23). In contrast, low-intensity seizure-inducing electrostimulation caused an opposite Arc expression profile (lowest in the dentate gyrus and highest in the perirhinal cortex), which indicates for Arc expression may be serving as a transcriptional threshold mechanism in CNS (23). Accordingly, Arc mRNA upregulation is positively correlated to

TABLE 3 Arc expression in non-genetic models of epilepsy in rat.

Gene set ID	Title	Structure	Study group(s)	Expression levels*	Differential expression	Mea- sure units
GSE137473 (100)	A systems approach delivers a functional microRNA catalog and expanded targets for seizure suppression in temporal lobe epilepsy	*hippocampus*	Perforant pathway stimulation (PPS) model ($n = 3$) vs. Ctrl ($n = 3$)	3.59–7.52	NS*	FPKM
GSE143555 (101)	RNA sequencing of laser-captured hippocampal deep and superficial CA1 subfields in epilepsy	*CA1*	kainic acid-induced status epilepticus ($n = 3$) and sham control ($n = 3$ group), deep and superficial CA1 subfields were studied separately	49,72–67,39 (superficial layer); 63.99–81.32 Ideep layer)	Downregulated in the superficial layer in kainite-treated animals (Padj < 0.0019)	CPM
GSE173885 (102)	Transcriptome of the audiogenic rat strain and identification of possible audiogenic epilepsy-associated genes	*corpora quadrigemina*	KM - audiogenic epilepsy rat strain ($n = 3$), Wistar rat ($n = 4$); outbred strain from KM rats ($n = 4$)	13.12–25.20	NS	CPM
GSE178409	Transcriptomic analysis of dorsal and ventral subiculum after the induction of acute seizures by the electric stimulation of the perforant pathway in rats	*subiculum*	Ventral and dorsal subiculum, after the induction of acute seizures by electric stimulation ($n = 5$) and in the control group ($n = 5$)	135.44–179.41 (dorsal); 30.91–63.16 (ventral)	Downregulated in dorsal subiculum in treated animals (Padj <0.0024)	CPM
GSE193580	Hippocampus RNA-sequencing of Q808 against PTZ-induced seizure model	*hippocampus*	Rats were randomly divided into vehicle control group ($n = 4$), PTZ + vehicle group ($n = 5$), and PTZ + Q808 group ($n = 5$)	35.06–80	NS	FPKM

*In control animals.

**NS, non-significant.

seizure burst ratio, burst amplitudes, and length of paroxysmal episodes (80).

3.2. Rodent models with Arc knock-out

Peebles et al. studied spine morphology and the general stability of the glutamatergic neuronal network and found both dependent on Arc expression, employing a mouse model (21). They have confirmed that Arc expression leads to an increase in spine density, but generally decreases synaptic efficacy by reducing surface GluR1. Authors have shown that regulated synaptic strength in neuronal networks determined by Arc is very important for network stability. Studying kainite-elicited seizure activity in WT and Arc–/– mice, authors have shown that Arc–/– mice are more susceptible to kainite-elicited seizures and neuronal changes associated with epilepsy. Also, Arc–/– mice had aberrant spontaneous cortical network discharge activity, highly associated with epilepsy (21). On the other side, prenatal or perinatal deletion of *Arc/Arg3.1* alters cortical network activity without excessive disruption of the balance of excitation and inhibition in the brain (88). Furthermore, Arc knockouts elevate AMPA receptor level expression in some brain regions including the nucleus accumbens which reduces the symptoms of epilepsy-associated pathologies (109). Pilocarpine-induced temporal lobe epilepsy causes a time-dependent decrease in Arc expression in hippocampal tissue (121).

Epilepsy is prevalent and often medically intractable in Angelman syndrome (AS). There are different models of AS. AS mouse models associated with UBE3A gene-deficient function (UBE3Am-/p+) shows reduced excitatory neurotransmission but a lower seizure threshold. Genetically decreased Arc expression additionally reduces abnormal EEGs and seizures in mice with Angelman syndrome associated with UBE3A gene-deficient function, because both Arc and UBE3A regulate surface expression of AMPA receptors. In another AS model, the so-called fragile X syndrome (FXS) mouse model, on the contrary, increased Arc is responsible for seizure phenotype (68, 114).

Comorbidity of schizophrenia and epilepsy are relatively common in clinical practice and animal models. Two different models of schizophrenia with seizures were developed, conditional KO (late-cKO) mice, in which Arc/Arg3.1 was deleted during late postnatal development, to investigate the causal relationship between *Arc/Arg3.1* deletion and schizophrenia-linked neurophysiological and behavioral phenotypes. Nevertheless, in an animal study genetic deletion of Arc/Arg3.1 *per se* did not cause schizophrenia-like behavior, and a significantly higher dosage of kainic acid was required to elicit epileptic seizures in the KO mice (88). This completely contradicts the results obtained in another model of Arc/Arg3.1 knockout mice by Managò et al. showing genetic mutation disrupting Arc produced a hyperactive phenotype and amphetamine supersensitivity consistent with rodents' correlates of schizophrenia-like symptoms (120). The authors also describe important differences in the dopaminergic system in KO and wild-type mice. Most likely, this inconsistency

TABLE 4 Animal epilepsy models and the role of Arc protein.

Animal epilepsy models	Epilepsy symptoms and manifestations	Possible role of Arc in the control of epileptogenic activity	References
Non-genetic models			
Mice' neuronal hippocampal and cortical cultures. Epileptogen's (4-Aminopyridine, bicuculline, forskolin) local administration	Synchronized network bursting in hippocampal cultures	Activity-induced Arc expression in neurons and astrocytes.	(106)
Temporal lobe epilepsy model (rats) pilocarpine-induced epilepsy	Status epilepticus	Optogenetics seizure control targeting intense ARC immunoreactive neurons Intense ARC immunoreactive neurons may have the potential to control epileptic seizures.	(112)
The mesial temporal lobe epilepsy model with the sclerotic hippocampus (mice) Optogenetically stimulated and kainic acid-induced epileptogenesis	Epileptiform events and status epilepticus in the hippocampus	The upregulation of Arc mRNA (1) is positively correlated with the epileptiform bursts, (2) increases during the increase of burst amplitudes and (3) increases with prolonged paroxysmal episodes. Arc is a possible mediator between synaptic plasticity and seizure activity.	(80)
Epilepsy after electroconvulsive shock treatment (rat) rat hippocampus and perirhinal cortex relationship between the current intensities that elicit seizures and the threshold for Arc mRNA transcription in the rat hippocampus and perirhinal cortex	Behavioral seizures with hind-limb extension and tonic–clonic motor responses	1. Intensive electrostimulation: the high proportion of Arc-positive neurons in the dentate gyrus, intermediate in the CA3 region of the hippocampus, lowest in the perirhinal cortex 2. Low-intensity electrostimulation: an opposite Arc expression profile (lowest in the dentate gyrus and highest in the perirhinal cortex)	(23)
Pentylenetetrazole-induced kindling in rats	The seizure intensity was classified according to the Racine scale	The most prominent increase in Arc expression during kindling was present in the entorhinal cortex, the dentate gyrus, and the basolateral nucleus of the amygdala	(107)
Intraperitoneal injection of pilocarpine to induce status epilepticus in rats	The seizure intensity was classified according to the Racine scale	Using Arc immunoreactivity as an indicator of granule cell activation, authors found that granule cells born after pilocarpine-induced SE did not express Arc more intensely than the surrounding granule cells and, in addition, transient seizure activity induced by pentylenetetrazol did not activate mature granule cells born after SE more intensely.	(110)
Electroconvulsive seizures in rats	Observation of generalized tonic/clonic seizure that lasted ~15 sec	Electroconvulsive seizures strongly induce prolonged Arc/Arg3.1 transcription in dentate granule cells. Assessment of Arc/Arg3.1 mRNA revealed that the induction of Arc/Arg3.1 transcription was blocked by NMDA receptor antagonists	(108)
Kainic acid-induced seizures in mice	Behavioral observation of the onset of seizure	Seizures elevated Arc/Arg3.1 protein in the granular cell layer and molecular layer of the dentate gyrus and in the pyramidal cells in CA1-3. The induction of a large number of activity-regulated genes, including Arc/Arg3.1, Arl5b, Gadd45b, Inhba, and Zwint, is indeed dependent on ERK phosphorylation.	(113)
Genetic models			
Angelman syndrome mouse model (mice). AS mice lack a functional copy of maternally inherited UBE3A but with a wild-type copy of the paternally inherited UBE3A allele.	Enhanced seizure-like response to an audiogenic stimulus	The reduction of the level of Arc expression has the potential to reverse the seizures associated with Angelman syndrome	(68)
Angelman syndrome UBE3A$^{m-/p+}$ model in mice	Field potential recording in brain slices	Local circuits of UBE3A$^{m-/p+}$ *in vitro* are hyperexcitable and display a unique epileptiform activity	(114)
Transgenic mice that express EGFP-Arc	A single generalized electroconvulsive tonic/clonic seizure that lasted approximately 15 s.	Arc mRNA degradation occurs via a mechanism with characteristics of nonsense-mediated mRNA decay (NMD). Rapid dendritic delivery of newly synthesized Arc mRNA after induction may depend in part on prior splicing of the 3′ UTR.	(115)
EGFP-tagged Arc in the primary culture of hippocampal neurons	Switch from tetrodotoxin-induced inactivity to BDNF treatment	Activity-induced Arc/Arg3.1 accumulates at spines during synaptic inactivity. Synaptic Arc/Arg3.1 reduces surface AMPAR levels in individual spines.	(29)
Patients with idiopathic generalized epilepsy including childhood absence epilepsy and juvenile myoclonic epilepsy	Absence epilepsy	Authors suggest the presence of an idiopathic generalized epilepsy susceptibility allele in the ARC gene.	(116)

(Continued)

TABLE 4 (Continued)

Animal epilepsy models	Epilepsy symptoms and manifestations	Possible role of Arc in the control of epileptogenic activity	References
Mutant mice with the deletion of the Drd1a gene to prevent dopamine D1 receptor expression	Behavioral and EEG observation of seizures	Administration of D1-type receptor agonists promotes the expression of Arc/Arg3.1 in the hippocampal dentate gyrus. Deletion of Drd1a gene prevents the effect	(105)
Wistar Albino Glaxo from Rijswijk (Wag/Rij) rats	Absence epilepsy	Hippocampal mGlu5 receptor-dependent synaptic plasticity is associated with the pathological phenotype of WAG/Rij rats. Arc is involved in mGluR-induced long-term synaptic depression (mGluR-LTD)	(117–119)
Arc−/− and Arc+/−mice	Electrical stimulation of dopamine neurons in the midbrain ventral tegmental area and Ca-imaging	Genetic disruption of Arc leads to concomitant hypoactive mesocortical and hyperactive mesostriatal dopamine pathways.	(120)
$Arc^{-/-}$ Mice Have Decreased Spine Density and Increased Spine Width. Kainite model	*$Arc^{-/-}$* mice are more susceptible to seizures in response to systemic challenges with pentylenetetrazol (PTZ).	Arc specifically reduces surface GluR1 internalization at thin spines, and Arc mutants that fail to facilitate AMPAR endocytosis do not increase the proportion of thin spines. Loss of Arc *in vivo* leads to a significant decrease in the proportion of thin spines and an epileptic-like network hyperexcitability.	(21)

can be explained by the different strategies used to create the two knockout mouse models.

4. Discussion and conclusion

The literature sources cited unanimously emphasize the paramount significance of Arc protein in regulating synaptic strength [reviewed by Zhang and Bramham (122)], which in turn determines the stability of the neuronal network, thus affecting epileptic seizure susceptibility (Figure 2) (21, 122). While the established mechanism of Arc-mediated influence relies on presynaptic NMDA-receptor mediated ionic currents in the glutamatergic pathway, it is also the primary mechanism that exerts direct cross-synaptic influence over postsynaptic spines morphology and their AMPARs (21). These spines are typically found at the postsynaptic site of most excitatory synapses in the mammalian brain and may be present on excitatory as well as inhibitory neurons (123). This implies that changes in Arc-protein-mediated activity can potentially affect the excitatory-inhibitory balance of the neuronal network, either reducing seizure threshold and promoting stability or inducing lability (88, 114).

These two possibilities are represented by the potential Arc-mediated changes (Figure 2). The primary known effect of the Arc protein is to decrease the strength of excitatory synapses, which could potentially reduce the destabilizing flow of excitatory signals to the existing epileptic focus or decrease auto-excitation by reducing internal excitatory connections (1). Conversely, Arc-mediated changes could also decrease excitatory feedback to inhibitory neurons, thereby reducing their inhibitory influence on the existing epileptic focus (2).

Arc knockouts will remove such effects: the literature reviewed and knockout experiments consistently show this two-sided effect on seizure susceptibility, if some existent epileptiform activity is present. While Arc definitely is activated in neurons participating in epileptic discharges, there is no evidence of the direct induction of epilepsy by Arc-protein mediated mechanisms.

These allow us to conclude that Arc activity-regulated expression directly participates in seizure susceptibility. Also, epileptic activation of Arc-mediated changes during the seizure may affect memory consolidation and many other important neuronal functions in epilepsy.

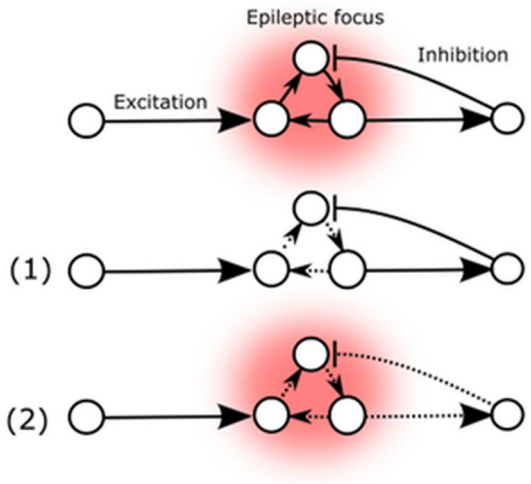

FIGURE 2
Arc mediated changes of seizure susceptibility. (1) Elevated Arc expression in epileptic focus weakens external AMPA-mediated excitatory influence. (2) Arc expression also decreases excitatory feedback to inhibitory neurons.

Author contributions

Conceptualization: DS, MI, AV, ANV, and VT. Writing: MI, DS, AI, AV, ANV, and VT. Review and editing and figures preparation: DS, AI, and MI. Editing: JA, AI, ES, LR, and PS. Supervision and project administration: MI, VT, and AV. Funding acquisition: MI, AV, and ANV. All authors have read and agreed to the published version of the manuscript.

Funding

This work was sponsored by the National Institute of General Medical Science (NIGMS) of the National Institute of Health (NIH) under awards U54GM133807 and SC3GM143983 which provided funding to JA and MI and NIH NIGMS RCMI award number G12MD007583 granted to the UCC. AV and ANV were supported by the project ID: 94030300 of the St. Petersburg State University, St. Petersburg, Russia. DS was supported by IEPHB Research program 075-0152-22-00.

Conflict of interest

The authors declare that the research was conducted in the absence of any commercial or financial relationships that could be construed as a potential conflict of interest.

Publisher's note

Author disclaimer

The content is solely the responsibility of the authors and does not necessarily represent the official views of the National Institute of Health.

References

1. Löwer R. The pathogenic potential of endogenous retroviruses: facts and fantasies. *Trends Microbiol.* (1999) 7:350–6. doi: 10.1016/S0966-842X(99)01565-6

2. Mustafin RN, Khusnutdinova EK. Involvement of transposable elements in neurogenesis. *Vavilovskii Zhurnal Genet Selektsii.* (2020) 24:209–18. doi: 10.18699/VJ20.613

3. Smit TK, Bos P, Peenze I, Jiang X, Estes MK, Steele AD. Seroepidemiological study of genogroup I and II calicivirus infections in South and southern Africa. *J Med Virol.* (1999) 59:227–31. doi: 10.1002/(SICI)1096-9071(199910)59:2<227::AID-JMV17>3.0.CO;2-8

4. Gonzalez-Cao M, Iduma P, Karachaliou N, Santarpia M, Blanco J, Rosell R. Human endogenous retroviruses and cancer. *Cancer Biol Med.* (2016) 13:483–8. doi: 10.20892/j.issn.2095-3941.2016.0080

5. Liu X, Liu Z, Wu Z, Ren J, Fan Y, Sun L, et al. Resurrection of endogenous retroviruses during aging reinforces senescence. *Cell.* (2023) 186:287–304.e26. doi: 10.1016/j.cell.2022.12.017

6. Denner J. Expression function of endogenous retroviruses in the placenta. *APMIS.* (2016) 124:31–43. doi: 10.1111/apm.12474

7. Frank JA, Singh M, Cullen HB, Kirou RA, Benkaddour-Boumzaouad M, Cortes JL, et al. Evolution antiviral activity of a human protein of retroviral origin. *Science.* (2022) 378:422–8. doi: 10.1126/science.abq7871

8. Redelsperger F, Raddi N, Bacquin A, Vernochet C, Mariot V, Gache V, et al. Genetic evidence that captured retroviral envelope syncytins contribute to myoblast fusion and muscle sexual dimorphism in mice. *PLoS Genet.* (2016) 12:1006289. doi: 10.1371/journal.pgen.1006289

9. Frese S, Ruebner M, Suhr F, Konou TM, Tappe KA, Toigo M, et al. Long-term endurance exercise in humans stimulates cell fusion of myoblasts along with fusogenic endogenous retroviral genes *in vivo*. *PLoS ONE.* (2015) 10:0132099. doi: 10.1371/journal.pone.0132099

10. Küry P, Nath A, Créange A, Dolei A, Marche P, Gold J, et al. Human endogenous retroviruses in neurological diseases. *Trends Mol Med.* (2018) 24:379–94. doi: 10.1016/j.molmed.2018.02.007

11. Römer C. Viruses and endogenous retroviruses as roots for neuroinflammation and neurodegenerative diseases. *Front Neurosci.* (2021) 15:175. doi: 10.3389/fnins.2021.648629

12. Lyford GL, Yamagata K, Kaufmann WE, Barnes CA, Sanders LK, Copeland NG, et al. Arc a growth factor and activity-regulated gene, encodes a novel cytoskeleton-associated protein that is enriched in neuronal dendrites. *Neuron.* (1995) 14:433–45. doi: 10.1016/0896-6273(95)90299-6

13. Link W, Konietzko U, Kauselmann G, Krug M, Schwanke B, Frey U, Kuhl, D. Somatodendritic expression of an immediate early gene is regulated by synaptic activity. *Proc Natl Acad Sci.* (1995) 92:5734–5738. doi: 10.1073/pnas.92.12.5734

14. Diering, Remembering GH, and forgetting in sleep: Selective synaptic plasticity during sleep driven by scaling factors Homer1a and Arc. *Neurobiol Stress.* (2022) 22:100512. doi: 10.1016/j.ynstr.2022.100512

15. Savino R, Polito AN, Marsala G, Ventriglio A, Di Salvatore M, De Stefano MI, et al. Agomelatine: a potential multitarget compound for neurodevelopmental disorders. *Brain Sci.* (2023) 13:734. doi: 10.3390/brainsci13050734

16. Casillas-Espinosa PM, Powell KL, O'Brien TJ. Regulators of synaptic transmission: roles in the pathogenesis and treatment of epilepsy. *Epilepsia.* (2012) 53:41–58. doi: 10.1111/epi.12034

17. Du X, Wei L, Yang B, Long S, Wang J, Sun A, et al. Cortical and subcortical morphological alteration in Angelman syndrome. *J Neurodev Disord.* (2023) 15:7. doi: 10.1186/s11689-022-09469-3

18. Husi H, Ward MA, Choudhary JS, Blackstock WP, Grant SGN. Proteomic analysis of NMDA receptor-adhesion protein signaling complexes. *Nat Neurosci.* (2000) 3:661–9. doi: 10.1038/76615

19. Giralt A, Brito V, Chevy Q, Simonnet C, Otsu Y, Cifuentes-DÍaz C, et al. Pyk2 modulates hippocampal excitatory synapses and contributes to cognitive deficits in a Huntington's disease model. *Nat Commun.* (2017) 8:15592. doi: 10.1038/ncomms15592

20. Ashley J, Cordy B, Lucia D, Fradkin LG, Budnik V, Thomson, T. Retrovirus-like Gag protein Arc1 binds RNA and traffics across synaptic boutons. *Cell.* (2018) 172:262. doi: 10.1016/j.cell.2017.12.022

21. Peebles CL, Yoo J, Thwin MT, Palop JJ, Noebels JL, Finkbeiner S. Arc regulates spine morphology and maintains network stability *in vivo*. *Proc Natl Acad Sci.* (2010) 107:18173–8. doi: 10.1073/pnas.1006546107

22. Pastuzyn ED, Day CE, Kearns RB, Kyrke-Smith M, Taibi AV, McCormick J, et al. The neuronal gene arc encodes a repurposed retrotransposon gag protein that mediates intercellular RNA transfer. *Cell.* (2018) 172:275–88.e18. doi: 10.1016/j.cell.2017.12.024

23. Chawla MK, Gray DT, Nguyen C, Dhaliwal H, Zempare M, Okuno H, et al. Seizure-induced arc mRNA expression thresholds in rat hippocampus and perirhinal cortex. *Front Syst Neurosci.* (2018) 12:53. doi: 10.3389/fnsys.2018.00053

24. Shepherd JD, Bear MF. New views of Arc, a master regulator of synaptic plasticity. *Nat Neurosci.* (2011) 14:279–84. doi: 10.1038/nn.2708

25. Korb E, Finkbeiner S. Arc in synaptic plasticity: from gene to behavior. *Trends Neurosci.* (2011) 34:591–8. doi: 10.1016/j.tins.2011.08.007

26. Mikuni T, Uesaka N, Okuno H, Hirai H, Deisseroth K, Bito H, et al. Arc/Arg31 is a postsynaptic mediator of activity-dependent synapse elimination in the developing cerebellum. *Neuron.* (2013) 78:1024–35. doi: 10.1016/j.neuron.2013.04.036

27. Rodriguez JJ, Davies HA, Silva AT, De Souza IEJ, Peddie CJ, Colyer FM, et al. Long-term potentiation in the rat dentate gyrus is associated with enhanced Arc/Arg31 protein expression in spines, dendrites and glia. *Eur J Neurosci.* (2005) 21:2384–96. doi: 10.1111/j.1460-9568.2005.04068.x

28. Raju CS, Fukuda N, López-Iglesias C, Göritz C, Visa N, Percipalle P. In neurons P, activity-dependent association of dendritically transported mRNA transcripts with the transacting factor CBF-A is mediated by A2RE/RTS elements. *Mol Biol Cell.* (2011) 22:1864. doi: 10.1091/mbc.e10-11-0904

29. Okuno H, Akashi K, Ishii Y, Yagishita-Kyo N, Suzuki K, Nonaka M, et al. Inverse synaptic tagging of inactive synapses via dynamic interaction of Arc/Arg31 with CaMKIIβ. *Cell.* (2012) 149:886–98. doi: 10.1016/j.cell.2012.02.062

30. Wu J, Petralia RS, Kurushima H, Patel H, Jung MY, Volk L, et al. Arc/Arg31 regulates an endosomal pathway essential for activity-dependent β-amyloid generation. *Cell.* (2011) 147:615–28. doi: 10.1016/j.cell.2011.09.036

31. Chowdhury S, Shepherd JD, Okuno H, Lyford G, Petralia RS, Plath N, et al. Arc/Arg31 interacts with the endocytic machinery to regulate AMPA receptor trafficking .*Neuron.* (2006) 52:445–59. doi: 10.1016/j.neuron.2006.08.033

32. Korb E, Wilkinson CL, Delgado RN, Lovero KL. Finkbeiner, S. Arc in the nucleus regulates PML-dependent GluA1 transcription and homeostatic plasticity. *Nat Neurosci.* (2013) 16:874–83. doi: 10.1038/nn.3429

33. Guzowski JF, Lyford GL, Stevenson GD, Houston FP, McGaugh JL, Worley PF. Barnes CA. Inhibition of activity-dependent arc protein expression in the rat hippocampus impairs the maintenance of long-term potentiation and the consolidation of long-term memory. *J Neurosci.* (2000) 20:3993–4001. doi: 10.1523/JNEUROSCI.20-11-03993.2000

34. Lituma PJ, Singer RH, Das S, Castillo PE. Real-time imaging of Arc/Arg3.1 transcription *ex vivo* reveals input-specific immediate early gene dynamics. *Proc Natl Acad Sci.* (2022) 119:e2123373119. doi: 10.1073/pnas.2123373119

35. de la Peña JB, Barragan-Iglesias P, Lou TF, Kunder N, Loerch S, Shukla T, et al. Intercellular arc signaling regulates vasodilation. *J Neurosci.* (2021) 41:7712–26. doi: 10.1523/JNEUROSCI.0440-21.2021

36. Bloomer WAC, VanDongen HMA, VanDongen, AMJ. Arc/Arg31 translation is controlled by convergent N-methyl-D-aspartate and Gs-coupled receptor signaling pathways. *J Biol Chem.* (2008) 283:582–92. doi: 10.1074/jbc.M702451200

37. Leung HW, Foo G, VanDonge A. Arc regulates transcription of genes for plasticity, excitability and Alzheimer's disease. *Biomedicines.* (2022) 10:1–44. doi: 10.3390/biomedicines10081946

38. Lingappa JR, Reed JC, Tanaka M, Chutiraka K, Robinson BA. How HIV-1 gag assembles in cells: Putting together pieces of the puzzle. *Virus Res.* (2014) 193:89–107. doi: 10.1016/j.virusres.2014.07.001

39. Burniston MT, Cimarelli A, Colgan J, Curtis SP, Luban J. Human immunodeficiency virus type 1 Gag polyprotein multimerization requires the nucleocapsid domain and RNA and is promoted by the capsid-dimer interface and the basic region of matrix protein. *J Virol.* (1999) 73:8527–40. doi: 10.1128/JVI.73.10.8527-8540.1999

40. Muriaux D, Mirro J, Nagashima K, Harvin D, Rein A. Murine leukemia virus nucleocapsid mutant particles lacking viral RNA encapsidate ribosomes. *J Virol.* (2002) 76:11405–13. doi: 10.1128/JVI.76.22.11405-11413.2002

41. Eckwahl MJ, Telesnitsky A, Wolin SL. Host RNA packaging by retroviruses: a newly synthesized story. *MBio.* (2016). 7:15. doi: 10.1128/mBio.02025-15

42. Coleman BM. Hill AF. Extracellular vesicles–Their role in the packaging and spread of misfolded proteins associated with neurodegenerative diseases. *Semin Cell Dev Biol.* (2015) 40:89–96. doi: 10.1016/j.semcdb.2015.02.007

43. Thompson PJ. Corcoran R. Everyday memory failures in people with epilepsy. *Epilepsia.* (1992) 33:S18–20.

44. Day C, Shepherd JD. Arc: building a bridge from viruses to memory. *Biochem.* (2015) 469:e1–e3. doi: 10.1042/BJ20150487

45. Hantak MP, Einstein J, Kearns RB. Shepherd JD. Intercellular communication in the nervous system goes viral. *Trends Neurosci.* (2021) 44:248–59. doi: 10.1016/j.tins.2020.12.003

46. Shepherd, J.D. Arc—an endogenous neuronal retrovirus? *Semin Cell Dev Biol.* (2018) 77:73–8. doi: 10.1016/j.semcdb.2017.09.029

47. Du J, Vegh V, Reutens DC. Small changes in synaptic gain lead to seizure-like activity in neuronal network at criticality. *Sci Rep.* (2019) 9:9. doi: 10.1038/s41598-018-37646-9

48. Erlendsson S, Morado DR, Cullen HB, Feschotte C, Shepherd JD. Briggs JAG. Structures of virus-like capsids formed by the Drosophila neuronal Arc proteins. *Nat Neurosci.* (2020) 23:172–5. doi: 10.1038/s41593-019-0569-y

49. Budnik V, Thomson T. Structure of an Arc-ane virus-like capsid. *Nat Neurosci.* (2020) 23:153–4. doi: 10.1038/s41593-019-0580-3

50. Eriksen MS, Nikolaienko O, Hallin EI, Grødem S, Bustad HJ, Flydal MI, et al. Arc self-association and formation of virus-like capsids are mediated by an N-terminal helical coil motif. *FEBS.* (2021) 288:2930–55. doi: 10.1111/febs.15618

51. Jenks KR, Kim T, Pastuzyn ED, Okuno H, Taibi AV, Bito H, et al. Arc restores juvenile plasticity in adult mouse visual cortex. *Proc Natl Acad Sci.* (2017) 114:9182–7. doi: 10.1073/pnas.1700866114

52. Nikolaienko O, Patil S, Eriksen MS. Bramham CR. Arc protein: a flexible hub for synaptic plasticity and cognition. *Semin Cell Dev Biol.* (2018) 77:33–42. doi: 10.1016/j.semcdb.2017.09.006

53. Zhang W, Wu J, Ward MD, Yang S, Chuang YA, Xiao M, et al. Structural basis of arc binding to synaptic proteins: implications for cognitive disease. *Neuron.* (2015) 86:490–500. doi: 10.1016/j.neuron.2015.03.030

54. Ufer F, Vargas P, Engler JB, Tintelnot J, Schattling B, Winkler H, et al. Arc/Arg3.1 governs inflammatory dendritic cell migration from the skin and thereby controls T cell activation. *Sci Immunol.* (2016) 1:aaf8665. doi: 10.1126/sciimmunol.aaf8665

55. Marsh APL, Edwards TJ, Galea C, Cooper HM, Engle EC, Jamuar SS, et al. DCC mutation update: Congenital mirror movements, isolated agenesis of the corpus callosum, and developmental split brain syndrome. *Hum Mutat.* (2018) 39:23–39. doi: 10.1002/humu.23361

56. Mans RA, Hinton KD, Rumer AE, Zellner KA, Blankenship EA. Expression of an arc-immunoreactive protein in the adult zebrafish brain increases in response to a novel environment. *Sch Contrib from Membsh Others Artic.* (2018) 76:2018. Available online at: https://digitalcommons.gaacademy.org/gjs/vol76/iss2/2/

57. Soucy SM, Huang J, Gogarten JP. Horizontal gene transfer: building the web of life. *Nat Rev Genet.* (2015) 16:472–82. doi: 10.1038/nrg3962

58. Emamalipour M, Seidi K, Zununi Vahed S, Jahanban-Esfahlan A, Jaymand M, Majdi H, et al. Horizontal gene transfer: from evolutionary flexibility to disease progression. *Front Cell Dev Biol.* (2020) 8:229. doi: 10.3389/fcell.2020.00229

59. Smit AF. Interspersed repeats and other mementos of transposable elements in mammalian genomes. *Curr Opin Genet Dev.* (1999) 9:657–63. doi: 10.1016/S0959-437X(99)00031-3

60. Potasiewicz A, Faron-Gorecka A, Popik P, Nikiforuk A. Repeated treatment with alpha 7 nicotinic acetylcholine receptor ligands enhances cognitive processes and stimulates Erk1/2 and Arc genes in rats. *Behav Brain Res.* (2021) 409:113338. doi: 10.1016/j.bbr.2021.113338

61. Boldridge M, Shimabukuro J, Nakamatsu K, Won C, Jansen C, Turner H, et al. Characterization of the C-terminal tail of the Arc protein. *PLoS ONE.* (2020) 15:239870. doi: 10.1371/journal.pone.0239870

62. Wang YY, Hsu SH, Tsai HY, Cheng FY. Cheng MC. Transcriptomic proteomic analysis of CRISPR/Cas9-mediated ARC-knockout HEK293 cells. *Int J Mol Sci.* (2022) 23:4498. doi: 10.3390/ijms23094498

63. Chuang YA, Hu TM, Chen CH, Hsu SH, Tsai HY, Cheng MC. Rare mutations and hypermethylation of the ARC gene associated with schizophrenia. *Schizophr Res.* (2016) 176:106–13. doi: 10.1016/j.schres.2016.07.019

64. Fromer M, Pocklington AJ, Kavanagh DH, Williams HJ, Dwyer S, Gormley P, et al. De novo mutations in schizophrenia implicate synaptic networks. *Nature.* (2014) 506:179. doi: 10.1038/nature12929

65. Rodríguez C, Areces D, García T, Cueli M, Gonzalez-Castro P. Neurodevelopmental disorders: An innovative perspective via the response to intervention model. *World J psychiatry.* (2021) 11:1017–26. doi: 10.5498/wjp.v11.i11.1017

66. Alhowikan AM. activity-regulated cytoskeleton-associated protein dysfunction may contribute to memory disorder and earlier detection of autism spectrum disorders. *Med Princ Pract.* (2016) 25:350–4. doi: 10.1159/000445351

67. Greer PL, Hanayama R, Bloodgood BL, Mardinly AR, Lipton DM, Flavell SW, et al. The angelman syndrome protein Ube3A regulates synapse development by ubiquitinating arc. *Cell.* (2010) 140:704–16. doi: 10.1016/j.cell.2010.01.026

68. Mandel-Brehm C, Salogiannis J, Dhamne SC, Rotenberg A, Greenberg ME. Seizure-like activity in a juvenile Angelman syndrome mouse model is attenuated by reducing Arc expression. *Proc Natl Acad Sci.* (2015) 112:5129–34. doi: 10.1073/pnas.1504809112

69. Samanta D. Pharmacotherapeutic management of seizures in patients with Angleman syndrome. *Expert Opin Pharmacother.* (2022) 23:1511–22. doi: 10.1080/14656566.2022.2105141

70. Crawford DC, Acuña JM. Sherman SL. fMR1 and the fragile X syndrome: human genome epidemiology review. *Genet Med.* (2001) 3:359. doi: 10.1097/00125817-200109000-00006

71. Berry-Kravis E. Epilepsy in fragile X syndrome. *Dev Med Child Neurol.* (2002) 44:724–8. doi: 10.1111/j.1469-8749.2002.tb00277.x

72. Westmark CJ. Fragile X APP: a decade in review, a vision for the future. *Mol Neurobiol.* (2018) 56:3904–21. doi: 10.1007/s12035-018-1344-x

73. Wilkerson JR, Albanesi JP, Huber KM. Roles for Arc in metabotropic glutamate receptor-dependent LTD and synapse elimination: implications in health and disease. *Semin Cell Dev Biol.* (2018) 77:51–62. doi: 10.1016/j.semcdb.2017.09.035

74. Fernández E, Collins MO, Frank RAW, Zhu F, Kopanitsa MV, Nithianantharajah J, et al. Arc requires PSD95 for assembly into postsynaptic complexes involved with neural dysfunction and intelligence. *Cell Rep.* (2017) 21:679–91. doi: 10.1016/j.celrep.2017.09.045

75. Guzowski JF. Insights into immediate-early gene function in hippocampal memory consolidation using antisense oligonucleotide and fluorescent imaging approaches. *Hippocampus.* (2002) 12:86–104. doi: 10.1002/hipo.10010

76. Borovkova M, Sieryi O, Lopushenko I, Kartashkina N, Pahnke J, Bykov A, et al. Screening of Alzheimer's disease with multiwavelength stokes polarimetry in a mouse model. *IEEE Trans Med Imaging.* (2022) 41:977–82. doi: 10.1109/TMI.2021.3129700

77. Kalchenko V, Harmelin A, Israeli D, Kateb B, Meglinski I, Tang Q, et al. Transcranial dynamic fluorescence imaging for the study of the epileptic seizures. In: Functional Brain Mapping: Methods and Aims. Tsytsarev V, Zhong N, Yamamoto V, (eds). Singapore: Springer Nature Singapore Pte Ltd. (2020). p. 49–66. doi: 10.1007/978-981-15-6883-1_3

78. Dynes JL. Steward O. Dynamics of bidirectional transport of Arc mRNA in neuronal dendrites. *J Comp Neurol.* (2007) 500:433–47. doi: 10.1002/cne.21189

79. Bye CM, McDona RJ. A specific role of hippocampal NMDA receptors and arc protein in rapid encoding of novel environmental representations and a more general long-term consolidation function. *Front Behav Neurosci.* (2019) 13:8. doi: 10.3389/fnbeh.2019.00008

80. Janz P, Hauser P, Heining K, Nestel S, Kirsch M, Egert U, et al. Position-time-dependent arc expression links neuronal activity to synaptic plasticity during epileptogenesis. *Front Cell Neurosci.* (2018) 12:244. doi: 10.3389/fncel.2018.00244

81. Engel JJ. Mesial temporal lobe epilepsy: what have we learned? *Neuroscientist.* (2001) 7:340–52. doi: 10.1177/107385840100700410

82. Walker C. Hippocampal sclerosis: causes and prevention. *Semin Neurol.* (2015) 35:193–200. doi: 10.1055/s-0035-1552618

83. Postnikova TY, Diespirov GP, Amakhin DV, Vylekzhanina EN, Soboleva EB, Zaitsev AV. Impairments of long-term synaptic plasticity in the hippocampus of young rats during the latent phase of the lithium-pilocarpine model of temporal lobe epilepsy. *Int J Mol Sci.* (2021) 22:13355. doi: 10.3390/ijms222413355

84. Malmgren K. Thom, Hippocampal sclerosis–origins M, and imaging. *Epilepsia.* (2012) 53 Suppl 4:19–33. doi: 10.1111/j.1528-1167.2012.03610.x

85. Thom, M. Review: Hippocampal sclerosis in epilepsy: a neuropathology review. *Neuropathol Appl Neurobiol.* (2014) 40:520–43. doi: 10.1111/nan.12150

86. Janz P, Savanthrapadian S, Häussler U, Kilias A, Nestel S, Kretz O, et al. Synaptic remodeling of entorhinal input contributes to an aberrant hippocampal network in temporal lobe epilepsy. *Cereb Cortex.* (2017) 27:2348–64. doi: 10.1093/cercor/bhw093

87. Swann JW. Hablitz, Cellular abnormalities JJ, and synaptic plasticity in seizure disorders of the immature nervous system. *Ment Retard Dev Disabil Res Rev.* (2000) 6:258–67. doi: 10.1002/1098-2779(2000)6:4<258::AID-MRDD5>3.0.CO;2-H

88. Gao X, Grendel J, Muhia M, Castro-Gomez S, Susens U, Isbrandt D, et al. Disturbed prefrontal cortex activity in the absence of schizophrenia-like behavioral dysfunction in Arc/Arg31 deficient mice. *J Neurosci.* (2019) 39:8149. doi: 10.1523/JNEUROSCI.0623-19.2019

89. Barrett T, Wilhite SE, Ledoux P, Evangelista C, Kim IF, Tomashevsky M, et al. NCBI GEO: archive for functional genomics data sets–update. *Nucleic Acids Res.* (2013) 41:gks1193. doi: 10.1093/nar/gks1193

90. Griffin NG, Wang Y, Hulette CM, Halvorsen M, Cronin KD, Walley NM, et al. Differential gene expression in dentate granule cells in mesial temporal lobe epilepsy with and without hippocampal sclerosis. *Epilepsia.* (2016) 57:376–85. doi: 10.1111/epi.13305

91. Morin-Brureau M, Milior G, Royer J, Chali F, LeDuigou C, Savary E, et al. Microglial phenotypes in the human epileptic temporal lobe. *Brain.* (2018) 141:3343–60. doi: 10.1093/brain/awy276

92. Kjær C, Barzaghi G, Bak LK, Goetze JP, Yde CW, Woldbye D, et al. Transcriptome analysis in patients with temporal lobe epilepsy. *Brain.* (2019) 142:E55. doi: 10.1093/brain/awz265

93. Robinson MD, McCarthy DJ. Smyth GK. edgeR: a Bioconductor package for differential expression analysis of digital gene expression data. *Bioinformatics.* (2010) 26:139–40. doi: 10.1093/bioinformatics/btp616

94. Papatheodorou I, Moreno P, Manning J, Fuentes AMP, George N, Fexova S, et al. Expression alas update: from tissues to single cells. *Nucleic Acids Res.* (2020) 48:D77–83. doi: 10.1093/nar/gkz947

95. Majewski L, Wojtas B, Maciag F, Kuznicki J. Changes in calcium homeostasis and gene expression implicated in epilepsy in hippocampi of mice overexpressing ORAI1. *Int J Mol Sci.* (2019). 20. doi: 10.3390/ijms20225539

96. Almeida Silva LF, Reschke CR, Nguyen NT, Langa E, Sanz-Rodriguez A, Gerbatin RR, et al. Genetic deletion of microRNA-22 blunts the inflammatory transcriptional response to status epilepticus and exacerbates epilepsy in mice. *Mol Brain.* (2020) 13:114. doi: 10.1186/s13041-020-00653-x

97. Kapur M, Ganguly A, Nagy G, Adamson SI, Chuang JH, Frankel WN, et al. Expression of the neuronal tRNA n-Tr20 regulates synaptic transmission and seizure susceptibility. *Neuron.* (2020) 108:193. doi: 10.1016/j.neuron.2020.07.023

98. Haigh JL, Adhikari A, Copping NA, Stradleigh T, Wade AA, Catta-Preta R, et al. Deletion of a non-canonical regulatory sequence causes loss of Scn1a expression and epileptic phenotypes in mice. *Genome Med.* (2021) 13:884. doi: 10.1186/s13073-021-00884-0

99. Ritchie ME, Phipson B, Wu D, Hu Y, Law CW, Shi W., Smyth GK. Limma powers differential expression analyses for RNA-sequencing and microarray studies. *Nucleic Acids Res.* (2015) 43:e47–e47. doi: 10.1093/nar/gkv007

100. Venø MT, Reschke CR, Morris G, Connolly NMC, Su J, Yan Y, et al. A systems approach delivers a functional microRNA catalog and expanded targets for seizure suppression in temporal lobe epilepsy. *Proc Natl Acad Sci.* (2020) 117:15977–88. doi: 10.1073/pnas.1919313117

101. Cid E, Marquez-Galera A, Valero M, Gal B, Medeiros DC, Navarron CM, et al. Sublayer- and cell-type-specific neurodegenerative transcriptional trajectories in hippocampal sclerosis. *Cell Rep.* (2021) 35:429560. doi: 10.1101/2021.02.03.429560

102. Chuvakova LN, Funikov SY, Rezvykh AP, Davletshin AI, Evgen'ev MB, Litvinova SA, et al. Transcriptome of the krushinsky-molodkina audiogenic rat strain and identification of possible audiogenic epilepsy-associated genes. *Front Mol Neurosci.* (2021) 14:738930. doi: 10.3389/fnmol.2021.738930

103. Park AY, Park YS, So D, Song IK, Choi JE, Kim HJ, et al. Activity-regulated cytoskeleton-associated protein (Arc/Arg3.1) is transiently expressed after heat shock stress and suppresses heat shock factor 1. *Sci Rep.* (2019) 9:1. doi: 10.1038/s41598-019-39292-1

104. Wall MJ, Collins DR, Chery SL, Allen ZD, Pastuzyn ED, George AJ, et al. The temporal dynamics of arc expression regulate cognitive flexibility. *Neuron.* (2018) 98:1124–32.e7. doi: 10.1016/j.neuron.2018.05.012

105. Gangarossa G, Benedetto Di, O'Sullivan M, Dunleavy M, Alcacer C, Bonito-Oliva A, et al. Convulsant doses of a dopamine D1 receptor agonist result in erk-dependent increases in Zif268 and Arc/Arg31 expression in mouse dentate gyrus. *PLoS ONE.* (2011) 6:e19415. doi: 10.1371/journal.pone.0019415

106. Jiang Y, VanDongen AMJ. Neuronal activity-dependent accumulation of arc in astrocytes. *bioRxiv.* (2020) 2020:11.10.376756. doi: 10.1101/2020.11.10.376756

107. Szyndler J, Maciejak P, Wislowska-Stanek A, Lehner M. Plaznik A. Changes in the Egr1 and Arc expression in brain structures of pentylenetetrazole-kindled rats. *Pharmacol Rep.* (2013) 65:368–78. doi: 10.1016/S1734-1140(13)71012-0

108. Chotiner JK, Nielson J, Farris S, Lewandowski G, Huang F, Banos K, et al. Assessment of the role of MAP kinase in mediating activity-dependent transcriptional activation of the immediate early gene Arc/Arg31 in the dentate gyrus *in vivo*. *Learn Mem.* (2010) 17:117–29. doi: 10.1101/lm.1585910

109. Penrod RD, Thomsen M, Taniguchi M, Guo Y, Cowan CW, Smith LN. The activity-regulated cytoskeleton-associated protein, Arc/Arg3.1, influences mouse cocaine self-administration. *Pharmacol Biochem Behav.* (2020) 188:172818. doi: 10.1016/j.pbb.2019.172818

110. Gao F, Song X, Zhu D, Wang X, Hao A, Victor Nadler J. Zhan, Dendritic morphology RZ, synaptic transmission, and activity of mature granule cells born following pilocarpine-induced status epilepticus in the rat. *Front Cell Neurosci.* (2015) 9:384. doi: 10.3389/fncel.2015.00384

111. Coenen AML. Van Luijtelaar EM. Genetic animal models for absence epilepsy: a review of the WAG/Rij strain of rats. *Behav Genet.* (2003) 33:635–55. doi: 10.1023/a:1026179013847

112. Borges FS, Gabrick EC, Protachevicz PR, Higa GSV, Lameu EL, Rodriguez PXR, et al. Intermittency properties in a temporal lobe epilepsy model. *Epilepsy Behav.* (2023) 139:109072. doi: 10.1016/j.yebeh.2022.109072

113. Blüthgen N, Van Bentum M, Merz B, Kuhl D, Hermey G. Profiling the MAPK/ERK dependent and independent activity regulated transcriptional programs in the murine hippocampus *in vivo*. *Sci Reports.* (2017) 7:1–14. doi: 10.1038/srep45101

114. Chung L, Bey AL, Towers AJ, Cao X, Kim IH, Jiang Y. Lovastatin suppresses hyperexcitability and seizure in Angelman syndrome model. *Neurobiol Dis.* (2018) 110:12–9. doi: 10.1016/j.nbd.2017.10.016

115. Steward O, Matsudaira Yee K, Farris S, Pirbhoy PS, Worley P, Okamura K, et al. Bito, Delayed degradation H, and impaired dendritic delivery of intron-lacking EGFP-Arc/Arg3.1 mRNA in EGFP-Arc transgenic mice. *Front Mol Neurosci.* (2018) 10:435. doi: 10.3389/fnmol.2017.00435

116. Haug K, Kremerskothen J, Hallmann K, Sander T, Dullinger J, Rau B, et al. Mutation screening of the chromosome 8q243-human activity-regulated cytoskeleton-associated gene (ARC) in idiopathic generalized epilepsy. *Mol Cell Probes.* (2000) 14:255–60. doi: 10.1006/mcpr.2000.0314

117. Di Cicco G, Marzano E, Iacovelli L, Celli R, van Luijtelaar G, Nicoletti F, et al. Group I metabotropic glutamate receptor-mediated long term depression is disrupted in the hippocampus of WAG/Rij rats modelling absence epilepsy. *Neuropharmacology.* (2021) 196:108686. doi: 10.1016/j.neuropharm.2021.108686

118. Mano T, Albanese A, Dodt HU, Erturk A, Gradinaru V, Treweek JB, et al. Whole-brain analysis of cells and circuits by tissue clearing and light-sheet microscopy. *J Neurosci.* (2018) 38:9330–7. doi: 10.1523/JNEUROSCI.1677-18.2018

119. Van Luijtelaar G, Hramov A, Sitnikova E. Koronovskii A. Spike-wave discharges in WAG/Rij rats are preceded by delta and theta precursor activity in cortex and thalamus. *Clin Neurophysiol.* (2011) 122:687–95. doi: 10.1016/j.clinph.2010.10.038

120. Managò F, Mereu M, Mastwal S, Mastrogiacomo R, Scheggia D, Emanuele M, et al. Genetic disruption of Arc/Arg31 in mice causes alterations in dopamine and neurobehavioral phenotypes related to schizophrenia. *Cell Rep.* (2016) 16:2116–28. doi: 10.1016/j.celrep.2016.07.044

121. Xing J, Han D, Xu D, Li X, Sun L. CREB protects against temporal lobe epilepsy associated with cognitive impairment by controlling oxidative neuronal damage. *Neurodegener Dis.* (2020) 19:225–7. doi: 10.1159/000507023

122. Zhang H, Bramham CR. Arc/Arg3.1 function in long-term synaptic plasticity: Emerging mechanisms and unresolved issues. *Eur J Neurosci.* (2020) 54:6696–712. doi: 10.1111/ejn.14958

123. Runge K, Cardoso C, de Chevigny A. Dendritic spine plasticity: function and mechanisms. *Front Synaptic Neurosci.* (2020) 12:36. doi: 10.3389/fnsyn.2020.00036

frontiers | Frontiers in Neurology

TYPE Review
PUBLISHED 23 August 2023
DOI 10.3389/fneur.2023.1223074

OPEN ACCESS

EDITED BY
Gilles van Luijtelaar,
Radboud University, Netherlands

REVIEWED BY
Victor Rodrigues Santos,
Federal University of Minas Gerais, Brazil
Vassiliy Tsytsarev,
University of Maryland, United States

*CORRESPONDENCE
Rita Citraro
✉ citraro@unicz.it

†These authors have contributed equally to this work and share first authorship

RECEIVED 15 May 2023
ACCEPTED 14 July 2023
PUBLISHED 23 August 2023

CITATION
Bosco F, Guarnieri L, Leo A, Tallarico M, Gallelli L, Rania V, Citraro R and De Sarro G (2023) Audiogenic epileptic DBA/2 mice strain as a model of genetic reflex seizures and SUDEP. *Front. Neurol.* 14:1223074. doi: 10.3389/fneur.2023.1223074

Audiogenic epileptic DBA/2 mice strain as a model of genetic reflex seizures and SUDEP

Francesca Bosco[1†], Lorenza Guarnieri[1†], Antonio Leo[1,2], Martina Tallarico[1], Luca Gallelli[1,2], Vincenzo Rania[1], Rita Citraro[1,2*] and Giovambattista De Sarro[1,2]

[1]Section of Pharmacology, Science of Health Department, School of Medicine, University "Magna Graecia" of Catanzaro, Catanzaro, Italy, [2]Research Center FAS@UMG, Department of Health Science, University "Magna Graecia" of Catanzaro, Catanzaro, Italy

Epilepsy is a chronic neurological disease characterized by abnormal brain activity, which results in repeated spontaneous seizures. Sudden unexpected death in epilepsy (SUDEP) is the leading cause of seizure-related premature death, particularly in drug-resistant epilepsy patients. The etiology of SUDEP is a structural injury to the brain that is not fully understood, but it is frequently associated with poorly controlled and repeated generalized tonic–clonic seizures (GTCSs) that cause cardiorespiratory and autonomic dysfunctions, indicating the involvement of the brainstem. Both respiratory and cardiac abnormalities have been observed in SUDEP, but not much progress has been made in their prevention. Owing to the complexity of SUDEP, experimental animal models have been used to investigate cardiac and/or respiratory dysregulation due to or associated with epileptic seizures that may contribute to death in humans. Numerous rodent models, especially mouse models, have been developed to better understand epilepsy and SUDEP physiopathology. This review synthesizes the current knowledge about dilute brown agouti coat color (DBA/2) mice as a possible SUDEP model because respiratory arrest (RA) and sudden death induced by audiogenic generalized seizures (AGSs) have been observed in these animals. Respiratory/cardiac dysfunction, brainstem arousal system dysfunction, and alteration of the neurotransmitter systems, which are observed in human SUDEP, have also been observed in these mice. In particular, serotonin (5-HT) alteration and adenosine neurotransmission appear to contribute to not only the pathophysiological mechanisms of medication but also seizure-related respiratory dysfunctions in this animal model. These neurotransmitter systems could be the relevant targets for medication development for chronic epilepsy and SUDEP prevention. We reviewed data on AGSs in DBA/2 mice and the relevance of this model of generalized tonic–clonic epilepsy to human SUDEP. Furthermore, the advantages of using this strain prone to AGSs for the identification of possible new therapeutic targets and treatment options have also been assessed.

KEYWORDS

generalized tonic–clonic seizure, sudden unexpected death in epilepsy, adenosine and serotonin neurotransmission, audiogenic seizures, DBA/2 mice, cardiorespiratory dysfunction

Introduction

Epilepsy is a chronic and debilitating neurologic disease with a high prevalence, which may substantially impair the quality of life. It is associated with cognitive decline and other neuropsychiatric comorbidities, as well as pharmacoresistance development, contributing to increased mortality (1). Sudden unexpected death in epilepsy (SUDEP) is the most frequent cause of epilepsy-related death in drug-resistant epileptic patients, and repeated generalized tonic–clonic seizures (GTCSs) are associated with SUDEP, leading to insistent brain activity damage and enhanced sympathetic activation (2). Seizure activation can propagate to distinct subcortical structures via synaptic connections or, more likely, via spreading depression, which can alter brainstem activity and impair cardiorespiratory function (3). The risk of sudden unexpected death is estimated to be 20 times higher in epileptic patients than in the general population (4). For treating SUDEP, new therapeutic treatments are needed to reduce disease progression and show efficacy against drug-resistant epilepsy, reducing the risk of SUDEP.

Given the unpredictable nature of SUDEP, it is difficult to study the mechanisms by which seizures propagate and impair brainstem function, producing the cardiorespiratory effects that induce it. Significant progress has been made in understanding the SUDEP mechanisms through clinical and experimental studies. Nevertheless, the etiology and pathogenesis of SUDEP are incompletely understood (1, 5). Different clinical and animal studies have indicated that SUDEP occurs due to multifactorial factors and that seizure-induced respiratory dysfunction, together with brainstem system dysfunction and neurotransmitter dysregulation, plays an important role in the mechanism of SUDEP in human and rodents (1, 6).

Genetic factors, such as channelopathies, or susceptibility to heat or audiogenic-induced seizures also contribute to increased predisposition to SUDEP in animal models (7). Studies on genetic mouse models allow for a better understanding of the pathophysiological modifications that lead to SUDEP (5). Usually, mouse models of sound-induced audiogenic generalized seizures (AGSs) are used to study the underlying mechanisms of SUDEP, with the aim of treating and preventing respiratory arrest (RA) due to AGSs (7). In audiogenic susceptible mice, intense auditory stimulation produces severe reflex tonic–clonic seizures that can frequently be lethal, mimicking those observed in human (8). The dilute brown agouti coat color (DBA/2) mice are a model well-established for audiogenic reflex epilepsy induced by sound stimulation, and they were used to investigate new antiseizure medications (ASMs) (9). These mice were also employed in the SUDEP model since they showed generalized convulsive seizures followed by respiratory arrest, which subsequently led to cardiac arrest and sudden death, similar to what is observed in human SUDEP (6, 10). Studies on DBA/2 mice have investigated drugs that reduce immediate RA and seizure-induced death (11). We reviewed the literature with information about DBA/2 mice as a model of SUDEP. We also reviewed the neuronal and biochemical mechanisms of reflex epilepsy and SUDEP, as well as the development of better treatment options.

SUDEP in epilepsy

SUDEP refers to an unexpected, non-traumatic death in children and adults with epilepsy, where postmortem examination does not reveal any anatomical or toxicological cause of death, including drowning (12, 13). Among the most important risk factors for SUDEP are uncontrolled or frequent GTCSs, the duration of epilepsy, prone position at the time of death, young age of first seizure, male sex, neurological comorbidities, polytherapy, ion channel or arrhythmia-related gene mutations, cardiac-respiratory dysfunction, intellectual disability, nocturnal seizures, and non-adherence to ASMs (12, 14). Severe GTCS with a frequency of >3/year have been clarified to induce changes in autonomic functions, resulting in the impairment of respiratory and cardiac functions and predisposing to SUDEP (1).

The incidence of SUDEP is estimated to be 24 times higher in epileptic patients than in the general population, with 1.16 cases per 1,000 epileptic patients per year, and the rate is higher in patients with refractory epilepsy (15). Furthermore, SUDEP reportedly affects all age groups, and its incidence is considered to be less common in young children than in adults, excluding rare diseases such as epileptic syndromes or genetic epilepsies (16). Recently, the risk of SUDEP in children has been found to be potentially greater than that in previous years (from 0.13 to 3.3 per 1,000 patients), especially in children with an increased severity of epilepsy in terms of frequency and type of seizures. Pediatric-specific risk factors include developmental delay and intellectual disability, structural abnormalities, and multiple ASM therapy (17).

The risk of SUDEP was markedly increased in children with genetic epilepsies, Dravet syndrome due to mutations in the *SCN1A*, *SCN8A* encephalopathies, or *DEPDC5* gene mutation-related epilepsy (18–20). However, the incidence of SUDEP in children and young people with epilepsy remains indeterminate because it varies depending on age range, type of epilepsies, epileptic syndromes, or genetic epilepsies, as well as the follow-up period and diagnosis (18). Successive cohort studies have suggested that the incidence of SUDEP is similar between adults and children (i.e., 1.2 per 1,000 people per year), although the incidence may be underestimated in children due to non-epilepsy-related deaths, as a post-mortem/autopsy is often not performed (21). To date, the exact incidence of SUDEP within subgroups of childhood epilepsy is not known.

All the SUDEP cases died at an early age (generally 10–40 years), particularly, patients with intellectual impairment, refractory epilepsy, and poorly controlled epilepsy with a high frequency of GTCS and nocturnal seizures. Studies have suggested a slight male predominance, with the male-to-female ratio being 229:159 (13, 22).

DBA/2 mouse

The DBA/2 inbred strain is genetically susceptible to AGSs, evoked by excessive auditory stimulation. AGSs consist of generalized reflex clonic–tonic convulsions, followed by seizure-induced respiratory arrest (S-IRA) (23). These events, observed in clinical SUDEP, make DBA/2 mice relevant models of SUDEP (23, 24). This strain has been well-described both phenotypically

and genetically (9). In DBA/2 mice, the susceptibility to AGSs varies with age when exposed to intense auditory stimulation (100–120 dB), being maximal between 21 and 28 days of age and then reduced or absent at 40–45 days (25). After intense sound stimulation, DBA/2 mice show seizure sequences characterized by brainstem-dependent wild runs and jumps, followed by clonic seizures characterized by violent convulsions and muscle spasms and, subsequently, tonic seizures characterized by muscle rigidity, culminating in S-IRA, cardiac dysfunction, and death. In DBA/2 mice, death occurs following an excessive tonic phase with hindlimb extension but not from clonic seizures (7), indicating that the tonic phase is probably responsible for S-IRA. Respiratory arrest is fatal unless the death is prevented through oxygenation or mechanical ventilation (26).

In ∼75% of these mice, AGSs are followed by RA, while the remaining 15% of DBA/2 mice exhibit AGSs without RA, indicating that they spontaneously recover from RA post-AGSs (25, 27). In DBA/2 with S-IRA, while RA is the main cause of death, electrocardiographic activity can be detected for ∼5 min after RA, suggesting that cardiac changes occur later (28).

The severity and susceptibility of the seizure to S-IRA decrease after 5 weeks of age due to hearing loss, with hearing thresholds elevated by 15–20 dB (29). This hearing loss may be due to the loss of sensory hair cells, the loss of spiral ganglion neurons, or striatal atrophy (30, 31). Progressive hearing loss has also been attributed to mutations in Cdh23 and Fscn2 (32, 33).

DBA/2 mice are the first example of polygenic heredity in which several mutations can be related to AGSs. More specifically, three loci, including Asp1, Asp2, and Asp3, located on chromosomes 12, 4, and 7, have been correlated with AGSs (34–36). In particular, Asp1 and Asp2 loci seem to be responsible for the manifestations of AGSs (35). These loci are also involved with the regulation of Ca^{2+}-ATPase activity, which is important for synaptic function and neurotransmitter release from synaptic vesicles (34).

DBA/2 mice also express an astrocyte-specific Kcnj10 deletion that has been shown to disrupt the activity of inward rectifying potassium (Kir) 4.1 channels and uptake glutamate (37); this results in low seizure threshold of audiogenic mice compared with the seizure-insensitive C57BL/6J mice (38).

Consequently, Kcnj10 gene polymorphism could play an important role in seizure-threshold differences between DBA/2 and C57BL/6J mice (37). DBA/2 mice are homozygous for allele 1473G and have a lower serotonin (5-HT) synthesis rate compared with C57BL/6J mice; this polymorphism, which alters brainstem serotonergic neurotransmission, contributes to AGSs and S-IRA in these mice (39, 40).

Pathophysiology of audiogenic seizures in DBA/2 mice

The production of AGSs resides in the interaction of brainstem sensory-motor structures in DBA/2 mice (27). In response to intense sound stimulation, a small population of hyperexcited neurons, which are located at the level of the inferior colliculus (IC) of the midbrain, induce the initiation and propagation of AGSs (8, 41). Thus, the IC is considered to be a crucial structure for AGSs onset, but other subcortical structures such as the rostral and medial subcortical regions may be involved (42), resulting in clonic and tonic seizures. These AGSs subsequently exert a negative effect on breathing, inducing S-IRA (41, 43). Studies on DBA/2 mice show that AGSs inhibit the ponto-medullary respiratory control network responsible for breathing control, which leads to apnea or respiratory arrest followed by asystole and death (44).

A key role of the IC in AGSs in DBA/2 mice has been shown by an experimental study, in which bilateral lesions of IC either eliminated or reduced AGS, whereas spreading depression of the cortex either increased latencies or decreased the severity but did not fully abolish AGSs (41). This does not seem to be due to the interruption of sensory input to the cerebral cortex because lesions of other relay nuclei fail to block AGSs (41). Studies based on fos immunochemistry have confirmed that the onset of AGSs is due to enhanced activity within the IC (45). The superior colliculus (SC) is an important modulatory structure in the network of AGSs, and its role is supported by the incomplete attenuation of AGSs through SC lesions (41). Epileptic foci have been also found in the cortex of DBA/2 mice, suggesting an involvement of cortical activities in the generation of AGSs (46). MEMRI data have demonstrated in DBA/1 mice, another model of AGS, changes involving various subcortical structures, such as the superior olivary complex (SOC) of the brainstem, the periaqueductal gray complex, and the amygdala, during AGS. In DBA/1 mice, pathways starting from the SOC play a key role in the neuronal network involved in audiogenic seizures; similarly, in DBA/2 mice, neuronal circuits in the brainstem, spinal cord, and all subcortical areas could also be important (47, 48).

Alteration of neurotransmissions in DBA/2 mice

The susceptibility and severity of AGSs in DBA/2 mice involved several neurotransmitters, such as serotonin (5-TH), adenosine, norepinephrine (NE), dopamine (DA), acetylcholine, glutamate, and GABA (56) (Table 1). Among these neurotransmitters, the serotonergic system is responsible for the generation and transmission of the respiratory rhythm in the brainstem (57), as well as in the modulation of epileptic seizures (58, 59). Accordingly, dysfunction in the brainstem 5-HT system, which results in impaired synaptic transmission and alterations in the expression of 5-TH receptors, is involved in respiratory dysfunction and is associated with a more severe respiratory phenotype in DBA/2 mice (25, 47). These mice generally have lower 5-HT tissue levels than C57/L6 control mice, and the lack of serotonergic signaling of raphe neurons contributes to their increased susceptibility to seizures and RA (39, 60, 61). Therefore, a reduction in 5-TH levels is believed to be responsible for increased seizure susceptibility, while the administration of its precursor 5-hydroxytryptophan (5-HTP), which increases 5-TH brain levels, can attenuate the propagation of AGSs in DBA/2 mice (62). Furthermore, 5-THP has also been found to counteract the reserpine-induced increase of AGSs in DBA/2 mice (63). Alterations of the serotonergic system may also be associated with a more severe respiratory phenotype because DBA/2 mice with fatal RA showed higher levels of tryptophan hydroxylase 2 (TPH2) and serotonin transporter (SERT) than DBA/2 mice with non-fatal RA (44). In addition, DBA/2 mice

TABLE 1 Effects of different monoaminergic receptors on the pathogenesis of SUDEP in DBA/2 mice.

Neurotransmitters	Type of effects	Type of receptors	Respiration	Audiogenic seizures/SUDEP	References
5-HT	Lower 5-HT levels	Increased expression of 5-HT2B	–	+	(25, 47)
		Decreased expression of 5-HT2C, 5-HT3, and 5-HT4	–	+	(11, 40)
Adenosine	Increases in extracellular adenosine	Over-stimulation of adenosine A1 and A2a	–	+	(49)
Noradrenaline	Lower levels	Reduced number of α1-adrenoceptor binding sites	*n*	+	(50)
Dopamine	Lower DA levels		*n*	+	(51)
Glutamate	Increased function	Upregulation of NMDA	*n*	+	(52)
GABA	Decreased function	$GABA_A$	*n*	+	(53–55)

+, activation; –, inhibition; *n*, no evidence.

showed altered expression of 5-HT receptors in the brainstem respiratory nuclei compared with C57BL/6J mice, with diminished expression of 5-HT2C, 5-HT3, and 5-HT4 receptors in the rostral ventral medulla respiratory region and enhanced expression of 5-HT2B receptors (11, 40). The changes in the brainstem 5-HT receptor expression are consistent with the increase of excitation mediated by 5-HT2B elevated expression, and the decrease of inhibition is mediated by decreased 5-HT2C expression; these changes are associated with susceptibility to AGSs and S-IRA in DBA/2 mice (40, 64). Antagonist compounds of 5-HT1C, 5-HT3, 5-HT4, and 5-HT7 receptors had anticonvulsant effects, increasing the latency of AGSs and decreasing the severity of seizures (65, 66), while antagonist compounds of 5-HT2 receptors increased the S-IRA incidence following seizures in DBA/2 mice (25).

Furthermore, the decrease of AGSs has been found with an inhibitor of tryptophan hydroxylase, parachlorophenylalanine (PCPA), or 5-HT receptor antagonists (66, 67). Therefore, reduced 5-TH neurotransmission due to depletion of the reserve or antagonism of 5-HT receptors are factors that may exert protection against AGSs in DBA/2 mice (40).

Owing to the effects exerted by 5-HT on respiration and seizures, it can be suggested that drugs that enhance the activity of this neurotransmitter might be useful in SUDEP prevention. Consequently, treatment with fluoxetine, a selective serotonin reuptake inhibitor (SSRI), has been found to be effective in preventing S-IRA and death, without affecting the severity of AGSs in DBA/2 mice (25).

Furthermore, the administration of fluoxetine at higher doses was able to reduce the occurrence of tonic seizures preceding the S-IRA (25). Additionally, the combined administration of serotonin uptake inhibitors and monoamine oxidase-A (MAO) inhibitors diminished AGSs in DBA/2J mice (62). On the contrary, the administration of cyproheptadine, a non-selective 5-HT receptor antagonist, increased susceptibility to S-IRA in 10% of DBA/2 mice, confirming further involvement of the serotonergic system in S-IRA (25). Therefore, genetic alterations of the 5-HT system, such as specific 5-HT receptor subtype expression abnormalities or reduced levels of the 5-HT-synthesizing enzyme tryptophan hydroxylase, can be responsible for the susceptibility to S-IRA of DBA/2 mice (40, 47).

Adenosine is another neurotransmitter that exerts its action on the respiratory centers of the brainstem, and an increase in its levels, induced by seizures, may contribute to SUDEP (68). From this neurotransmitter, that serotonin and adenosine show the opposite effects on respiratory suppression. While elevated serotonin levels in the brainstem can prevent S-RIA and death in DBA/2 mice, overstimulation of adenosine receptors in the brainstem can induce respiratory arrest (28). Some studies have shown that molecules such as caffeine, a non-selective adenosine receptor antagonist, or SCH 442416, an A2A receptor antagonist, decrease the occurrence of S-IRA in DBA/2 mice. Other studies have demonstrated that DPCPX, a selective adenosine A1 antagonist, did not alter S-IRA, suggesting that excessive A2A receptor activation makes DBA/2 mice more vulnerable to S-IRA (28, 69). The inhibition of adenosine metabolism by pretreatment with 5-iodotubercidin (5-ITU) increased the susceptibility to S-IRA of DBA/2 mice, which initially displayed only AGSs, indicating that excessive adenosine signaling may contribute to seizure-induced death in these mice (28). Reduced brain levels of NE and DA are also responsible for increased AGS susceptibility (51). Generally, DBA/2 mice show lower levels of NE and DA in the brain than C57BL/6J mice; the administration of Levodopa (L-DOPA) was found to attenuate AGS in DBA/2 mice by increasing the brain levels of these neurotransmitters, particularly DA, which is the active principle formed from L-DOPA (51, 70).

In addition to L-DOPA, dopaminergic receptor agonists, such as apomorphine and other related compounds, showed protection against AGS in DBA/2 mice (71).

Alterations in the glutamatergic and GABAergic neurotransmission are also involved in the generation of AGS in DBA/2 mice (9, 72). Regarding glutamatergic neurotransmission, an increased NMDA-mediated glutamate release has been found to occur in 21–30-day-old DBA/2 mice through a nitric oxide (NO)-mediated mechanism (73). At this age and following audiogenic stimulation, the enhanced NO generation in DBA/2 mice was 2-fold compared with DBA/2 mice, which were not exposed to acoustic stimulation, indicating the involvement of

NO in the occurrence of AGS (74). The antagonists of ionotropic and metabotropic glutamatergic receptors exerted inhibitory effects on AGS, supporting the involvement of glutamatergic neurotransmission (75–78). In particular, a functional NMDA-mediated upregulation responsible for the generation of AGS has been shown in DBA/2 mice, and the administration of an antisense probe for the NMDA receptor (NR1 subunit) has been shown to induce a complete suppression of AGS, accompanied by a small (20%) reduction in the NMDA receptor levels (79).

A deficit of GABAergic neurotransmission, in IC neurons, is also implicated in the AGS susceptibility of DBA/2 mice (80), and drugs that increase GABA concentration or mimic its postsynaptic actions reduced the occurrence and severity of AGS (81, 82). In DBA/2 mice at various ages, before, during, and after the period of maximal AGS, no changes in brain GABA concentration and glutamic acid decarboxylase (GAD) activity were found, which means that the susceptibility to AGS does not result from the reduced ability to synthesize and store GABA (83). Instead, lower binding sites for GABA in the brain of DBA/2 mice, compared with other non-susceptible strains, have been reported (84), and this reduction has been correlated with the age of susceptibility seizures (83). However, the affinities of these binding sites were found to be higher in DBA/2 mice than in control mice of the same age (85, 86). Studies on receptor binding, chloride flux, and response to $GABA_A$ receptor drugs have suggested $GABA_A$ receptor alterations in DBA/2 mice (53–55). In particular, a decreased density of benzodiazepine 3H-flunitrazepam binding sites in 28- to 29-day-old DBA/2 mice has been reported, suggesting a delayed development of these binding sites (85). Other studies have found an increase in benzodiazepine 3H-flunitrazepam binding sites in DBA/2 mice (at ∼22 days of age) compared with age-matched C57BL/6J mice (87). For these reasons, the use of $GABA_A$ agonists, GABA transaminase inhibitors, and some inhibitors of GABA reuptake may be useful in reducing the incidence and severity of AGS in DBA/2 mice (85, 88–90). An indirect involvement of GABA neurotransmission in AGS in DBA/2 has been also suggested by another study, in which gastrin-releasing peptide (GRP), a selective agonist for the BB2 subtype of bombesin receptor, was able to reduce AGS in audiogenic DBA/2 mice, probably through an increase of GABAergic function (91) (Figure 1).

In addition to neurotransmitters, synaptic hyperactivity and the sustained increase in circulating catecholamines are also involved in AGS and S-IRA; repeated induction of generalized seizures in DBA/2 mice can lead to Ca^{2+} overload and oxidative stress, which trigger mitochondrial dysfunction by generating reactive oxygen species (ROS) with consequent cardiomyocyte death (92–94).

Efficacy studies of different drugs on AGS in DBA/2 mice

DBA/2 mice have been widely used not only as a genetic model of generalized reflex epilepsy but also for screening novel compounds to predict the clinical utility of novel treatments for drug-resistant epilepsy (78, 95).

All clinically used ASMs (carbamazepine, oxcarbazepine, felbamate, gabapentin, lamotrigine, phenytoin, phenobarbital, ethosuximide, levetiracetam, topiramate, valproate, brivaracetam, and perampanel) have shown efficacy against AGS in DBA/2 mice (9, 95–97) (Table 2).

In addition, different studies have demonstrated the efficacy of classical benzodiazepines and their derivatives, 1,4-benzodiazepines and 1,5-benzodiazepines (82, 102). The different degree of anticonvulsant activity appears to be related to the benzodiazepine binding affinity (inhibition of [3H]flunitrazepam binding) (82, 89, 102). Compounds blocking the uptake of GABA (ethyl nipecotate and nipecotic acid) into neurons or glia and structurally diverse positive allosteric modulators of $GABA_B$ receptors showed protection against AGS in DBA/2 mice (81, 103). Compounds that block excitatory neurotransmission by acting as antagonists at the NMDA and AMPA receptors showed the anticonvulsant effects in DBA/2 mice (75, 104).

Riluzole, a drug approved for the treatment of amyotrophic lateral sclerosis, was found to be protective against AGS in DBA/2 mice, with full protection against sound-induced tonic extension; this effect is reportedly due to the interaction of riluzole with glycine/NMDA and AMPA/kainate receptors (105).

Co-treatment of topiramate (TPM) with L-type Ca^{2+} channel modulators (nifedipine and Bay k 8644) or with AMPA/kainate receptor antagonists (NBQX and CFM) showed protection against tonic and clonic seizures in audiogenic mice (106).

The anticonvulsant effects of various other compounds, such as substances that enhance the 5-HT system (107), ligands for adenosine receptors (28, 69, 108), and carbapenem derivatives (109), have been also evaluated in DBA/2 mice. Treatment with cannabinoid receptor (CB1R) agonists has shown anticonvulsant effects against AGS, suggesting the involvement of these receptors in the susceptibility of DBA/2 mice to AGS (110). Similarly, cannabis-derived compounds, such as cannabidiol (CBD) and cannabidivarin (CBDV), have been shown to reduce AGS incidence, and the co-administration of CBD and CBDV showed synergic effects against AGS in audiogenic mice, blocking both clonic and tonic seizures through different mechanisms of CB1R (111, 112). Carbenoxolone, a chemical gap junction blocker, was shown to reduce the severity of AGS in DBA/2 mice, suggesting the role of connexins in epileptic seizures (113). Gap junctions play an important role in the neuronal network for both synchronized neuronal activity and field potential oscillations. During epileptic seizures and intercritical phases, electroencephalogram (EEG) signals and the degree of electrical coupling to the astrocytic gap junction were found to be correlated, contributing to the synchronization of the neuronal cell networks and inducing recurrent epileptiform activity (114). The antiepileptic effects of carbenoxolone could be due to its capacity to block both spontaneous bursts and epileptiform activity of neurons, although it does not do so directly. It seems to block the gap junction between astrocytes, suppressing their synchronization and supporting the possible direct involvement of the astrocytic gap junction in epileptiform activity and the indirect involvement in neurons (115). Among the different connexins (CX26, CX36, and CX32), CX43 has been found to affect epileptic seizures; its expression and electrical conduction have been found to increase after seizure, which can be reduced by carbenoxolone (114, 116).

The potential synergism of carbenoxolone with ASM, as well as the pharmacodynamic potentiation of ASM effects by statins, cannabinoid receptors agonists (98, 110), beta-adrenoceptor

10.3389/fneur.2023.1223074

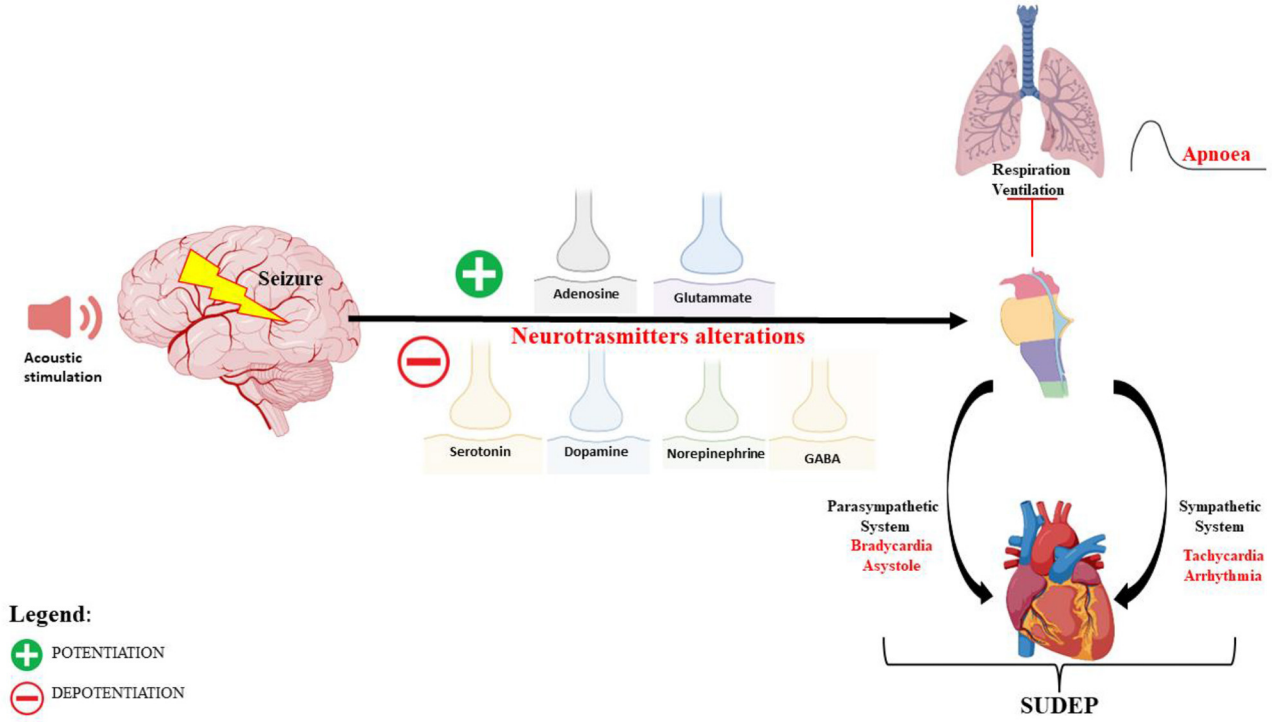

FIGURE 1
Schematic representation of the neuronal network and mechanisms of autonomic central cardiorespiratory dysfunction during seizure following audiogenic stimulation in DBA/2 mice.

TABLE 2 ED50 values (±95% confidence limits) of some ASMs against audiogenic seizures in DBA/2 mice.

ASM	Wild running	Clonus	Tonus	References
Carbamazepine	10.6 (8.1–13.8)	4.4 (3.6–5.4)	3.0 (2.6–3.8)	(98, 99)
Diazepam	0.49 (0.34–0.71)	0.28 (0.2–0.39)	0.24 (0.15–0.39)	(98, 99)
Ethosuximide	290 (207–406)	138 (96–198)	90 (70–116)	(98, 99)
Felbamate	114.6 (92–142.7)	48.8 (35–67)	23.1 (12.1–44)	(98, 99)
Gabapentin	38 (16–51)	20.3 (13.7–30.2)	13.9 (8.7–22.3)	(98, 99)
Gabapentin	38 (16–51)	20.3 (13.7–30.2)	13.9 (8.7–22.3)	(98, 99)
Lamotrigine	6.1 (4.6–8.1)	3.5 (2.4–5.1)	1.1 (0.7–1.8)	(98, 99)
Levetiracetam	15.38 (12.17–19.45)	9.77 (7.22–13.22)	7.89 (5.89–10.57)	(98, 99)
Oxcarbazepine	11.4 (9.7–13.3)	4.2 (3.0–5.88)	3.2 (2.7–3.79)	(98, 99)
Perampanel	ND	ND	0.47	(100)
Phenobarbital	7.1 (5.6–9.0)	3.4 (2.3–5.0)	2.4 (1.7–3.4)	(98, 99)
Phenytoin	4.3 (3.1–6.0)	2.5 (1.8–3.5)	2.0 (1.6–2.5)	(98, 99)
Retigabine	12.52 (9.92–15.8)	6.78 (4.60–9.99)	4.83 (2.98–7.83)	(98, 99)
Topiramate	22.9 (15.8–33.9)	12.12 (6.94–21.15)	6.12 (3.48–20.88)	(98, 99)
Valproate	84 (63–114)	43 (33–56)	31 (22–43)	(98, 99)
Brivaracetam	ND	2.4 (1.4–4.0)	ND	(101)
Unmodified CBDV BDS	127.56 (92. 39–176.12)	73.81 (53.24–102.34)	50.93 (29.85–86.88)	Unpublished data

Data are expressed in mg/kg. ND, not determined.

antagonists (117), and D-cycloserine, has been also studied in audiogenic DBA/2 mice (118). The potential anticonvulsant effects of a natural product, i.e., flavonoid-rich extract from orange juice (OJe), and its possible mechanism of action, were also studied on AGS-sensible DBA/2 (119). Finally, the protective effects of the new isoquinoline sulfonamides on AGS in DBA/2 mice were investigated by selectively inhibiting the isoforms of human carbonic anhydrase II and VII (hCA II and hCA VII) (120).

DBA/2 mice as relevant models of human SUDEP

Animal models, in particular, genetically altered mice, develop spontaneous or induced seizures leading to death, and these models are able to show the role of autonomic dysregulation respiratory mechanisms that precede death. DBA/2 mice experience AGS when they are exposed to high-intensity acoustic stimulation, and these seizures are followed by a high occurrence of S-IRA, cardiac arrest, and sudden death, making these mice a valid model of human SUDEP (7, 121, 122) (Figure 2). In these mice, S-IRA, resulting from AGS, leads to subsequent death if not rapidly prevented by oxygen administration or mechanical ventilation, similar to epileptic patients (6, 26). Generalized seizures, particularly uncontrolled ones, are important risk factors for SUDEP because they propagate trans-synaptically or by spreading depression and interrupt the brainstem functions that control cardiorespiratory activity and its connections to cortical, diencephalic, and spinal cord areas. This causes RA with subsequent cardiac failure, mechanisms that are proposed as the main cause of human SUDEP (122, 124).

DBA/2 mice die in the tonic phase with hindlimb extension similar to human SUDEP with motor convulsive seizures (125). Death immediately following an AGS occurs with sequential events, including immediate respiratory failure followed by cardiac depression; this is observed in DBA/2 mice and is similarly observed in human SUDEP (24, 126). In DBA/2 mice, RA always precedes cardiac arrest, similar to terminal apnea, which is commonly responsible for human SUDEP. Therefore, altered brainstem function is linked with respiratory and cardiac dysfunctions, followed by terminal apnea and asystole, leading to SUDEP in both DBA/2 mice and epileptic patients.

The common cardiopulmonary events that contribute to death make DBA/2 mice an important model for evaluating the mechanisms of these events and translating this knowledge into the development of new strategies for SUDEP prevention.

The advantage of using DBA/2 mice as the SUDEP model is given by the predictability of seizures, allowing for the resuscitation of these mice and the repetition of tests and, consequently, the possibility to determine the mechanisms of RA (28).

In DBA/2 mice, AGS spreads to brainstem laryngomotor areas, causing laryngospasm and associated obstructive apnea with consequent death; the implantation of a surrogate airway protecting against death suggests that both laryngospasm and associated obstructive apnea are part of a common mechanism that leads to SUDEP in epileptic patients and murine species (24, 127). DBA/2 mice not only present many key features of human SUDEP, including autonomic dysregulation, apnea, hypoventilation, and cardiac arrhythmias, but also suggest the potential molecular mechanisms of SUDEP, such as modifications of serotonergic and adenosinergic neurotransmission, which significantly alter not only the seizure activity but also the brainstem respiratory network. 5-HT and adenosine show opposite effects on respiratory function (11, 28). Serotonergic neurons stimulate breathing, and the loss of brainstem serotonergic control of cardiorespiratory function induced by seizures can cause prolonged hypoventilation or apnea, contributing to SUDEP (128). In DBA/2 mice, the loss of serotonergic neurons reportedly induces S-IRA, the main factor for SUDEP (47), and the enhancement of 5-HT function in the brainstem with SSRI treatment reportedly reduces the occurrence of S-IRA (128). Similarly, dysregulation of serotonergic brainstem neurons, which regulate brainstem respiratory centers, and spreading of depolarization have been found in epileptic drug-resistant patients, and they have been correlated with an increased risk of human SUDEP (11, 25). Consequently, SSRI treatment has shown some protective effects by reducing the incidence of central apnea in SUDEP patients (129, 130). In addition, DBA/2 mice were found to exhibit diminished expression of 5-HT2C, 5-HT3, and 5-HT4 receptors in the rostral ventral medulla respiratory region; similar abnormalities of these 5-HT receptors expression were found in sudden infant death syndrome (131). Therefore, in addition to the evidence of the effect of serotonergic neurotransmission on seizure susceptibility, increases in 5-HT may positively affect seizure-related respiratory events associated with SUDEP in animal models and humans.

Furthermore, adenosine is also a possible contributor to SUDEP (49); excessive adenosine release and overactivation of adenosine receptors, induced by seizures, may give rise to excessive inhibition of brainstem respiratory centers; this causes lethal apnea or cardiac arrest, potentiating SUDEP through respiratory suppression in DBA/2 mice (28). The administration of caffeine, an adenosine receptor antagonist, reduced the incidence of seizure-induced RA, thus preventing SUDEP in audiogenic DBA/2 mice (28). Similarly, in different brain areas of epileptic patients, an altered adenosinergic system has been observed with the overactivation of A2A receptors, resulting in cardiorespiratory dysfunctions and increased risk of SUDEP (132). Consequently, the blockade of adenosine receptors should prevent SUDEP in human and experimental models (133, 134).

The translational research obtained in this experimental model has allowed us to identify that the serotonergic and adenosine neuronal networks of the brainstem may share a common final pathway with human SUDEP, and drugs that act on these neurotransmission systems may be potential targets for SUDEP prevention. Furthermore, the knowledge of cardiac and/or respiratory alterations due to AGS, which may contribute to sudden death in DBA/2 mice, indicates the translational potential of the use of these animals in clinical studies on SUDEP (135).

The elevated occurrence of death after AGS in DBA/2 mice suggests the existence of a genetic predisposition to respiratory depression, supporting the hypothesis of the presence of genetic predictors of SUDEP (40, 136).

Compared with other models, such as kainic acid (KA) or the pilocarpine animal model of status epilepticus (SE), the DBA/2

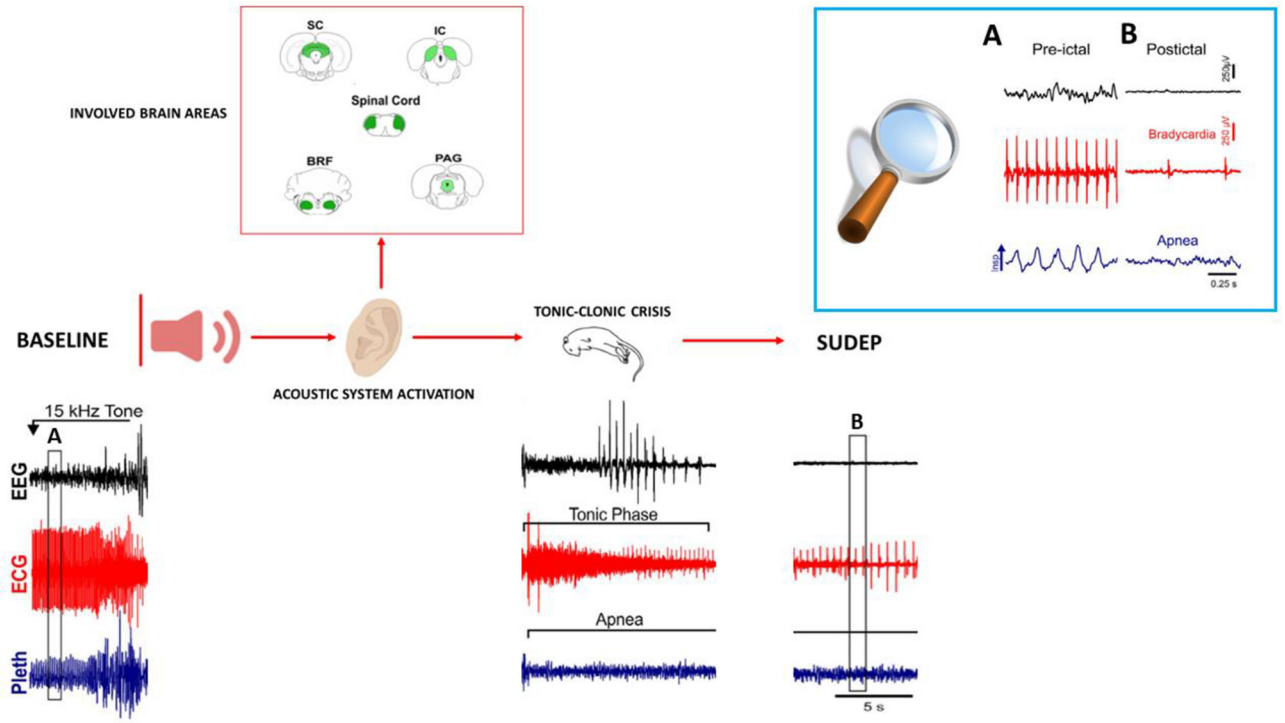

FIGURE 2
Representation of brain areas involved in AGS, and representative patterns of EEG (electroencephalogram), ECG (electrocardiogram) changes, and respiration (plethysmometer) before seizure onset, during the tonic–clonic phase up to SUDEP in audiogenic DBA/2 mice. The upper right box **(A, B)** shows the expanded traces from the corresponding boxes of the recordings shown below. All patterns are re-adapted by Wenker (123) in "Postictal death is associated with tonic phase apnea in a mouse model of sudden unexpected death in epilepsy."

model has several advantages. One advantage of DBA/2 mice is that their death is not associated with SE, and they exhibit sudden death immediately after AGS. Their death is a result of RA, leading to subsequent cardiac failure, in agreement with the findings obtained in many cases of human SUDEP (3, 26). This distinct feature makes DBA/2 mice relevant SUDEP models. KA or pilocarpine-induced SE is useful as a model for human temporal lobe epilepsy (137), but these models do not induce SUDEP-like seizures. In fact, pilocarpine or KA injection produces SE in a healthy brain, a condition that is excluded from the current definition of SUDEP (2). Seizures appear in limbic and neocortical structures, but the seizure onset is believed to reside in the hippocampal formation with consequent hippocampal neurodegeneration and neuroinflammation, unlike what is observed in DBA/2 mice (138, 139).

Variability in SE induction and in the frequency and severity of spontaneous seizures, as well as variable mortality among different rodent strains, have also been found in SE animal models, causing difficulty not only in reproducing the TLE model but also in considering it a SUDEP model (140–142). Regarding the variability in the mechanisms of death, the mortality ranges from 5 to 30% in the SE KA-induced model (138), while in the pilocarpine model, mortality is much higher since ∼30–40% of treated animals do not survive SE, and there are difficulties in SE induction due to pilocarpine-resistant animals (143, 144). Therefore, in these models, mice that died within 7 days from SE induction are believed to have failed to develop SE. Therefore, they are not considered to have died of SUDEP since they likely did not develop spontaneous seizures. Unlike audiogenic DBA/2 mice in which seizure-induced respiratory depression leads to sudden death, some of these animals can show small seizure activity, some can also show transient apnea, and others can show respiratory depression. Therefore, it is not possible to understand which of these behaviors are related to SUDEP manifestation. Additionally, in these animal models of SE, significant changes in cardiac structure and function are found after the SE period (145).

Some studies reported obstructive apnea, cardiac dysfunction, and death as a response to KA-induced seizure (146), while other studies showed that some mice, survived by pilocarpine-induced SE, died suddenly after several weeks when they developed spontaneous seizures (147, 148). However, these responses to KA or pilocarpine-induced SE are different from mechanisms that cause respiratory depression and death in the DBA/2 model. In addition, genetic mutations together with neurotransmission alterations can explain the higher susceptibility to AGS and the consequent death of DBA/2 mice.

Although this audiogenic model more strongly resembles human SUDEP in many respects, DBA/2 mice present some limitations to achieving a full comprehension of respiratory dysfunction in chronic epilepsy and SUDEP, which is because AGS and S-IRA are induced by intense acoustic stimulation, and these mice do not develop spontaneous recurrent seizures unlike

what occurs in human SUDEP, which in any case results from spontaneous seizures (28). Furthermore, in DBA/2 mice, there is a high incidence of death after AGSs, while the probability of sudden death after an epileptic seizure is lower in patients (5). In particular, in DBA/2 mice, if AGS-induced fatal RA is not prevented, they die (11), whereas epileptic patients who die of SUDEP can have numerous seizures before the fatal event occurs (1).

In addition, the susceptibility to AGS of DBA/2 mice seems to be age-dependent, being high in young mice (21–28 days postnatal) and decreasing with age. The young age at which DBA/2 mice show susceptibility to AGS could be a limitation in transferring the results to human settings, particularly in investigating any chronic treatment, which would be needed for human SUDEP prevention. For this, DBA/2 mice may be appropriate as an acute mouse model of SUDEP. However, the young age at epilepsy onset and the duration of the seizure disorder, which often occurs during childhood, are the main risks of human SUDEP (17). In particular, the risk of SUDEP is greater for patients with childhood-onset epilepsy that is chronic and persists into adulthood than for patients with epileptic seizures that appear in adulthood. The clinical implication of this age-dependent susceptibility to seizure may be related to the higher incidence of sudden death in children with severe forms of epilepsy than in adults. However, recent studies in children have documented a similar incidence to that of adults (21). Despite these differences, studies of sudden death in young AGS-susceptible mice may be useful for increasing the knowledge of complex pathophysiologic mechanisms underlying human SUDEP and for assessing potential therapies to prevent SUDEP.

Conclusion

In epilepsy, SUDEP is a major clinical problem for epileptic patients and their families. Although different studies have identified numerous risk factors for SUDEP, we are still unable to prevent or diminish the incidence of SUDEP. Furthermore, although adherence patterns in ASM can limit seizures in most patients, they do not alter long-term prognosis or prevent epilepsy progression or the risk of SUDEP. The high mortality rate associated with certain types of epilepsy points to respiratory depression, decreased heart frequency, autonomic dysfunction, and altered neurotransmitter systems in the brainstem. Although treatments such as SSRIs and adenosine antagonists have been experimented with, their clinical application remains limited.

Studies in animal models of epilepsy are essential to help understand the pathophysiological mechanisms associated with seizures and SUDEP. In particular, DBA/2 strains are inbred mice prone to AGS-induced fatal RA and frequently used as SUDEP models. These mice not only summarize numerous key features of human SUDEP, including altered cardiorespiratory function and pulmonary impairment following audiogenic seizures, but also allow for accurate investigations of molecular mechanisms present in SUDEP, such as serotonergic and adenosinergic dysfunctions and genetic susceptibility. Brainstem neurotransmitters may provide new targets for interventions to prevent premature death from SUDEP.

Translation of basic experimental research into human epilepsy could be represented by DBA/2 mice, whose response to ASM has permitted the development of new medications and therapy trials.

However, in this experimental model, SUDEP susceptibility is related to acoustic stress only at a young age. Therefore, DBA/2 mice could represent only an acute SUDEP model. However, given the translational value of the knowledge that can emerge from using this animal model, it would be advisable to carry out further and more specific studies.

Author contributions

FB, LGa, and AL conceptualized the manuscript framework, performed literature research, and drafted the manuscript. MT, LGu, and VR were also involved in drafting the manuscript and creating the tables. RC and GD critically reviewed the manuscript. All authors reviewed the drafted manuscript for critical content and approved the final version.

Funding

AL, RC, and GD received funding from #NEXTGENERATIONEU (NGEU), the Ministry of University and Research (MUR), the National Recovery and Resilience Plan (NRRP), and the MNESYS (PE0000006) project–a multiscale integrated approach to the study of the nervous system in health and disease (DN. 1553 11.10.2022).

Conflict of interest

The authors declare that the research was conducted in the absence of any commercial or financial relationships that could be construed as a potential conflict of interest.

Publisher's note

References

1. Zhao H, Long L, Xiao B. Advances in sudden unexpected death in epilepsy. *Acta Neurol Scand.* (2022) 146:716–22. doi: 10.1111/ane.13715

2. Mesraoua B, Tomson T, Brodie M, Asadi-Pooya AA. Sudden unexpected death in epilepsy (SUDEP): Definition, epidemiology, and significance of education. *Epilepsy Behav.* (2022) 132:108742. doi: 10.1016/j.yebeh.2022.108742

3. Katayama PL. Cardiorespiratory dysfunction induced by brainstem spreading depolarization: a potential mechanism for SUDEP. *J Neurosci.* (2020) 40:2387. doi: 10.1523/JNEUROSCI.3053-19.2020

4. Bauer J, Devinsky O, Rothermel M, Koch H. Autonomic dysfunction in epilepsy mouse models with implications for SUDEP research. *Front Neurol.* (2023) 13:1040648. doi: 10.3389/fneur.2022.1040648

5. Pansani AP, Colugnati DB, Scorza CA, De Almeida ACG, Cavalheiro EA, Scorza FA. Furthering our understanding of SUDEP: the role of animal models. *Expert Rev Neurother.* (2016) 16:561–72. doi: 10.1586/14737175.2016.1169925

6. Manolis TA, Manolis ASA, Melita H, Manolis ASA. Sudden unexpected death in epilepsy: the neuro-cardio-respiratory connection. *Seizure.* (2019) 64:65–73. doi: 10.1016/j.seizure.2018.12.007

7. Martin B, Dieuset G, Pawluski JL, Costet N, Biraben A. Audiogenic seizure as a model of sudden death in epilepsy: a comparative study between four inbred mouse strains from early life to adulthood. *Epilepsia.* (2020) 61:342–9. doi: 10.1111/epi.16432

8. Ross KC, Coleman JR. Developmental and genetic audiogenic seizure models: behavior and biological substrates. *Neurosci Biobehav Rev.* (2000) 24:639–53. doi: 10.1016/S0149-7634(00)00029-4

9. De Sarro G, Russo E, Citraro R, Meldrum BS. Genetically epilepsy-prone rats (GEPRs) and DBA/2 mice: two animal models of audiogenic reflex epilepsy for the evaluation of new generation AEDs. *Epilepsy Behav.* (2017) 71:165–73. doi: 10.1016/j.yebeh.2015.06.030

10. Mameli O, Caria MA. *Sudden Death in Epilepsy : Forensic and Clinical Issues (1).* In: Lathers CM, Schraeder PL, Bungo MW, editors. (2010). p. 591–613. Available online at: https://www.routledge.com/Sudden-Death-in-Epilepsy-Forensic-and-Clinical-Issues/Lathers-Schraeder-Bungo-Leestma/p/book/9781439802229 (accessed April 17, 2023).

11. Feng HJ, Faingold CL. Abnormalities of serotonergic neurotransmission in animal models of SUDEP. *Epilepsy Behav.* (2017) 71:174–80. doi: 10.1016/j.yebeh.2015.06.008

12. Sveinsson O, Andersson T, Mattsson P, Carlsson S, Tomson T. Clinical risk factors in SUDEP: a nationwide population-based case-control study. *Neurology.* (2020) 94:e419–29. doi: 10.1212/WNL.0000000000008741

13. Yan F, Zhang F, Yan Y, Zhang L, Chen Y. Sudden unexpected death in epilepsy: investigation of autopsy-based studies. *Front Neurol.* (2023) 14:1126652. doi: 10.3389/fneur.2023.1126652

14. Sahly AN, Shevell M, Sadleir LG, Myers KA. SUDEP risk and autonomic dysfunction in genetic epilepsies. *Auton Neurosc.i.* (2022) 237:102907. doi: 10.1016/j.autneu.2021.102907

15. Donnan AM, Schneider AL, Russ-Hall S, Churilov L, Scheffer IE. Rates of status epilepticus and sudden unexplained death in epilepsy in people with genetic developmental and epileptic encephalopathies. *Neurology.* (2023) 100:e1712–e1722. doi: 10.1212/WNL.0000000000207080

16. Abdel-Mannan O, Taylor H, Donner EJ, Sutcliffe AG. A systematic review of sudden unexpected death in epilepsy (SUDEP) in childhood. *Epilepsy Behav.* (2019) 90:99–106. doi: 10.1016/j.yebeh.2018.11.006

17. Whitney R, Sharma S, Ramachandrannair R. Sudden unexpected death in epilepsy in children. *Dev Med Child Neurol.* (2023). doi: 10.1111/dmcn.15553

18. Trivisano M, Muccioli L, Ferretti A, Lee HF, Chi CS, Bisulli F. Risk of SUDEP during infancy. *Epilepsy Behav.* (2022) 131:107896. doi: 10.1016/j.yebeh.2021.107896

19. Mastrangelo M, Esposito D. Paediatric sudden unexpected death in epilepsy: from pathophysiology to prevention. *Seizure.* (2022) 101:20. doi: 10.1016/j.seizure.2022.07.020

20. Shmuely S, Sisodiya SM, Gunning WB, Sander JW, Thijs RD. Mortality in Dravet syndrome: a review. *Epilepsy Behav.* (2016) 64:69–74. doi: 10.1016/j.yebeh.2016.09.007

21. Keller AE, Whitney R, Li SA, Pollanen MS, Donner EJ. Incidence of sudden unexpected death in epilepsy in children is similar to adults. *Neurology.* (2018) 91:e107–11. doi: 10.1212/WNL.0000000000005762

22. Abdel-Mannan O, Venkatesan TC, Sutcliffe AG. Paediatric sudden unexpected death in epilepsy (SUDEP): is it truly unexplained? *Paediatr Child Health.* (2022) 32:382–7. doi: 10.1016/j.paed.2022.07.010

23. Faingold C, Tupal S, N'Gouemo P. Genetic Models of Reflex Epilepsy and SUDEP in Rats and Mice. *Model Seiz Epilep Second Ed.* (2017) 441–53. Chapter 31. doi: 10.1016/B978-0-12-804066-9.00032-8

24. Irizarry R, Sukato D, Kollmar R, Schild S, Silverman J, Sundaram K, et al. Seizures induce obstructive apnea in DBA/2J audiogenic seizure-prone mice: lifesaving impact of tracheal implants. *Epilepsia.* (2020) 61:e13–6. doi: 10.1111/epi.16431

25. Tupal S, Faingold CL. Evidence supporting a role of serotonin in modulation of sudden death induced by seizures in DBA/2 mice. *Epilepsia.* (2006) 47:21–6. doi: 10.1111/j.1528-1167.2006.00365.x

26. Venit EL, Shepard BD, Seyfried TN. Oxygenation prevents sudden death in seizure-prone mice. *Epilepsia.* (2004) 45:993–6. doi: 10.1111/j.0013-9580.2004.02304.x

27. Faingold CL, Tupal S. Neuronal network interactions in the startle reflex, learning mechanisms, and cns disorders, including sudden unexpected death in epilepsy. *Neuronal Networks Brain Funct CNS Disord Ther.* (2014) 407–18. Chapter 29. doi: 10.1016/B978-0-12-415804-7.00029-0

28. Faingold CL, Randall M, Kommajosyula SP. Susceptibility to seizure-induced sudden death in DBA/2 mice is altered by adenosine. *Epilepsy Res.* (2016) 124:49–54. doi: 10.1016/j.eplepsyres.2016.05.007

29. Seo MS, Lee B, Kang KK, Sung SE, Choi JH, Lee SJ, et al. Phenotype of the aging-dependent spontaneous onset of hearing loss in DBA/2 mice. *Vet Sci.* (2021) 8:49. doi: 10.3390/vetsci8030049

30. Yang L, Zhang H, Han X, Zhao X, Hu F, Li P, et al. Attenuation of hearing loss in DBA/2J mice by anti-apoptotic treatment. *Hear Res.* (2015) 327:109–16. doi: 10.1016/j.heares.2015.05.006

31. Ahn JH, Kang HH, Kim TY, Shin JE, Chung JW. Lipoic acid rescues DBA mice from early-onset age-related hearing impairment. *Neuroreport.* (2008) 19:1265–9. doi: 10.1097/WNR.0b013e328308b338

32. Johnson KR, Longo-Guess C, Gagnon LH Yu H, Zheng QY. A locus on distal chromosome 11 (ahl8) and its interaction with Cdh23 ahl underlie the early onset, age-related hearing loss of DBA/2J mice. *Genomics.* (2008) 92:219–25. doi: 10.1016/j.ygeno.2008.06.007

33. Suzuki S, Ishikawa M, Ueda T, Ohshiba Y, Miyasaka Y, Okumura K, et al. Quantitative trait loci on chromosome 5 for susceptibility to frequency-specific effects on hearing in DBA/2J mice. *Exp Anim.* (2015) 64:241–51. doi: 10.1538/expanim.14-0110

34. Neumann PE, Seyfried TN. Mapping of two genes that influence susceptibility to audiogenic seizures in crosses of C57BL/6J and DBA/2J mice. *Behav Genet.* (1990) 20:307–23. doi: 10.1007/BF01067798

35. Neumann PE, Collins RL. Confirmation of the influence of a chromosome 7 locus on susceptibility to audiogenic seizures. *Mamm Genome.* (1992) 3:250–3. doi: 10.1007/BF00292152

36. Jawahar MC, Sari CI, Wilson YM, Lawrence AJ, Brodnicki T, Murphy M. Audiogenic seizure proneness requires the contribution of two susceptibility loci in mice. *Neurogenetics.* (2011) 12:253–7. doi: 10.1007/s10048-011-0289-2

37. Ferraro TN, Golden GT, Smith GG, Martin JF, Lohoff FW, Gieringer TA, et al. Fine mapping of a seizure susceptibility locus on mouse chromosome 1: nomination of Kcnj10 as a causative gene. *Mamm Genome.* (2004) 15:239–51. doi: 10.1007/s00335-003-2270-3

38. Inyushin M, Kucheryavykh LY, Kucheryavykh YV, Nichols CG, Buono RJ, Ferraro TN, et al. Potassium channel activity and glutamate uptake are impaired in astrocytes of seizure susceptible DBA/2 mice. *Epilepsia.* (2010) 51:1707–13. doi: 10.1111/j.1528-1167.2010.02592.x

39. Cervo L, Canetta A, Calcagno E, Burbassi S, Sacchetti G, Caccia S, et al. Genotype-dependent activity of tryptophan hydroxylase-2 determines the response to citalopram in a mouse model of depression. *J Neurosci.* (2005) 25:8165–72. doi: 10.1523/JNEUROSCI.1816-05.2005

40. Uteshev V, Tupal S, Mhaskar Y, Faingold CL. Abnormal serotonin receptor expression in DBA/2 mice associated with susceptibility to sudden death due to respiratory arrest. *Epilepsy Res.* (2010) 88:183–8. doi: 10.1016/j.eplepsyres.2009.11.004

41. Willott JF, Lu SM. Midbrain pathways of audiogenic seizures in DBA/2 mice. *Exp Neurol.* (1980) 70:288–99. doi: 10.1016/0014-4886(80)90028-X

42. Willott JF, Demuth RM, Lu SM. Excitability of auditory neurons in the dorsal and ventral cochlear nuclei of DBA/2 and C57BL/6 mice. *Exp Neurol.* (1984) 83:495–506. doi: 10.1016/0014-4886(84)90118-3

43. Suthakar K, Ryugo DK. Descending projections from the inferior colliculus to medial olivocochlear efferents: Mice with normal hearing, early onset hearing loss, and congenital deafness. *Hear Res.* (2017) 343:34–49. doi: 10.1016/j.heares.2016.06.014

44. Kouchi H, Ogier M, Dieuset G, Morales A, Georges B, Rouanet JL, et al. Respiratory dysfunction in two rodent models of chronic epilepsy and acute seizures and its link with the brainstem serotonin system. *Sci Rep.* (2022) 12:10248. doi: 10.1038/s41598-022-14153-6

45. Le Gal La Salle G, Naquet R. Audiogenic seizures evoked in DBA/2 mice induce c-fos oncogene expression into subcortical auditory nuclei. *Brain Res.* (1990) 518:308–12. doi: 10.1016/0006-8993(90)90988-N

46. Takao T, Murakami H, Fukuda M, Kawaguchi T, Kakita A, Takahashi H, et al. Transcranial imaging of audiogenic epileptic foci in the cortex of DBA/2J mice. *Neuroreport.* (2006) 17:267–71. doi: 10.1097/01.wnr.0000201505.61373.42

47. Faingold CL, Randall M, Mhaskar Y, Uteshev V. Differences in serotonin receptor expression in the brainstem may explain the differential ability of a serotonin agonist to block seizure-induced sudden death in DBA/2 vs. DBA/1 mice. *Brain Res.* (2011) 1418:104–10. doi: 10.1016/j.brainres.2011.08.043

48. Kommajosyula SP, Randall ME, Brozoski TJ, Odintsov BM, Faingold CL. Specific subcortical structures are activated during seizure-induced death in a model of sudden unexpected death in epilepsy (SUDEP): a manganese-enhanced magnetic resonance imaging study. *Epilepsy Res.* (2017) 135:87–94. doi: 10.1016/j.eplepsyres.2017.05.011

49. Shen HY Li T, Boison D. A novel mouse model for sudden unexpected death in epilepsy (SUDEP): role of impaired adenosine clearance. *Epilepsia.* (2010) 51:465–8. doi: 10.1111/j.1528-1167.2009.02248.x

50. Jazrawi SP, Horton RW. Brain adrenoceptor binding sites in mice susceptible (DBA/2J) and resistant (C57 Bl/6) to audiogenic seizures. *J Neurochem.* (1986) 47:173–7. doi: 10.1111/j.1471-4159.1986.tb02846.x

51. Dailey JW, Jobe PC. Effect of increments in the concentration of dopamine in the central nervous system on audiogenic seizures in DBA/2J mice. *Neuropharmacology.* (1984) 23:1019–24. doi: 10.1016/0028-3908(84)90123-0

52. Chapman AG, Elwes RD, Millan MH, Polkey CE, Meldrum BS. Role of glutamate and aspartate in epileptogenesis; contribution of microdialysis studies in animal and man. *Epilepsy Res.* (1996) 12(Suppl.):239–46.

53. Marley RJ, Wehner JM. Correlation between the enhancement of flunitrazepam binding by GABA and seizure susceptibility in mice. *Life Sci.* (1987) 40:2215–24. doi: 10.1016/0024-3205(87)90056-7

54. Schwartz RD, Seale TW, Skolnick P, Paul SM. Differential seizure sensitivities to picrotoxinin in two inbred strains of mice (DBA/2J and BALB/c ByJ): parallel changes in GABA receptor-mediated chloride flux and receptor binding. *Brain Res.* (1989) 481:169–74. doi: 10.1016/0006-8993(89)90499-X

55. Yu O, Ito M, Chiu TH, Rosenberg HC. GABA-gated chloride ion influx and receptor binding studies in C57BL6J and DBA2J mice. *Brain Res.* (1986) 399:374–8. doi: 10.1016/0006-8993(86)91531-3

56. Jobe PC, Laird HE. Neurotransmitter abnormalities as determinants of seizure susceptibility and intensity in the genetic models of epilepsy. *Biochem Pharmacol.* (1981) 30:3137–44. doi: 10.1016/0006-2952(81)90510-4

57. Hilaire G, Voituron N, Menuet C, Ichiyama RM, Subramanian HH, Dutschmann M, et al. Dysfunction. *Respir Physiol Neurobiol.* (2010) 174:76. doi: 10.1016/j.resp.2010.08.017

58. Richerson GB, Buchanan GF. The serotonin axis: Shared mechanisms in seizures, depression, and SUDEP. *Epilepsia.* (2011) 52(Suppl. 1):28–38. doi: 10.1111/j.1528-1167.2010.02908.x

59. Buchanan GF, Murray NM, Hajek MA, Richerson GB. Serotonin neurones have anti-convulsant effects and reduce seizure-induced mortality. *J Physiol.* (2014) 592:4395. doi: 10.1113/jphysiol.2014.277574

60. Calcagno E, Canetta A, Guzzetti S, Cervo L, Invernizzi RW. Strain differences in basal and post-citalopram extracellular 5-HT in the mouse medial prefrontal cortex and dorsal hippocampus: relation with tryptophan hydroxylase-2 activity. *J Neurochem.* (2007) 103:1111–20. doi: 10.1111/j.1471-4159.2007.04806.x

61. Schlesinger K, Boggan W, Freedman DX, Genetics of audiogenic seizures: I. Relation to brain serotonin and norepinephrine in mice. *Life Sci.* (1965) 4:2345–51. doi: 10.1016/0024-3205(65)90289-4

62. Sparks DL, Buckholtz NS. Combined inhibition of serotonin uptake and oxidative deamination attenuates audiogenic seizures in DBA/2J mice. *Pharmacol Biochem Behav.* (1985) 23:753–7. doi: 10.1016/0091-3057(85)90067-X

63. Boggan WO, Seiden LS. 5-Hydroxytryptophan reversal of reserpine enhancement of audiogenic seizure susceptibility in mice. *Physiol Behav.* (1973) 10:9–12. doi: 10.1016/0031-9384(73)90077-2

64. Jordan D. Vagal control of the heart: central serotonergic (5-HT) mechanisms. *Exp Physiol.* (2005) 90:175–81. doi: 10.1113/expphysiol.2004.029058

65. Bourson A, Kapps V, Zwingelstein C, Rudler A, Boess FG, Sleight AJ. Correlation between 5-HT7 receptor affinity and protection against sound-induced seizures in DBA/2J mice. *Naunyn Schmiedebergs Arch Pharmacol.* (1997) 356:820–6. doi: 10.1007/PL00005123

66. Semenova TP, Ticku MK. Effects of 5-HT receptor antagpnist on seizure susceptibility and locomotor activity in DBA/2 mice. *Brain Res.* (1992) 588:229–36. doi: 10.1016/0006-8993(92)91580-8

67. Peters RI, Lack DB. Audiogenic seizures and brain serotonin after L-tryptophan and p-chlorophenylalanine. *Exp Neurol.* (1985) 90:540–8. doi: 10.1016/0014-4886(85)90151-7

68. Purnell B, Murugan M, Jani R, Boison D. The good, the bad, and the deadly: adenosinergic mechanisms underlying sudden unexpected death in epilepsy. *Front Neurosci.* (2021) 15:708304. doi: 10.3389/fnins.2021.708304

69. De Sarro G, De Sarro A, Di Paola ED, Bertorelli R. Effects of adenosine receptor agonists and antagonists on audiogenic seizure-sensible DBA/2 mice. *Eur J Pharmacol.* (1999) 371:137–45. doi: 10.1016/S0014-2999(99)00132-6

70. Boggan WO, Seiden LS. Dopa reversal of reserpine enhancement of audiogenic seizure susceptibility in mice. *Physiol Behav.* (1971) 6:215–7. doi: 10.1016/0031-9384(71)90028-X

71. Anlezark GM, Blackwood DHR, Meldrum BS, Ram VJ, Neumeyer JL. Comparative assessment of dopamine agonist aporphines as anticonvulsants in two models of reflex epilepsy. *Psychopharmacology.* (1983) 81:135–9. doi: 10.1007/BF00429007

72. Chapman AG, Croucher MJ, Meldrum BS. Evaluation of anticonvulsant drugs in DBA/2 mice with sound-induced seizures. *Arzneimittelforschung.* (1984) 34:1261–4. http://www.ncbi.nlm.nih.gov/pubmed/6542784

73. Rowley HL, Ellis Y, Davies JA. Age-related effects of NMDA-stimulated concomitant release of nitric oxide and glutamate in cortical slices prepared from DBA/2 mice. *Brain Res.* (1993) 613:49–53. doi: 10.1016/0006-8993(93)90452-S

74. Bashkatova VG, Mikoyan VD, Malikova LA, Raevskii KS. Role of nitric oxide and lipid peroxidation in pathophysiological mechanisms of audiogenic seizures in GEP Rats and DBA/2 mice. *Bull Exp Biol Med.* (2003) 136:7–10. doi: 10.1023/A:1026064107856

75. Moldrich RX, Beart PM, Jane DE, Chapman AG, Meldrum BS. Anticonvulsant activity of 3,4-dicarboxyphenylglycines in DBA/2 mice. *Neuropharmacology.* (2001) 40:732–5. doi: 10.1016/S0028-3908(01)00002-8

76. Moldrich RX, Chapman AG, De Sarro G, Meldrum BS. Glutamate metabotropic receptors as targets for drug therapy in epilepsy. *Eur J Pharmacol.* (2003) 476:3–16. doi: 10.1016/S0014-2999(03)02149-6

77. Conti P, Pinto A, Tamborini L, Grazioso G, De Sarro G, Bräuner-Osborne H, et al. Synthesis of conformationally constrained glutamic acid homologues and investigation of their pharmacological profiles. *ChemMedChem.* (2007) 2:1639–47. doi: 10.1002/cmdc.200700118

78. Gitto R, Caruso R, Orlando V, Quartarone S, Barreca ML, Ferreri G, et al. Synthesis and anticonvulsant properties of tetrahydroisoquinoline derivatives. *Farmaco.* (2004) 59:7–12. doi: 10.1016/j.farmac.2003.10.003

79. Chapman AG, Woodburn VL, Woodruff GN, Meldrum BS. Anticonvulsant effect of reduced NMDA receptor expression in audiogenic DBA/2 mice. *Epilepsy Res.* (1996) 26:25–35. doi: 10.1016/S0920-1211(96)00036-8

80. Faingold CL. Role of GABA abnormalities in the inferior colliculus pathophysiology - Audiogenic seizures. *Hear Res.* (2002) 168:223–37. doi: 10.1016/S0378-5955(02)00373-8

81. Horton RW, Collins JF, Anlezark GM, Meldrum BS. Convulsant and anticonvulsant actions in DBA/2 mice of compounds blocking the reuptake of GABA. *Eur J Pharmacol.* (1979) 59:75–83. doi: 10.1016/0014-2999(79)90026-8

82. Gatta E, Cupello A, Di Braccio M, Grossi G, Robello M, Scicchitano F, et al. Anticonvulsive activity in audiogenic DBA/2 mice of 1,4-benzodiazepines and 1,5-benzodiazepines with different activities at cerebellar granule cell GABAA receptors. *J Mol Neurosci.* (2016) 60:539–47. doi: 10.1007/s12031-016-0838-0

83. Sykes CC, Horton RW. Cerebral glutamic acid decarboxylase activity and gamma-aminobutyric acid concentrations in mice susceptible or resistant to audiogenic seizures. *J Neurochem.* (1982) 39:1489–91. doi: 10.1111/j.1471-4159.1982.tb12597.x

84. De Luca G, Di Giorgio RM, Macaione S, Calpona PR, Costantino S, Di Paola ED, et al. Susceptibility to audiogenic seizure and neurotransmitter amino acid levels in different brain areas of IL-6-deficient mice. *Pharmacol Biochem Behav.* (2004) 78:75–81. doi: 10.1016/j.pbb.2004.02.004

85. Horton RW, Prestwich SA, Meldrum BS. Gamma-aminobutyric acid and benzodiazepine binding sites in audiogenic seizure-susceptible mice. *J Neurochem.* (1982) 39:864–70. doi: 10.1111/j.1471-4159.1982.tb07972.x

86. Ticku MK. Differences in γ-aminobutyric acid receptor sensitivity in inbred strains of mice. *J Neurochem.* (1979) 33:1135–8. doi: 10.1111/j.1471-4159.1979.tb05253.x

87. Robertson HA. Audiogenic seizures: increased benzodiazepin receptor binding in a susceptible strain of mice. *Eur J Pharmacol.* (1980) 66:249–52. doi: 10.1016/0014-2999(80)90149-1

88. Dalby NO. GABA-level increasing and anticonvulsant effects of three different GABA uptake inhibitors. *Neuropharmacology.* (2000) 39:2399–407. doi: 10.1016/S0028-3908(00)00075-7

89. De Sarro G, Carotti A, Campagna F, McKernan R, Rizzo M, Falconi U, et al. Benzodiazepine receptor affinities, behavioral, and anticonvulsant activity of 2-aryl-2,5-dihydropyridazino[4,3-b]indol- 3(3H)-ones in mice. *Pharmacol Biochem Behav.* (2000) 65:475–87. doi: 10.1016/S0091-3057(99)00230-0

90. De Sarro G, Chimirri A, McKernan R, Quirk K, Giusti P, De Sarro A. Anticonvulsant activity of azirino[1,2-d][1,4]benzodiazepines and related 1,4-benzodiazepines in mice. *Pharmacol Biochem Behav.* (1997) 58:281–9. doi: 10.1016/S0091-3057(96)00565-5

91. Andrews N, Davis B, Gonzalez MI, Oles R, Singh L, McKnight AT. Effect of gastrin-releasing peptide on rat hippocampal extracellular GABA levels and seizures in the audiogenic seizure-prone DBA/2 mouse. *Brain Res.* (2000) 859:386–9. doi: 10.1016/S0006-8993(00)02010-2

92. Korff S, Riechert N, Schoensiegel F, Weichenhan D, Autschbach F, Katus HA, et al. Calcification of myocardial necrosis is common in mice. *Virchows Arch.* (2006) 448:630–8. doi: 10.1007/s00428-005-0071-7

93. Zhao H, Zhang H, Schoen FJ, Schachter SC, Feng HJ. Repeated generalized seizures can produce calcified cardiac lesions in DBA/1 mice. *Epilep Behav.* (2019) 95:169–74. doi: 10.1016/j.yebeh.2019.04.010

94. Dong R, Liu P, Wee L, Butany J, Sole MJ. Verapamil ameliorates the clinical and pathological course of murine myocarditis. *J Clin Invest.* (1992) 90:2022–30. doi: 10.1172/JCI116082

95. Donato Di Paola E, Gareri P, Davoli A, Gratteri S, Scicchitano F, Naccari C, et al. Influence of levetiracetam on the anticonvulsant efficacy of conventional antiepileptic drugs against audiogenic seizures in DBA/2 mice. *Epilepsy Res.* (2007) 75:112–21. doi: 10.1016/j.eplepsyres.2007.04.008

96. De Sarro G, Ongini E, Bertorelli R, Aguglia U, De Sarro A. Excitatory amino acid neurotransmission through both NMDA and non-NMDA receptors is involved in the anticonvulsant activity of felbamate in DBA/2 mice. *Eur J Pharmacol.* (1994) 262:11–9. doi: 10.1016/0014-2999(94)90022-1

97. De Sarro G, Di Paola ED, Conte G, Pasculli MP, De Sarro A. Influence of retigabine on the anticonvulsant activity of some antiepileptic drugs against audiogenic seizures in DBA/2 mice. *Naunyn Schmiedebergs Arch Pharmacol.* (2001) 363:330–6. doi: 10.1007/s002100000361

98. Russo E, Donato Di Paola E, Gareri P, Siniscalchi A, Labate A, Gallelli L, et al. Pharmacodynamic potentiation of antiepileptic drugs' effects by some HMG-CoA reductase inhibitors against audiogenic seizures in DBA/2 mice. *Pharmacol Res.* (2013) 70:1–12. doi: 10.1016/j.phrs.2012.12.002

99. De Sarro G, Paola ED Di, Gratteri S, Gareri P, Rispoli V, Siniscalchi A, et al. Fosinopril and zofenopril, two angiotensin-converting enzyme (ACE) inhibitors, potentiate the anticonvulsant activity of antiepileptic drugs against audiogenic seizures in DBA/2 mice. *Pharmacol Res.* (2012) 65:285–96. doi: 10.1016/j.phrs.2011.11.005

100. Hanada T, Hashizume Y, Tokuhara N, Takenaka O, Kohmura N, Ogasawara A, et al. Perampanel: a novel, orally active, noncompetitive AMPA-receptor antagonist that reduces seizure activity in rodent models of epilepsy. *Epilepsia.* (2011) 52:1331–40. doi: 10.1111/j.1528-1167.2011.03109.x

101. Matagne A, Margineanu DG, Kenda B, Michel P, Klitgaard H. Anti-convulsive and anti-epileptic properties of brivaracetam (ucb 34714), a high-affinity ligand for the synaptic vesicle protein, SV2A. *Br J Pharmacol.* (2008) 154:1662–71. doi: 10.1038/bjp.2008.198

102. De Sarro G, Ferreri G, Gareri P, Russo E, De Sarro A, Gitto R, et al. Comparative anticonvulsant activity of some 2,3-benzodiazepine derivatives in rodents. *Pharmacol Biochem Behav.* (2003) 74:595–602. doi: 10.1016/S0091-3057(02)01040-7

103. Brown JW, Moeller A, Schmidt M, Turner SC, Nimmrich V, Ma J, et al. Anticonvulsant effects of structurally diverse GABA(B) positive allosteric modulators in the DBA/2J audiogenic seizure test: comparison to baclofen and utility as a pharmacodynamic screening model. *Neuropharmacology.* (2016) 101:358–69. doi: 10.1016/j.neuropharm.2015.10.009

104. Micale N, Zappalà M, Grasso S, Puja G, De Sarro G, Ferreri G, et al. Novel potent AMPA/kainate receptor antagonists: synthesis and anticonvulsant activity of a series of 2-[(4-alkylsemicarbazono)-(4-amino-phenyl)methyl]-4,5-methylenedioxyphenylacetic acid alkyl esters. *J Med Chem.* (2002) 45:4433–42. doi: 10.1021/jm020863y

105. De Sarro G, Siniscalchi A, Ferreri G, Gallelli L, De Sarro A. NMDA and AMPA/kainate receptors are involved in the anticonvulsant activity of riluzole in DBA/2 mice. *Eur J Pharmacol.* (2000) 408:25–34. doi: 10.1016/S0014-2999(00)00709-3

106. Russo E, Constanti A, Ferreri G, Citraro R, De Sarro G. Nifedipine affects the anticonvulsant activity of topiramate in various animal models of epilepsy. *Neuropharmacology.* (2004) 46:865–78. doi: 10.1016/j.neuropharm.2003.11.028

107. Sparks DL, Buckholtz NS. Effects of 6-methoxy-1,2,3,4-tetrahydro-beta-carboline (6-MeO-THbetaC) on audiogenic seizures in DBA/2J mice. *Pharmacol Biochem Behav.* (1980) 12:119–24. doi: 10.1016/0091-3057(80)90425-6

108. De Sarro G, Donato Di Paola E, Falconi U, Ferreri G, De Sarro A. Repeated treatment with adenosine A1 receptor agonist and antagonist modifies the anticonvulsant properties of CPPene. *Eur J Pharmaco.l.* (1996) 317:239–45. doi: 10.1016/S0014-2999(96)00746-7

109. De Sarro A, Imperatore C, Mastroeni P, De Sarro G. Comparative convulsant potencies of two carbapenem derivatives in C57 and DBA/2 mice. *J Pharm Pharmacol.* (1995) 47:292–6. doi: 10.1111/j.2042-7158.1995.tb05798.x

110. Citraro R, Russo E, Leo A, Russo R, Avagliano C, Navarra M, et al. Pharmacokinetic-pharmacodynamic influence of N-palmitoylethanolamine, arachidonyl-2′-chloroethylamide and WIN 55,212-2 on the anticonvulsant activity of antiepileptic drugs against audiogenic seizures in DBA/2 mice. *Eur J Pharmacol.* (2016) 791:523–34. doi: 10.1016/j.ejphar.2016.09.029

111. Hill AJ, Mercier MS, Hill TDM, Glyn SE, Jones NA, Yamasaki Y, et al. Cannabidivarin is anticonvulsant in mouse and rat. *Br J Pharmacol.* (2012) 167:1629–42. doi: 10.1111/j.1476-5381.2012.02207.x

112. Hill TDM, Cascio MG, Romano B, Duncan M, Pertwee RG, Williams CM, et al. Cannabidivarin-rich cannabis extracts are anticonvulsant in mouse and rat via a CB1 receptor-independent mechanism. *Br J Pharmacol.* (2013) 170:679–92. doi: 10.1111/bph.12321

113. Gareri P, Condorelli D, Belluardo N, Gratteri S, Ferreri G, Donato Di Paola E, et al. Influence of carbenoxolone on the anticonvulsant efficacy of conventional antiepileptic drugs against audiogenic seizures in DBA/2 mice. *Eur J Pharmacol.* (2004) 484:49–56. doi: 10.1016/j.ejphar.2003.10.047

114. Vincze R, Péter M, Szabó Z, Kardos J, Héja L, Kovács Z. Connexin 43 differentially regulates epileptiform activity in models of convulsive and non-convulsive epilepsies. *Front Cell Neurosci.* (2019) 13:173. doi: 10.3389/fncel.2019.00173

115. Volnova A, Tsytsarev V, Ganina O, Vélez-Crespo GE, Alves JM, Ignashchenkova A, Inyushin M. The anti-epileptic effects of carbenoxolone *in vitro* and *in vivo*. *Int J Mol Sci.* (2022) 23:663. doi: 10.3390/ijms23020663

116. Liu B, Ran X, Yi Y, Zhang X, Chen H, Hu Y. Anticonvulsant effect of carbenoxolone on chronic epileptic rats and its mechanism related to connexin and high-frequency oscillations. *Front Mol Neurosc.i.* (2022) 15:870947. doi: 10.3389/fnmol.2022.870947

117. De Sarro G, Di Paola ED, Ferreri G, De Sarro A, Fischer W. Influence of some beta-adrenoceptor antagonists on the anticonvulsant potency of antiepileptic drugs against audiogenic seizures in DBA/2 mice. *Eur J Pharmacol.* (2002) 442:205–13. doi: 10.1016/S0014-2999(02)01536-4

118. De Sarro G, Gratteri S, Naccari F, Pasculli MP, De Sarro A. Influence of D-cycloserine on the anticonvulsant activity of some antiepileptic drugs against audiogenic seizures in DBA/2 mice. *Epilepsy Res.* (2000) 40:109–21. doi: 10.1016/S0920-1211(00)00113-3

119. Citraro R, Navarra M, Leo A, Di Paola ED, Santangelo E, Lippiello P, et al. The anticonvulsant activity of a flavonoid-rich extract from orange juice involves both NMDA and GABA-benzodiazepine receptor complexes. *Molecules.* (2016) 21. doi: 10.3390/molecules21091261

120. Bruno E, Buemi MR, De Luca L, Ferro S, Monforte AM, Supuran CT, et al. *In vivo* evaluation of selective carbonic anhydrase inhibitors as potential anticonvulsant agents. *ChemMedChem.* (2016) 11:1812–8. doi: 10.1002/cmdc.201500596

121. Garbuz DG, Davletshin AA, Litvinova SA, Fedotova IB, Surina NM, Poletaeva II. Rodent models of audiogenic epilepsy: genetic aspects, advantages, current problems and perspectives. *Biomedicines.* (2022) 10:2934. doi: 10.3390/biomedicines10112934

122. Schraeder P, Lathers C. DBA mice as models of sudden unexpected death in epilepsy. *Sudd Death Epileps.y.* (2010) 695–712.

123. Wenker IC, Teran FA, Wengert ER, Wagley PK, Panchal PS, Blizzard EA, et al. Postictal death is associated with tonic phase apnea in a mouse model of sudden unexpected death in epilepsy. *Ann Neurol.* (2021) 89:1023–35. doi: 10.1002/ana.26053

124. Nei M, Pickard A. The role of convulsive seizures in SUDEP. *Auton Neurosci.* (2021) 235:102856. doi: 10.1016/j.autneu.2021.102856

125. Faingold CL, Tupal S, Randall M. Prevention of seizure-induced sudden death in a chronic SUDEP model by semichronic administration of a selective serotonin reuptake inhibitor. *Epilepsy Behav.* (2011) 22:186–90. doi: 10.1016/j.yebeh.2011.06.015

126. Ryvlin P, Nashef L, Lhatoo SD, Bateman LM, Bird J, Bleasel A, et al. Incidence and mechanisms of cardiorespiratory arrests in epilepsy monitoring units (MORTEMUS): a retrospective study. *Lancet Neurol.* (2013) 12:966–77. doi: 10.1016/S1474-4422(13)70214-X

127. Stewart M, Kollmar R, Nakase K, Silverman J, Sundaram K, Orman R, et al. Obstructive apnea due to laryngospasm links ictal to postictal events in SUDEP cases and offers practical biomarkers for review of past cases and prevention of new ones. *Epilepsia.* (2017) 58:e87–90. doi: 10.1111/epi.13765

128. Petrucci AN, Joyal KG, Purnell BS, Buchanan GF. Serotonin and sudden unexpected death in epilepsy. *Exp Neurol.* (2020) 325:113145. doi: 10.1016/j.expneurol.2019.113145

129. Bateman LM Li CS, Lin TC, Seyal M. Serotonin reuptake inhibitors are associated with reduced severity of ictal hypoxemia in medically refractory partial epilepsy. *Epilepsia.* (2010) 51:2211–4. doi: 10.1111/j.1528-1167.2010.02594.x

130. Lacuey N, Martins R, Vilella L, Hampson JP, Rani MRS, Strohl K, et al. The association of serotonin reuptake inhibitors and benzodiazepines with ictal central apnea. *Epilepsy Behav.* (2019) 98(Pt A):73–79. doi: 10.1016/j.yebeh.2019.06.029

131. Kinney HC, Richerson GB, Dymecki SM, Darnall RA, Nattie EE. The brainstem and serotonin in the sudden infant death syndrome. *Annu Rev Pathol.* (2009) 4:517–50. doi: 10.1146/annurev.pathol.4.110807.092322

132. Patodia S, Paradiso B, Garcia M, Ellis M, Diehl B, Thom M, et al. Adenosine kinase and adenosine receptors A1 R and A2A R in temporal lobe epilepsy and hippocampal sclerosis and association with risk factors for SUDEP. *Epilepsia.* (2020) 61:787–97. doi: 10.1111/epi.16487

133. Guo M, Li T. Adenosine dysfunction in epilepsy and associated comorbidities. *Curr Drug Targets.* (2022) 23:344–57. doi: 10.2174/1389450122666210928145258

134. Shen HY, Baer SB, Gesese R, Cook JM, Weltha L, Coffman SQ, et al. Adenosine-A2A receptor signaling plays a crucial role in sudden unexpected death in epilepsy. *Front Pharmacol.* (2022) 13:910535. doi: 10.3389/fphar.2022.910535

135. Maguire MJ, Jackson CF, Marson AG, Nevitt SJ. Treatments for the prevention of Sudden Unexpected Death in Epilepsy (SUDEP). *Cochrane database Syst Rev.* (2020) 4. doi: 10.1002/14651858.CD011792.pub3

136. Generoso JS, Giridharan V, Lee J, Macedo D, Barichello T. The role of the microbiota-gut-brain axis in neuropsychiatric disorders. *Rev Bras Psiquiatr.* (2021) 43:293–305. doi: 10.1590/1516-4446-2020-0987

137. Nirwan N, Vyas P, Vohora D. Animal models of status epilepticus and temporal lobe epilepsy: a narrative review. *Rev Neurosci.* (2018) 29:757–70. doi: 10.1515/revneuro-2017-0086

138. Rusina E, Bernard C, Williamson A. The kainic acid models of temporal lobe epilepsy. *eNeuro.* (2021) 8. doi: 10.1523/ENEURO.0337-20.2021

139. Lévesque M, Avoli M, Bernard C. Animal models of temporal lobe epilepsy following systemic chemoconvulsant administration. *J Neurosci Methods.* (2016) 260:45–52. doi: 10.1016/j.jneumeth.2015.03.009

140. McKhann GM, Wenzel HJ, Robbins CA, Sosunov AA, Schwartzkroin PA. Mouse strain differences in kainic acid sensitivity, seizure behavior, mortality, and hippocampal pathology. *Neuroscience.* (2003) 122:551–61. doi: 10.1016/S0306-4522(03)00562-1

141. Schauwecker PE. Strain differences in seizure-induced cell death following pilocarpine-induced status epilepticus. *Neurobiol Dis.* (2012) 45:297. doi: 10.1016/j.nbd.2011.08.013

142. Müller CJ, Gröticke I, Hoffmann K, Schughart K, Löscher W. Differences in sensitivity to the convulsant pilocarpine in substrains and sublines of C57BL/6 mice. *Genes, Brain Behav.* (2009) 8:481–92. doi: 10.1111/j.1601-183X.2009.00490.x

143. Curia G, Longo D, Biagini G, Jones RSG, Avoli M. The pilocarpine model of temporal lobe epilepsy. *J Neurosci Methods.* (2008) 172:143–57. doi: 10.1016/j.jneumeth.2008.04.019

144. Ahmed Juvale II, Che Has AT. The evolution of the pilocarpine animal model of status epilepticus. *Heliyo.n.* (2020) 6:e04557. doi: 10.1016/j.heliyon.2020.e04557

145. González A, Nome CG, Bendiksen BA, Sjaastad I, Zhang L, Aleksandersen M, et al. Assessment of cardiac structure and function in a murine model of temporal lobe epilepsy. *Epilepsy Res.* (2020) 161:106300. doi: 10.1016/j.eplepsyres.2020.106300

146. Nakase K, Kollmar R, Lazar J, Arjomandi H, Sundaram K, Silverman J, et al. Laryngospasm, central and obstructive apnea during seizures: defining pathophysiology for sudden death in a rat model. *Epilepsy Res.* (2016) 128:126–39. doi: 10.1016/j.eplepsyres.2016.08.004

147. Shibley H, Smith BN. Pilocarpine-induced status epilepticus results in mossy fiber sprouting and spontaneous seizures in C57BL/6 and CD-1 mice. *Epilepsy Res.* (2002) 49:109–20. doi: 10.1016/S0920-1211(02)00012-8

148. Derera ID, Delisle BP, Smith BN. Functional neuroplasticity in the nucleus tractus solitarius and increased risk of sudden death in mice with acquired temporal lobe epilepsy. *eNeuro.* (2017) 4. doi: 10.1523/ENEURO.0319-17.2017

frontiers | Frontiers in Neurology

TYPE Original Research
PUBLISHED 26 September 2023
DOI 10.3389/fneur.2023.1243301

OPEN ACCESS

EDITED BY
Evgenia Sitnikova,
Institute of Higher Nervous Activity and Neurophysiology (RAS), Russia

REVIEWED BY
Anna B. Volnova,
Saint Petersburg State University, Russia
Ben Duffy,
Subtle Medical, Inc., United States

*CORRESPONDENCE
Tomokazu Ohshiro
✉ toshiro@med.tohoku.ac.jp

RECEIVED 20 June 2023
ACCEPTED 29 August 2023
PUBLISHED 26 September 2023

CITATION
Liu D, Fujihara K, Yanagawa Y, Mushiake H and Ohshiro T (2023) *Gad1* knock-out rats exhibit abundant spike-wave discharges in EEG, exacerbated with valproate treatment. *Front. Neurol.* 14:1243301. doi: 10.3389/fneur.2023.1243301

Gad1 knock-out rats exhibit abundant spike-wave discharges in EEG, exacerbated with valproate treatment

Dongyu Liu[1], Kazuyuki Fujihara[2], Yuchio Yanagawa[3], Hajime Mushiake[1] and Tomokazu Ohshiro[1]*

[1]Department of Physiology, Graduate School of Medicine, Tohoku University, Sendai, Japan, [2]Department of Psychiatry and Neuroscience, Graduate School of Medicine, Gunma University, Maebashi, Japan, [3]Department of Genetic and Behavioral Neuroscience, Graduate School of Medicine, Gunma University, Maebashi, Japan

Objective: To elucidate the functional role of gamma-aminobutyric acid (GABA)-ergic inhibition in suppressing epileptic brain activities such as spike-wave discharge (SWD), we recorded electroencephalogram (EEG) in knockout rats for *Glutamate decarboxylase 1* (*Gad1*), which encodes one of the two GABA-synthesizing enzymes in mammals. We also examined how anti-epileptic drug valproate (VPA) acts on the SWDs present in *Gad1* rats and affects GABA synthesis in the reticular thalamic nucleus (RTN), which is known to play an essential role in suppressing SWD.

Methods: Chronic EEG recordings were performed in freely moving control rats and homozygous knockout *Gad1* (−/−) rats. Buzzer tones (82 dB) were delivered to the rats during EEG monitoring to test whether acoustic stimulation could interrupt ongoing SWDs. VPA was administered orally to the rats, and the change in the number of SWDs was examined. The distribution of GABA in the RTN was examined immunohistochemically.

Results: SWDs were abundant in EEG from *Gad1* (−/−) rats as young as 2 months old. Although SWDs were universally detected in older rats irrespective of their *Gad1* genotype, SWD symptom was most severe in *Gad1* (−/−) rats. Acoustic stimulation readily interrupted ongoing SWDs irrespective of the *Gad1* genotype, whereas SWDs were more resistant to interruption in *Gad1* (−/−) rats. VPA treatment alleviated SWD symptoms in control rats, however, counterintuitively exacerbated the symptoms in *Gad1* (−/−) rats. The immunohistochemistry results indicated that GABA immunoreactivity was significantly reduced in the somata of RTN neurons in *Gad1* (−/−) rats but not in their axons targeting the thalamus. VPA treatment greatly increased GABA immunoreactivity in the RTN neurons of *Gad1* (−/−) rats, which is likely due to the intact GAD2, another GAD isozyme, in these neurons.

Discussion: Our results revealed two opposing roles of GABA in SWD generation: suppression and enhancement of SWD. To account for these contradictory roles, we propose a model in which GABA produced by GAD1 in the RTN neuronal somata is released extrasynaptically and mediates intra-RTN inhibition.

KEYWORDS

animal model of absence epilepsy, gamma-aminobutyric acid (GABA), glutamate decarboxylase (GAD), reticular thalamic nucleus, valproate

1. Introduction

An absence seizure is a non-convulsive epilepsy accompanied by a spike-wave discharge (SWD) that appears suddenly in a patient's electroencephalogram (EEG) and lasts for several seconds (1–3). Human patients temporarily lose consciousness while paroxysmal activity emerges in the EEG. Therefore, the appearance of SWDs in an EEG is a useful clinical observation for the diagnosis of absence epilepsy. SWDs can be identified by a characteristic composite waveform consisting of a primary oscillation lasting up to 30 s (frequency: approximately 3 Hz) and large spikes superimposed on and in phase with the oscillation (1, 2). Genetic rat models for SWD have long been established (4–6); these model rats exhibit SWDs reproducibly in EEGs, with dominant oscillation frequencies of approximately 7–12 Hz (5, 7). Common laboratory rats such as Brown Norway, Long-Evans, and even wild-caught rats were recently demonstrated to exhibit abundant SWDs in EEGs (8, 9). Although SWDs in these rats are usually accompanied by the absence of seizure-like symptoms such as behavioral immobility, both naïve and genetic model rats can behaviorally detect and respond appropriately to sensory or reward cues presented when an SWD appeared on their EEG (9–12). Therefore, whether SWDs in rodents represent pathological or physiological brain activity remains controversial (7–9, 13, 14).

SWDs originate primarily within the reticular thalamic nucleus (RTN)–thalamus–cortex network (15–19). The RTN consists of GABAergic neurons that surround and innervate the thalamus, providing synaptic inhibition to thalamocortical (TC) relay neurons (20). The firing of RTN neurons elicits hyperpolarization in TC neurons, which in turn activates low-threshold T-type Ca^{2+} channels and evokes post-inhibitory rebound bursting in TC neurons (21). These TC neurons project axon collaterals back to the RTN; the re-excitation of RTN neurons leads to recurrent intra-thalamic oscillation, i.e., SWD (19).

Gamma-aminobutyric acid (GABA), the main inhibitory neurotransmitter, is synthesized from glutamate by two isoenzymes, namely, glutamate decarboxylase (GAD) 1 (67 kDa) and GAD2 (65 kDa) in mammalians. GAD2 is localized primarily in the inhibitory synapse and therefore plays an important role in synaptic inhibition (22, 23). *Gad2* knockout mice or rats are viable but suffer from spontaneous convulsive seizures (24–26). By contrast, GAD1 is primarily localized in the cytoplasm of GABAergic neurons (27, 28). Knockout rats for *Gad1* that were recently created through clustered regularly interspaced short palindromic repeats (CRISPR)/Cas9-mediated gene editing showed schizophrenia-like symptoms (29). However, whether these *Gad1* (–/–) homozygous knockout rats show any other neurological symptoms, such as epilepsy, remains to be determined.

In this study, we conducted EEG monitoring of *Gad1* (–/–) rats to evaluate their SWD symptoms in comparison with control rats. We attempted to interrupt ongoing SWDs through acoustic stimulation and conducted a pharmacological experiment using the anti-epilepsy drug valproate (VPA). Finally, we immunohistochemically analyzed the GABA expression level in RTN neurons to examine the effects of VPA treatment.

2. Materials

2.1. Animals

Gad1 knockout rats were generated using CRISPR/Cas9-mediated gene editing (29) in the Long-Evans background. Knockout rats were crossed with Long-Evans rats (Japan SLC, Inc., Japan) and bred in the *Gad1* heterozygous (+/–) state in our laboratory. *Gad1* (–/–) and *Gad1* wild-type (+/+) rats were obtained from sibling mating between heterozygotes. All rats were reared under standard laboratory conditions under a 12-h/12-h light/dark cycle. All experimental procedures were approved by the Animal Care and Experimentation Committee of Gunma University and the Tohoku University Committee for Animal Research.

2.2. Surgery and EEG recordings

Implant surgery and EEG recording were performed as described previously (25). Briefly, rats were anesthetized with medetomidine, midazolam, and butorphanol mixture and placed on the stereotaxic apparatus. Heart rates and SpO_2 were continuously monitored. The scalp was excised, and the parietal skull bone was exposed. Small burr holes (~0.9 mm diameter) were made bilaterally over the skull, and twisted-pair wire electrodes (114 μm diameter, TFA-coated silver wire, Med Wire, USA) and/or silver-pleated screw electrodes (M1 × 3 mm, Unique Medical, Japan) were aseptically implanted. The tips of the twisted-pair wire electrodes were inserted into the cortex at a depth of 1 mm and firmly supported through a ceramic guide tube (KyoCera, Japan). After the implant surgery, the rats were returned to the home cage and were allowed to recover from the surgery for 1 to 2 days before the first recording was made. On the EEG recording, the rat with the implant was transferred from the home cage to a clear plexiglass cage (60 × 60 × 60 cm), on whose walls two piezoelectric speakers (Digi-Key Electronics, Thief River Falls, MN, USA) were pasted. A wired head-stage amplifier (HST/8o50-G1-GR; Plexon, Inc., Dallas, TX, USA) or wireless head-stage amplifier (TBSI Wireless Neural Recording System, Global Bio Inc., Mount Laurel, NJ, USA) were used for EEG recording. Raw electrical signals were further amplified and digitized using the Omniplex multichannel recording system (Plexon). In total, 45 rats of both sexes, including 20 *Gad1* (–/–), 9 *Gad1* (+/–), and 16 *Gad1* (+/+) rats, were used in this study. The rats were separated into two age groups, younger (<2 months) and older (≥2 months), and their EEGs were examined for SWDs. Because SWDs were rare in younger *Gad1* (+/–) and *Gad1* (+/+) rats, only EEG data from older rats were further analyzed. Thus, in total, 100 h of EEG data were collected and analyzed from 10 *Gad1* (–/–) rats (age: 2–11 months), 45 h from 6 *Gad1* (+/–) rats (age: 3–12 months), and 70 h from 7 *Gad1* (+/+) rats (age: 2–12 months). EEG recording was performed for up to 5 h per day, and recording lasted for up to 3 months in a single animal. Some EEG recording sessions were videotaped to record rat behavior.

2.3. Acoustic stimulation experiment

In the acoustic stimulation experiment, a rat was placed in a clear plexiglass cage while wearing an EEG headset. The experimenter continuously monitored the EEG for SWDs and applied a series of acoustic stimulations from piezoelectric speakers (dominant frequency: 2 kHz; loudness: 82 dB [measured at the cage center]; ambient loudness: 44 dB) as soon as an SWD appeared on the monitor. The recording was started without acoustic stimulation for 1–2 h and continued for another 1–2 h with acoustic stimulation. In total, 22 h of EEG recording data were obtained from five *Gad1* (−/−) rats (age: 2–10 months), as well as 28 h of EEG recording data from two *Gad1* (+/−) rats and four *Gad1* (+/+) rats (age: 3–9 months). Because *Gad1* (+/−) and *Gad1* (+/+) rats yielded similar results, the data from these genotype groups were merged and used as control group data.

2.4. Offline SWD detection

All EEG recording data were analyzed offline for SWDs using custom-made programs written in MATLAB code. Briefly, raw voltage signals sampled at 1 kHz were subjected to high-pass filtering (cutoff: 0.9 Hz) and wavelet-transformed (30). SWDs were extracted from the total spectral power time series data by imposing frequency thresholds at 5 and 32 Hz; this interval contained most of the SWD oscillation power (Figure 1). The extracted SWDs were checked visually, and mechanical noise caused by rats tapping the cable or chewing food pellets was excluded from the data. By our definition, a spike-train waveform lasting <1 s was not regarded as an SWD.

2.5. VPA treatment

We initially examined the effect of intraperitoneal (i.p.) injections of VPA (150–300 mg/kg, dissolved in 1 ml of saline) using three *Gad1* (−/−), two *Gad1* (+/−), and two *Gad1* (+/+) rats. In this pilot experiment, we observed that all became drowsy and inactive after the injection, except for one *Gad1* (+/+) rat. To avoid acute poisoning and the need for repeated i.p. administration, we next tried a milder oral formulation of the drug, using another set of rats (two *Gad1* (−/−), four *Gad1* (+/−), and two *Gad1* (+/+) rats). VPA (10 mg/ml) was dissolved in water and made available to the rats *ad libitum* for 7 days. At the end of this period, we collected the blood serum samples from these animals and outsourced them to a local biochemistry lab (Nagahama Life Science Laboratory, Shiga, Japan) for the VPA blood concentration measurement. VPA concentration was measured based on the enzyme immunoassay method (Emit2000 valproate assay, Siemens Healthcare, Japan). The average blood concentration of VPA was 40.4 ± 10.4 μg/ml (24.1–73.7; n = 8 animals). The effective blood concentration of VPA for the treatment of epilepsy in humans is 50–100 μg/ml (31). Based on these observations, we decided to adopt the oral administration of the drug for the EEG recording experiment and the GABA immunohistochemistry. For the recording experiment, a pre-medication EEG recording was performed 2–3 days before starting drug administration [control group: VPA (−)]. EEG recording was resumed on the 3rd day after the initiation of drug administration and performed for a total of 2–3 days until the 7th day of the VPA treatment [experimental group: VPA (+)] (Table 1). In total, we obtained 70 h of EEG recording data from four *Gad1* (−/−) rats (age: 5–11 months) and 68 h from four *Gad1* (+/+) rats (age: 5–12 months). The water intake and body weight were monitored during the experiment (Table 2).

2.6. Immunohistochemistry

Four *Gad1* (+/+) VPA (−), five *Gad1* (+/+) VPA (+), four *Gad1* (−/−) VPA (−), and four *Gad1* (−/−) VPA (+) rats were euthanized by intraperitoneal injection of pentobarbital (150 mg/kg animal) and perfused with one-half Karnovsky fixative (2% paraformaldehyde and 2% glutaraldehyde in phosphate-buffered saline). The fixed brain was immersed in 30% sucrose in 0.1 M phosphate buffer for cryoprotection and embedded in Tissue-Tek OCT compound (Sakura Finetek Japan, Tokyo, Japan). The frozen brain was cut into 10-μm-thick sections using a cryostat (CM1950, Leica, Wetzlar, Germany) and mounted onto coated slide glasses (MAS-01, Matsunami Glass, Kishiwada, Japan). Coronal sections (ca. bregma −2.7 mm) were selected to examine the RTN and neighboring thalamic nuclei. Immunostaining was performed using a STAINperfect Immunostaining Kit (ImmuSmol, Bordeaux, France), following the manufacturer's instructions. The primary antibodies used in these experiments included chicken polyclonal anti-GABA (1:500 dilution; ImmuSmol), rabbit polyclonal anti-parvalbumin (PV) (1:2,000, GTX134110, Genetex, Hsinchu, Taiwan), chicken normal serum (for negative control, 1:2,000 dilution; Jackson ImmunoResearch), and the secondary antibodies were preabsorbed Alexa Fluor-488 conjugated goat anti-chicken IgY (1:500 dilution; ab150173, Abcam, Cambridge, UK) and preabsorbed Alexa Fluor-568 conjugated goat anti-rabbit IgG (1:500 dilution; ab175695, Abcam, Cambridge, UK). For fluorescent nucleus staining, we used a CellStain−4′,6-diamidino-2-phenylindol (DAPI) solution (1:500 dilution, Dojindo Kumamoto, Mashiki, Japan). Fluorescence images were acquired using an LSM 780 laser confocal microscope (Zeiss, Oberkochen, Germany) and a 63× oil objective lens (numerical aperture: 1.4) and analyzed using the ZEN confocal image analysis software (Zeiss) and ImageJ software (National Institutes of Health, Bethesda, MD, USA), respectively (32–34) (Supplementary Figures S1, S2).

2.7. Statistical analyses and graphics

Median values were compared using the Wilcoxon rank-sum, Wilcoxon signed-rank, and Kruskal–Wallis tests using the MATLAB Statistics and Machine Learning Toolbox. Multiple comparisons were performed using the *multicompare* function with Fisher's least significant difference option in the same toolbox. All plots were drawn using Excel software (Microsoft Corp., Redmond, WA, USA). In the box-whisker plot, the upper (lower) whisker was drawn from the top (bottom) of the box, up (down), to the

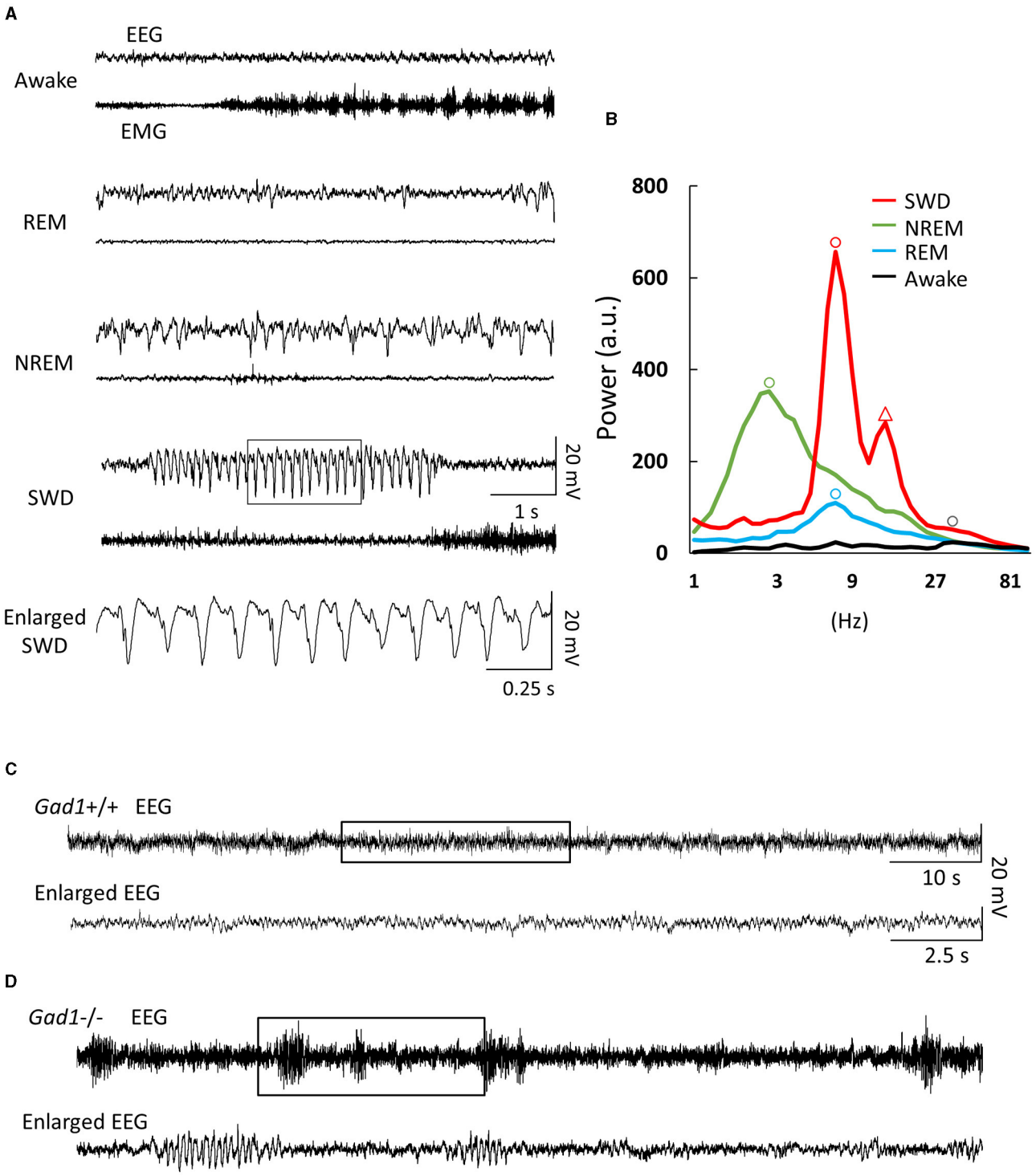

FIGURE 1
Electroencephalogram (EEG) and electromyogram (EMG) patterns. **(A)** EEG/EMG patterns from a *Gad1* homozygous (−/−) knockout rat. Similar patterns were observed in both *Gad1* heterozygous (+/−) and wild-type (+/+) rats. In the awake state, the animals showed a rapid, small-amplitude EEG pattern and a highly active EMG pattern. Rapid-eye-movement (REM) sleep was associated with complete muscle atonia, despite the active EEG pattern. Non-REM (NREM) sleep was associated with a slow, large-amplitude EEG pattern. Spike-wave discharges (SWDs) (framed section of the EEG, enlarged at the bottom) appeared suddenly while the rats were awake, although they tended to remain still. **(B)** EEG power spectrum with arbitrary units (a.u.). Peaks are indicated by circles. The dominant frequencies for SWD, NREM sleep, REM sleep, and wakefulness were 8, 3, 7, and 30 Hz, respectively. The SWD power spectrum also showed a second prominent peak (triangle) at the first harmonic, i.e., 16 Hz, reflecting a spiky waveform shape. **(C)** EEG pattern from a 7-week-old *Gad1* (+/+) rat. Few SWDs were seen at ages of <2 months. The framed section (top) is enlarged at the bottom. **(D)** EEG patterns from a 5-week-old *Gad1* (−/−) rat showed many SWDs. The framed section (top) is enlarged at the bottom.

10.3389/fneur.2023.1243301

TABLE 1 EEG recording time before and during the VPA treatment.

Animal ID	Pre-medication	VPA treatment						
	2–3 days	1st day	2nd day	3rd day	4th day	5th day	6th day	7th day
1. *Gad1* (+/+)	10 h in total	-	-	4 h	-	4 h	-	2 h
2. *Gad1* (+/+)	9 h	-	-	-	4 h	-	3 h	2 h
3. *Gad1* (+/+)	5 h	-	-	-	5 h	-	-	-
4. *Gad1* (+/+)	10 h	-	-	5 h	5 h	-	-	-
1. *Gad1* (−/−)	7 h	-	-	-	4 h	-	3 h	-
2. *Gad1* (−/−)	10 h	-	-	5 h	-	-	-	5 h
3. *Gad1* (−/−)	10 h	-	-	-	5 h	-	2 h	3 h
4. *Gad1* (−/−)	8 h	-	-	4 h	-	4 h	-	-

TABLE 2 Amounts of water/VPA intake (average) and rat's weight (range) before, during, and after VPA treatment.

Animal ID	Pre-medication (2–3 days)	VPA treatment (7 days)	VPA cessation (3 days)
1. *Gad1* (+/+)	37 ml/day, 502–510 g	25 ml/day, 489–478 g	40 ml/day, 498 g
2. *Gad1* (+/+)	22 ml/day, 282–276 g	12 ml/day, 260–252 g	27 ml/day, 275 g
3. *Gad1* (+/+)	33 ml/day, 316–324 g	30 ml/day, 302–298 g	N.D.
4. *Gad1* (+/+)	25 ml/day, 272–277 g	20 ml/day, 247–242 g	30 ml/day, 263 g
1. *Gad1* (−/−)	33 ml/day, 308–312 g	23 ml/day, 300–294 g	30 ml/day, 300 g
2. *Gad1* (−/−)	45 ml/day, 476–477 g	23 ml/day, 458–465 g	50 ml/day, 474 g
3. *Gad1* (−/−)	30 ml/day, 310–300 g	20 ml/day, 288–272 g	30 ml/day, 284 g
4. *Gad1* (−/−)	31 ml/day, 281–282 g	18 ml/day, 256–255 g	N.D.

The body weight and the water intake of the rats were decreased by valproate treatment (VPA, 10 mg/ml, per os), but recovered after cessation of VPA treatment. N.D. (no data).

largest (smallest) data point within 1.5-fold of the interquartile range. Outliers outside the upper and lower whiskers are not shown in the plot.

3. Results

3.1. Abundant SWDs in young *Gad1* (−/−) rats

EEG patterns in *Gad1* (−/−) rats during the awake or sleep (rapid eye movement and non-rapid eye movement) states appeared to be similar to those in normal animals (32) (Figure 1A). However, on visual inspection of the EEG data, frequent large-amplitude spiky waveforms caught the attention (Figure 1A, SWD), which lasted a few seconds and oscillated at approximately 8 Hz (Figure 1B). These features are suggestive of spike-wave discharges in rodents (5, 7). These SWDs were observed while the rats were awake but quiet or at rest after active exploration. SWDs were observed in *Gad1* (−/−) rats as early as 2 months of age, whereas they were rarely detected in *Gad1* (+/−) or *Gad1* (+/+) rats at similar ages (Figures 1C, D, Table 3). Only one out of seven rats showed SWDs (29 SWDs were detected from a total of 10 h of recording). The other six control rats did not show SWD in their EEG (a total of 175 h of recording). However, even in *Gad1* (+/+) rats, SWDs eventually prevailed in the EEG at older ages. No overt convulsive seizures or other epileptic activity were observed in *Gad1* (−/−) rats (data not shown).

TABLE 3 Proportion of rats showing SWDs sorted by age.

Gad1 genotype	Younger than 2 months old	Older than 2 months old
(−/−)	7/8	16/16
(+/−)	0/4	6/6
(+/+)	1/3	14/16

The rats were separated into two age groups (young and old) and examined for the presence of spike-wave discharges (SWDs) in EEG. In all, 45 rats were recorded; 4 out of 20 Gad1 (−/−) rats, 1 out of 9 Gad1 (+/−) rats, and 3 out of 16 Gad1 (+/+) rats were examined in both age groups.

As SWDs were rare in young *Gad1* (+/−) and *Gad1* (+/+) rats, only SWDs from older rats were analyzed and compared among the three genotypes (Figure 2). SWDs were significantly longer in *Gad1* (−/−) rats (median: 2.3 s; $n = 7{,}305$ SWDs from 10 rats) than in *Gad1* (+/−) rats (2.0 s; n = 1,749 SWDs from 6 rats) or *Gad1* (+/+) rats (2.1 s; n = 3,766 SWDs from 7 rats) (Figure 2A; $P = 4.2 \times 10^{-13}$; Kruskal–Wallis test). The difference between *Gad1* (+/+) and *Gad1* (+/−) rats was not statistically significant ($P = 0.41$; Wilcoxon rank-sum test). The SWD length shows long-tailed

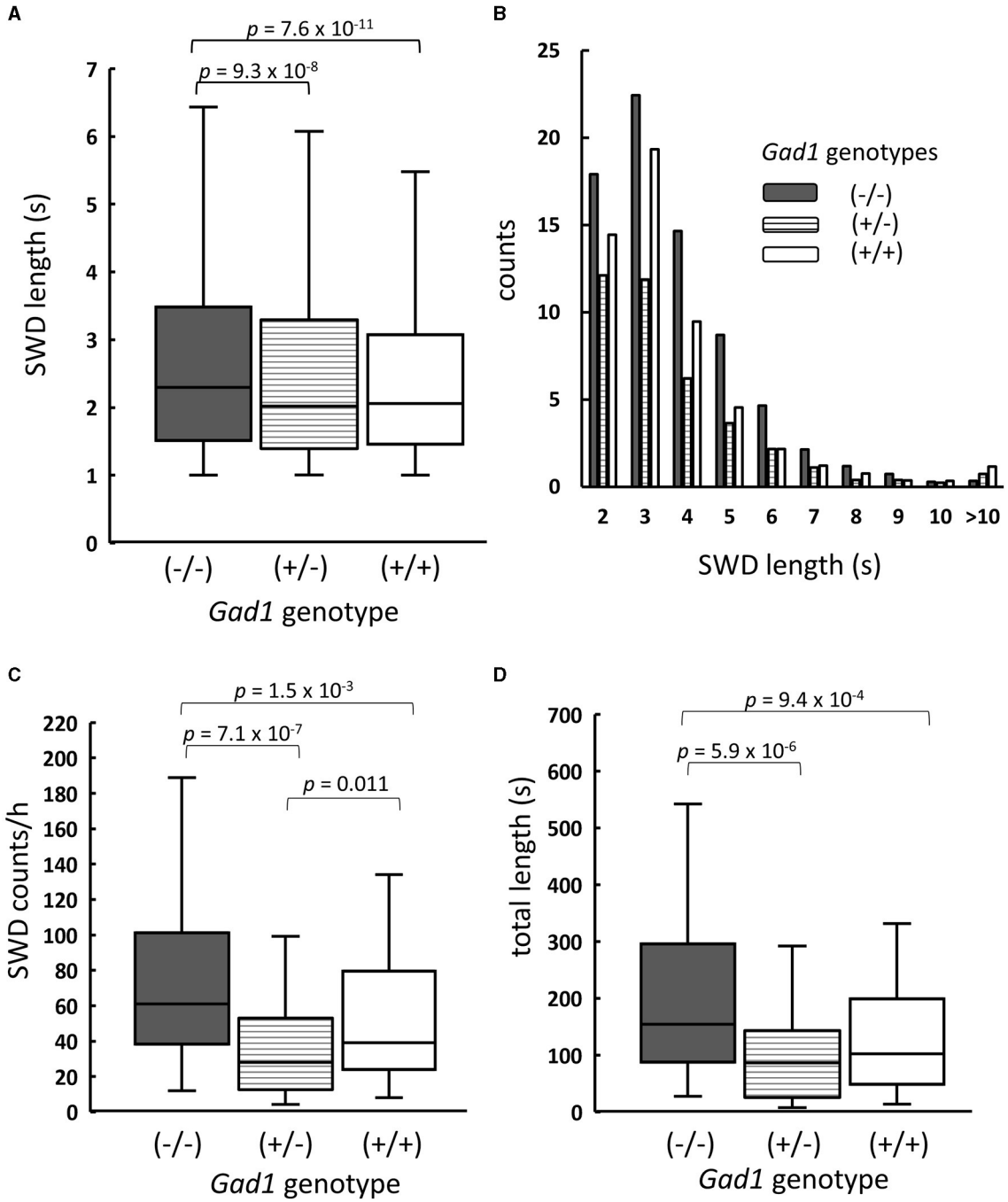

FIGURE 2
Summary of SWDs from *Gad1* (−/−) rats (shaded), *Gad1* (+/−) rats (lined), and *Gad1* (+/+) rats (unshaded). **(A)** Box and whisker plots of individual SWD lengths. The median SWD length was greatest in the *Gad1* (−/−) group. **(B)** Distribution of SWD counts per hour, sorted by length. Most SWDs lasted for 5 s. **(C)** Accumulated SWD counts per hour. The median count was highest in the *Gad1* (−/−) group. **(D)** Accumulated lengths of individual SWDs per hour. The median length was greatest in the *Gad1* (−/−) group. In the graphs, SWD data were merged within the same experimental group, and the medians of each group were compared (Wilcoxon rank-sum test), i.e., *P*-values were obtained based on events but not animals. See the text for detailed statistical information.

distributions (Figure 2B), with the longest SWD lasting longer than 10 s. Most SWDs were shorter than 5 s in duration, regardless of genotype. The median SWD count in *Gad1* (−/−) rats (61/h) was the largest among the three genotypes ($P = 8.3 \times 10^{-7}$; Kruskal–Wallis test) (Figure 2C), while the median SWD in *Gad1* (+/−) rats (28/h) was significantly smaller than in *Gad1* (+/+) rats (39/h) ($P = 0.011$; Wilcoxon rank-sum test). Therefore, the total SWD time per hour was greatest in *Gad1* (−/−) rats (median: 155 s/h), which was significantly different from *Gad1* (+/−) and *Gad1* (+/+) rats (median: 86 and 102 s/h, respectively, $P = 5.7 \times 10^{-6}$; Kruskal–Wallis test) (Figure 2D). The total SWD time in *Gad1* (+/−) was shorter than *Gad1* (+/+) rats, however the difference

was insignificant ($P = 0.09$; Wilcoxon rank-sum test). These results indicate that *Gad1* (−/−) rats had the most severe SWD phenotype and that GAD1 plays a role in suppressing SWD generation in rats.

3.2. Interruption of SWD by acoustic stimulations

In human patients with absence seizures, SWD appears abruptly in EEG, while the patients temporally lose consciousness and are often unaware of external sensory stimuli (1–3). Therefore, we investigated whether the rats were responsive to external acoustic stimulation when SWDs appeared in the EEG. We presented buzzer tones through speakers to awake-behaving animals during live EEG monitoring. The experimenter presented the buzzer tone as soon as an SWD was detected in the EEG displayed on a monitor. *Gad1* (−/−) and control rats responded overtly to these buzzer tones (Table 4). Most SWDs were interrupted readily by a single volley of buzzer tones (Case 1 SWD, Figure 3A), whereas the remaining SWDs were not (Case 2 SWD, Figure 3B). The appearance of SWDs in EEG was highly correlated with the inactivity of animals caused by reward withdrawal or a loss of motivation to achieve the reward during behavioral tasks (33). Because buzzer stimulations were not associated with reward and did not require a voluntary response, the SWDs observed in the rats, including in Case 2, likely reflect the animal's gradual loss of interest in, or sensory adaptation to, repeated buzzer tones (11, 33). If this is true, the number of SWDs should increase over time. To test this possibility, the SWDs were categorized into the first and second halves of the 1-h recording session. The total SWD count, including that of Cases 1 and 2, was not significantly different between the first and second halves of the session in *Gad1* (−/−) rats (median: 63 and 48 per 30 min, respectively; n = 9; $p = 0.82$, Wilcoxon signed-rank test) and control rats (median: 37 and 9 per 30 min, respectively; $n = 11$; $p = 0.10$) (Figure 3C). Similarly, the SWD counts of Case 2 were not significantly different between the first and second halves of the session in *Gad1* (−/−) rats (median: 6 and 16 per 30 min, respectively; $p = 0.51$) or control rats (median: 2 and 0 per 30 min, respectively; $p = 0.11$). We extended three recording sessions for an additional hour and observed no significant increase in SWD counts in any group (data not shown). Therefore, our results do not suggest that the SWDs were produced by sensory adaptation or a loss of motivation over time. Interestingly, the SWD count in Case 2 was significantly higher in *Gad1* (−/−) rats (median Case2/(Case1 + Case2) ratio: 18%; n = 18) than in the control group (median ratio: 5%; n = 20) ($p = 0.015$, Wilcoxon rank-sum test) (Figure 3D). These results indicate that rats responded to sensory stimuli when SWDs appeared in EEG, and *Gad1* (−/−) rats had more SWDs resistant to sensory interruption.

3.3. Anti-epileptic drug test

We next examined VPA, a medication commonly used to treat both the absence and the myoclonic seizure, which inhibits GABA degradative enzymes such as GABA transaminase (34, 35), thereby increasing the GABA level in the brain. As SWD was a common symptom in both older *Gad1* (+/+) and *Gad1* (−/−) rats, we expected that an increase in GABA caused by VPA would alleviate the SWD phenotype in both genotypes. Consistent with this expectation, the SWD phenotype in *Gad1* (+/+) rats ($n = 4$) was significantly alleviated by VPA treatment (Figure 4). The median length of individual SWDs was decreased by VPA treatment, from 2.2 s (without VPA treatment; $n = 2{,}516$ SWDs) to 1.9 s (with VPA treatment; n = 1,625 SWDs) (Figure 4A). A decrease in SWD length was observed over the entire range of SWD sizes (Figure 4B). The median count of SWD appearances per hour decreased from 73 to 51 (Figure 4C); thus, the accumulated SWD length per hour decreased from 200 to 127 s following VPA treatment (Figure 4D).

Counterintuitively, the SWD phenotype in the *Gad1* (−/−) rats ($n = 4$) was worsened by VPA treatment (Figure 5). The median SWD length without treatment (median: 2.4 s; $n = 3{,}113$ SWDs) increased to 3.0 s following VPA treatment ($n = 3{,}132$ SWDs) (Figure 5A). Notably, SWDs shorter than 4 s in duration decreased in number, whereas those lasting longer than 5 s became more frequent (Figure 5B). The number of SWD occurrences, irrespective of size, did not differ significantly between treatment groups (Figure 5C). Overall, accumulated SWD length per hour increased from 289 to 307 s; however, this increase was not significant (Figure 5D). In summary, VPA treatment exacerbated the SWD symptom in *Gad1* (−/−) rats, unlike in control rats, suggesting that a mere increase in GABA level by the drug cannot compensate for GAD1 deficiency.

TABLE 4 Results of hearing ability test.

Genotype group	Total	Responses
Gad1 (−/−) group	300	281
Control group	300	277

Three Gad1 (−/−) rats, one Gad1 (+/−) rats (control group), and two Gad1 (+/+) rats (control group) were presented with a short buzzer tone (300 times in each group), and their overt responses to the tone, e.g., twitching a body part (pinna, neck, whisker pad, and so forth) or interrupting their behavior (chewing pellets, exploring on the floor, and so forth) were counted. A total of 281 responses were recorded in the Gad1 (−/−) group, and 277 responses were recorded in the control group, indicating that all genotypes had similar hearing abilities.

3.4. GABA immunoreactivity in reticular thalamic nucleus

GAD1 is abundantly expressed in GABAergic neurons in the RTN, which plays an important role in SWD generation (15–19). We finally examined GABA immunoreactivity in the RTN (Figure 6). We identified GABAergic RTN neurons and their axons through co-immunostaining with an antibody against parvalbumin (PV), a peptide marker for the GABAergic RTN neurons (36–39). In *Gad1* (+/+) rats without VPA treatment [VPA(−)], a strong GABA immunoreactivity was detected in the somata of RTN neurons (Figure 6A, left). A further enhanced GABA immunoreactivity was observed after VPA treatment [VPA(+)] (Figure 6B, left). As expected, GAD1 deficiency reduced GABA immunoreactivity in the somata (Figure 6C, left). VPA treatment

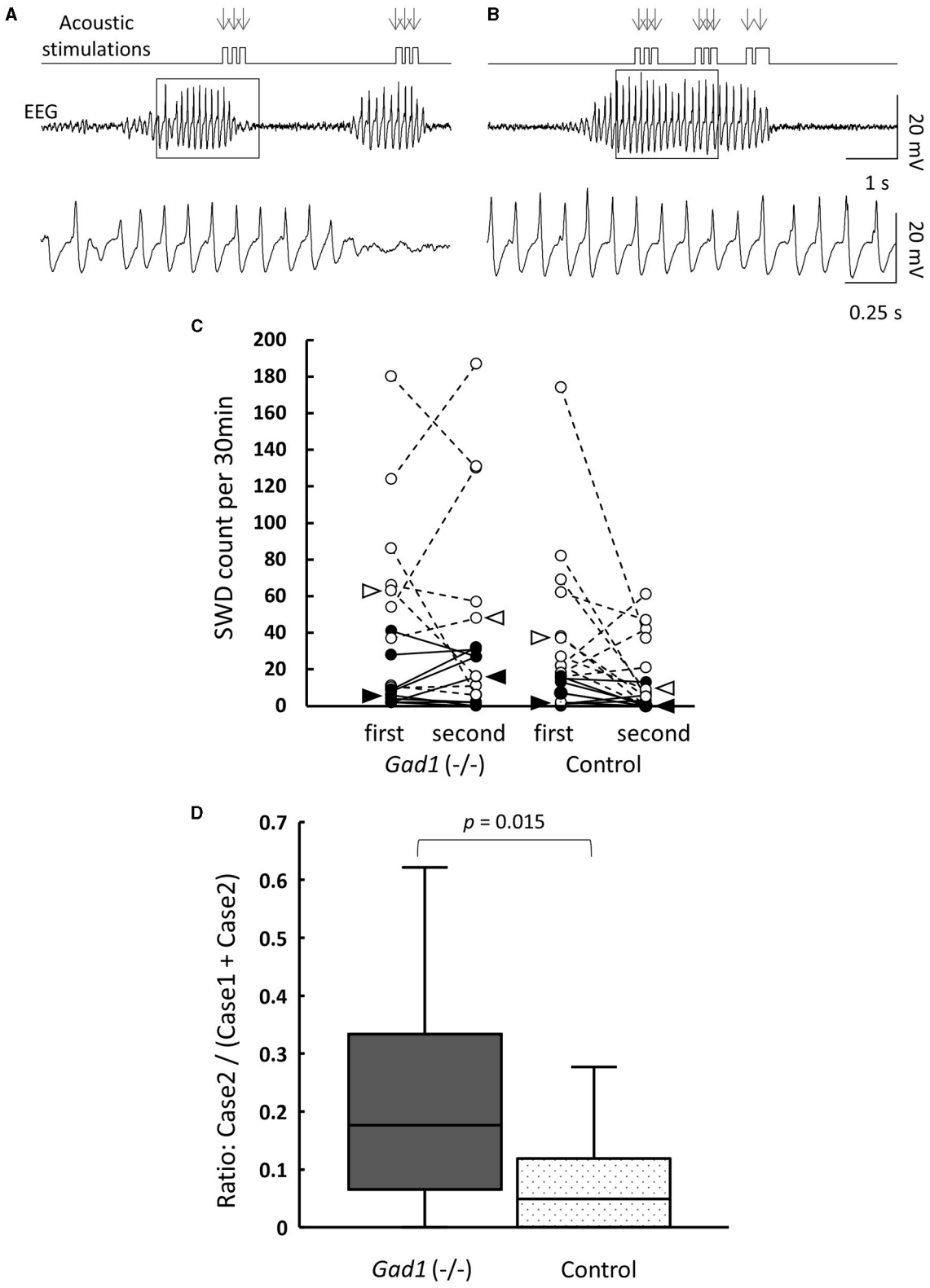

FIGURE 3
Interruption of SWDs by auditory stimuli (AS). **(A)** Case 1: SWDs on the EEG were readily interrupted by AS. The timing of AS presentation is indicated by arrows. The framed section of the SWD data is enlarged at the bottom. **(B)** Case 2: SWDs were not interrupted by AS. The framed section of the SWD data is enlarged at the bottom. Both examples are from a *Gad1* (−/−) rat. The other genotypes showed similar patterns. **(C)** SWD counts according to genotype and occurrence period (first or second half) during the 1-h recording session. Total SWD counts, including both Cases 1 and 2, are indicated by open circles, and Case 2 counts are indicated by filled circles. Circles from the same rat are connected. Medians are indicated by open arrowhead (Cases 1 and 2) or filled arrowhead (Case 2 only). **(D)** Accumulated Case 2 ratio (Case 2/[Cases 1 and 2]) sorted by genotype. *P*-values were calculated using the Wilcoxon rank-sum test.

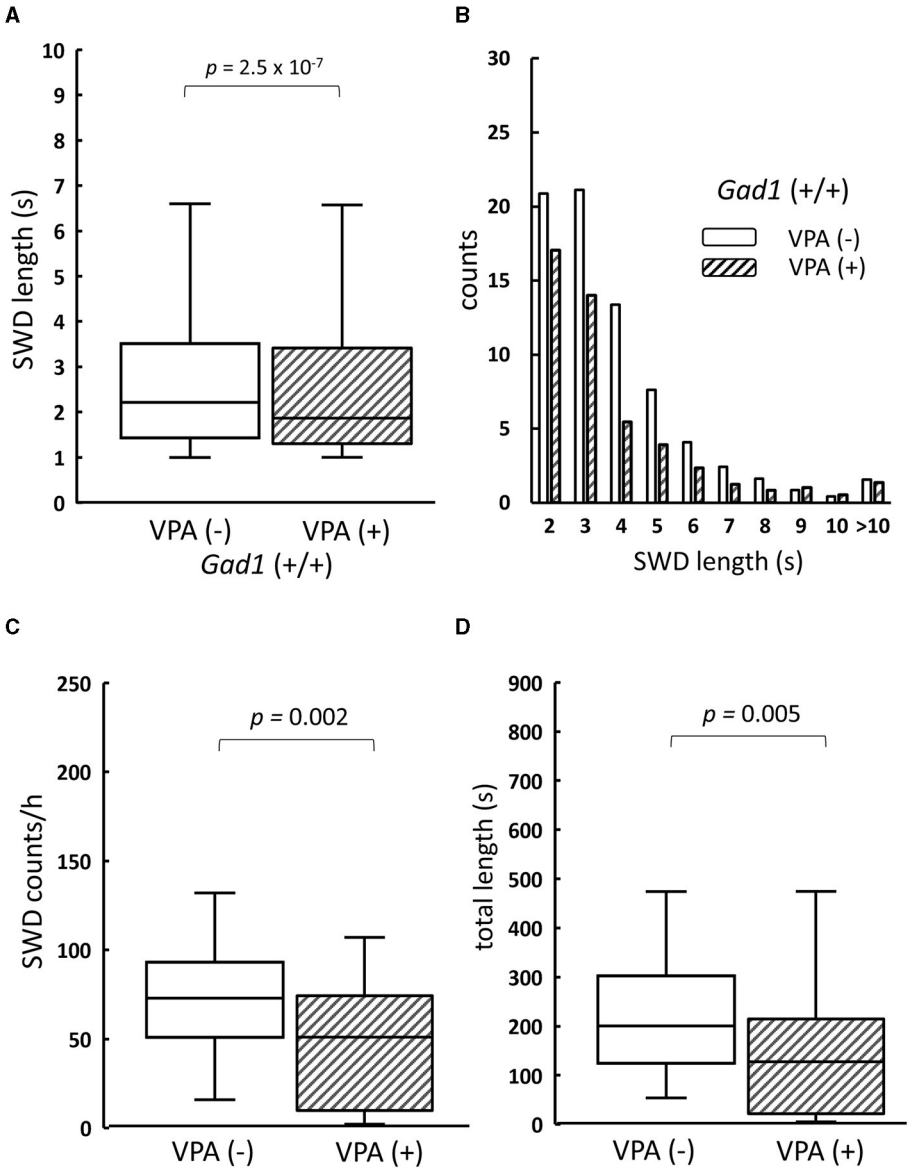

FIGURE 4
The effect of valproate treatment on SWD in *Gad1* (+/+) rats. **(A)** The median SWD length before valproate treatment [VPA(−)] was significantly decreased by VPA administration [VPA (+)]. **(B)** SWD counts per hour decreased in almost all SWD length categories following VPA administration. **(C)** The median SWD count per hour was significantly decreased by VPA treatment. **(D)** The median accumulated SWD time per hour was significantly decreased by VPA treatment. SWD data were merged within the same experimental group, and the medians of each group were compared (the Wilcoxon rank-sum test).

restored GABA immunoreactivity in the somata of *Gad1* (−/−) rats (Figure 6D, left). These results are quantified and summarized in Figure 6E. GABA immunoreactivity was significantly lower in *Gad1* (−/−) rats ($P = 7.4 \times 10^{-9}$; Kruskal–Wallis test). The GABA immunoreactivity was restored in *Gad1* (−/−) after VPA treatment, comparable to that of *Gad1* (+/+) rats ($P = 0.69$; Wilcoxon rank-sum test).

By contrast, the patterns of GABA immunoreactivity in the RTN axons targeting the thalamus were different from those found in the RTN somata. The GABA immunoreactivity in the RTN axons was similar between *Gad1* (+/+) (Figure 6A, right) and *Gad1* (−/−) rats (Figure 6C, right). VPA treatment led to a marked increase in GABA immunoreactivity in the axons of both *Gad1* (+/+) rats (Figure 6B, right) and *Gad1* (−/−) rats (Figure 6D, right) to a similar degree. These results are summarized in Figure 6F. The difference in GABA immunoreactivity was not significantly different between the two genotypes without VPA treatment [VPA(−)] ($P = 0.54$; Wilcoxon rank-sum test) or with VPA treatment [VPA(+)] ($P = 0.73$). These results suggest that GAD1 has a less influential role in axonal GABA production. In summary, we detected a significant

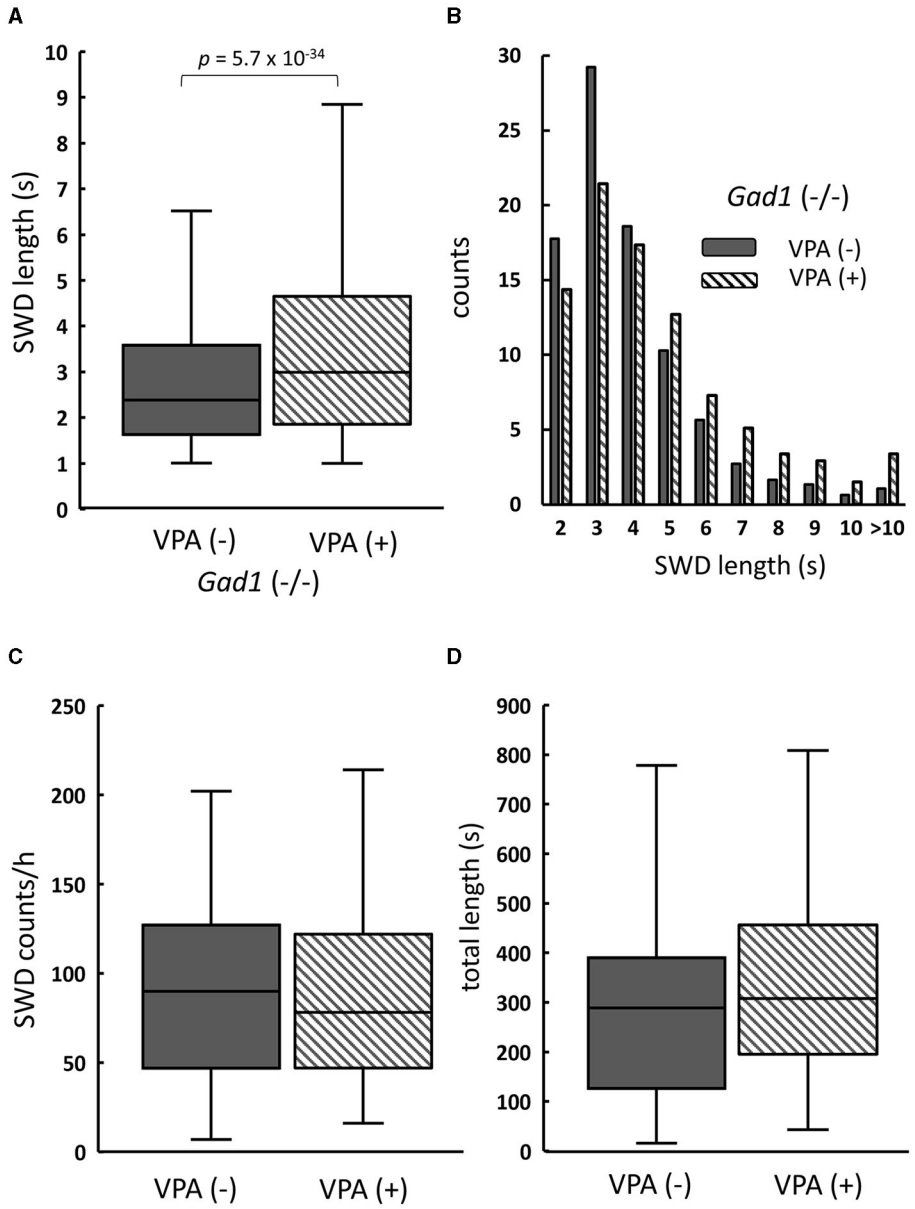

FIGURE 5
The effect of valproate treatment in *Gad1* (−/−) rats. **(A)** The median SWD length before valproate treatment [VPA(−)] was significantly increased by VPA administration [VPA(+)]. **(B)** Following VPA treatment, SWD counts per hour decreased for shorter SWDs but increased for longer SWDs. **(C)** The median SWD count per hour was slightly decreased by VPA, but the effect was not statistically significant ($P = 0.77$). **(D)** The median SWD length per hour was increased by VPA, but the effect was not statistically significant ($P = 0.23$). SWD data were merged within the same experimental group, and the medians of each group were compared (the Wilcoxon rank-sum test).

reduction in GABA immunoreactivity in the RTN neuronal somata in *Gad1* (−/−) rats, consistent with the notion that GAD1 is essential for GABA synthesis in the RTN. The residual GABA in *Gad1* (−/−) rats and excess GABA after VPA treatment are presumably produced by another GABA-synthesizing enzyme, GAD2, which is also expressed in RTN neurons and predominantly localized in the axons (28). The absence of functional GAD1 in the RTN and the excess GABA production in the axons after VPA treatment may account for the contradictory VPA treatment effect observed in *Gad1* (−/−) rats (see the "Discussion" section).

4. Discussion

In this study, we demonstrated that SWD appeared in EEGs at younger ages and more frequently in *Gad1* (−/−) rats than in control rats, indicating that GAD1 plays an important role in SWD suppression. Even control rats exhibited SWDs (Figure 2), which increased in number with age (Table 3) and were alleviated by VPA treatment (Figure 4). Both GAD1 protein and mRNA levels have been reported to decrease spontaneously in the auditory cortex and hippocampus of common laboratory rats (40, 41), suggesting that

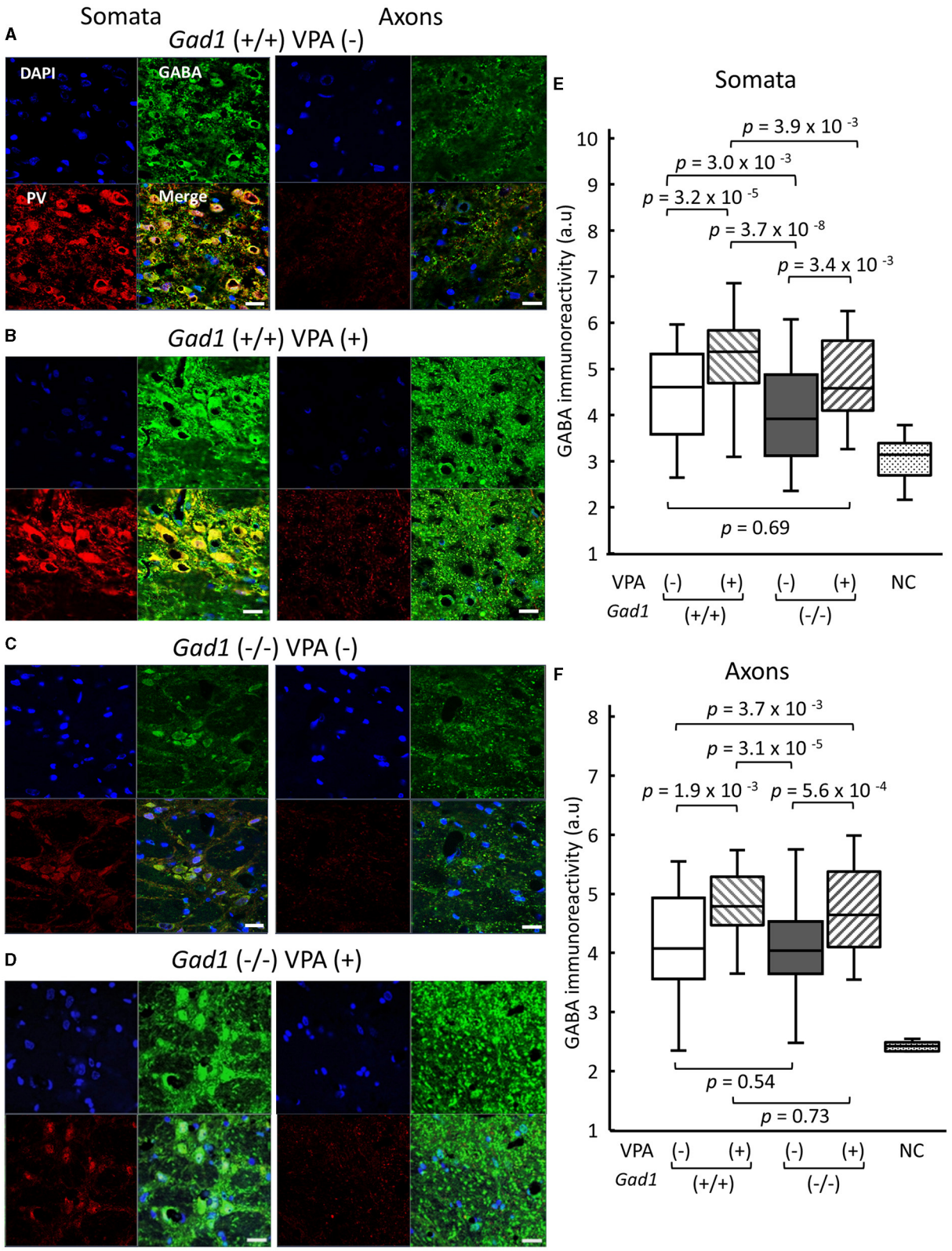

FIGURE 6
GABA immunoreactivity in neuronal soma of RTN neurons and their axons targeting the thalamus. White scale bar: 20 μm. Immunohistochemical detection of gamma aminobutyric acid (GABA, green) and parvalbumin (PV, red) in **(A)** *Gad1* (+/+) VPA (−) rats, **(B)** *Gad1* (+/+) VPA (+) rats, **(C)** *Gad1* (−/−) VPA (−) rats, and **(D)** *Gad1* (−/−) VPA (+) rat. Cell nuclei were labeled with DAPI (blue). **(E)** GABA immunoreactivity was significantly lower in the RTN neuronal soma of *Gad1* (−/−) rats without VPA treatment. **(F)** GABA immunoreactivity in the RTN axons was not significantly different between *Gad1* (−/−) and *Gad1* (+/+) rats, irrespective of VPA treatment. *P* values in the graphs were calculated by pairwise comparisons (the Wilcoxon rank-sum test). Negative control (NC) was included to indicate the background immunoreactivity level, in which chicken normal serum was used as the primary antibody in place of the chicken anti-GABA antibody.

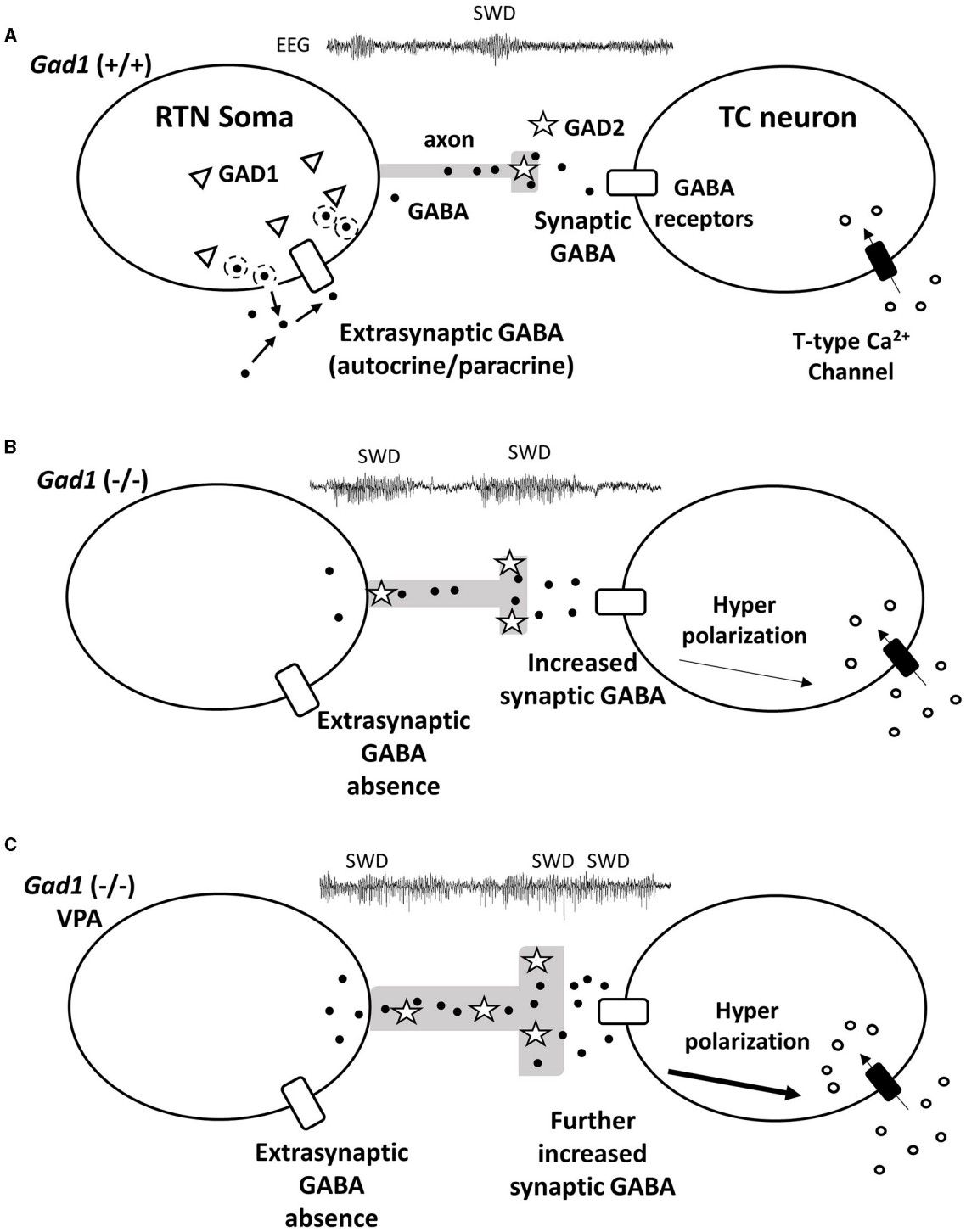

FIGURE 7
Hypothetical mechanism for GABA (black dots) signal transduction between reticular thalamic nucleus (RTN) neurons and thalamocortical (TC) relay neurons underlying SWD generation. **(A)** In the RTN neurons of *Gad1* (+/+) rats, GABA generated by GAD1 (triangles) is released extrasynaptically. The extrasynaptic GABA acts on GABA receptors (white rectangles) localized on the cell body of the RTN neuron and regulates neural activity in an autocrine/paracrine manner. **(B)** RTN neurons of *Gad1* (−/−) rats are disinhibited due to the lack of extrasynaptic GABA. Synaptic GABA synthesis is continued by intact GAD2 (stars) and is enhanced due to disinhibition. GABA binds to synaptic GABA receptors on TC neurons, resulting in deep membrane hyperpolarization and a rebound Ca^{2+} influx mediated by T-type Ca^{2+} channels. **(C)** In *Gad1* (−/−) rats with VPA treatment, synaptic GABA synthesis and release are further enhanced, resulting in profound rebound bursting of TC neurons and exacerbation of the SWD phenotype.

the overall efficacy of GABAergic signal transduction in the brain decreases with age and that this decrease underlies the increase in SWDs observed in older control rats.

We observed that the SWD counts per hour in *Gad1* (+/–) rats were significantly smaller than those in *Gad1* (+/+) rats (Figure 2C), contrary to the observation that the SWD phenotype in *Gad1* (+/–) rats was not significantly different from that in *Gad1* (+/+) rats (Figure 2A). One likely explanation for this unexpected order relation is that one of the *Gad1* (+/+) rats used for this experiment particularity showed a severe SWD phenotype similar to that of the *Gad1* (–/–) rat. Therefore, we do not suggest that the difference seen between *Gad1* (+/–) and *Gad1* (+/+) rats reflects a biologically meaningful difference.

SWDs have been studied in rodent models of epilepsy (4–6). Rodent models have shown that SWDs associated with behavioral immobility could be readily interrupted by external acoustic stimulations or voluntarily controlled with reward cues (9–12, 33, 42), which is consistent with our observation that most SWDs and the associated behavioral immobility were interrupted by buzzer tones (Case 1 SWD, Figure 3A). However, these findings are inconsistent with the clinical observation in human cases that loss of consciousness (absence seizure) is associated with SWDs (1–3). Previous studies have suggested that SWDs in rodents may reflect regular brain activities such as those associated with whisker twitching or attentive mu rhythm (14, 43–45). Nevertheless, we demonstrated that modest numbers of SWDs were resistant to interruption by buzzer tones (Case 2 SWD, Figure 3B) (12). Our data do not strongly suggest that these SWDs were produced by sensory adaptation or loss of motivation over time. Although our buzzer stimuli were not associated with any reward or required behavioral response, they were strong enough to suppress the ongoing SWDs in the control rats for ∼95% of the SWDs, comparable to ∼90% reported by Rodgers et al. (12), in which their acoustic stimuli were associated with no reward as in ours. Importantly, in our *Gad1* (–/–) rats, the same stimulus achieved suppression for ∼82% of the SWDs, which was significantly lower than the control rats, supporting our interpretation that *Gad1* (–/–) rats showed more severe SWDs resistant to external sensory stimuli. Further studies are required to clarify whether Case 2 SWDs indicate true epileptic activity intermixed with Case 1 SWDs, which may represent a regular brain rhythm.

The interplay between glutamatergic excitatory inputs and GABAergic inhibitory inputs to the thalamus, RTN, and cortex plays an essential role in generating SWDs. Synchronous neuronal excitation in TC neurons is associated with the depolarization of membrane potential after prolonged hyperpolarization by GABAergic inputs from RTN neurons (19, 46–49). The excitatory activity in TC neurons is transferred to the cortex through TC projections; in turn, cortical neurons provide corticothalamic input to the subcortical RTN and thalamus as feedback. The postinhibitory rebound depolarization requires T-type Ca^{2+} channels (19, 21), which are effectively blocked by ethosuximide (ETX) (9, 31). Indeed, we observed that ETX administration fully suppressed SWDs in both *Gad1* (–/–) and *Gad1* (+/+) rats (Supplementary Figure S3), confirming the involvement of T-type Ca^{2+} channels in SWD generation in these animals. Although the responsible genetic mutations in the epilepsy model rats have not been fully identified, a mutation in the gene encoding a T-type Ca^{2+} channel subunit has been suggested (5).

Our immunohistochemical experiment showed that GABA synthesis was greatly reduced in the RTN neuronal soma and minimally affected in the RTN axons in *Gad1* (–/–) rats (Figure 6). GAD2, a GAD isozyme, is also expressed in RTN neurons (28) and is likely responsible for the residual GABA synthesis. Therefore, GABAergic neurotransmission should remain functional at the inhibitory synapses on the TC neurons in *Gad1* (–/–) rats. We explored the role of GAD1 in suppressing SWD within the RTN neuronal soma. Interestingly, synaptic GABAergic connections are rare among the RTN neurons (50), and tonic inhibition mediated through extrasynaptic GABA receptors is dominant in these neurons (51). We propose that the GABA produced by GAD1 is released in an autocrine/paracrine manner from the RTN neuronal soma to inhibit RTN neurons extrasynaptically. Previous studies have demonstrated extrasynaptic GABA release in the retina (52). Our results can be accounted for by non-synaptic GABAergic inhibition within RTN neurons (Figure 7A). The GABA produced by GAD1 is released from the RTN neuronal cell bodies and maintains the basal activity of these inhibitory neurons through mutual extrasynaptic GABAergic neurotransmission. This model accounts for the enhanced SWD phenotype in *Gad1* (–/–) rats (Figure 7B). RTN neurons are tonically active (disinhibited) in these rats due to a deficiency of extrasynaptic GABA. However, GABA synthesis in the axons continues due to intact synaptic GAD2 and can even be elevated due to the compensatory increase in GAD2 expression in *Gad1* (–/–) rats (28). Therefore, GABA release at the inhibitory synapses between the disinhibited RTN axon terminals and target TC neurons should be significantly increased. The increased activation of synaptic GABA receptors on TC neurons induces deep hyperpolarization in these neurons, followed by profound rebound bursting. This rebound bursting is involved in sustained SWD generation (19, 21). A further increase in synaptic GABA production after VPA treatment (Figure 7C) results in longer and deeper hyperpolarization of TC neurons, leading to the paradoxical exacerbation of SWD symptoms in *Gad1* (–/–) rats.

In conclusion, we demonstrated that GAD1 deficiency in rats results in abundant SWDs in EEG data from an early age, comparable to other epilepsy-model rodents. *Gad1* (–/–) rats exhibited SWDs resistant to interruption by buzzer tones more frequently than control rats; therefore, we suggest that true epileptic activity may have occurred, together with regular brain rhythms. We revealed two opposing roles for GABA: suppression and enhancement of SWD generation. Our interpretation of these results depends on the hypothetical extrasynaptic GABA produced by GAD1 from the RTN neuronal soma. Further molecular and neurophysiological experiments are necessary to confirm the role played by GAD1 in extrasynaptic GABAergic transduction in the RTN.

Data availability statement

The original contributions presented in the study are included in the article/Supplementary material, further inquiries can be directed to the corresponding author.

Ethics statement

The animal study was approved by Tohoku University Committee for Animal Research. The study was conducted in accordance with the local legislation and institutional requirements.

Author contributions

DL and TO designed the research, analyzed the data, and wrote the manuscript. DL conducted the experiments and collected the data. All authors contributed to the article and approved the submitted version.

Funding

This study was supported by JSPS KAKENHI Grants 16K06984 and 19K22464 (TO), 23K18159, 22H04922, and MEXT Grants 19H03337 (HM).

Acknowledgments

We thank Dr. Toshikazu Kakizaki for his helpful comments on the manuscript.

Conflict of interest

The authors declare that the research was conducted in the absence of any commercial or financial relationships that could be construed as a potential conflict of interest.

Publisher's note

Supplementary material

The Supplementary Material for this article can be found online at: https://www.frontiersin.org/articles/10.3389/fneur.2023.1243301/full#supplementary-material

References

1. Blumenfeld H. Consciousness and epilepsy: why are patients with absence seizures absent? *Prog Brain Res.* (2005) 150:271–86. doi: 10.1016/S0079-6123(05)50020-7

2. Blumenfeld H. Epilepsy and the consciousness system: transient vegetative state? *Neurol Clin.* (2011) 29:801–23. doi: 10.1016/j.ncl.2011.07.014

3. Remi J, Vollmar C, Noachtar S. No response to acoustic stimuli: absence or akinetic seizure? *Epilep Behav.* (2011) 21:478–9. doi: 10.1016/j.yebeh.2011.06.008

4. Gilles van Luijtelaar TC. "Genetic models of absence epilepsy in the rat," In: *Models of Seizures and Epilepsy.* (2006) p. 233-48.

5. Coenen AM, Van Luijtelaar EL. Genetic animal models for absence epilepsy: a review of the WAG/Rij strain of rats. *Behav Genet.* (2003) 33:635–55. doi: 10.1023/a:1026179013847

6. Danober L, Deransart C, Depaulis A, Vergnes M, Marescaux C. Pathophysiological mechanisms of genetic absence epilepsy in the rat. *Prog Neurobiol.* (1998) 55:27–57. doi: 10.1016/S0301-0082(97)00091-9

7. Shaw FZ. 7-12 Hz high-voltage rhythmic spike discharges in rats evaluated by antiepileptic drugs and flicker stimulation. *J Neurophysiol.* (2007) 97:238–47. doi: 10.1152/jn.00340.2006

8. Taylor JA, Reuter JD, Kubiak RA, Mufford TT, Booth CJ, Dudek FE, et al. Spontaneous recurrent absence seizure-like events in wild-caught rats. *J Neurosci.* (2019) 39:4829–41. doi: 10.1523/JNEUROSCI.1167-18.2019

9. Taylor JA, Rodgers KM, Bercum FM, Booth CJ, Dudek FE, Barth DS. Voluntary control of epileptiform spike-wave discharges in awake rats. *J Neurosci.* (2017) 37:5861–9. doi: 10.1523/JNEUROSCI.3235-16.2017

10. Saillet S, Gharbi S, Charvet G, Deransart C, Guillemaud R, Depaulis A, et al. Neural adaptation to responsive stimulation: a comparison of auditory and deep brain stimulation in a rat model of absence epilepsy. *Brain Stimul.* (2013) 6:241–7. doi: 10.1016/j.brs.2012.05.009

11. Drinkenburg WHIM, Schuurmans MLEJ, Coenen AML, Vossen JMH, van Luijtelaar ELJM. Ictal stimulus processing during spike-wave discharges in genetic epileptic rats. *Behav Brain Res.* (2003) 143:141–6. doi: 10.1016/S0166-4328(03)00031-7

12. Rodgers KM, Dudek FE, Barth DS. Progressive, seizure-like, spike-wave discharges are common in both injured and uninjured Sprague-Dawley rats: implications for the fluid percussion injury model of post-traumatic epilepsy. *J Neurosci.* (2015) 35:9194–204. doi: 10.1523/JNEUROSCI.0919-15.2015

13. Shaw FZ. Is spontaneous high-voltage rhythmic spike discharge in Long Evans rats an absence-like seizure activity? *J Neurophysiol.* (2004) 91:63–77. doi: 10.1152/jn.00487.2003

14. Wiest MC, Nicolelis MA. Behavioral detection of tactile stimuli during 7-12 Hz cortical oscillations in awake rats. *Nat Neurosci.* (2003) 6:913–4. doi: 10.1038/nn1107

15. Gorji A, Mittag C, Shahabi P, Seidenbecher T, Pape HC. Seizure-related activity of intralaminar thalamic neurons in a genetic model of absence epilepsy. *Neurobiol Dis.* (2011) 43:266–74. doi: 10.1016/j.nbd.2011.03.019

16. Hu B, Guo Y, Shi F, Zou X, Dong J, Pan L, et al. The generation mechanism of spike-and-slow wave discharges appearing on thalamic relay nuclei. *Sci Rep.* (2018) 8:4953. doi: 10.1038/s41598-018-23280-y

17. Meeren HK, Pijn JP, Van Luijtelaar EL, Coenen AM, Lopes da Silva FH. Cortical focus drives widespread corticothalamic networks during spontaneous absence seizures in rats. *J Neurosci.* (2002) 22:1480–95. doi: 10.1523/JNEUROSCI.22-04-01480.2002

18. Sitnikova E. Thalamo-cortical mechanisms of sleep spindles and spike-wave discharges in rat model of absence epilepsy (a review). *Epilepsy Res.* (2010) 89:17–26. doi: 10.1016/j.eplepsyres.2009.09.005

19. Fogerson PM, Huguenard JR. Tapping the brakes: cellular and synaptic mechanisms that regulate thalamic oscillations. *Neuron.* (2016) 92:687–704. doi: 10.1016/j.neuron.2016.10.024

20. Pinault D. The thalamic reticular nucleus: structure, function and concept. *Brain Res Rev.* (2004) 46:1–31. doi: 10.1016/j.brainresrev.2004.04.008

21. Leresche N, Lambert RC. GABA receptors and T-type Ca^{2+} channels crosstalk in thalamic networks. *Neuropharmacology.* (2018) 136:37–45. doi: 10.1016/j.neuropharm.2017.06.006

22. Wu H, Jin Y, Buddhala C, Osterhaus G, Cohen E, Jin H, et al. Role of glutamate decarboxylase (GAD) isoform, GAD65, in GABA synthesis and transport into synaptic vesicles-evidence from GAD65-knockout mice studies. *Brain Res.* (2007) 1154:80–3. doi: 10.1016/j.brainres.2007.04.008

23. Walls AB, Eyjolfsson EM, Smeland OB, Nilsen LH, Schousboe I, Schousboe A, et al. Knockout of GAD65 has major impact on synaptic GABA synthesized from astrocyte-derived glutamine. *J Cereb Blood Flow Metab.* (2011) 31:494–503. doi: 10.1038/jcbfm.2010.115

24. Stork O, Ji FY, Kaneko K, Stork S, Yoshinobu Y, Moriya T, et al. Postnatal development of a GABA deficit and disturbance of neural functions in mice lacking GAD65. *Brain Res.* (2000) 865:45–58. doi: 10.1016/S0006-8993(00)02206-X

25. Kakizaki T, Ohshiro T, Itakura M, Konno K, Watanabe M, Mushiake H, et al. Rats deficient in the GAD65 isoform exhibit epilepsy and premature lethality. *FASEB J.* (2021) 35:e21224. doi: 10.1096/fj.202001935R

26. Qi J, Kim M, Sanchez R, Ziaee SM, Kohtz JD, Koh S. Enhanced susceptibility to stress and seizures in GAD65 deficient mice. *PLoS ONE.* (2018) 13:e0191794. doi: 10.1371/journal.pone.0191794

27. Esclapez M TN, Kaufman DL, Tobin AJ, Houser CR. Comparative. Comparative localization of two forms of glutamic acid decarboxylase and their mRNAs in rat brain supports the concept of functional differences between the forms. *Neuroscience.* (1994) 14:834–1855. doi: 10.1523/JNEUROSCI.14-03-01834.1994

28. Panthi S, Lyons NMA, Leitch B. Impact of dysfunctional feed-forward inhibition on glutamate decarboxylase isoforms and gamma-aminobutyric acid transporters. *Int J Mol Sci.* (2021) 22:14. doi: 10.3390/ijms22147740

29. Fujihara K, Yamada K, Ichitani Y, Kakizaki T, Jiang W, Miyata S, et al. CRISPR/Cas9-engineered *Gad1* elimination in rats leads to complex behavioral changes: implications for schizophrenia. *Transl Psychiatry.* (2020) 10:426. doi: 10.1038/s41398-020-01108-6

30. Kuki T, Ohshiro T, Ito S, Ji ZG, Fukazawa Y, Matsuzaka Y, et al. Frequency-dependent entrainment of neocortical slow oscillation to repeated optogenetic stimulation in the anesthetized rat. *Neurosci Res.* (2013) 75:35–45. doi: 10.1016/j.neures.2012.10.007

31. Loscher W. The pharmacokinetics of antiepileptic drugs in rats: consequences for maintaining effective drug levels during prolonged drug administration in rat models of epilepsy. *Epilepsia.* (2007) 48:1245–58. doi: 10.1111/j.1528-1167.2007.01093.x

32. Fang G, Xia Y, Zhang C, Liu T, Yao D. Optimized single electroencephalogram channel sleep staging in rats. *Lab Anim.* (2010) 44:312–22. doi: 10.1258/la.2010.009081

33. Vergnes M, Marescaux C, Boehrer A, Depaulis A. Are rats with genetic absence epilepsy behaviorally impaired? *Epilepsy Res.* (1991) 9:97–104. doi: 10.1016/0920-1211(91)90019-C

34. Watanabe Y, Takechi K, Fujiwara A, Kamei C. Effects of antiepileptics on behavioral and electroencephalographic seizure induced by pentetrazol in mice. *J Pharmacol Sci.* (2010) 112:282–9. doi: 10.1254/jphs.09225FP

35. Loscher W. Basic pharmacology of valproate—a review after 35 years of clinical use for the treatment of epilepsy. *CNS Drugs.* (2002) 16:669–94. doi: 10.2165/00023210-200216100-00003

36. Kawaguchi Y, Kondo S. Parvalbumin, somatostatin and cholecystokinin as chemical markers for specific GABAergic interneuron types in the rat frontal cortex. *J Neurocytol.* (2002) 31:277–87. doi: 10.1023/A:1024126110356

37. Kajita Y, Mushiake H. Heterogeneous GAD65 Expression in subtypes of GABAergic neurons across layers of the cerebral cortex and hippocampus. *Front Behav Neurosci.* (2021) 15:750869. doi: 10.3389/fnbeh.2021.750869

38. Steullet P, Cabungcal JH, Bukhari SA, Ardelt MI, Pantazopoulos H, Hamati F, et al. The thalamic reticular nucleus in schizophrenia and bipolar disorder: role of parvalbumin-expressing neuron networks and oxidative stress. *Mol Psychiatry.* (2018) 23:2057–65. doi: 10.1038/mp.2017.230

39. Williams SM, Goldman-Rakic PS, Leranth C. The synaptology of parvalbumin-immunoreactive neurons in the primate prefrontal cortex. *J Comp Neurol.* (1992) 320:353–69. doi: 10.1002/cne.903200307

40. Ling LL, Hughes LF, Caspary DM. Age-related loss of the GABA synthetic enzyme glutamic acid decarboxylase in rat primary auditory cortex. *Neuroscience.* (2005) 132:1103–13. doi: 10.1016/j.neuroscience.2004.12.043

41. Stanley DP, Shetty AK. Aging in the rat hippocampus is associated with widespread reductions in the number of glutamate decarboxylase-67 positive interneurons but not interneuron degeneration. *J Neurochem.* (2004) 89:204–16. doi: 10.1111/j.1471-4159.2004.02318.x

42. Li X, Ouyang G, Richards DA. Predictability analysis of absence seizures with permutation entropy. *Epilepsy Res.* (2007) 77:70–4. doi: 10.1016/j.eplepsyres.2007.08.002

43. Shaw FZ, Liao YF. Relation between activities of the cortex and vibrissae muscles during high-voltage rhythmic spike discharges in rats. *J Neurophysiol.* (2005) 93:2435–48. doi: 10.1152/jn.00999.2004

44. Nicolelis MA, Fanselow EE. Thalamocortical correction of thalamcortical optimization of tactile processing according to behavioral state. *Nat Neurosci.* (2002) 5:517–23. doi: 10.1038/nn0602-517

45. Shaw FZ, Liao YF, Chen RF, Huang YH, Lin RC. The zona incerta modulates spontaneous spike-wave discharges in the rat. *J Neurophysiol.* (2013) 109:2505–16. doi: 10.1152/jn.00750.2011

46. Guillery RW, Feig SL, Lozsadi DA. Paying attention to the thalamic reticular nucleus. *Trends Neurosci.* (1998) 21:28–32. doi: 10.1016/S0166-2236(97)01157-0

47. Clemente-Perez A, Makinson SR, Higashikubo B, Brovarney S, Cho FS, Urry A, et al. Distinct thalamic reticular cell types differentially modulate normal and pathological cortical rhythms. *Cell Rep.* (2017) 19:2130–42. doi: 10.1016/j.celrep.2017.05.044

48. Schofield CM, Kleiman-Weiner M, Rudolph U, Huguenard JR, A. gain in GABAA receptor synaptic strength in thalamus reduces oscillatory activity and absence seizures. *Proc Natl Acad Sci U S A.* (2009) 106:7630–5. doi: 10.1073/pnas.0811326106

49. Huntsman MM, Porcello DM, Homanics GE, DeLorey TM, Huguenard JR. Reciprocal inhibitory connections and network synchrony in the mammalian thalamus. *Science.* (1999) 283:541–3. doi: 10.1126/science.283.5401.541

50. Hou G, Smith AG, Zhang ZW. Lack of intrinsic GABAergic connections in the thalamic reticular nucleus of the mouse. *J Neurosci.* (2016) 36:7246–52. doi: 10.1523/JNEUROSCI.0607-16.2016

51. Crabtree JW, Lodge D, Bashir ZI, Isaac JT, GABAA. NMDA and mGlu2 receptors tonically regulate inhibition and excitation in the thalamic reticular nucleus. *Eur J Neurosci.* (2013) 37:850–9. doi: 10.1111/ejn.12098

52. Hirasawa H, Contini M, Raviola E. Extrasynaptic release of GABA and dopamine by retinal dopaminergic neurons. *Philos Trans R Soc Lond B Biol Sci.* (2015) 370:1672. doi: 10.1098/rstb.2014.0186

frontiers | Frontiers in Neuroscience

TYPE Brief Research Report
PUBLISHED 13 October 2023
DOI 10.3389/fnins.2023.1282201

OPEN ACCESS

EDITED BY
Evgenia Sitnikova,
Institute of Higher Nervous Activity and Neurophysiology (RAS), Russia

REVIEWED BY
Severine Deforges,
UMR5297 Institut Interdisciplinaire de Neurosciences (IINS), France
Alexander Bryson,
University of Melbourne, Australia

*CORRESPONDENCE
Sophie F. Hill
✉ sfhill@umich.edu

RECEIVED 23 August 2023
ACCEPTED 25 September 2023
PUBLISHED 13 October 2023

CITATION
Hill SF, Jafar-Nejad P, Rigo F and Meisler MH (2023) Reduction of *Kcnt1* is therapeutic in mouse models of *SCN1A* and *SCN8A* epilepsy.
Front. Neurosci. 17:1282201.
doi: 10.3389/fnins.2023.1282201

Reduction of *Kcnt1* is therapeutic in mouse models of *SCN1A* and *SCN8A* epilepsy

Sophie F. Hill[1,2]*, Paymaan Jafar-Nejad[3], Frank Rigo[3] and Miriam H. Meisler[1,2,4]

[1]Neuroscience Graduate Program, University of Michigan, Ann Arbor, MI, United States, [2]Department of Human Genetics, University of Michigan, Ann Arbor, MI, United States, [3]Ionis Pharmaceuticals, Carlsbad, CA, United States, [4]Department of Neurology, University of Michigan, Ann Arbor, MI, United States

Developmental and epileptic encephalopathies (DEEs) are severe seizure disorders with inadequate treatment options. Gain- or loss-of-function mutations of neuronal ion channel genes, including potassium channels and voltage-gated sodium channels, are common causes of DEE. We previously demonstrated that reduced expression of the sodium channel gene *Scn8a* is therapeutic in mouse models of sodium and potassium channel mutations. In the current study, we tested whether reducing expression of the potassium channel gene *Kcnt1* would be therapeutic in mice with mutation of the sodium channel genes *Scn1a* or *Scn8a*. A *Kcnt1* antisense oligonucleotide (ASO) prolonged survival of both *Scn1a* and *Scn8a* mutant mice, suggesting a modulatory effect for KCNT1 on the balance between excitation and inhibition. The cation channel blocker quinidine was not effective in prolonging survival of the *Scn8a* mutant. Our results implicate *KCNT1* as a therapeutic target for treatment of *SCN1A* and *SCN8A* epilepsy.

KEYWORDS

***Scn8a*, *Scn1a*, *Kcnt1*, epilepsy, ASO, sodium channel, potassium channel**

1. Introduction

Developmental and epileptic encephalopathies (DEEs) are among the most severe epileptic disorders. The typical disease course begins with onset of seizures during the first year of life, followed by developmental delay, movement disorders, intellectual disability, sleep disturbances, and feeding difficulties (Scheffer and Nabbout, 2019; Meisler et al., 2021; Johannesen et al., 2022). Seizures are often resistant to treatment with current antiepileptic drugs (Scheffer and Nabbout, 2019; Meisler et al., 2021; Johannesen et al., 2022).

Many DEEs result from mutations in sodium and potassium channel genes (Lindy et al., 2018; Symonds et al., 2019). Based on their roles in the neuronal action potential, excessive sodium current or insufficient potassium current would be predicted to cause hyperexcitability and epilepsy. In agreement with expectation, many missense mutations in the voltage-gated sodium channel gene *SCN8A* result in excessive sodium current ("gain-of-function", or GOF, mutations) and *SCN8A*-DEE (Veeramah et al., 2012; Meisler et al., 2021; Johannesen et al., 2022). Experimental expression of an *SCN8A* GOF mutation in excitatory neurons is sufficient to cause seizures and premature death, while expression limited to inhibitory neurons does not (Bunton-Stasyshyn et al., 2019).

Loss-of-function (LOF) mutations of the sodium channel gene *SCN1A* and GOF mutations of the potassium channel gene *KCNT1* can also cause epilepsy (Barcia et al., 2012; Scheffer and

Nabbout, 2019; Gribkoff and Winquist, 2023). *SCN1A* haploinsufficiency reduces the excitability of inhibitory neurons, altering excitation/inhibition balance (Cheah et al., 2012; Tai et al., 2014; Favero et al., 2018). The epileptogenic mechanism of *KCNT1* GOF mutations is not well established, but a similar disinhibitory mechanism may be involved (Shore et al., 2020; Gertler et al., 2022; Wu et al., 2023).

KCNT1 is a sodium-activated potassium channel (also known as Slo2.2, $K_{Na}1.1$, or Slack) with widespread expression in the central nervous system (Rizzi et al., 2016). KCNT1 regulates afterhyperpolarization amplitude and action potential threshold (Martinez-Espinosa et al., 2015; Quraishi et al., 2019; Shore et al., 2020; Gertler et al., 2022; Wu et al., 2023). *KCNT1* GOF mutations enhance bursting behavior in excitatory neurons and reduce action potential firing in inhibitory neurons (Quraishi et al., 2019; Shore et al., 2020; Gertler et al., 2022; Wu et al., 2023).

In the mouse, homozygous knock-in of *KCNT1* GOF mutations results in spontaneous seizures, reduced threshold for seizure induction, behavioral abnormalities, and premature lethality (Quraishi et al., 2020; Shore et al., 2020; Burbano et al., 2022; Gertler et al., 2022). Burbano et al. (2022) described an antisense oligonucleotide (ASO) that reduces expression of *Kcnt1*. Administration of the ASO to a homozygous *Kcnt1* GOF mouse prolonged survival, reduced seizure frequency, and corrected behavioral abnormalities. Conversely, homozygous loss of *Kcnt1* also improves survival after electrically induced seizrues (Quraishi et al., 2020).

Reducing expression of *Scn8a* prolongs survival of epileptic mice with mutations in the potassium channel genes *Kcna1* and *Kcnq2* (Hill et al., 2022). Here, we asked whether modulating expression of a potassium channel can improve the phenotype of sodium channel mutants. Administration of the *Kcnt1* ASO (Burbano et al., 2022) on postnatal day 2 doubled the lifespan of *Scn8a* mutant mice and extended survival of *Scn1a* haploinsufficient mice. Our results suggest a new therapeutic intervention for DEEs caused by mutations of *SCN1A* and *SCN8A*.

2. Methods

2.1. Mice

The *Scn8a*^{cond} allele, abbreviated W, contains two tandem copies of exon 26, the final coding exon of *Scn8a* (Bunton-Stasyshyn et al., 2019). The upstream copy, designated 26a, is a floxed exon that encodes the wildtype channel. Deletion of exon 26a by Cre results in expression of exon 26b encoding the variant p.R1872W. This variant has been identified in multiple individuals with *SCN8A* epilepsy (Bunton-Stasyshyn et al., 2019; Johannesen et al., 2022). *Scn8a*$^{cond/cond}$ male mice were crossed with *EIIa-Cre*/+ female mice (JAX 003724) to generate *Scn8a*$^{cond/+}$,*EIIa-Cre* double heterozygous mice expressing the R1872W variant (designated W/+ mice). Both the *Scn8a*^{cond} allele and the *EIIa-Cre* transgene were maintained on a C57Bl/6J genetic background.

Scn1a$^{+/-}$ mice with deletion of exon 1 were maintained on the protective 129S6/SvEvTac strain background and activated in (C57BL/6J X 129S6/SvEvTac) F1 mice (Miller et al., 2014). Both male and female mice were used for all experiments. Experiments were approved by the Committee on the Use and Care of Animals at the University of Michigan.

2.2. ASOs

ASOs were synthesized by Ionis Pharmaceuticals as described (Swayze et al., 2007). Both the non-targeting control and *Kcnt1* ASOs are 20-bp gap-mers with 5 2'-*O*-methoxyethyl modifications on the first and last 5 bases and phosphorothioate modifications on all 20 bases. The *Kcnt1* ASO (5' GCT TCA TGC CAC TTT CCA GA 3′) is complementary to the 3' UTR of mouse *Kcnt1* and was previously described (Burbano et al., 2022). The non-targeting control ASO (5' CCT ATA GGA CTA TTC AGG AA 3′) is well-tolerated and is not complementary to any transcript encoded by the mouse genome (Swayze et al., 2007). Animals treated with control ASO received a 30 μg dose.

2.3. Intracerebroventricular (ICV) injections

At postnatal day 2 (P2), mice were cryo-anesthetized for 3 min. ASO was diluted in PBS (2 μL injection volume) and manually injected into the left ventricle as described (Lenk et al., 2020). Animals were allowed to recover for 10 min at 37°C before being returned to the home cage.

2.4. qRT-PCR

Brain and spinal cord from 3-week-old mice treated with control or *Kcnt1* ASO were homogenized in TRIzol (Invitrogen Cat. #15596026, Waltham, MA). RNA was extracted using the Direct-zol RNA Mini Prep kit from Zymo Research (Irvina, CA). cDNA was synthesized with the LunaScript kit from New England Biolabs (Ipwsich, MA). *Scn8a* (Mm00488110_m1), *Kcnt1* (Mm01330661_g1), and *Tbp* (Mm01277042_m1) transcripts were quantified using TaqMan gene expression assays (Applied Biosystems, Foster City, CA).

2.5. Quinidine administration

Quinidine (Sigma Aldrich, St. Louis, MO) was diluted in phosphate-buffered saline (50 or 100 mg/kg) and administered by daily intraperitoneal injection beginning at P10, the youngest age at which daily intraperitoneal injections were feasible.

3. Results

3.1. Characterization of the *Kcnt1* ASO

We used an ASO to reduce expression of mouse *Kcnt1*. The 20 base-pair "gap-mer" ASO targets the 3' UTR of the mouse *Kcnt1* gene (Figure 1A) and recruits RNaseH1 to degrade the transcript (Burbano et al., 2022). We first administered the ASO to wild-type animals by ICV injection at P2. Three weeks later, we measured gene expression in brain and spinal cord by qRT-PCR (Figure 1B; Supplementary Table S1). *Kcnt1* expression was reduced in both brain and spinal cord (two-way ANOVA, $p < 0.0001$). For example, adminsitration of 45 μg *Kcnt1* ASO reduced *Kcnt1* expression in brain to 0.25 ± 0.04 of control (mean ± SD, $n = 3$) (Supplementary Table S1). Reduction of *Kcnt1* transcript reduces KCNT1 protein expression

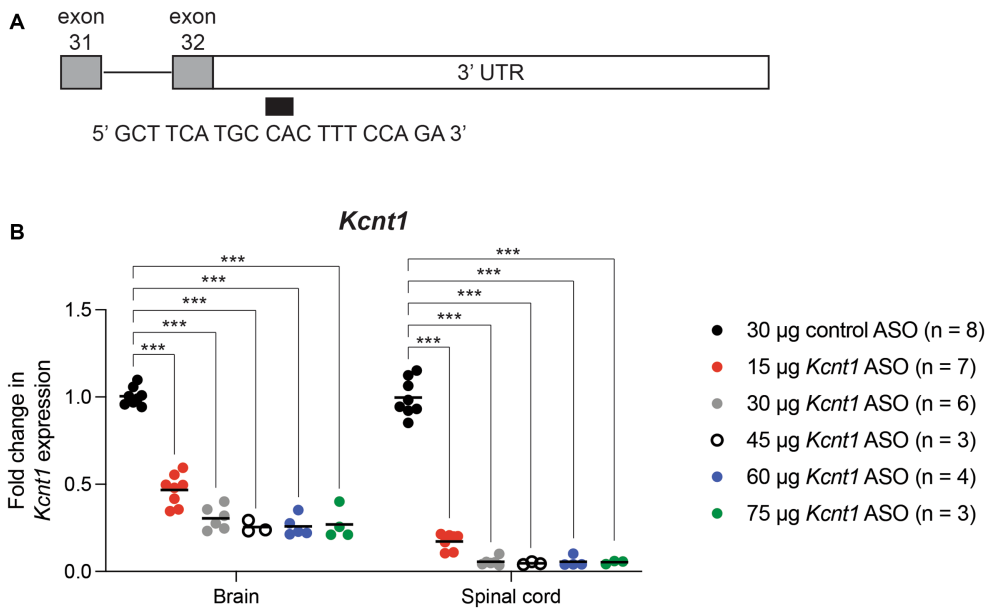

FIGURE 1
Kcnt1 ASO reduces *Kcnt1* transcript abundance. **(A)** The *Kcnt1* ASO targets the proximal 3'UTR of the *Kcnt1* transcript. **(B)** Expression of *Kcnt1* in brain and spinal cord from P21 wildtype mice treated with *Kcnt1* ASO on P2, measured by qRT-PCR (***=p<0.0001, Sidak's multiple comparisons test).

(Burbano et al., 2022). Expression of *Scn8a* was unaffected by the *Kcnt1* ASO (Supplementary Figure S1). No changes in *Kcnt1* expression were detected in previous studies of *Scn1a* and *Scn8a* mutant mice (Sprissler et al., 2017; Hawkins et al., 2019; Valassina et al., 2022).

3.2. ASO-mediated reduction of *Kcnt1* extends the lifespan of an *SCN8A* DEE mouse

We previously generated a mouse with Cre-dependent expression of the patient mutation p.R1872W (Bunton-Stasyshyn et al., 2019). Expression of this mutation by crossing with the ubiquitously expressed *EIIa-Cre* results in a single, lethal seizure at P14 (Bunton-Stasyshyn et al., 2019). We treated *Scn8a*$^{cond/+}$,*EIIa-Cre* (W/+) animals with 15–75 µg *Kcnt1* ASO by ICV injection at P2. Mice treated with the control ASO exhibited median survival of 16 days (Figure 2). Mice treated with 15 µg *Kcnt1* ASO lived three days longer (median survival = 19 days, p = 0.0493, Mantel-Cox log-rank test). Treatment with 30 µg *Kcnt1* ASO extended median survival to 27 days (p < 0.0001, Mantel- Cox log-rank test). Mice treated with 45 µg, the optimal dose, exhibited median survival of 36 days, more than double the lifespan of control ASO-treated mice (p < 0.0001, Mantel-Cox log-rank test, Figure 2). Treatment with 60 or 75 µg *Kcnt1* ASO did not further reduce *Kcnt1* expression (Figure 1B) or further extend survival (Supplementary Figure S2).

3.3. Quinidine does not extend survival in the *SCN8A* DEE mouse

Quinidine is a nonspecific cation channel blocker used to treat cardiac arrhythmia. *In vitro*, quinidine blocks KCNT1 channel activity, suggesting that it could be a precision therapy for patients with gain-of-function *KCNT1* mutations (Mori et al., 1998; Milligan et al., 2014). *In vivo*, quinidine has mixed efficacy in *KCNT1* epilepsy patients (Mikati et al., 2015; Numis et al., 2018; Fitzgerald et al., 2019; Cole et al., 2021).

To determine whether inhibition of KCNT1 channels by quinidine would be therapeutic in *Scn8a* mutant mice, we administered 50 or 100 mg/kg quinidine by daily intraperitoneal injection beginning at P10 (Figure 3). Untreated mice exhibited median survival of 15 days (n = 47). Treatment with 50 or 100 mg/kg quinidine did not extend the lifespan of the *SCN8A*-DEE mice (median survival = 14 days; n = 7 & 9, respectively; Figure 3).

3.4. ASO-mediated reduction of *Kcnt1* extends the lifespan of a mouse model of *SCN1A* haploinsufficiency

We also tested the effect of the *Kcnt1* ASO in *Scn1a*$^{+/-}$ mice, a model of Dravet Syndrome. Consistent with previous studies (Miller et al., 2014; Favero et al., 2018), approximately 1/3 of untreated *Scn1a*$^{+/-}$ mice died between 3 and 4 weeks of age, and during the remaining 6-month monitoring period, there were several sporadic deaths (Figure 4). We administered 45 µg *Kcnt1* ASO to *Scn1a*$^{+/-}$ mice at P2. None of the treated mice died in the first 4 weeks, indicating that reduced *Kcnt1* expression during this critical period is sufficient to prevent death (p = 0.0513, Mantel-Cox log-rank test, Figure 4). There were four deaths during the 6-month monitoring period, all after 9 weeks of age (Figure 4). Since quinidine was not effective in the *Scn8a* mutant mice, we did not treat the *Scn1a* mutant mice.

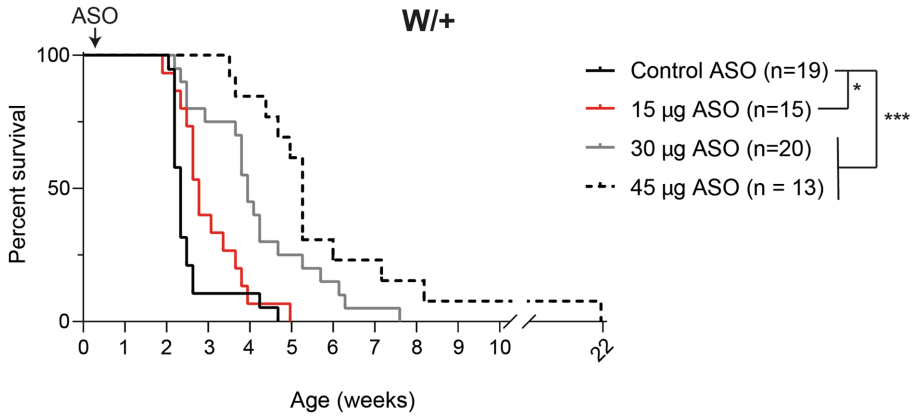

FIGURE 2
Kcnt1 ASO prolongs survival of *Scn8a* mutant mice. Survival of *Scn8a*$^{cond/+}$,*Ella-Cre* (W/+) mice treated with 15–45 µg *Kcnt1* ASO at P2 compared with a cohort of contemporaneous control mice treated with control ASO [Control data was previously published in Lenk et al. (2020)]. Asterisks indicate significance of Mantel-Cox log-rank tests: * = $p < 0.05$, *** = $p < 0.0001$.

4. Discussion

Developmental and epileptic encephalopathies are frequently caused by pathological variants of ion channel genes. Here, we showed that reduction of *Kcnt1* expression is protective in mouse models of *Scn1a* and *Scn8a* epilepsy. Our findings suggest that patients with mutations of *SCN1A* and *SCN8A* could benefit from treatment with a *KCNT1* ASO or KCNT1-specific channel blocker.

A previous study demonstrated that the *Kcnt1* ASO improved the survival, seizure, and behavioral phenotypes of *Kcnt1* GOF mice (Burbano et al., 2022). Interestingly, the *Kcnt1* ASO was therapeutic at lower doses in *Kcnt1* mutant mice than in the *Scn8a* mutant studied here. In neonatal *Kcnt1* mutant mice, 3.4 µg extended the median survival by more than 100 days (Burbano et al., 2022). In contrast, doses of 15–45 µg added only 20 days to survival of the *Scn8a* mutant mice. These observations suggest that the effect in the *Scn8a* mutant may be indirect. For example, gain-of-function of *Kcnt1* reduces excitability of parvalbumin interneurons (Gertler et al., 2022). Reduced expression of *Kcnt1* may enhance excitability of parvalbumin interneurons and thereby reduce seizure susceptibility. Consistent with this hypothesis, homozygous knockout of *Kcnt1* reduces the lethality of electrically-induced seizures by more than half (Quraishi et al., 2020). Further investigation may identify other types of epilepsy that respond to reduction of *KCNT1*.

We previously demonstrated that reducing *Scn8a* expression is therapeutic in *Scn1a*$^{+/-}$ mice (Lenk et al., 2020) and in mice with epilepsy caused by loss of the potassium channel genes *Kcna1* and *Kcnq2* (Hill et al., 2022). P2 administration of the *Scn8a* ASO completely rescued the *Scn1a*$^{+/-}$ mice (Lenk et al., 2020). In contrast, 4/14 of the *Scn1a*$^{+/-}$ mice treated with the *Kcnt1* ASO died between two and six months of age. The deaths after 2 months may result from turnover of the *Kcnt1* ASO; alternatively, reduced *Kcnt1* may be effective only in the interval between 3–4 weeks. The long-term effectiveness of the *Scn8a* ASO in *Scn1a* mutant mice is interesting, since the effect on *Scn8a* expression persists for only 6 weeks (Lenk et al., 2020). Viral overexpression of the *Kcna1* channel is protective against seizures induced by tetanus neurotoxin or pentylenetetrazole (Snowball et al., 2019; Qiu et al., 2022). Taken together, these observations suggest that modulation of ion channel expression to compensate for epileptogenic mutations is a promising therapeutic strategy.

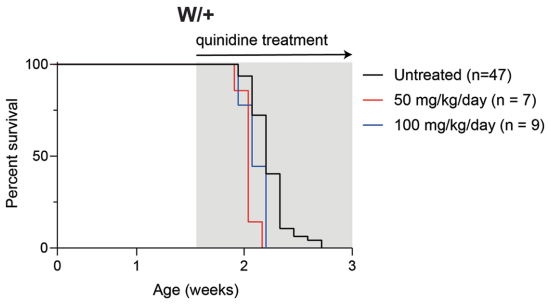

FIGURE 3
Quinidine does not prolong survival of *Scn8a* mutant mice. Survival of *Scn8a*$^{cond/+}$,*Ella-Cre* (W/+) mice daily treated with 50 or 100 mg/kg quinidine compared to untreated mice. Grey shading indicates treatment period.

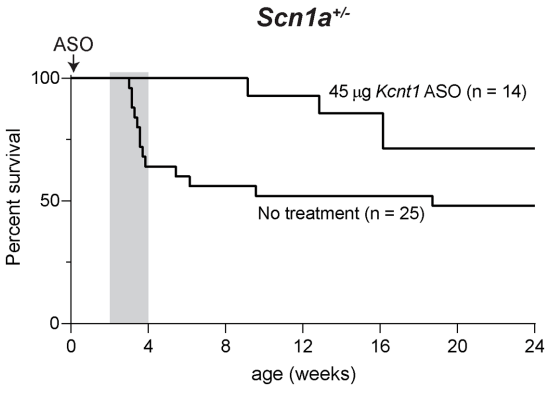

FIGURE 4
Kcnt1 ASO prolongs survival of *Scn1a*$^{+/-}$ mice. Survival of *Scn1a*$^{+/-}$ mice treated with 45 µg *Kcnt1* ASO at P2 compared to untreated mice ($p = 0.0513$, Mantel-Cox log-rank test). Grey shading indicates the critical period in the development of Dravet Syndrome.

Among the ion channel genes that could be targeted to treat channelopathies, *KCNT1* is an attractive choice because reduced expression is well tolerated. Heterozygous loss-of-function mutations of *KCNT1* are present in the general population and not associated with disease (Lek et al., 2016; Karczewski et al., 2020). *Kcnt1*$^{-/-}$ mice are healthy and fertile, with minor abnormalities such as impaired reversal learning and slightly elevated pain sensitivity (Bausch et al., 2015; Lu et al., 2015; Martinez-Espinosa et al., 2015; Quraishi et al., 2020). In contrast, heterozygous loss of *Scn8a* is not present in the healthy population (probability of loss-of-function intolerance, pLI = 1) (Lek et al., 2016; Karczewski et al., 2020) and homozygous loss is lethal in the mouse (Burgess et al., 1995).

Quinidine has been proposed as a therapy for patients with *KCNT1* epilepsy because of the effectiveness of high doses for correction of GOF mutations *in vitro* (Milligan et al., 2014; Numis et al., 2018). The effects of quinidine are not specific to KCNT1 (Roden, 2014). Clinical application of quinidine in *KCNT1* epilepsy has mixed success. Some individuals achieved seizure freedom (Mikati et al., 2015; Fitzgerald et al., 2019), but most patients report no benefit or worsening seizures (Mikati et al., 2015; Numis et al., 2018; Cole et al., 2020). Quinidine concentration sufficiently high to block KCNT1 may be difficult to achieve *in vivo* without deleterious effects on other ion channels (Liu et al., 2022). We found that quinidine was not protective in *Scn8a* mutant mice. More specific KCNT1 channel blockers (Cole et al., 2020; Griffin et al., 2021) may be more effective for treatment of *KCNT1*, *SCN8A*, and *SCN1A* epilepsy.

Data availability statement

The original contributions presented in the study are included in the article/Supplementary material, further inquiries can be directed to the corresponding author.

Ethics statement

The animal study was approved by University of Michigan Institutional Animal Care & Use Committee. The study was conducted in accordance with the local legislation and institutional requirements.

Author contributions

SH: Conceptualization, Data curation, Formal Analysis, Investigation, Methodology, Visualization, Writing – original draft, Writing – review & editing. PJ-N: Conceptualization, Resources, Writing – review & editing. FR: Conceptualization, Resources, Writing – review & editing. MM: Conceptualization, Funding acquisition, Supervision, Writing – review & editing.

Funding

The author(s) declare financial support was received for the research, authorship, and/or publication of this article. Supported by NINDS grant R01 NS34509 (MM) and a Rackham Predoctoral Fellowship from the Rackham School of Graduate Studies, University of Michigan (SH).

Conflict of interest

PJ-N and FR are paid employees of Ionis Pharmaceuticals.

The remaining authors declare that the research was conducted in the absence of any commercial or financial relationships that could be construed as a potential conflict of interest.

Publisher's note

Supplementary material

The Supplementary material for this article can be found online at: https://www.frontiersin.org/articles/10.3389/fnins.2023.1282201/full#supplementary-material

References

Barcia, G., Fleming, M. R., Deligniere, A., Gazula, V. R., Brown, M. R., Langouet, M., et al. (2012). De novo gain-of-function KCNT1 channel mutations cause malignant migrating partial seizures of infancy. *Nat. Gen.* 44, 1255–1259. doi: 10.1038/ng.2441

Bausch, A. E., Dieter, R., Nann, Y., Hausmann, M., Meyerdierks, N., Kaczmarek, L. K., et al. (2015). The sodium-activated potassium channel slack is required for optimal cognitive flexibility in mice. *Learn. Mem.* 22, 323–335. doi: 10.1101/lm.037820.114

Bunton-Stasyshyn, R. K. A., Wagnon, J. L., Wengert, E. R., Barker, B. S., Faulkner, A., Wagley, P. K., et al. (2019). Prominent role of forebrain excitatory neurons in SCN8A encephalopathy. *Brain* 142, 362–375. doi: 10.1093/brain/awy324

Burbano, L. E., Li, M., Jancovski, N., Jafar-Nejad, P., Richards, K., Sedo, A., et al. (2022). Antisense oligonucleotide therapy for KCNT1 encephalopathy. *JCI Insight* 7:e146090. doi: 10.1172/JCI.INSIGHT.146090

Burgess, D. L., Kohrman, D. C., Galt, J., Plummer, N. W., Jones, J. M., Spear, B., et al. (1995). Mutation of a new sodium channel gene, Scn8a, in the mouse mutant "motor endplate disease". *Nat. Genet.* 10, 461–465. doi: 10.1038/ng0895-461

Cheah, C. S., Yu, F. H., Westenbroek, R. E., Kalume, F. K., Oakley, J. C., Potter, G. B., et al. (2012). Specific deletion of NaV1.1 sodium channels in inhibitory interneurons causes seizures and premature death in a mouse model of Dravet syndrome. *Proc. Natl. Acad. Sci. U. S. A.* 109, 14646–14651. doi: 10.1073/pnas.1211591109

Cole, B. A., Clapcote, S. J., Muench, S. P., and Lippiat, J. D. (2021). Targeting KNa1.1 channels in KCNT1-associated epilepsy. *Trends Pharmacol. Sci.* 42, 700–713. doi: 10.1016/J.TIPS.2021.05.003

Cole, B. A., Johnson, R. M., Dejakaisaya, H., Pilati, N., Fishwick, C. W. G., Muench, S. P., et al. (2020). Structure-based identification and characterization of inhibitors of the epilepsy-associated KNa1.1 (KCNT1) Potassium Channel. *iScience* 23:101100. doi: 10.1016/J.ISCI.2020.101100

Favero, M., Sotuyo, N. P., Lopez, E., Kearney, J. A., and Goldberg, E. M. (2018). A transient developmental window of fast-spiking interneuron dysfunction in a mouse model of dravet syndrome. *J. Neurosci.* 38, 7912–7927. doi: 10.1523/JNEUROSCI.0193-18.2018

Fitzgerald, M. P., Fiannacca, M., Smith, D. M., Gertler, T. S., Gunning, B., Syrbe, S., et al. (2019). Treatment responsiveness in KCNT1-related epilepsy. *Neurotherapeutics* 16, 848–857. doi: 10.1007/s13311-019-00739-y

Gertler, T. S., Cherian, S., DeKeyser, J. M., Kearney, J. A., and George, A. L. Jr. (2022). KNa1.1 gain-of-function preferentially dampens excitability of murine parvalbumin-positive interneurons. *Neurobiol. Dis.* 168:105713. doi: 10.1016/j.nbd.2022.105713

Gribkoff, V. K., and Winquist, R. J. (2023). Potassium channelopathies associated with epilepsy-related syndromes and directions for therapeutic intervention. *Biochem. Pharmacol.* 208:115413. doi: 10.1016/J.BCP.2023.115413

Griffin, A. M., Kahlig, K. M., Hatch, R. J., Hughes, Z. A., Chapman, M. L., Antonio, B., et al. (2021). Discovery of the first orally available, selective K(Na)1.1 inhibitor: in vitro and in vivo activity of an Oxadiazole series. *ACS Med. Chem. Lett.* 12, 593–602. doi: 10.1021/acsmedchemlett.0c00675

Hawkins, N. A., Calhoun, J. D., Huffman, A. M., and Kearney, J. A. (2019). Gene expression profiling in a mouse model of Dravet syndrome. *Exp. Neurol.* 311, 247–256. doi: 10.1016/J.EXPNEUROL.2018.10.010

Hill, S. F., Ziobro, J. M., Jafar-Nejad, P., Rigo, F., and Meisler, M. H. (2022). Genetic interaction between Scn8a and potassium channel genes Kcna1 and Kcnq2. *Epilepsia* 63, e125–e131. doi: 10.1111/EPI.17374

Johannesen, K. M., Liu, Y., Koko, M., Gjerulfsen, C. E., Sonnenberg, L., Schubert, J., et al. (2022). Genotype-phenotype correlations in SCN8A-related disorders reveal prognostic and therapeutic implications. *Brain* 145, 2991–3009. doi: 10.1093/BRAIN/AWAB321

Karczewski, K. J., Francioli, L. C., Tiao, G., Cummings, B. B., Alföldi, J., Wang, Q., et al. (2020). The mutational constraint spectrum quantified from variation in 141,456 humans. *Nature* 581, 434–443. doi: 10.1038/s41586-020-2308-7

Lek, M., Karczewski, K. J., Minikel, E. V., Samocha, K. E., Banks, E., Fennell, T., et al. (2016). Analysis of protein-coding genetic variation in 60,706 humans. *Nature* 536, 285–291. doi: 10.1038/nature19057

Lenk, G. M., Jafar-Nejad, P., Hill, S. F., Huffman, L. D., Smolen, C. E., Wagnon, J. L., et al. (2020). Scn8a antisense oligonucleotide is protective in mouse models of SCN8A encephalopathy and Dravet syndrome. *Ann. Neurol.* 87, 339–346. doi: 10.1002/ana.25676

Lindy, A. S., Stosser, M. B., Butler, E., Downtain-Pickersgill, C., Shanmugham, A., Retterer, K., et al. (2018). Diagnostic outcomes for genetic testing of 70 genes in 8565 patients with epilepsy and neurodevelopmental disorders. *Epilepsia* 59, 1062–1071. doi: 10.1111/epi.14074

Liu, R., Sun, L., Wang, Y., Wang, Q., and Wu, J. (2022). New use for an old drug: quinidine in KCNT1-related epilepsy therapy. *Neurol. Sci.* 44, 1201–1206. doi: 10.1007/S10072-022-06521-X/FIGURES/1

Lu, R., Bausch, A. E., Kallenborn-Gerhardt, W., Stoetzer, C., Debruin, N., Ruth, P., et al. (2015). Slack channels expressed in sensory neurons control neuropathic pain in mice. *J. Neurosci. Off. J. Soc. Neurosci.* 35, 1125–1135. doi: 10.1523/JNEUROSCI.2423-14.2015

Martinez-Espinosa, P. L., Wu, J., Yang, C., Gonzalez-Perez, V., Zhou, H., Liang, H., et al. (2015). Knockout of Slo2.2 enhances itch, abolishes KNa current, and increases action potential firing frequency in DRG neurons. *elife* 4:e10013. doi: 10.7554/eLife.10013

Meisler, M. H., Hill, S. F., and Yu, W. (2021). Sodium channelopathies in neurodevelopmental disorders. *Nat. Rev. Neurosci.* 22, 152–166. doi: 10.1038/s41583-020-00418-4

Mikati, M. A., Jiang, Y. H., Carboni, M., Shashi, V., Petrovski, S., Spillmann, R., et al. (2015). Quinidine in the treatment of KCNT1-positive epilepsies. *Ann. Neurol.* 78, 995–999. doi: 10.1002/ana.24520

Miller, A. R., Hawkins, N. A., McCollom, C. E., and Kearney, J. A. (2014). Mapping genetic modifiers of survival in a mouse model of Dravet syndrome. *Genes Brain Behav.* 13, 163–172. doi: 10.1111/gbb.12099

Milligan, C. J., Li, M., Gazina, E. V., Heron, S. E., Nair, U., Trager, C., et al. (2014). KCNT1 gain of function in 2 epilepsy phenotypes is reversed by quinidine. *Ann. Neurol.* 75, 581–590. doi: 10.1002/ana.24128

Mori, K., Kobayashi, S., Saito, T., Masuda, Y., and Nakaya, H. (1998). Inhibitory effects of class I and IV antiarrhythmic drugs on the Na+−activated K+ channel current in guinea pig ventricular cells. *Naunyn Schmiedeberg's Arch. Pharmacol.* 358, 641–648. doi: 10.1007/pl00005306

Numis, A. L., Nair, U., Datta, A. N., Sands, T. T., Oldham, M. S., Patel, A., et al. (2018). Lack of response to quinidine in KCNT1-related neonatal epilepsy. *Epilepsia* 59, 1889–1898. doi: 10.1111/epi.14551

Qiu, Y., O'Neill, N., Maffei, B., Zourray, C., Almacellas-Barbanoj, A., Carpenter, J. C., et al. (2022). On-demand cell-autonomous gene therapy for brain circuit disorders. *Science* 378, 523–532. doi: 10.1126/SCIENCE.ABQ6656

Quraishi, I. H., Mercier, M. R., McClure, H., Couture, R. L., Schwartz, M. L., Lukowski, R., et al. (2020). Impaired motor skill learning and altered seizure susceptibility in mice with loss or gain of function of the Kcnt1 gene encoding slack (KNa1.1) Na+−activated K+ channels. *Sci. Rep.* 10:3213. doi: 10.1038/S41598-020-60028-Z

Quraishi, I. H., Stern, S., Mangan, K. P., Zhang, Y., Ali, S. R., Mercier, M. R., et al. (2019). An epilepsy-associated KCNT1 mutation enhances excitability of human iPSC-derived neurons by increasing slack K Na currents. *J. Neurosci.* 39, 7438–7449. doi: 10.1523/JNEUROSCI.1628-18.2019

Rizzi, S., Knaus, H.-G., and Schwarzer, C. (2016). Differential distribution of the sodium-activated potassium channels slick and slack in mouse brain. *J. Comp. Neurol.* 524, 2093–2116. doi: 10.1002/cne.23934

Roden, D. M. (2014). Pharmacology and toxicology of Nav1.5-class 1 anti-arrhythmic drugs. *Card. Electrophysiol. Clin.* 6, 695–704. doi: 10.1016/j.ccep.2014.07.003

Scheffer, I. E., and Nabbout, R. (2019). SCN1A-related phenotypes: epilepsy and beyond. *Epilepsia* 60, S17–S24. doi: 10.1111/epi.16386

Shore, A. N., Colombo, S., Tobin, W. F., Petri, S., Cullen, E. R., Dominguez, S., et al. (2020). Reduced GABAergic neuron excitability, altered synaptic connectivity, and seizures in a KCNT1 gain-of-function mouse model of childhood epilepsy. *Cell Rep.* 33:108303. doi: 10.1016/j.celrep.2020.108303

Snowball, A., Chabrol, E., Wykes, R. C., Shekh-Ahmad, T., Cornford, J. H., Lieb, A., et al. (2019). Epilepsy gene therapy using an engineered potassium channel. *J. Neurosci.* 39, 3159–3169. doi: 10.1523/JNEUROSCI.1143-18.2019

Sprissler, R. S., Wagnon, J. L., Bunton-Stasyshyn, R. K., Meisler, M. H., and Hammer, M. F. (2017). Altered gene expression profile in a mouse model of SCN8A encephalopathy. *Exp. Neurol.* 288, 134–141. doi: 10.1016/J.EXPNEUROL.2016.11.002

Swayze, E., Siwkowski, A. M., Wancewicz, E. V., Migawa, M. T., Wyrzykiewicz, T. K., Hung, G., et al. (2007). Antisense oligonucleotides containing locked nucleic acid improve potency but cause significant hepatotoxicity in animals. *Nucleic Acids Res.* 35, 687–700. doi: 10.1093/NAR/GKL1071

Symonds, J. D., Zuberi, S. M., Stewart, K., McLellan, A., O'Regan, M., MacLeod, S., et al. (2019). Incidence and phenotypes of childhood-onset genetic epilepsies: a prospective population-based national cohort. *Brain* 142, 2303–2318. doi: 10.1093/BRAIN/AWZ195

Tai, C., Abe, Y., Westenbroek, R. E., Scheuer, T., and Catterall, W. A. (2014). Impaired excitability of somatostatin- and parvalbumin-expressing cortical interneurons in a mouse model of Dravet syndrome. *Proc. Natl. Acad. Sci. U. S. A.* 111, E3139–E3148. doi: 10.1073/pnas.1411131111

Valassina, N., Brusco, S., Salamone, A., Serra, L., Luoni, M., Giannelli, S., et al. (2022). Scn1a gene reactivation after symptom onset rescues pathological phenotypes in a mouse model of Dravet syndrome. *Nat. Commun.* 13:161. doi: 10.1038/S41467-021-27837-W

Veeramah, K. R., O'Brien, J. E., Meisler, M. H., Cheng, X., Dib-Hajj, S. D., Waxman, S. G., et al. (2012). De novo pathogenic SCN8A mutation identified by whole-genome sequencing of a family quartet affected by infantile epileptic encephalopathy and SUDEP. *Am. J. Hum. Genet.* 90, 502–510. doi: 10.1016/j.ajhg.2012.01.006

Wu, J., Quraishi, I. H., Zhang, Y., Bromwich, M., and Kaczmarek, L. K. (2023). Disease-causing slack potassium channel mutations produce opposite effects on excitability of excitatory and inhibitory neurons. *bioRxiv*. doi: 10.1101/2023.02.14.528229

frontiers | Frontiers in Neurology

TYPE Original Research
PUBLISHED 07 November 2023
DOI 10.3389/fneur.2023.1255097

OPEN ACCESS

EDITED BY
Evgenia Sitnikova,
Institute of Higher Nervous Activity and Neurophysiology (RAS), Russia

REVIEWED BY
Beatrice Paradiso,
University of Milan, Italy
Laetitia Francelle,
Northwestern University, United States

*CORRESPONDENCE
Kai-Feng Shen
✉ shenkaifengk@tmmu.edu.cn
Ping Liang
✉ liangping868@sina.com

RECEIVED 08 July 2023
ACCEPTED 06 October 2023
PUBLISHED 07 November 2023

CITATION
Zhang L, Huang J, Dai L, Zhu G, Yang X-L, He Z, Li Y-H, Yang H, Zhang C-Q, Shen K-F and Liang P (2023) Expression profiles of α-synuclein in cortical lesions of patients with FCD IIb and TSC, and FCD rats. *Front. Neurol.* 14:1255097. doi: 10.3389/fneur.2023.1255097

Expression profiles of α-synuclein in cortical lesions of patients with FCD IIb and TSC, and FCD rats

Li Zhang[1], Jun Huang[2], Lu Dai[3], Gang Zhu[2], Xiao-Lin Yang[2], Zeng He[2], Yu-Hong Li[4], Hui Yang[2,3], Chun-Qing Zhang[2], Kai-Feng Shen[2]* and Ping Liang[1]*

[1]Department of Neurosurgery, Children's Hospital of Chongqing Medical University, National Clinical Research Center for Child Health and Disorders, Ministry of Education Key Laboratory of Child Development and Disorders, Chongqing Key Laboratory of Pediatrics, Chongqing, China, [2]Department of Neurosurgery, Epilepsy Research Center of PLA, Xinqiao Hospital, Army Medical University, Chongqing, China, [3]Chongqing Institute for Brain and Intelligence, Guang Yang Bay Laboratory, Chongqing, China, [4]Department of Cell Biology, Basic Medical College, Army Medical University, Chongqing, China

Background: Focal cortical dysplasia (FCD) IIb and tuberous sclerosis complex (TSC) are common causes of drug-resistant epilepsy in children. However, the etiologies related to the development of FCD IIb and TSC are not fully understood. α-synuclein (α-syn) is a member of synucleins family that plays crucial roles in modulating synaptic transmission in central nervous system. Here, we explored the expression profiles and potential pathogenic functions of α-syn in cortical lesions of epileptic patients with FCD IIb and TSC.

Methods: Surgical specimens from epileptic patients with FCD IIb and TSC, as well as FCD rats generated by *in utero* X-ray-radiation were adopted in this study and studied with immunohistochemistry, immunofluorescence, western blotting, and co-immunoprecipitation etc. molecular biological techniques.

Result: Our results showed that α-syn expression was reduced in FCD IIb and TSC lesions. Specifically, α-syn protein was intensely expressed in dysplastic neurons (DNs) and balloon cells (BCs) in FCD IIb lesions, whereas was barely detected in DNs and giant cells (GCs) of TSC lesions. Additionally, p-α-syn, the aggregated form of α-syn, was detected in DNs, BCs, GCs, and glia-like cells of FCD IIb and TSC lesions. We previous showed that the function of N-methyl-D-aspartate receptor (NMDAR) was enhanced in FCD rats generated by X-ray-radiation. Here, we found the interaction between α-syn and NMDAR subunits NMDAR2A, NMDAR2B were augmented in cortical lesions of FCD patients and FCD rats.

Conclusion: These results suggested a potential role of α-syn in the pathogenesis of FCD IIb and TSC by interfering with NMDAR.

KEYWORDS

FCD IIb, TSC, FCD rats, α-syn, NMDAR

1. Introduction

Malformations of cortical development (MCDs), including focal cortical dysplasia (FCDs) and tuberous sclerosis complex (TSC), are the most common pathological causes of drug-resistant epilepsy in children (1). FCDs were classified into FCD type I, IIa, and IIb according to the current international consensus classification established by the International League against Epilepsy (ILAE). Type I FCD is characterized histologically with microcolumnar neurons, and type II is characterized by cortical dyslamination and dysplastic neurons (DNs) with (Type IIb) or without balloon cells (BCs) (Type IIa) (2). Similar to the pathological characteristics of FCD IIb, TSC lesions are characterized with DNs and giant cells (GC) under pathological examination (3). Plentiful investigations were conducted to reveal the etiology of FCD IIb and TSC; however, present studies are still

insufficient to elucidate the pathological and epileptic mechanisms of FCD IIb and TSC.

α-synuclein (α-syn), a member of the synuclein family, plays various routes to cellular dysfunction by inducing synaptic dysfunction, mitochondrial impairment, defective endoplasmic reticulum (ER) function, autophagy–lysosomal pathway, and nuclear dysfunction (4). α-syn widely localizes in presynaptic terminals as a monomer and plays crucial roles in regulating neurotransmitter release, synaptic function, and plasticity in the central nervous system (5). Additionally, studies have shown that α-syn monomers tend to aggregate in structures of higher molecular weights leading to the formation of α-syn oligomers, protofibrils, and eventually fibrils, the main components of Lewy bodies in neurodegenerative diseases (6). Thus, the versatile roles of α-syn in mediating cellular function intrigue us on whether it plays important roles in the etiology of FCD IIb and TSC.

Due to ethical limitations, many investigations cannot be carried out in humans. To address the etiology and pathogenesis of FCD, many animal models of FCD have been established to investigate the mechanisms of epileptogenesis and novel therapeutics for epilepsy. Historically, chemical or physical induction during early life was adopted to create the FCD model in animals, including neonatal freeze lesions (7, 8) or *in utero* irradiation to generate microgyria and focal heterotopia (9–11), *in utero* exposure to methylazoxymethanol (MAM) acetate (12–17), carmustine 1–3-bis-chloroethyl-nitrosourea (BCNU) (18), and neonatal exposure ibotenic acid to generate focal cortical malformations (19). Transgenic and *in utero* electroporation-based animal models were used to target genes of the mTOR pathway and recapitulate, to various degrees, the cortical malformations and recurrent spontaneous seizures in recent years (20–22). However, there is no "perfect" animal model as no single model recapitulates all the human phenotypes associated with FCD. Rat models are more economic and easier to establish, e.g., compared with the ferret model (14–17). When compared with mice, rats are larger in size. More importantly, rats are closer to humans with less genomic differences and greater physiological similarities in consequence, making them the ideal and classical animal for constructing FCD models (23–26), whereas chemical or physical stimulation-induced mouse models of FCD have been rarely reported. In the study, we used *in utero* irradiation of pregnant rats to X-ray to generate FCD rats in consistent with the procedures used in our previous study (27). Striking the loss of normal six-layered cortex, varying degrees of cytomegalic or dysmorphic cells and spontaneous seizures were reported in these animals (9, 28, 29).

Thus, to explore the potential function of α-syn in the pathogenesis of FCD IIb and TSC, we conducted a study using surgical specimens from epileptic patients with FCD IIb and TSC, as well as FCD rats generated by *in utero* X-ray-radiation, to investigate the expression patterns of α-syn in cortical lesions and the interplay of α-syn and N-methyl-D-aspartate receptor (NMDAR), which is the primary receptor mediating excitatory synaptic transmission in central nervous system.

In the study, we found that α-syn was reduced, whereas the interaction between α-syn and NMDAR was strengthened in the cortical lesions of patients with FCD IIb and TSC, suggesting a complex function of α-syn in the pathogenesis of FCD. Cortical dyslamination and thinning were the most prominent histological abnormities in FCD rats during our observation from 7 to 28 days, in parallel with the alteration of α-syn and NMDAR in the cellular level, which highly simulated the pathological features of human FCD and suggested the disruption of brain function, including epileptogenesis in FCD rats. Immunotherapeutic approaches have been used to reduce α-syn pathology in rodent models with neurodegenerative diseases. However, many challenges existed before achieving an effective treatment strategy, including the overcoming of the blood–brain barrier and the complex heterogeneity of α-syn (30). Similar progresses have been achieved in unraveling the pathology of α-syn in neurodegenerative diseases, and further studies to address the key pathology of α-syn in the pathogenesis of FCD IIb, and TSC might benefit and have the potential to alter the progression of FCD IIb and TSC.

2. Materials and methods

2.1. Human brain tissue specimens

This study was conducted in accordance with the Declaration of Helsinki and the guidelines for the conduction of research involving human subjects, as established by the Ethics Committee of Xinqiao Hospital, Army Medical University. FCD IIb and TSC-induced pediatric drug-resistant epilepsy were diagnosed according to the current international consensus classification proposed by the ILAE. Invasive depth electrode recordings were performed if the epileptic lesions could not be precisely located by scalp electroencephalogram before the surgery. Only epileptogenic tissues that were identified with the dysplastic cortex by magnetic resonance imaging and further confirmed *post-hoc* by neuropathological correction were used in the study. Informed written consent was obtained from all participants or legal guardians for the use of the dissected tissue for research purposes only.

In the present study, 15 FCD IIb and 24 TSC lesions were examined. The general clinical information of all the patients is summarized in Table 1, and detailed clinical information of each patient is presented in Supplementary Tables S1, S2. Among the 26 control cortex (CTX) used in this study, 23 control tissues were obtained from patients with craniocerebral tumors in accordance with the criteria reported in previous studies during surgery (31, 32). None of any other neurological diseases or history of seizures were detected in these patients, and only the normal-appearing tissues without reactive astrogliosis, inflammation, or necrosis were included in the study. The other three control cortical specimens were obtained from individuals who were diagnosed with increased intracranial pressure due to traumatic brain injury and without any neurological disease in history. The samples distant from the directly injured area were obtained in <6h after brain injury (33) after comprehensive presurgical assessment, including history, neuroimaging studies, and neurological examination according to

Abbreviations: α-syn, α-synuclein; p-α-syn, phosphorylated α-synuclein; DNs, dysplastic neurons; BCs, balloon cells; GCs, giant cells; MCD, malformation cortical development.

TABLE 1 Summary of the clinical characteristics of patients with FCD IIb and TSC lesions.

	FCD IIb	TSC
Male/female	10/5	14/10
Median age of surgery (years)	13.3(3.5–34.0)	8.9(2.0–32.0)
Median age at onset of seizure (years)	5.1(0.2–18.0)	3.0(0.3–14.8)
Seizure type	FAS (1/6.7%) FIAS (1/6.7%) FBTCS (2/13.3%) GAS (1/6.7%) GTS (3/20%) GTCS (7/46.7%)	FAS (3/12.5%) FIAS (5/20.83%) FBTCS (1/4.1%) GAS (2/8.3%) GTCS (13/54.17%)
Lesion location	Frontal (9/60%) Temporal (5/33.3%) Parietal (1/6.7%)	Frontal (15/62.5%) Temporal (4/16.7%) Parietal (3/12.5%) Occipital (2/8.3%)
Median duration of epilepsy (years)	4.3 (0.9–20.0)	2.50 (0.2–30.0)
Median seizure frequency (per month)	105.0 (1–3000)	12.5 (1–300)
Postoperative outcome (Engle's class)	I (13/86.7%) III (1/6.7%) IV (1/6.7%)	I (18/75%) II (2/8.3%) III (2/8.3%) IV (2/8.3%)

the criteria (27, 34). The detailed information of each control subject is shown in Supplementary Table S3.

2.2. Animal experiments

Sprague–Dawley rats were obtained from Army Medical University and housed under standard conditions with room temperature of 23 ± 1°C, humidity of 60%, and 12-h light/12-h dark cycle with food and water *ad libitum*. Randomly chosen female rats were exposed to X-ray (145 cGy, 60 s) (RS-2000, Rad Source Technologies) at post-pregnancy day 17 to disrupt the normal development of cortex *in utero*, and newborn rats were weaned at postnatal day 21 (P21) after normal delivery according to previous procedures (9). A total of 58 rats (both male and female) were used in this study, including 16 rats at 7 days: male/female: 7/9, 22 rats at 14 days: male/female: 12/10, and 20 rats at 28 days: male/female: 10/10. The number ratio of male to female was close to 1:1.

All experimental procedures were conducted in accordance with the guidelines of the Ethical Committee of Army Medical University and approved by the Internal Animal Care and Use Committee of Army Medical University.

2.3. RT-PCR

The total RNA was extracted from each specimen using the TRIzol reagent following the manufacture protocol (Invitrogen, Carlsbad, CA). RNA concentration was determined using a nanodrop spectrophotometer (Ocean Optics, Dunedin, FL) at 260/280 nm with a ratio of 1.8–2.0. Single-stranded cDNA was reverse-transcribed from 1 μg RNA using oligo dT primers (Takara, Otsu, Japan). The primers used in this study were as follows: human *α-syn* (forward: 5'GACAGCAGTAGCCCAGAAGACAG3', reverse: 5'GCATTTCATAAGCCTCATTGTCAG3'); human *GAPDH* (forward: 5'CACTCCTCCACCTTTGACGC3', reverse: 5'CTGTTGCTGTAGCCAAATTCGT3'), rat *syn* (forward: 5'GTTTTGTCAAGAAGGACCAGATG3', reverse: 5'GGCATTTCATAAGCCTCACTG3'); rat *GAPDH* (forward: 5'AAGTTCAACGGCACAGTCAAGG3', reverse: 5'CGCCAGTAGACTCCACGACATA3').

The PCR cycle was set as follows: 95°C for 30 s (one cycle), and 95°C for 5 s and 60°C for 40 s (49 cycles) to denaturation, 65°C for 5 s to anneal, and 95°C for 5s to extension. Each quantitative PCR reaction was repeated three times, and the quantitative PCR analysis was repeated by at least two independent experiments. The relative expression of α-syn mRNA in each sample was determined by the $2^{-\Delta\Delta Ct}$ method with GAPDA as internal control.

2.4. Western blotting

Protein of each specimen was extracted by the homogenizing tissue in RIPA lysis buffer supplemented with a mixture of protease and phosphatase inhibitors (cat.no: P0013B, Beyotime Biotechnology), and the concentration was determined using the Bradford protein assay (cat.no: P0010, Beyotime Biotechnology). An equal amount of protein (40 mg/ lane) was separated on 12% SDS-polyacrylamide gels and transferred to polyvinylidene fluoride membranes with a pore size of 0.2 μm. Membranes were blocked in 5% non-fat milk for 1 h and incubated with primary antibody overnight at 4°C (α-syn: 1:500, cat.no: 10842–1-AP, Proteintech; GAPDH:1:5000, cat.no: HRP-60004, Proteintech). Membranes were washed three times with Tris-buffered saline containing 0.1% Tween-20 (TBST) and then incubated with a peroxidase-conjugated goat anti-rabbit secondary antibody (1:1.000, cat.no: SA00001–2, Proteintech) for 1 h at 37°C. The signal was detected using chemiluminescent substrates (cat.no: SQ201L, Epizyme Biomedical Technology) after washing three times with TBST. GAPDH was used as the loading control. Densitometric analysis was performed using ImageJ to quantify the optical density (OD value) of each protein band.

2.5. Immunostaining

Paraffin-embedded tissues were sectioned at a thickness of 4 μm and mounted on polylysine-coated slides. Antigen retrieval was performed by heating sections in citrate buffer solution (0.01 M, pH 6.0) at 100°C for 30 min after deparaffinization and rehydration. After cooling to room temperature, the sections were washed with PBS. Sections were treated with 0.3% H_2O_2 to remove endogenous peroxidase activity. After blocked with 0.3% H_2O_2 for 10 min at 37°C, sections were incubated with primary antibodies: α-syn (1:200, cat.no:10842–1-AP, Proteintech, Wuhan), p-α-syn antibody (1:200, cat.no: PA5118553, Thermo Fisher) or NMDAR2A (1:100, cat.no: #M264, Sigma-Aldrich), or NMDAR2B (1:100, cat.no: 21920-1-AP, Proteintech) overnight at 4°C. Sections were incubated with HRP-conjugated secondary antibody (ZLI-9018, ZSBIO) for 1 h at 37°C and developed with the DAB Chromogenic Kit (ZLI-9018, ZSBIO) after washing three times

with PBS. Counterstaining was performed with hematoxylin. For hematoxylin and eosin (HE) staining, sections were incubated with hematoxylin for 5 min and eosin for 20 s consecutively after deparaffinization and rehydration. An inverted bright-field microscope (BX63, OLYPUS, Japan) was used to acquire images.

For immunofluorescent staining, paraffin-embedded sections were blocked in 10% goat serum after deparaffinization and antigen retrieval and incubated with corresponding primary antibodies: α-syn (1:200, cat.no: 10842-1-AP, Proteintech), p-α-syn antibody (1:200, cat.no: PA5118553, Thermo Fisher), vesicular glutamate transporters 2 VGLUT2 (1:200, cat.no: ab211869, Abcam), vesicular GABA transporters VGAT (1:50, cat.no: ab211534, Abcam), vimentin (1:500, cat.no: 60330-1-Ig, Proteintech), NeuN (1:5000, cat.no: ab104224, Abcam), GFAP (1:400, cat.no: C9205, Sigma-Aldrich), Iba1 (1:500, cat.no: OB-PGP049, Biofarm), and Olig2 (1:500, cat.no:OB-PGP040-02, Biofarm) overnight at 4°C. After washing three times with PBS, the sections were incubated with Alexa Fluor 488-conjugated anti-rabbit antibody (1:1000, cat.no: #A-11008, Thermo Fisher Scientific), Alexa Fluor 555-conjugated anti-rabbit antibody (1:1000, cat.no: #A-21428, Thermo Fisher Scientific), Alexa Fluor 555-conjugated anti-mouse antibody (1:1000, cat.no: #A-21422, Thermo Fisher Scientific), or Alexa Fluor 488-conjugated anti-Guinea pig antibody (1:1000, cat.no: ab150185, Abcam) for 1 h at 37°C. Sections were subsequentially nuclear stained by Hoechst 33258 and photographed by a confocal microscope (LSM880; ZEISS, Germany).

Notably, the distinct morphology of BCs and astrocytes helps to distinguish them in FCD samples. BCs have eccentric nuclei, a ballooned cytoplasm, and do not exhibit clear axonal or dendritic processes (35). However, astrocytes exhibit a morphology of several stem branches that give rise to many finely branching processes in a uniform distribution. Additionally, Vimentin is generally used as a marker of immature glia and neurons during development (36) and was also used as a maker for BCs traditionally, which were demonstrated to be immature neurons in FCD lesions (37–40). However, GFAP is commonly used as a mature astrocytic marker (41, 42) and rarely detected in BCs in FCD lesions (27, 43, 44).

2.6. Co-immunoprecipitation

In brief, proteins were extracted from cortical tissues of FCD patients and rats using the Universal Magnetic Co-IP Kit protocol (cat. no: 54002, Active motif) under manufacturer's instructions. Protein extracts were incubated with protein G PLUS-Agarose (Santa Cruz, Biotechnology) for 1 h at 4 °C to eliminate non-specific binding. After incubation, the precleared supernatants containing 1 mg of protein were incubated with corresponding primary antibodies: α-syn (cat.no: #4179S, cell signaling technology), NMDAR2A (cat.no: #M264, Sigma-Aldrich), NMDAR2B (cat.no: #14544, cell signaling technology), or IgG (cat.no: #5127, cell signaling technology) overnight at 4 °C. Lysates were incubated with protein G PLUS-Agarose for 3 h at 4 °C with rotation. Beads were washed four times with complete Co-IP/wash buffer. Pre-IP lysates and bound proteins eluted from the immune complexes were denatured by heating to 95 °C for 5 min and used for Western blot analysis (12% gel for α-syn, 6% gel for NMDAR2A and NMDAR2B).

2.7. Evaluation of IHC

The immunoreactivity of α-syn and p-α-syn in DNs, BCs, and GCs was evaluated following an evaluation scheme reported previously (45), and the relative number of positive cells within cortical lesions was semi-quantified according to a three-point frequency score: 1: 0–10% (rare); 2: 11–50% (sparse); 3: > 50% (high), and the staining intensity was semi-quantified to a 4-point scale: 0 (absence), 1 (weak), 2 (moderate), and 3 (strong). The product of these two scores (frequency and intensity) yielded the total score. All the areas of the slices were evaluated, and the score represents the predominant cell staining intensity in each section.

The immunoreactivity of α-syn in neuropils, p-α-syn, NMDAR2A, and NMDAR2B was evaluated with image J in consistent with our previous study (46). In short, non-overlapping fields (400× magnification, 0.3481 mm × 0.2621 mm width) were defined in the center of the lesions. Three sections from each specimen were selected, and three visions were captured in each section, and the ODs of the nine areas were averaged for the specimen. The immunoreactivity was evaluated by two histologists who were blind to the clinical data.

2.8. Statistics

The proper sample size and study power were estimated according to the previously established experimental settings (47). Data acquisition and analysis were done blindly and were presented as mean ± SEM. For comparisons between two independent groups, the unpaired two-tailed *t*-test was used. Spearman's rank correlation test was used for bivariate correlation analyses. Statistical methods and the number of replicates were indicated when used. Normality and equal variance tests were performed for all statistical analyses. GraphPad Prism 7 software was used for data plotting and analysis. A p-value of < 0.05 was considered as statistically significant.

3. Results

3.1. The expression profiles of α-syn in lesions of patients with FCD IIb and TSC

We first examined the expression differences of α-syn between FCD IIb, TSC lesions, and control cortex (CTX) individually. RT-PCR results showed the expression of α-syn mRNA was significantly reduced in FCD IIb lesions (Figure 1A, $^{**}p < 0.01$, unpaired two-tailed *t*-test), α-syn band was detected at approximately 18 kDa by Western blotting, and quantitative analysis showed the expression of α-syn was significantly reduced in FCD IIb lesions (Figure 1B, $^{*}p < 0.05$, unpaired two-tailed *t*-test). Interestingly, RT-PCR results showed α-syn mRNA was significantly increased in TSC lesions (Figure 1C, $^{*}p < 0.05$, unpaired two-tailed *t*-test), while α-syn protein was reduced

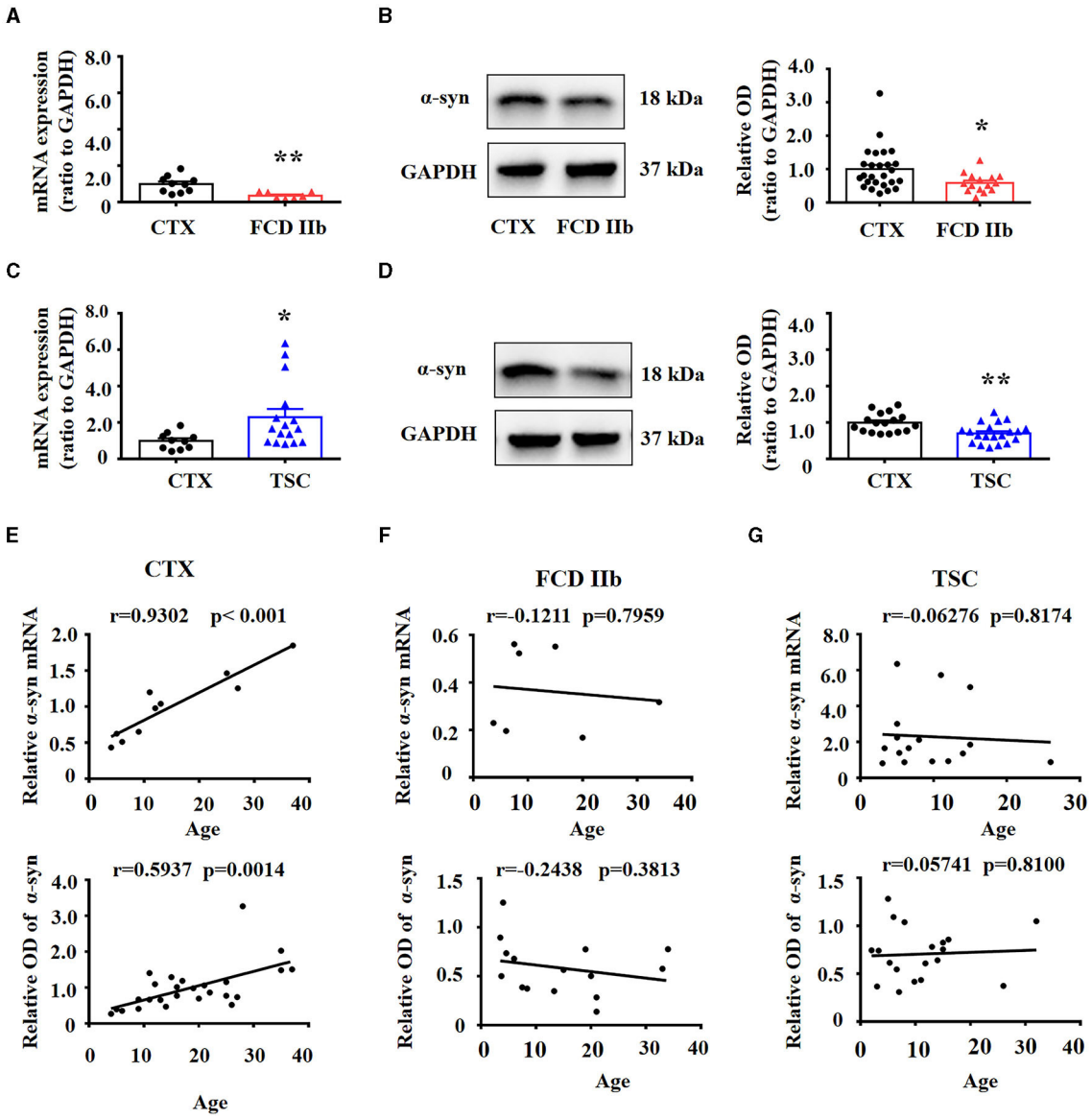

FIGURE 1
Expression of α-syn mRNA and protein in cortical lesions of patients with FCD IIb and TSC. **(A)** Statistical analysis showed that α-syn mRNA was significantly reduced in FCD IIb lesions ($^{**}p < 0.01$, unpaired two-tailed *t*-test, $n = 10$, 7 specimens for each group). **(B)** Representative immunoblot bands showing α-syn was detected at approximately 18 kDa, and GAPDH (37 kDa) was used as the loading control. Densitometric analysis showed that α-syn protein was significantly reduced in FCD IIb lesions ($^{*}p < 0.05$, unpaired two-tailed *t*-test, $n = 26$, 15 specimens for each group). **(C)** Statistical analysis showed that α-syn mRNA was increased in TSC lesions ($^{*}p < 0.05$, unpaired two-tailed *t*-test, $n = 10$, 16 specimens for each group). **(D)** Immunoblot bands showing α-syn (18 kDa) and GAPDH (37 kDa) in total homogenates from CTX and TSC lesions. Densitometric analysis showed α-syn protein was significantly decreased in TSC lesions ($^{**}p < 0.01$, unpaired two-tailed *t*-test, $n = 17$, 20 specimens for each group). **(E)** Spearman's correlation analysis showed that both α-syn mRNA ($r = 0.9302$, $^{***}p < 0.001$) and protein ($r = 0.5937$, $p = 0.0014$) were positively correlated with the ages of control subjects. **(F)** No significant correlation was observed between α-syn mRNA ($r = -0.1211$, $p = 0.7959$), protein ($r = -0.2438$, $p = 0.3813$), and ages of patients with FCD IIb. **(G)** No significant correlation was observed between α-syn mRNA ($r = -0.06276$, $p = 0.8174$), protein ($r = 0.05741$, $p = 0.8100$), and ages of patients with TSC.

(Figure 1D, $^{**}p < 0.01$, unpaired two-tailed *t*-test). α-syn protein expression was increased gradually along with the development in the brain (48, 49). We found that both the mRNA and protein expression of α-syn were positively correlated with the ages of control subjects by Spearman's correlation analysis (Figure 1E). However, the positive correlation between α-syn and age was lost in patients with FCD IIb (Figure 1F) and TSC (Figure 1G).

3.2. Expression patterns of α-syn in FCD IIb and TSC lesions

We investigated the cellular expression and distribution of α-syn in FCD IIb and TSC lesions with IHC. Moderate-to-strong immunoreactivity of α-syn was observed in the neuropils of CTX, while the immunoreactivity of α-syn was barely detected in the

10.3389/fneur.2023.1255097

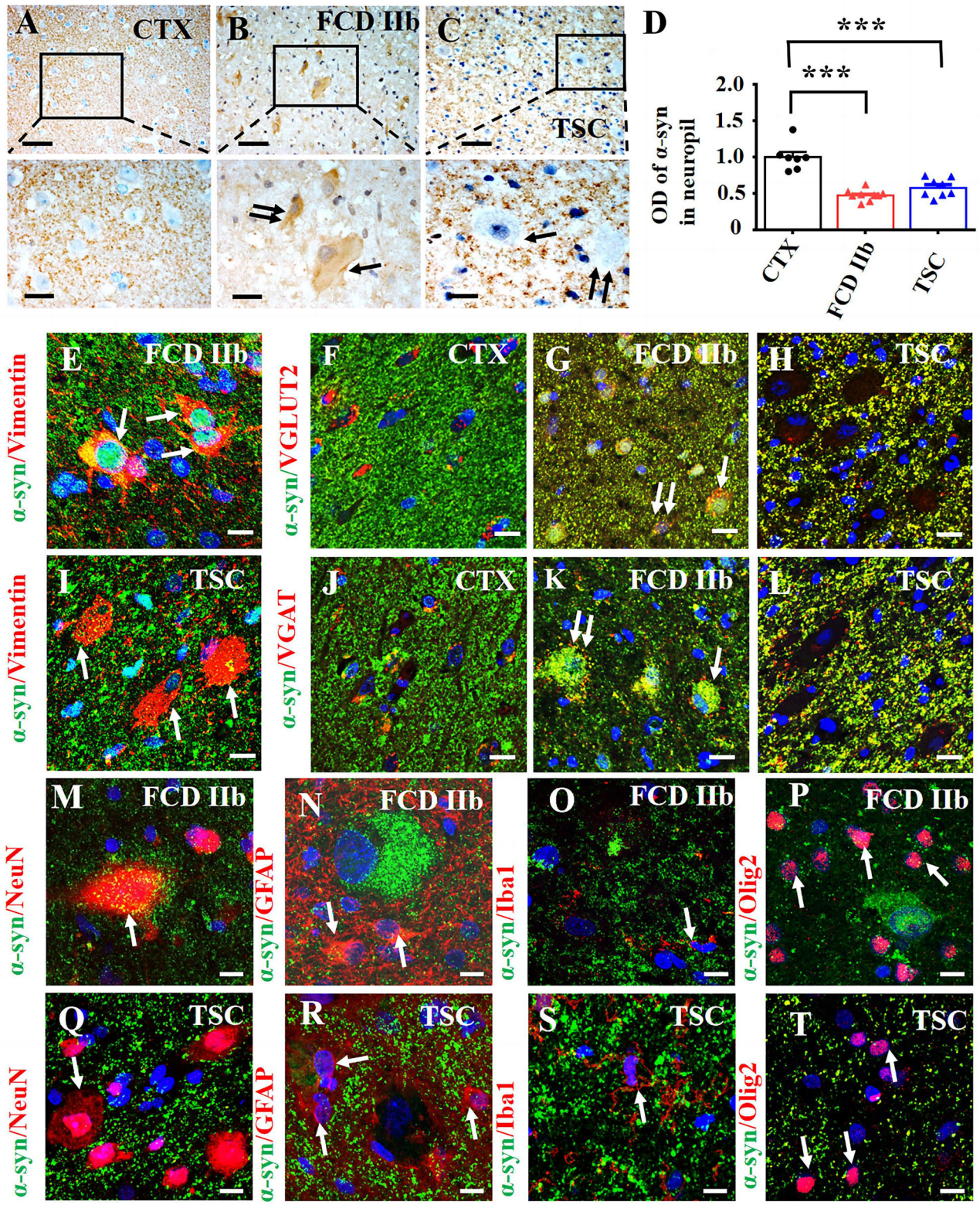

FIGURE 2
Expression profiles of α-syn in lesions of patients with FCD IIb and TSC. **(A)** Moderate-to-strong α-syn immunoreactivity was observed in the neuropils of CTX but was neglectable in the neuronal cytoplasm. **(B)** Representative image showing weak α-syn signal in the neuropils of FCD IIb lesions and moderate α-syn immunoreactivity in DN (double arrow) and BC (arrow) of FCD IIb lesions. **(C)** Strong but less of α-syn positive signal was observed in the neuropils of TSC lesions, and α-syn immunoreactivity was barely detected in DN (arrow) and GC (double arrow) of TSC lesions. **(D)** Statistical analysis results showing that the average OD value of α-syn was reduced in neuropils of both FCD IIb and TSC lesions (***$p < 0.001$, unpaired two-tailed t-test, $n = 7, 9, 8$ specimens for each group). **(E)** Representative images showing α-syn was expressed in vimentin-positive BC in FCD IIb lesions (arrows). **(F)** α-syn was barely expressed in VGLUT2-positive excitatory neurons in CTX. **(G)** Representative image showing the

(Continued)

FIGURE 2 (Continued)
co-expression of α-syn and VGLUT2 was intensified in the neuropils, DN (double arrow), and BC (arrow) in FCD IIb lesions. **(H)** The co-expression of α-syn and VGLUT2 was intensified in the neuropils of TSC lesions as well but not observed in DN and BC. **(I)** α-syn was not detected in vimentin-positive GCs in TSC lesions. **(J)** Representative image showing α-syn was barely expressed in VGAT-positive neurons in CTX. **(K)** Representative image showing significant co-expression of α-syn and VGAT in DN (double arrow) and BC (arrow) of FCD IIb lesions. **(L)** The co-expression of α-syn and VGAT was intensified in the neuropils of TSC lesions but not observed in DN and GC of TSC lesions. **(M)** Representative image showing slightly α-syn expression in a NeuN-positive neuron and nearby neuropils in FCD IIb lesions (arrow). **(N–P)** Representative images showing α-syn was not detected in GFAP-positive astrocytes (**(N)**, arrows), Iba1-positive microglia (**O**, arrow), and Olig2-positive oligodendrocytes (**(P)**, arrows) in FCD IIb lesions. **(Q–T)** Representative images showing α-syn was not expressed in NeuN-positive neurons in TSC lesions (**(Q)**, arrow), GFAP-positive (**(R)**, arrows), Iba1-positive microglia (**(S)**, arrows), and Olig2-positive oligodendrocytes in TSC lesions (**(T)**, arrow). Scale bars: 50 μm for the upper panel of **(A–C)**, 20 μm for the bottom panel of **(A–C)**, and 10 μm for images **(E–T)**.

TABLE 2 α-syn and p-α-syn immunoreactivity score in cortical lesions of patients with FCD IIb and TSC.

		Control	FCD IIb	TSC
α-syn	DNs	—	$3.67 \pm 0.44^{***}$	0 ± 0
	BCs/GCs	—	3.33 ± 0.33	0 ± 0
P-α-syn	DNS	2.86 ± 0.13	$6.88 \pm 0.67^{***}$	$8.14 \pm 0.86^{***}$
	BCs/GCs	—	7.86 ± 0.56	5.43 ± 1.09

$^{***}p < 0.001$, FCD IIb, TSC vs. CTX, respectively. Unpaired two-tailed t-test, n = 7–9 specimens for each group.

cytoplasm of neurons (Figure 2A). However, weak-to-moderate α-syn immunoreactivity was detected in DNs (double arrows) and BCs (arrows) in FCD IIb lesions (Figure 2B). Interestingly, α-syn immunoreactivity was barely observed in DNs (double arrows) in TSC lesions nor GCs (arrows) (Figure 2C). Additionally, weak α-syn immunoreactivity was observed in the neuropils of FCD IIb and TSC lesions (Figures 2B, C). Statistical analysis showed that the average optical density (OD) of α-syn was significantly reduced both in FCD IIb and TSC lesions (Figure 2D, $^{***}p < 0.001$, unpaired two-tailed *t*-test).

Additionally, we evaluated the immunoreactivity score of α-syn in the cytoplasm of control neurons, DNs, BCs, and GCs of FCD IIb and TSC lesions with methods reported in previous studies (35, 45) and summarized the information in Table 2. Specifically, α-syn immunoreactivity was not observed in the cytoplasm of neurons in CTX and was scored zero, but it was significantly increased in DNs, BCs of FCD IIb lesions and scored 3.67 ± 0.44, 3.33 ± 0.33, respectively ($^{***}p < 0.001$, unpaired two-tailed *t*-test), and α-syn was not observed in DNs and GCs of TSC lesions and scored zero individually.

Double immunofluorescent staining results showed that α-syn was expressed in vimentin-positive BCs in FCD IIb lesions (arrows in Figure 2E). α-syn was intensively expressed in the neuropils of CTX and sparsely co-localized with VGLUT2, a marker of excitatory neurons in CTX (Figure 2F). However, the immunoreactivity of VGLUT2 was intensely increased in the neuropils of both FCD IIb and TSC lesions, as shown by the co-expression of α-syn and VGLUT2 (Figures 2G, H). Importantly, co-expression of α-syn and VGLUT2 was observed in DNs (double arrows) and BCs (arrows) in FCD IIb lesions (Figure 2G) but not in the GCs of TSC lesions (Figure 2H). In TSC lesions, α-syn signal was not detected in vimentin-positive GCs (Figure 2I) nor in VGAT-positive inhibitory neurons in the CTX (Figure 2J). However, the co-expression of α-syn and VGAT was intensified in DNs and BCs of FCD IIb lesions (Figure 2K) and neuropils of TSC lesions (Figure 2L). Thus, these results suggested that α-syn might contribute to regulating the excitatory and inhibitory synaptic transmission both in FCD IIb and TSC lesions.

α-syn was expressed both in the cytoplasm of NeuN-positive neurons and nearby neuropils (Figure 2M) but not in GFAP-positive astrocytes (Figure 2N), Iba1-positive microglia (Figure 2O), and Olig2-positive oligodendrocytes (Figure 2P) in FCD IIb lesions. Interestingly, α-syn was not expressed in NeuN-positive neurons (Figure 2Q) in TSC lesions, GFAP-positive astrocytes (Figure 2R), Iba1-positive microglia (Figure 2S), and Olig2-positive oligodendrocytes (Figure 2T).

3.3. Expression patterns of p-α-syn in FCD IIb and TSC lesions

p-α-syn, in which α-syn is phosphorylated at Ser129, is the major pathological form of α-syn. The aggregation of p-α-syn in the cytoplasm and nuclei of neurons was identified as pathological markers of Parkinson's disease and multiple system atrophy in the central nervous system, respectively (50). We evaluated the immunoreactivity score of p-α-syn in the DNs, BCs, and GCs of FCD IIb and TSC lesions as well. As illustrated in Table 2, weak p-α-syn immunoreactivity was observed in the neurons of CTX and scored 2.86 ± 0.13. However, the immunoreactivity score of p-α-syn was significantly increased in the DNs and BCs of FCD IIb lesions, which scored 6.88 ± 0.67 and 7.86 ± 0.56, respectively ($^{***}p < 0.001$, unpaired two-tailed *t*-test), and DNs and GCs of TSC lesions, which scored 8.14 ± 0.86 and 5.43 ± 1.09, individually ($^{***}p < 0.001$, unpaired two-tailed *t*-test).

As shown by the representative images, weak-to-moderate immunoreactivity of p-α-syn was observed in neurons of CTX specimens (Figure 3A). In contrast, moderate-to-strong p-α-syn immunoreactivity was observed in DN (arrow), BC (double arrow), and glia-like cells (arrowheads) of FCD IIb lesions (Figure 3B). Strong p-α-syn immunoreactivity was detected in the cytoplasm and nuclei of DN (arrow) and glia-like cells (arrowheads) in TSC lesions (Figure 3C), while the intensity was relatively reduced in GC (double arrow) of TSC lesions (Figure 3D). Additionally, statistical analysis indicated the overall OD value of p-α-syn was increased in FCD IIb and TSC lesions (Figure 3E, $^{***}p < 0.001$, unpaired two-tailed *t*-test), suggesting that α-syn was abnormally aggregated in

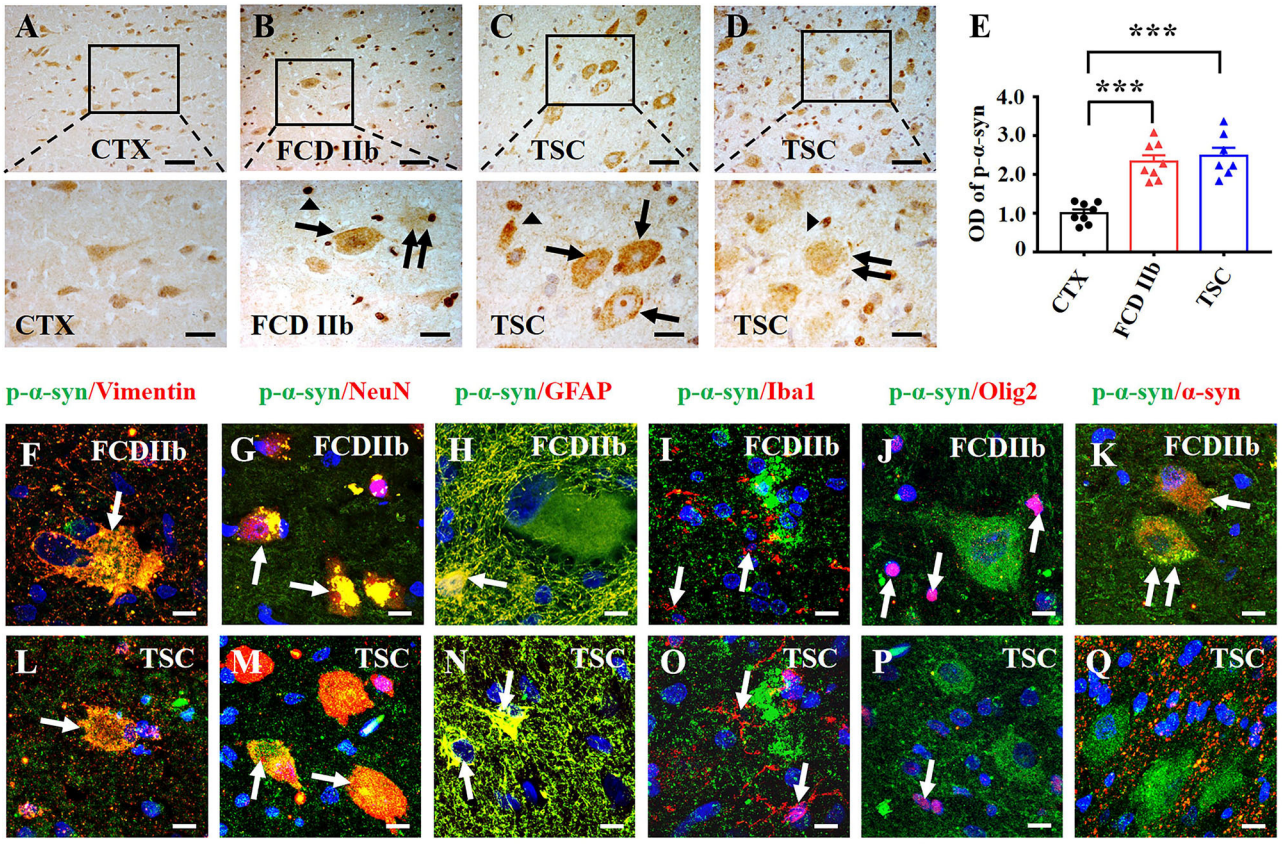

FIGURE 3
Expression profiles of p-α-syn in lesions of patients with FCD IIb and TSC. **(A)** Representative images showing moderate p-α-syn immunoreactivity in neurons of the CTX. **(B)** Moderate-to-strong p-α-syn immunoreactivity was observed in the cytoplasm of DN (arrow) and BC (double arrow) in FCD IIb lesions, and strong p-α-syn signal was detected in the nuclei of dysplastic neurons and glia-like cells (arrowhead). **(C, D)** Representative images showing strong p-α-syn immunoreactivity in DNs (arrow) and glia-like cells (arrowheads) of TSC lesions, and moderate p-α-syn immunoreactivity was observed in GC (double arrow). **(E)** Statistical analysis demonstrated that the average OD of p-α-syn was increased in cortical lesions of patients with FCD IIb and TSC (***$p < 0.001$, unpaired two-tailed t-test, $n = 8, 8, 7$ specimens for each group). **(F)** Representative image showing p-α-syn signal in vimentin-positive BC (arrow) in FCD IIb lesions. **(G, H)** Representative images showing p-α-syn immunoreactivity in NeuN-positive neurons (**G**, arrows) and GFAP-positive astrocytes in FCD IIb lesions (**H**, arrow). **(I, J)** Representative image showing p-α-syn was barely expressed in Iba1-positive microglia (**I**, arrows) and Olig2-positive oligodendrocytes (**J**, arrow). **(K)** Representative image showing p-α-syn and α-syn were co-expressed in in BC (arrow) and DN (double arrows) of FCD IIb lesions. **(L)** Representative image showing p-α-syn was expressed in the vimentin-positive GC in TSC lesions (arrow). **(M, N)** Representative images showing p-α-syn was detected in the NeuN-positive neurons (**M**, arrows) and GFAP-positive astrocytes in TSC lesions (**N**, arrow). **(O, P)** p-α-syn was barely observed in Iba1-positive microglia (**O**, arrow) and Olig2-positive oligodendrocytes (**P**, arrows) in TSC lesions. **(Q)** Representative images showing p-α-syn and α-syn were barely co-expressed in TSC lesions. Scale bars: 50 μm for upper panel of **(A–D)**, 20 μm for bottom panel of **(A–D)**, 10 μm for **(F–Q)**.

the dysplastic neurons in cortical lesions of patients with FCD IIb and TSC.

Double immunofluorescent staining results showed that p-α-syn was identified in vimentin-positive BC (Figure 3F) and NeuN-positive neurons in FCD IIb lesions (Figure 3G). Additionally, p-α-syn was detected in the GFAP-positive astrocytes (Figure 3H) but not in Iba1-positive microglia (Figure 3I) and Oligo2-positive oligodendrocytes (Figure 3J) in FCD IIb lesions. Furthermore, co-expression of α-syn and p-α-syn was observed in DN (arrow) and BC (double arrows) in FCD IIb lesions (Figure 3K). Intense p-α-syn signal was detected in vimentin-positive BC in TSC lesions (Figure 3L), NeuN-positive neurons (Figure 3M), and GFAP-positive astrocytes (Figure 3N). However, p-α-syn signal was not detected in Iba1-positive microglia (Figure 3O) and Olig2-positive oligodendrocytes (Figure 3P) in TSC lesions. Additionally, p-α-syn was barely co-expressed with α-syn in TSC lesions (Figure 3Q).

3.4. α-syn interacted with NMDAR in the cortical lesions of patients with FCD IIb and TSC

N-methyl-D-aspartic acid receptor (NMDAR) plays important role in mediating glutamate-induced excitatory synaptic transmission in the central nervous system (51). The molecular composition of NMDAR was found to be altered in the cortical samples of patients with FCD and relevant animal models (31, 52–54). Studies have shown that α-syn could alter synaptic transmission and plasticity by interfering with different NMDAR subunits (55–58). Therefore, we wondered whether α-syn regulates the expression of primary NMDAR subunits NMDAR2A and NMDAR2B in the cortical lesions of patient with FCD IIb and TSC and of FCD rats.

First, we investigated the expression profiles of NMDAR2A and NMDAR2B in cortical lesions of patients with FCD IIb and TSC. As shown by the representative images (Figures 4A–C, E–G), in comparison with the immunoreactivity of NMDAR2A and NMDAR2B in CTX, NMDAR2A and NMDAR2B immunoreactivity were intensively increased in the dysplastic neurons of FCD IIb and TSC lesions. Statistical analysis results showed that the immunoreactivity of both NMDAR2A and NMDAR2B was significantly increased in FCD IIb and TSC lesions (Figures 4D, H). Furthermore, we verified the interaction of α-syn with NMDAR2A and NMDAR2B in cortical lesions of patients with FCD IIb and TSC with Co-IP. Representative images and immunoblotting bands (Figure 4I) showed that the interaction of α-syn/NMDAR2A was not significantly altered, but the α-syn/NMDAR2B complex was augmented in FCD IIb and TSC lesions. However, reverse verification bands showed that the NMDAR2A/α-syn complex was significantly augmented both in FCD IIb and TSC lesions (Figure 4J, upper panel). In comparison with the blotting bands of NMDAR2A, the expression of NMDAR2B was relatively weak in the homogenates of CTX, FCD IIb, and TSC lesions (Figure 4J, bottom panel). However, the NMDAR2B/α-syn complex was significantly strengthened both in FCD IIb and TSC lesions, suggesting strong interactions of α-syn with NMDAR2A and NMDAR2B in the cortical lesions of patients with FCD IIb and TSC.

3.5. The expression profiles of α-syn and p-α-syn in FCD rats

Consistent with previous studies (9, 27), we utilized *in utero* X-ray radiated rats to replicate the pathological characteristics of FCD. We used RT-PCR to determine α-syn mRNA expression in the FCD rats first. Statistical analysis showed that α-syn mRNA was significantly reduced in FCD rats from 7, 14, to 28 days after birth (Figure 5A, $^{**}p < 0.01$, unpaired two-tailed *t*-test). Pyramidal neurons in layer V are the principal output neurons in the cortex (59, 60). Thus, we explored the expression profiles of α-syn and p-α-syn in layer V of cortical lesions. IHC results showed that α-syn immunoreactivity was significantly reduced in layer V of cortical lesions in FCD rats from 7, 14, to 28 days after birth (Figures 5B, C). Conversely, IHC results showed that p-α-syn immunoreactivity was significantly increased in layer V of cortical lesions in FCD rats from 7, 14, to 28 days after birth (Figures 5D, E). As shown by the representative images, the appearance of the brain of X-ray-radiated rats (FCD rats) at 28 days after birth was dramatically deformed, illustrated by an apparent reduction in bulk volume, telencephalon, and cerebellum (Figure 5F). Furthermore, HE-staining results showed that the cortical structure was significantly disrupted, as shown by a much thinner cortex (indicated by the occurrence of corpus callosum) and non-obvious lamellar structure (Figure 5G), which was highly similar to the pathological characteristics of cortical dyslamination in FCD patients. Additionally, Western blotting results showed that α-syn protein expression was significantly reduced in FCD rats at 28 days after birth (Figure 5H).

3.6. α-syn interacted with NMDAR in the cortex of FCD rats

Consistent with the experiments performed in FCD IIb and TSC patients, we investigated the expression of NMDAR2A and NMDAR2B in cortical neurons of layer V in FCD rats. IHC results showed that both the immunoreactivity of NMDAR2A and NMDAR2B were increased in the cortical neurons of FCD rats, as shown by the representative images and statistical results (Figures 6A–D) ($^{**}p < 0.01$, unpaired two-tailed *t*-test.). To test whether α-syn interacts with NMDAR2A and NMDAR2B, we performed Co-IP to investigate the interaction between α-syn and NMDAR2A and NMDAR2B. As shown by the representative immunoblotting bands (Figure 6E), this qualitative approach suggested an augmentation in the levels of the α-syn/NMDAR2A and α-syn /NMDAR2B complex in FCD rats at 28 days after birth, and IgG was used as negative control. Reverse Co-IP was performed to confirm the interaction of NMDAR2A and NMDAR2B with α-syn. As shown by the representative immunoblotting bands (Figure 6F), the NMDAR2A/α-syn complex did not significantly differ between control and FCD rats by pulling down NMDAR2A, whereas the NMDAR2B/α-syn complex was intensified in FCD rats at 28 days after birth.

We also investigated the interaction of α-syn and NMDAR in FCD and control rats at postnatal 7 days and 14 days. At 7 days after birth, as shown in representative immunoblotting bands (Supplementary Figure S1A), α-syn/NMDAR2A complex and α-syn/NMDAR2B complex were reduced in the FCD rats. Reverse immunoblotting bands (Supplementary Figure S1B) showed that the NMDAR2A/α-syn complex did not significantly differ between the control and FCD rats by pulling down NMDAR2A, while the NMDAR2B/α-syn complex was augmented. At 14 days after birth, the immunoblotting bands (Supplementary Figure S1C) indicated that both α-syn/NMDAR2A complex and α-syn/NMDAR2B complex were intensified in the FCD rats, while reverse Co-IP immunoblotting bands (Supplementary Figure S1D) showed that NMDAR2A/α-syn and NMDAR2B/α-syn complex were reduced in the FCD rats. Together, these results suggested that α-syn might contribute to regulating the synaptic transmission in FCD rats by interfering with NMDAR from an early developmental stage.

4. Discussion

The present study highlighted the distinctive expression profiles of α-syn and p-α-syn, and the interaction of α-syn with NMDAR in the cortical lesions of patients with FCD IIb and TSC, and FCD rats generated by X-ray-radiation, suggesting a potential role of α-syn/NMDAR complex in the pathogenesis and epileptogenesis of FCD IIb and TSC.

α-syn is shown to be concentrated in nerve terminals in close proximity to synaptic vesicles, with little staining in somata and dendrites, implicated in crucial roles for in vesicular trafficking, neurotransmitter release, and neurotransmission (61, 62). Here, we found the expression of α-syn protein was significantly reduced in the cortical lesions of patients with FCD IIb and TSC. The inconsistency of increased mRNA level but reduced protein expression of α-syn in TSC patients was intriguing, and

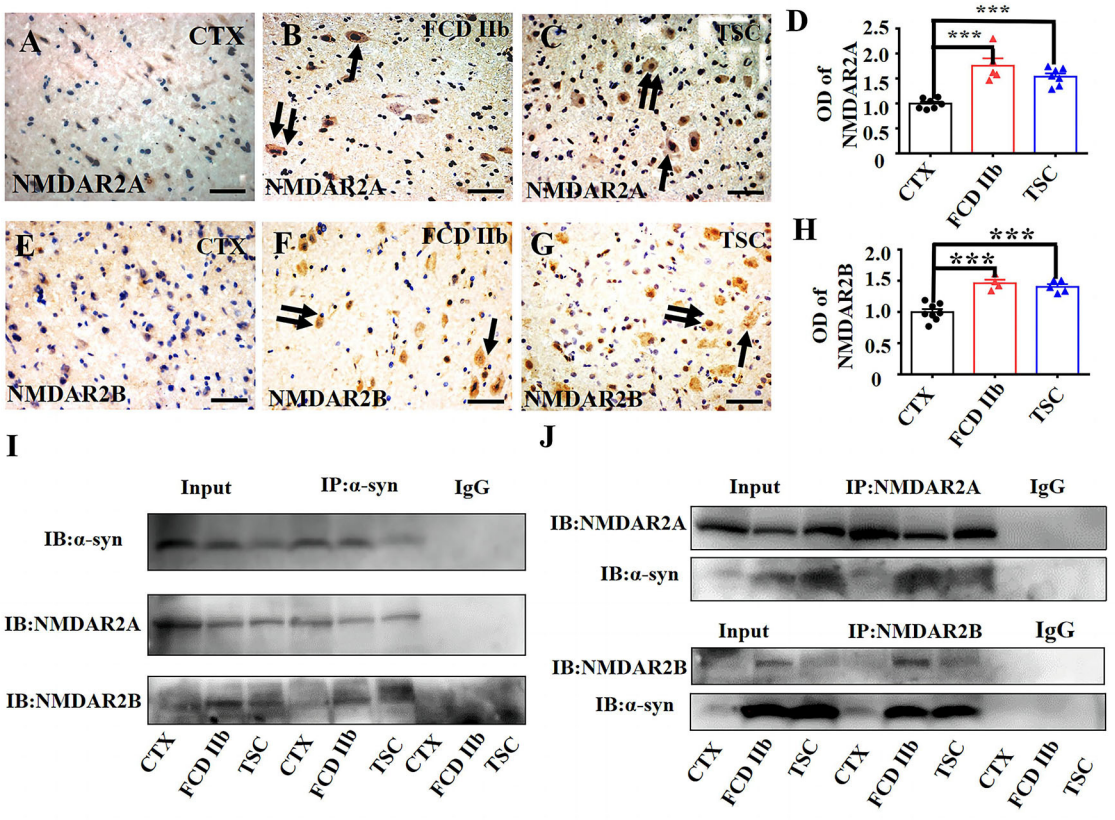

FIGURE 4
α-syn interacted with NMDAR in cortical lesions of patients with FCD IIb and TSC. **(A)** Weak NMDAR2A immunoreactivity was detected in the neurons in CTX. **(B, C)** Representative images showing strong NMDAR2A immunoreactivity in DNs (arrow) and BCs (double arrows) of FCD IIb lesions and also DNs (arrow) and BCs (double arrows) of TSC lesions. **(D)** Statistical analysis showed that the average OD of NMDAR2A was increased both in the FCD IIb and TSC lesions ($^{***}p < 0.001$, unpaired two-tailed *t*-test, $n = 7, 5, 7$ specimens for each group). **(E)** Representative image showing weak NMDAR2B immunoreactivity in neurons of CTX. **(F, G)** Representative images showing strong NMDAR2B immunoreactivity in DNs (arrow) and BCs (double arrows) of FCD IIb lesions, and DNs (arrow) and GCs (double arrows) of TSC lesions. **(H)** Statistical analysis showed that the average OD of NMDAR2B was increased both in the FCD IIb and TSC leisons ($^{***}p < 0.001$, unpaired two tailed *t*-test, $n = 8, 4, 5$ specimens for each group). **(I)** Representative immunoblotting bands showing that α-syn/NMDAR2A complex was not significantly altered, while α-syn/NMDAR2B complex was augmented both in FCD IIb and TSC lesions. IgG was used as negative control. **(J)** Representative immunoblotting bands showing significant augmentation of both NMDAR2A/α-syn and NMDAR2B/α-syn complex in FCD IIb and TSC lesions. IgG was used as negative control.

we speculated that mechanisms concerning posttranscriptional translation contribute to the discrepancy (63–65). However, the co-expression of α-syn with both VGLUT2 and VGAT was intensified in cortical lesions of patients with FCD IIb and TSC, suggesting a potential role of α-syn in regulating synaptic transmission during epileptic activity in patients with FCD IIb and TSC.

Fibrillary aggregates of α-syn protein, p-α-syn in the cytoplasm of neurons and glia termed as synucleinopathies, have been implicated in several neurodegenerative diseases, including Parkinson's disease, Alzheimer's disease, and multiple sclerosis atrophy (66). Studies reported that α-syn protein aggregation, including oligomeric deposits, protofibrils deposits, and fibrils, can spread across neurons and glias similar to the pathological characteristics of prionic diseases (67–69). Here, we found that p-α-syn was specifically aggregated in the cytoplasm, nuclei of BCs and GCs, dysplastic neurons, and astrocytes in the cortical lesions of patients with FCD IIb and TSC as well and further verified the neuropathological characteristics of dysplastic neurons and BCs and GCs in FCD IIb and TSC. Conversely, α-syn was absent in DNs and GCs of TSC lesions. These phenomena can be explained by the following reasons. α-syn was synthesized in neuronal cytoplasm and transported to nerve terminals gradually for functioning during development (70, 71). However, DN and GCs are typical dysplastic neurons with eccentric nuclei, giant cytoplasm, and without clear axonal or dendritic processes, suggesting that critical cytological deficits existed in these cells, which might indicate the underlying deficiency of α-syn in DN and GCs. Interestingly, positive p-α-syn immunoreactivity was observed in the cytoplasm of DN and GCs, possibly attributing to the disturbed activity of various kinases and signaling cascades in TSC lesions after the abnormal activation of mTOR pathway (72).

Our previous studies have shown that NMDAR-mediated currents were significantly increased in the dysplastic neurons in FCD rats (27). Consistent with the functional augmentation of NMDAR, we found that the immunoreactivity of NMDAR2A and NMDAR2B was consistently increased in the cortical lesions of patients with FCD IIb and TSC and also FCD rats in this study.

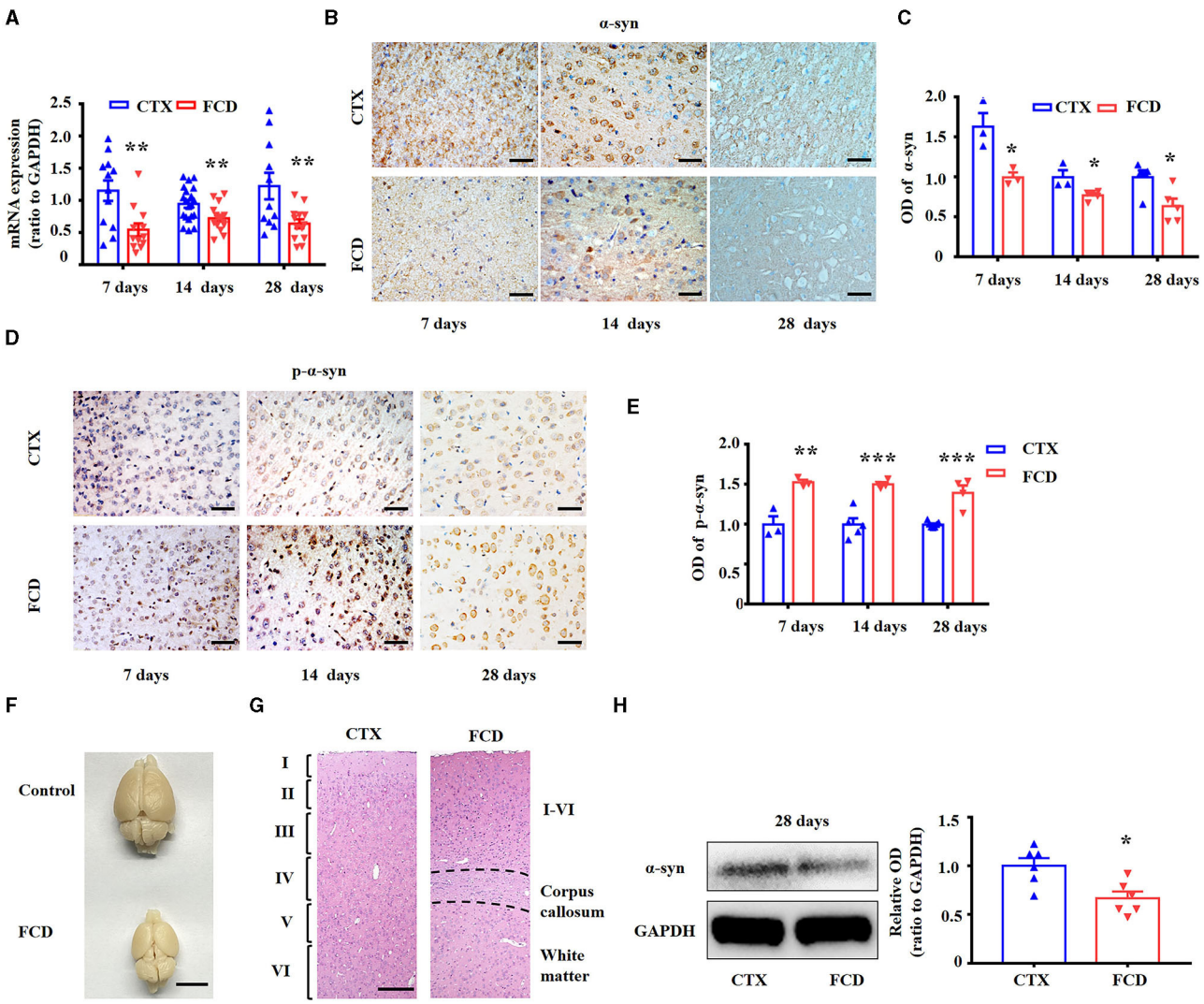

FIGURE 5
Expression profiles of α-syn and p-α-syn in FCD rats. **(A)** RT-PCR results showed α-syn mRNA expression was significantly reduced in FCD rats at postnatal 7, 14, and 28 days (**$p < 0.01$, unpaired two-tailed *t*-test, $n = 11–20$ rats for each group). **(B)** Representative images showing strong α-syn immunoreactivity in the neuronal membrane and cytoplasm or neuropils in the cortex of control rats but weak-to-moderate α-syn immunoreactivity in the cortex of FCD rats at 7, 14, and 28 days after birth. Scale bars: 50 μm. **(C)** Statistical analysis showed that the α-syn protein was significantly decreased in FCD rats ($p < 0.05$, unpaired two-tailed *t*-test, $n = 3–5$ rats for each group). **(D)** Weak p-α-syn immunoreactivity was observed in the neuronal membrane of control rats, whereas it was strengthened in the cortical neurons of FCD rats at 7, 14, and 28 days after birth. Scale bars: 50 μm. **(E)** Statistical analysis showed that the p-α-syn protein was significantly increased in FCD rats (**$p < 0.01$, ***$p < 0.001$, unpaired two-tailed *t*-test, $n = 3–7$ rats for each group). **(F)** Representative images showing deformed brain in FCD rats at 28 days after birth, as shown by reduced telencephalon and cerebellum volume, and uncovered quadrigemina. Scale bar: 1 cm. **(G)** HE staining images showing thinner cortex (indicated by the occurrence of corpus callosum) and disrupted lamellar structure in FCD rats at 28 days after birth. Scale bar: 200 μm. **(H)** Representative immunoblot bands of α-syn and GAPDH in total homogenates from the cortex of control and FCD rats at 28 days after birth, and statistical analysis results showing that α-syn protein was significantly decreased in FCD rats (*$p < 0.05$, unpaired two-tailed *t*-test, $n = 6$ rats for each group).

Several studies have pointed out that α-syn could interact with NMDAR to induce synaptic dysfunction in the central nervous system, leading to memory and cognitive impairments in animals (55–57, 73, 74). Additionally, α-syn was reported to modulate the NMDAR2B activation and internalization in cultured cortical neurons (75). Here, we found that the direct interaction of α-syn with NMDAR2A and NMDAR2B was significantly intensified in FCD rats since postnatal 7 days, which suggested that α-syn might contribute to the synaptic dysfunction in FCD lesions by modulating the internalization and activation of NMDAR. Thus, our study here suggested a causal relationship between disturbed α-syn expression and abnormal NMDAR function in the pathogenesis and epileptogenesis of FCD IIb and TSC.

5. Conclusion

Taking together, our study characterized the disturbed expression of α-syn and p-α-syn in FCD and TSC lesions and demonstrated a stronger interaction between α-syn and NMDAR in cortical lesions of patients with FCD IIb and TSC, and FCD rats, proposing a potential linkage between α-syn and NMDAR

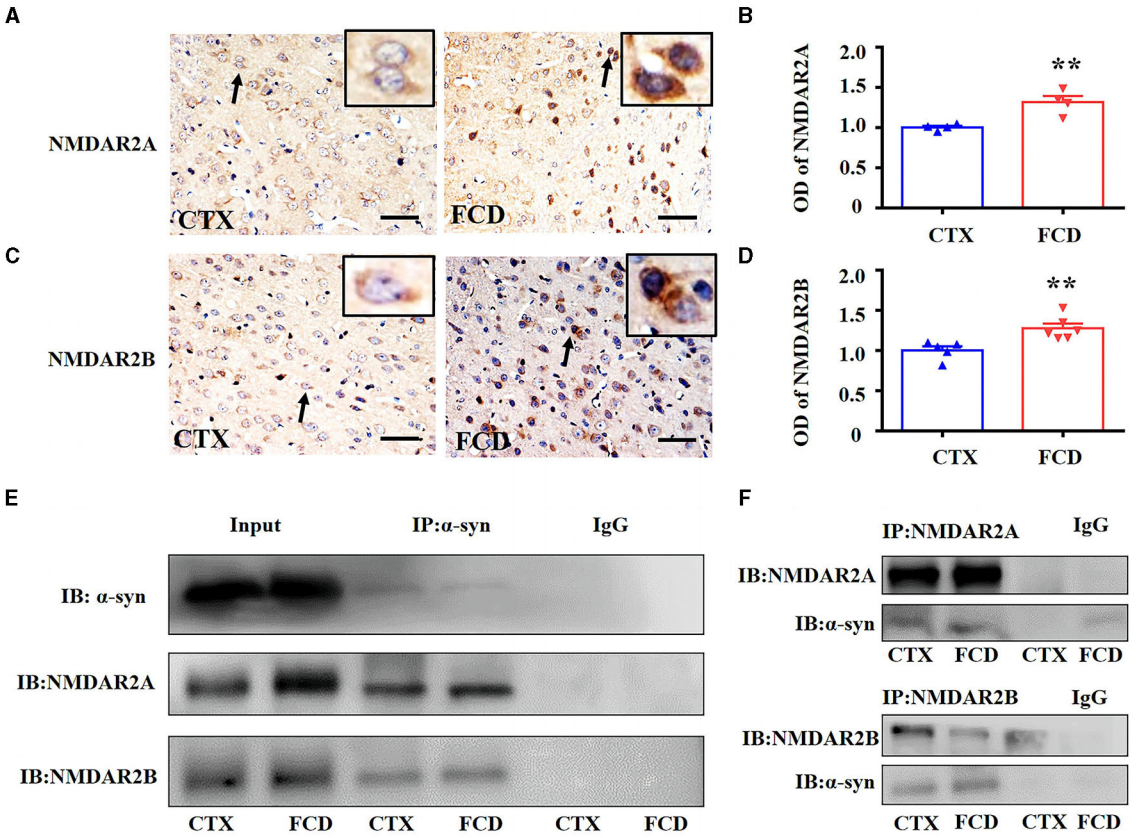

FIGURE 6
α-syn interacted with NMDAR in the cortex of FCD rats at postnatal 28 days. **(A)** Representative images showing moderate NMDAR2A immunoreactivity on layer V cortical neuronal membrane of control rats (arrow and inset) but was intensified both in the membrane and cytoplasm of cortical neurons in FCD rats (arrow and inset). **(B)** Statistical analysis showing NMDAR2A immunoreactivity was increased in the cortex of FCD rats (**$p < 0.01$, unpaired two-tailed *t*-test, $n = 4$ rats for each group). **(C)** Weak NMDAR2B immunoreactivity was observed in the cytoplasm of cortical neurons in control rats (arrow and inset) but increased immunoreactivity in the cortical neurons of FCD rats (arrow and inset). **(D)** Statistical analysis showed NMDAR2B immunoreactivity was significantly increased in the cortex of FCD rats (**$p < 0.01$, unpaired two-tailed *t*-test, $n = 5$, 6 rats for each group). **(E)** Representative Western blotting bands showing immunoprecipitation of α-syn in the cortex of control and FCD rats. Membranes were immunoblotted with anti-NMDAR2A and anti-NMDAR2B antibodies. Augmented α-syn/NMDAR2A and α-syn/NMDAR2B complex was observed in the cortical homogenates of FCD rats. IgG was used as negative control. **(F)** Representative Western blotting bands showing immunoprecipitation of NMDAR2A or NMDAR2B, membranes were immunoblotted with anti-α-syn antibody, and the augmentation of NMDAR2B/α-syn was more apparent in FCD rats. IgG was used as negative control.

in the pathogenesis and epileptogenesis of FCD. These results advanced our understanding of the potential function of α-syn by mediating NMDAR during the pathological development of FCD IIb and TSC. Studies concerning the modulating effects of α-syn on seizure activity in future would expand our understanding of the pathogenesis of FCD IIb and TSC further.

Data availability statement

The original contributions presented in the study are included in the article/Supplementary material, further inquiries can be directed to the corresponding authors.

Ethics statement

The studies involving humans were approved by the Ethics Committee of Xinqiao Hospital, Army Medical University. The studies were conducted in accordance with the local legislation and institutional requirements. Written informed consent for participation in this study was provided by the participants' legal guardians/next of kin. The animal study was approved by the Ethical Committee of Army Medical University and approved by the Internal Animal Care and Use Committee of Army Medical University. The study was conducted in accordance with the local legislation and institutional requirements. Written informed consent was obtained from the individual(s), and minor(s)' legal guardian/next of kin, for the publication of any potentially identifiable images or data included in this article.

Author contributions

LZ: Data curation, Writing—original draft. JH: Methodology, Resources, Writing—review & editing. LD: Methodology, Writing—review & editing. GZ: Methodology, Writing—review & editing. X-LY: Formal Analysis, Methodology, Writing—review &

editing. ZH: Methodology, Software, Writing—review & editing. Y-HL: Conceptualization, Resources, Writing—review & editing. HY: Resources, Writing—review & editing. C-QZ: Funding acquisition, Investigation, Methodology, Project administration, Resources, Writing—review & editing. K-FS: Formal Analysis, Investigation, Methodology, Software, Supervision, Writing—review & editing. PL: Methodology, Supervision, Writing—review & editing.

Funding

This work was supported by the grant from National Natural Science Foundation of China (no. 82171463).

Conflict of interest

The authors declare that the research was conducted in the absence of any commercial or financial relationships that could be construed as a potential conflict of interest.

Publisher's note

All claims expressed in this article are solely those of the authors and do not necessarily represent those of their affiliated organizations, or those of the publisher, the editors and the reviewers. Any product that may be evaluated in this article, or claim that may be made by its manufacturer, is not guaranteed or endorsed by the publisher.

Supplementary material

The Supplementary Material for this article can be found online at: https://www.frontiersin.org/articles/10.3389/fneur.2023.1255097/full#supplementary-material

References

1. Kielbinski M, Gzielo K, Soltys Z. Review: Roles for astrocytes in epilepsy: insights from malformations of cortical development. *Neuropathol Appl Neurobiol.* (2016) 42:593–606. doi: 10.1111/nan.12331

2. Najm I, Lal D, Alonso Vanegas M, Cendes F, Lopes-Cendes I, Palmini A, et al. The ILAE consensus classification of focal cortical dysplasia: an update proposed by an ad hoc task force of the ILAE diagnostic methods commission. *Epilepsia.* (2022) 63:1899–919. doi: 10.1111/epi.17301

3. Schick V, Majores M, Koch A, Elger CE, Schramm J, Urbach H, et al. Alterations of phosphatidylinositol 3-kinase pathway components in epilepsy-associated glioneuronal lesions. *Epilepsia.* (2007) 48:65–73. doi: 10.1111/j.1528-1167.2007.01291.x

4. Wong YC, Krainc D. α-synuclein toxicity in neurodegeneration: mechanism and therapeutic strategies. *Nat Med.* (2017) 23:1–13. doi: 10.1038/nm.4269

5. Alarcón-Arís D, Recasens A, Galofré M, Carballo-Carbajal I, Zacchi N, Ruiz-Bronchal E, et al. Selective α-synuclein knockdown in monoamine neurons by intranasal oligonucleotide delivery: potential therapy for Parkinson's disease. *Mol Ther.* (2018) 26:550–67. doi: 10.1016/j.ymthe.2017.11.015

6. Lashuel HA, Overk CR, Oueslati A, Masliah E. The many faces of α-synuclein: from structure and toxicity to therapeutic target. *Nat Rev Neurosci.* (2013) 14:3406. doi: 10.1038/nrn3406

7. Takase K, Shigeto H, Suzuki SO, Kikuchi H, Ohyagi Y, Kira J. Prenatal freeze lesioning produces epileptogenic focal cortical dysplasia. *Epilepsia.* (2008) 49:997–1010. doi: 10.1111/j.1528-1167.2008.01558.x

8. Campbell SL, Hablitz JJ, Olsen ML. Functional changes in glutamate transporters and astrocyte biophysical properties in a rodent model of focal cortical dysplasia. *Front Cell Neurosci.* (2014) 8:425. doi: 10.3389/fncel.2014.00425

9. Kellinghaus C, Kunieda T, Ying Z, Pan A, Lüders HO, Najm IM. Severity of histopathologic abnormalities and in vivo epileptogenicity in the in utero radiation model of rats is dose dependent. *Epilepsia.* (2004) 45:583–91. doi: 10.1111/j.0013-9580.2004.41103.x

10. Oghlakian RO, Tilelli CQ, Hiremath GK, Alexopoulos AV, Najm IM. Single injection of a low dose of pentylenetetrazole leads to epileptogenesis in an animal model of cortical dysplasia. *Epilepsia.* (2009) 50:801–10. doi: 10.1111/j.1528-1167.2008.01815.x

11. Nemes AD, O'Dwyer R, Najm IM, Ying Z, Gonzalez-Martinez J, Alexopoulos AV. Treatment with lacosamide impedes generalized seizures in a rodent model of cortical dysplasia. *Epilepsia.* (2017) 58:1755–61. doi: 10.1111/epi.13856

12. Harrington EP, Möddel G, Najm IM, Baraban SC. Altered Glutamate Receptor—transporter expression and spontaneous seizures in rats exposed to methylazoxymethanol in utero. *Epilepsia.* (2007) 48:158–68. doi: 10.1111/j.1528-1167.2006.00838.x

13. Bassanini S, Hallene K, Battaglia G, Finardi A, Santaguida S, Cipolla M, et al. Early cerebrovascular and parenchymal events following prenatal exposure to the putative neurotoxin methylazoxymethanol. *Neurobiol Dis.* (2007) 26:481–95. doi: 10.1016/j.nbd.2007.02.008

14. Gierdalski M, Sardi SP, Corfas G, Juliano SL. Endogenous neuregulin Restores radial glia in a (ferret) model of cortical dysplasia. *J Neurosci.* (2005) 25:8498–504. doi: 10.1523/JNEUROSCI.1476-05.2005

15. Abbah J, Juliano SL. Altered migratory behavior of interneurons in a model of cortical dysplasia: the influence of elevated GABAA activity. *Cereb Cortex.* (2014) 24:2297–308. doi: 10.1093/cercor/bht073

16. Schaefer AW, Juliano SL. Migration of transplanted neural progenitor cells in a ferret model of cortical dysplasia. *Exp Neurol.* (2008) 210:67–82. doi: 10.1016/j.expneurol.2007.10.005

17. Poluch S, Juliano SL, A. normal radial glial scaffold is necessary for migration of interneurons during neocortical development. *Glia.* (2007) 55:822–30. doi: 10.1002/glia.20488

18. Inverardi F, Chikhladze M, Donzelli A, Moroni RF, Regondi MC, Pennacchio P, et al. Cytoarchitectural, behavioural and neurophysiological dysfunctions in the BCNU-treated rat model of cortical dysplasia. *Eur J Neurosci.* (2013) 37:150–62. doi: 10.1111/ejn.12032

19. Takano T, Sawai C, Takeuchi Y. Radial and tangential neuronal migration disorder in ibotenate-induced cortical lesions in hamsters: immunohistochemical study of reelin, vimentin, and calretinin. *J Child Neurol.* (2004) 19:107–15. doi: 10.1177/088307380401900205O1

20. Shao Y, Ge Q, Yang J, Wang M, Zhou Y, Guo J-X, et al. Pathological networks involving dysmorphic neurons in type II focal cortical dysplasia. *Neurosci Bull.* (2022) 38:1007–24. doi: 10.1007/s12264-022-00828-7

21. Hsieh LS, Wen JH, Nguyen LH, Zhang L, Getz S, Torres-Reveron J. Ectopic HCN4 expression drives mTOR-dependent epilepsy in mice. *Sci Transl Med.* (2020) 12:eabc1492. doi: 10.1126/scitranslmed.abc1492

22. Hsieh LS, Wen JH, Claycomb K, Huang Y, Harrsch FA, Naegele JR, et al. Convulsive seizures from experimental focal cortical dysplasia occur independently of cell misplacement. *Nat Commun.* (2016) 7:11753. doi: 10.1038/ncomms11753

23. Strzemecki D, Guzowska M, Grieb P. Survival rates of homozygotic Tp53 knockout rats as a tool for preclinical assessment of cancer prevention and treatment. *Cell Mol Biol Lett.* (2017) 22:9. doi: 10.1186/s11658-017-0039-z

24. Aitman T, Dhillon P, Geurts AM, A. RATional choice for translational research? *Dis Model Mech.* (2016) 9:1069–72. doi: 10.1242/dmm.027706

25. Abbott A. The renaissance rat. *Nature.* (2004) 428:464–6. doi: 10.1038/428464a

26. Gibbs RA, Weinstock GM, Metzker ML, Muzny DM, Sodergren EJ, Scherer S, et al. Genome sequence of the Brown Norway rat yields insights into mammalian evolution. *Nature.* (2004) 428:493–521.

27. Shen K-F, Duan Q-T, Duan W, Xu S-L, An N, Ke Y-Y, et al. Vascular endothelial growth factor-C modulates cortical NMDA receptor activity in cortical lesions of

young patients and rat model with focal cortical dysplasia. *Brain Pathol.* (2022) 32:e13065. doi: 10.1111/bpa.13065

28. Kielbinski M, Setkowicz Z, Gzielo K, Weglarz W, Janeczko K. Altered electroencephalography spectral profiles in rats with different patterns of experimental brain dysplasia. *Birth Defects Res.* (2018) 110:303–16. doi: 10.1002/bdr2.1131

29. Wong M. Animal models of focal cortical dysplasia and tuberous sclerosis complex. Recent progress toward clinical applications. *Epilepsia.* (2009) 50:34–44. doi: 10.1111/j.1528-1167.2009.02295.x

30. Brundin P, Dave KD, Kordower JH. Therapeutic approaches to target alpha-synuclein pathology. *Exp Neurol.* (2017) 298:225–35. doi: 10.1016/j.expneurol.2017.10.003

31. Finardi A, Colciaghi F, Castana L, Locatelli D, Marras CE, Nobili P, et al. Long-duration epilepsy affects cell morphology and glutamatergic synapses in type IIB focal cortical dysplasia. *Acta Neuropathol.* (2013) 126:219–35. doi: 10.1007/s00401-013-1143-4

32. Gruber V-E, Luinenburg MJ, Colleselli K, Endmayr V, Anink JJ, Zimmer TS, et al. Increased expression of complement components in tuberous sclerosis complex and focal cortical dysplasia type 2B brain lesions. *Epilepsia.* (2022) 63:364–74. doi: 10.1111/epi.17139

33. Hynd MR, Lewohl JM, Scott HL, Dodd PR. Biochemical and molecular studies using human autopsy brain tissue. *J Neurochem.* (2003) 85:543–62. doi: 10.1046/j.1471-4159.2003.01747.x

34. Huang K, Wang Z, He Z, Li Y, Li S, Shen K, et al. Downregulated formyl peptide receptor 2 expression in the epileptogenic foci of patients with focal cortical dysplasia type IIb and tuberous sclerosis complex. *Immun Inflamm Dis.* (2022) 10:e706. doi: 10.1002/iid3.706

35. Zurolo E, Iyer A, Maroso M, Carbonell C, Anink JJ, Ravizza T, et al. Activation of toll-like receptor, RAGE and HMGB1 signalling in malformations of cortical development. *Brain.* (2011) 134:1015–32. doi: 10.1093/brain/awr032

36. LeVine SM, Goldman JE. Embryonic divergence of oligodendrocyte and astrocyte lineages in developing rat cerebrum. *J Neurosci.* (1988) 8:3992–4006. doi: 10.1523/JNEUROSCI.08-11-03992.1988

37. Zimmer TS, Broekaart DWM, Luinenburg M, Mijnsbergen C, Anink JJ, Sim NS, et al. Balloon cells promote immune system activation in focal cortical dysplasia type 2b. *Neuropathol Appl Neurobiol.* (2021) 47:826–39. doi: 10.1111/nan.12736

38. Ying Z, Gonzalez-Martinez J, Tilelli C, Bingaman W, Najm I. Expression of neural stem cell surface marker CD133 in balloon cells of human focal cortical dysplasia. *Epilepsia.* (2005) 46:1716–23. doi: 10.1111/j.1528-1167.2005.00276.x

39. Boer K, Lucassen PJ, Spliet WGM, Vreugdenhil E, van Rijen PC, Troost D, et al. Doublecortin-like (DCL) expression in focal cortical dysplasia and cortical tubers. *Epilepsia.* (2009) 50:2629–37. doi: 10.1111/j.1528-1167.2009.02191.x

40. Zimmer TS, Ciriminna G, Arena A, Anink JJ, Korotkov A, Jansen FE, et al. Chronic activation of anti-oxidant pathways and iron accumulation in epileptogenic malformations. *Neuropathol Appl Neurobiol.* (2020) 46:546–63. doi: 10.1111/nan.12596

41. Roll L, Eysel UT, Faissner A. Laser lesion in the mouse visual cortex induces a stem cell niche-like extracellular matrix, produced by immature astrocytes. *Front Cell Neurosci.* (2020) 14:102. doi: 10.3389/fncel.2020.00102

42. Saggu H, Pilkington GJ. Immunocytochemical characterization of the A15 A5 transplantable brain tumour model in vivo. *Neuropathol Appl Neurobiol.* (1986) 12:291–303. doi: 10.1111/j.1365-2990.1986.tb00141.x

43. Sun F-J, Zhang C-Q, Chen X, Wei Y-J, Li S, Liu S-Y, et al. Downregulation of CD47 and CD200 in patients with focal cortical dysplasia type IIb and tuberous sclerosis complex. *J Neuroinflam.* (2016) 13:85. doi: 10.1186/s12974-016-0546-2

44. Wang Z, Huang K, Yang X, Shen K, Yang L, Ruan R, et al. Downregulated GPR30 expression in the epileptogenic foci of female patients with focal cortical dysplasia type IIb and tuberous sclerosis complex is correlated with 18F-FDG PET-CT values. *Brain Pathol.* (2021) 31:346–64. doi: 10.1111/bpa.12925

45. Zhang C-Q, Shu H-F, Yin Q, An N, Xu S-L, Yin J-B, et al. Expression and cellular distribution of vascular endothelial growth factor-C system in cortical tubers of the tuberous sclerosis complex. *Brain Pathol.* (2012) 22:205–18. doi: 10.1111/j.1750-3639.2011.00519.x

46. Wang Z, Xie R, Yang X, Yin H, Li X, Liu T, et al. Female mice lacking ERβ display excitatory/inhibitory synaptic imbalance to drive the pathogenesis of temporal lobe epilepsy. *Theranostics.* (2021) 11:6074–89. doi: 10.7150/thno.56331

47. Faul F, Erdfelder E, Lang A-G, Buchner A. G*Power 3: a flexible statistical power analysis program for the social, behavioral, and biomedical sciences. *Behav Res Methods.* (2007) 39:175–91. doi: 10.3758/BF03193146

48. Li W, Lesuisse C, Xu Y, Troncoso JC, Price DL, Lee MK. Stabilization of alpha-synuclein protein with aging and familial Parkinson's disease-linked A53T mutation. *J Neurosci.* (2004) 24:7400–9. doi: 10.1523/JNEUROSCI.1370-04.2004

49. Hsu LJ, Mallory M, Xia Y, Veinbergs I, Hashimoto M, Yoshimoto M, et al. Expression pattern of synucleins (non-Abeta component of Alzheimer's disease amyloid precursor protein/alpha-synuclein) during murine brain development. *J Neurochem.* (1998) 71:338–44. doi: 10.1046/j.1471-4159.1998.71010338.x

50. Villar-Piqué A, Lopes da Fonseca T, Outeiro TF. Structure, function and toxicity of alpha-synuclein: the Bermuda triangle in synucleinopathies. *J Neurochem.* (2016) 139:240–55. doi: 10.1111/jnc.13249

51. Luo Y, Ma H, Zhou J-J, Li L, Chen S-R, Zhang J, et al. Focal cerebral ischemia and reperfusion induce brain injury through α2δ-1–bound NMDA receptors. *Stroke.* (2018) 49:2464–72. doi: 10.1161/STROKEAHA.118.022330

52. Deshmukh A, Leichner J, Bae J, Song Y, Valdés-Hernández PA, Lin W-C, et al. Histological characterization of the irritative zones in focal cortical dysplasia using a preclinical rat model. *Front Cell Neurosci.* (2018) 12:52. doi: 10.3389/fncel.2018.00052

53. Hagemann G, Kluska MM, Redecker C, Luhmann HJ, Witte OW. Distribution of glutamate receptor subunits in experimentally induced cortical malformations. *Neuroscience.* (2003) 117:991–1002. doi: 10.1016/S0306-4522(02)00959-4

54. DeFazio RA, Hablitz JJ. Alterations in NMDA receptors in a rat model of cortical dysplasia. *J Neurophysiol.* (2000) 83:315–21. doi: 10.1152/jn.2000.83.1.315

55. Ferreira DG, Temido-Ferreira M, Vicente Miranda H, Batalha VL, Coelho JE, Szegö ÉM, et al. α-synuclein interacts with PrPC to induce cognitive impairment through mGluR5 and NMDAR2B. *Nat Neurosci.* (2017) 20:1569–79. doi: 10.1038/nn.4648

56. Diógenes MJ, Dias RB, Rombo DM, Vicente Miranda H, Maiolino F, Guerreiro P, et al. Extracellular alpha-synuclein oligomers modulate synaptic transmission and impair LTP via NMDA-receptor activation. *J Neurosci.* (2012) 32:11750–62. doi: 10.1523/JNEUROSCI.0234-12.2012

57. Durante V, de Iure A, Loffredo V, Vaikath N, De Risi M, Paciotti S, et al. Alpha-synuclein targets GluN2A NMDA receptor subunit causing striatal synaptic dysfunction and visuospatial memory alteration. *Brain.* (2019) 142:1365–85. doi: 10.1093/brain/awz065

58. Navarria L, Zaltieri M, Longhena F, Spillantini MG, Missale C, Spano P. Alpha-synuclein modulates NR2B-containing NMDA receptors and decreases their levels after rotenone exposure. *Neurochem Int.* (2015) 86:14–23. doi: 10.1016/j.neuint.2015.03.008

59. Pirone A, Alexander J, Lau LA, Hampton D, Zayachkivsky A, Yee A, et al. conditional knock-out mouse is a model of infantile spasms with elevated neuronal β-catenin levels, neonatal spasms, and chronic seizures. *Neurobiol Dis.* (2017) 98:149–57. doi: 10.1016/j.nbd.2016.11.002

60. Bock T, Stuart GJ. The impact of BK channels on cellular excitability depends on their subcellular location. *Front Cell Neurosci.* (2016) 10:206. doi: 10.3389/fncel.2016.00206

61. Vekrellis K, Rideout HJ, Stefanis L. Neurobiology of α-synuclein. *Mol Neurobiol.* (2004) 30:1–21. doi: 10.1385/MN:30:1:001

62. Sharma M, Burré J. α-Synuclein in synaptic function and dysfunction. *Trends Neurosci.* (2023) 46:153–66. doi: 10.1016/j.tins.2022.11.007

63. Holm A, Karlsson T, Vikström E. Pseudomonas aeruginosa lasI/rhlI quorum sensing genes promote phagocytosis and aquaporin 9 redistribution to the leading and trailing regions in macrophages. *Front Microbiol.* (2015) 6:915. doi: 10.3389/fmicb.2015.00915

64. Zhang YT, Zhang YL, Chen SX, Yin GH, Yang ZZ, Lee S, et al. Proteomics of methyl jasmonate induced defense response in maize leaves against Asian corn borer. *BMC Genomics.* (2015) 16:224. doi: 10.1186/s12864-015-1363-1

65. Yang W-K, Kang C-K, Hsu A-D, Lin C-H, Lee T-H. Different modulatory mechanisms of renal FXYD12 for Na(+)-K(+)-ATPase between two closely related Medakas upon salinity challenge. *Int J Biol Sci.* (2016) 12:730–45. doi: 10.7150/ijbs.15066

66. Brás IC, Dominguez-Meijide A, Gerhardt E, Koss D, Lázaro DF, Santos PI, et al. Synucleinopathies: where we are and where we need to go. *J Neurochem.* (2020) 153:433–54. doi: 10.1111/jnc.14965

67. Martinelli AHS, Lopes FC, John EBO, Carlini CR, Ligabue-Braun R. Modulation of disordered proteins with a focus on neurodegenerative diseases and other pathologies. *Int J Mol Sci.* (2019) 20:1322. doi: 10.3390/ijms20061322

68. Busquets MA, Espargaró A, Estelrich J, Sabate R. Could α-synuclein amyloid-like aggregates trigger a prionic neuronal invasion? *Biomed Res Int.* (2015) 2015:172018. doi: 10.1155/2015/172018

69. Aisenbrey C, Borowik T, Byström R, Bokvist M, Lindström F, Misiak H, et al. How is protein aggregation in amyloidogenic diseases modulated by biological membranes? *Eur Biophys J.* (2008) 37:247–55. doi: 10.1007/s00249-007-0237-0

70. Murphy DD, Rueter SM, Trojanowski JQ, Lee VM-Y. Synucleins Are Developmentally expressed, and α-synuclein regulates the size of the presynaptic vesicular pool in primary hippocampal neurons. *J Neurosci.* (2000) 20:3214–20. doi: 10.1523/JNEUROSCI.20-09-03214.2000

71. Withers GS, George JM, Banker GA, Clayton DF. Delayed localization of synelfin (synuclein, NACP) to presynaptic terminals in cultured rat hippocampal neurons. *Brain Res Dev Brain Res.* (1997) 99:87–94. doi: 10.1016/S0165-3806(96)00210-6

72. Nguyen LH, Mahadeo T, Bordey A. mTOR hyperactivity levels influence the severity of epilepsy and associated neuropathology in an experimental model of tuberous sclerosis complex and focal cortical dysplasia. *J Neurosci.* (2019) 39:2762–73. doi: 10.1523/JNEUROSCI.2260-18.2019

73. Tozzi A, de Iure A, Bagetta V, Tantucci M, Durante V, Quiroga-Varela A, et al. Alpha-synuclein produces early behavioral alterations via striatal cholinergic synaptic dysfunction by interacting with glun2d n-methyl-d-aspartate receptor subunit. *Biol Psychiatry*. (2016) 79:402–14. doi: 10.1016/j.biopsych.2015.08.013

74. Ma Z, Liu K, Li X-R, Wang C, Liu C, Yan D-Y, et al. Alpha-synuclein is involved in manganese-induced spatial memory and synaptic plasticity impairments via TrkB/Akt/Fyn-mediated phosphorylation of NMDA receptors. *Cell Death Dis.* (2020) 11:834. doi: 10.1038/s41419-020-03051-2

75. Xuan Q, Xu S-L, Lu D-H, Yu S, Zhou M, Uéda K, et al. Increased expression of α-synuclein in aged human brain associated with neuromelanin accumulation. *J Neural Transm.* (2011) 118:1575–83. doi: 10.1007/s00702-011-0636-3

frontiers | Frontiers in Neurology

TYPE Original Research
PUBLISHED 30 November 2023
DOI 10.3389/fneur.2023.1282494

OPEN ACCESS

EDITED BY
Hua-Jun Feng,
Harvard Medical School, United States

REVIEWED BY
Shu Wang,
Capital Medical University, China
Yueqing Peng,
Columbia University, United States

*CORRESPONDENCE
Filiz Onat
✉ filiz.onat@acibadem.edu.tr

RECEIVED 24 August 2023
ACCEPTED 10 November 2023
PUBLISHED 30 November 2023

CITATION
Toplu A, Mutlu N, Erdeve ET, Sariyildiz Ö, Çelik M, Öz-Arslan D, Akman Ö, Molnár Z, Çarçak N and Onat F (2023) Involvement of orexin type-2 receptors in genetic absence epilepsy rats.
Front. Neurol. 14:1282494.
doi: 10.3389/fneur.2023.1282494

Involvement of orexin type-2 receptors in genetic absence epilepsy rats

Aylin Toplu[1,2], Nursima Mutlu[3], Elif Tuğçe Erdeve[4], Özge Sariyildiz[2], Musa Çelik[5], Devrim Öz-Arslan[2,5,6], Özlem Akman[7], Zoltan Molnár[8], Nihan Çarçak[2,9] and Filiz Onat[2,10]*

[1]Department of Medical Pharmacology, School of Medicine, Marmara University, Istanbul, Türkiye, [2]Department of Neuroscience, Health Sciences Institute, Acibadem Mehmet Ali Aydinlar University, Istanbul, Türkiye, [3]Department of Molecular Biotechnology and Genetics, Institute of Science, Istanbul University, Istanbul, Türkiye, [4]Department of Pharmacology, Health Sciences Institute, Istanbul University, Istanbul, Türkiye, [5]Department of Biophysics, Health Sciences Institute, Acibadem Mehmet Ali Aydinlar University, Istanbul, Türkiye, [6]Department of Biophysics, School of Medicine, Acibadem Mehmet Ali Aydinlar University, Istanbul, Türkiye, [7]Department of Physiology, Faculty of Medicine, Demiroglu Bilim University, Istanbul, Türkiye, [8]Department of Physiology, Anatomy and Genetics, University of Oxford, Oxford, United Kingdom, [9]Department of Pharmacology, Faculty of Pharmacy, Istanbul University, Istanbul, Türkiye, [10]Department of Medical Pharmacology, School of Medicine, Acibadem Mehmet Ali Aydinlar University, Istanbul, Türkiye

Introduction: Orexin is a neuropeptide neurotransmitter that regulates the sleep/wake cycle produced by the lateral hypothalamus neurons. Recent studies have shown the involvement of orexin system in epilepsy. Limited data is available about the possible role of orexins in the pathophysiology of absence seizures. This study aims to understand the role of orexinergic signaling through the orexin-type 2 receptor (OX2R) in the pathophysiology of absence epilepsy. The pharmacological effect of a selective OX2R agonist, YNT-185 on spike-and-wave-discharges (SWDs) and the OX2R receptor protein levels in the cortex and thalamus in adult GAERS were investigated.

Methods: The effect of intracerebroventricular (ICV) (100, 300, and 600 nmol/10 µL), intrathalamic (30 and 40 nmol/500 nL), and intracortical (40 nmol/500 nL) microinjections of YNT-185 on the duration and number of spontaneous SWDs were evaluated in adult GAERS. The percentage of slow-wave sleep (SWS) and spectral characteristics of background EEG were analyzed after the ICV application of 600 nmol YNT-185. The level of OX2R expression in the somatosensory cortex and projecting thalamic nuclei of adult GAERS were examined by Western blot and compared with the non-epileptic Wistar rats.

Results: We showed that ICV administration of YNT-185 suppressed the cumulative duration of SWDs in GAERS compared to the saline-administered control group ($p < 0.05$). However, intrathalamic and intracortical microinjections of YNT-185 did not show a significant effect on SWDs. ICV microinjections of YNT-185 affect sleep states by increasing the percentage of SWS and showed a significant treatment effect on the 1–4 Hz delta frequency band power during the 1–2 h post-injection period where YNT-185 significantly decreased the SWDs. OXR2 protein levels were significantly reduced in the cortex and thalamus of GAERS when compared to Wistar rats.

Conclusion: This study investigated the efficacy of YNT-185 for the first time on absence epilepsy in GAERS and revealed a suppressive effect of OX2R agonist on SWDs as evidenced by the significantly reduced expression of OX2R in the cortex and thalamus. YNT-185 effect on SWDs could be attributed to its regulation

of wake/sleep states. The results constitute a step toward understanding the effectiveness of orexin neuropeptides on absence seizures in GAERS and might be targeted by therapeutic intervention for absence epilepsy.

KEYWORDS

absence epilepsy, orexin type-2 receptor, spike-and-wave discharge, YNT-185, epilepsy

Introduction

Orexin-A and -B (hypocretins) which are the neuropeptides mainly derived from orexin-containing neurons in the hypothalamus play a crucial role in circadian rhythm and specifically mediating wakefulness in the sleep–wake system (1–4). Orexinergic neurons project to the cortex and virtually all subcortical arousal systems and exert their effects by binding to orexin type-1 (OX1R) and orexin type-2 receptors (OX2R) (2, 5). The orexinergic system has recently been investigated in the sleep-arousal network and disorders related to the sleep architecture, such as epilepsy (6, 7). Limited evidence is available about the possible role of the orexinergic system in the pathophysiology of generalized epilepsies (8, 9). Therefore, the orexinergic system has become the focus of much attention for its possible involvement in the modulation of genetic generalized epilepsies. It has also been stated that convulsive seizures can be reduced by improving sleep quality by using orexin antagonists (10). Absence epilepsy occupies a prominent position in genetic generalized epilepsies since absence seizures are quite common, accounting for 10–17% of all cases of epilepsy diagnosed in children (11, 12). Spontaneous spike-and-wave discharges (SWDs), a pathognomonic feature of the EEG in typical absence seizures of absence epilepsy, start and end abruptly on a normal EEG background in a state of quiet wakefulness (13, 14). It has recently been shown that OX1R protein levels are significantly lower in the thalamus and the somatosensory cortex of adult genetic absence epilepsy rats from Rijswijk (WAG/Rij model) that is well-validated and commonly used genetic model of absence epilepsy (15).

Despite this initial work, the link between orexinergic signaling and absence epilepsy remains to be demonstrated. In order to better understand the link between orexinergic system and absence seizures, further studies involving other models of absence epilepsy are required. The other genetic model including naturally occurring mutations in rats from Strasbourg (GAERS), serves as a model for the approach to experimental and translational paths to the understanding of absence seizures and absence epileptogenesis (16). Revealing the role of the orexinergic system in GAERS will help solidify the knowledge in the field of absence epilepsy. In addition, the function of OX2R in the epileptogenesis of absence seizures and the *in-vivo* effects of orexin ligands on absence seizures in genetic absence epilepsy models are still unknown. Clarification of these issues will further contribute to a better understanding of the pathophysiological mechanisms of generalized genetic epilepsies related to sleep–wakefulness states.

Here we investigated whether orexinergic transmission through OX2R modulates absence seizures in rats with absence epilepsy namely GAERS. First, we demonstrated the pharmacological effect of the OX2R agonist, YNT-185, applied by intracerebroventricular (ICV) or intraparenchymal microinjections in adult GAERS. We also examined the effect of YNT-185 on slow-wave sleep (SWS) and conducted spectral analysis of EEG. Finally, we investigated the OX2R receptor protein levels by immunoblotting in the cortex and thalamus of adult GAERS and compared them with adult non-epileptic Wistar rats.

Materials and methods

Animals

Experiments were performed in adult (3–4 months old), 300–350 g male GAERS and Wistar rats. The experiments were performed in Acibadem Mehmet Ali Aydinlar University, *Laboratory Animal* Application and *Research Center* (ACU-DEHAM). Animals were kept within cycles of 12 h in light, 12 h in dark environment, and with a room temperature of 22–24°C. This study was approved by the Acibadem University Ethical Committee for Experimental Animals (ACU-HADYEK) conforming with the EU Directive 2010/63/EU for animal experiments (HDK-2022/36).

Stereotaxic surgery

Animals were anesthetized using inhalation isoflurane (2.5–3%, the flow rate of oxygen was ˜0.8 L/min) anesthesia and placed into a stereotaxic instrument (Stoelting Model 51,600, Stoelting Co. Illinois, USA). For ICV microinjections, a stainless-steel guide cannulla (C313G; Plastics One, Roanoke, VA, USA) was implanted unilaterally according to the coordinates from the atlas of Paxinos and Watson (17) (AP: −1.0 mm, ML: −1.4 mm, DV: 4.1 mm from bregma). For intraparenchymal microinjections, stainless steel guide cannulas (C315G; Plastics One, Roanoke, VA, USA) were implanted bilaterally targeting ventrobasal complex of thalamus (VB) or somatosensorial cortex (S1) according to the coordinates from the atlas of Paxinos and Watson (17) (VB coordinates: AP: −3.2 mm, ML: ±4.8 mm, DV: 5.5 with an angle of 16°; S1 coordinates: AP: −2.1 mm, ML: ±5.5 mm, DV: 3.5 mm from bregma). EEG recording electrodes were implanted bilaterally over the fronto-parietal cortices. Dental acrylic was used to protect each implant onto the skull. A stainless-steel dummy was also inserted into the guide cannulas until the microinjection. Following the surgery, the animals were returned to their cages for routine care as single animals per cage, and allowed to recover for one week before the EEG recordings. The experimental design is

presented in Supplementary Figure S1, and was created by using BioRender.com.

Intracerebral microinjections

After a 1-week recovery period, each animal was placed in a plexiglass recording chamber and habituated for 40 min. Then a 3-h baseline EEG (from 9 a.m. to 12 p.m.) was recorded from GAERS in order to confirm the occurrence of typical absence seizures after stereotaxic surgery. The next day, an internal cannula for ICV or intraparenchymal (VB or S1) was inserted into the guide cannula, extending 1 mm below the tip of the guide. Then the different doses of YNT-185 solution or an equal volume of sterile saline (%0.9 NaCl) were delivered via a microinfusion pump (at a rate of 10 µL/5 min for ICV or at a rate of 500 nL/5 min for intraparenchymal microinjections). EEG was recorded for 180 min after the microinjections. The cumulative seizure duration, number of seizures, and duration of individual seizures were analyzed and compared among the groups.

EEG recording and analysis

EEG was amplified through a BioAmp ML 136 amplifier, with band pass filter settings at 1–40 Hz, recorded and analyzed using Chart v.8.1 program (PowerLab8S ADI Instruments, Oxfordshire, UK). The total time spent in seizure, and the number and duration of individual seizure were evaluated. In both the baseline recording and the recording after administration, only SWD complexes with a train of SWD (7–11 Hz) and an amplitude at least twice that of the background EEG were found at periods longer than 1 s and were assessed (See Supplementary Figure S2). The cumulative seizure duration, the number of seizures, and the duration of individual seizures (duration of each SWD) were evaluated in the EEG recording taken over 3 h.

Slow-wave sleep scoring and spectral analysis of background EEG

EEG sleep scoring and spectral analysis were conducted in a blinded manner by a neurophysiologist. EEG segments showing slow frequencies in the EEG background, including high-amplitude delta waves, were categorized as slow-wave sleep (SWS) following previously established criteria (18). Due to the absence of video and electromyographic recordings, it was not possible to score active wakefulness, passive wakefulness, and REM states. The percentage of SWS was quantified in both the 600 nmol/10 µL ICV YNT-185 group, in which YNT-185 significantly suppressed SWDs, and the saline-treated vehicle group. The 3-h EEG recordings following YNT-185 or saline administration were compared to baseline EEG EEG recordings obtained one day before the injections in each group. To confirm the SWS scores obtained from EEG recordings of the 600 nmol/10 µL-YNT-185 group, in which YNT-185 significantly increased SWS, and to evaluate other frequency changes due to YNT-185 administration, the spectral characteristics of the background EEG were analyzed by computing the power spectra using fast Fourier transform (FFT; MATLAB 9.5, MathWorks), as previously described (19). To assess the effects of YNT-185 on EEG characteristics, we analyzed 0–1 h, 1–2 h, and 2–3 h post-injection EEG data from the right cerebral cortex of animals and compared it to its baseline EEG recordings. FFT was performed on 2000 randomly picked artifact-free epochs of 2-s duration of background EEG, without any SWD pattern, tapered with a Hamming window, and a frequency resolution of 0.5 Hz. The absolute power spectra were divided into 1–4 Hz (delta), 4.5–8 Hz (theta), 8.5–13 Hz (alpha), 13.5–30 Hz (beta) frequency bands, and the mean power for each of these frequency bands was computed.

Histological verification

The location of each cannula was confirmed by histological verification. After the EEG recordings, the location of the ICV cannula was confirmed by anesthetizing each rat, inserting a needle into the guide cannula, and injecting 10 µL of 1% methylene blue into the lateral ventricle. The needle was kept at the injection site for at least 60 s before removal. After decapitation, the brain was removed, and the traces of methylene blue were inspected to determine the sites of ICV injection.

For the VB or S1 groups, after the recordings, the rats were decapitated under anesthesia, and their brains were isolated and placed in a 30% formalin-sucrose mixture. Frozen sections were cut at 40 µm on a cryostat (Thermo Fisher, Cryotome™ FSE Cryostats, FE Model, 230 V 50 Hz) and stained with thionin for light microscopic examination of injection sites according to Paxinos and Watson rat brain atlas (Figures 1D, 2D and 3D). Only animals with correctly placed cannulas were included in this study.

Western blot

The cortex and thalamus tissues were dissected and then immediately snap-freezed using liquid nitrogen. The dissected tissues were stored at −80°C until protein extraction. The tissues were homogenized in the ice-cold RIPA lysis buffer (50 mM Tris–HCl, pH 7.4, 150 mM NaCl, 1% NP-40, 0.25% sodium deoxycholate, 1 mM EDTA, 1 mM PMSF, 1 mM sodium orthovanadate, 1 mM sodium fluoride with 1X protease inhibitor cocktail) using a tissue Dounce homogenizer. The homogenized samples were then sonicated by Omni Ruptor 4,000 sonicator approximately for 1 s. The lysates were centrifuged at 14.000Xg for 15 min at 4°C to collect the supernatants. The concentration of extracted protein was quantified using Bradford protein assay (Bio-Rad, USA), and 20 µg of protein from each sample was separated by 10% SDS-polyacrylamide gel electrophoresis, then transferred to a nitrocellulose membrane using a semi-dry transfer system (40 min, 25 V) (Bio-rad, Transblot). The membranes were incubated with 5% bovine serum albumin for 1 h at RT. Afterward, the membranes were incubated with primary antibodies against OX2R (1:1000, Thermo Fisher Scientific, USA), and β-actin (1,10.000, Thermo Fisher Scientific, USA) overnight at 4°C. The membrane was rinsed three times with TBS-T for 10 min., and then probed with appropriate secondary antibodies 1:5000 (Rabbit for OX2R and mouse for β-actin) for 1 h at RT and then washed three times with TBS-T for 10 min. The protein bands were visualized by an enhanced chemiluminescence reagent (SuperSignal™ West Femto Maximum Sensitivity Substrate, Thermo Scientific, USA). Finally, the relative

10.3389/fneur.2023.1282494

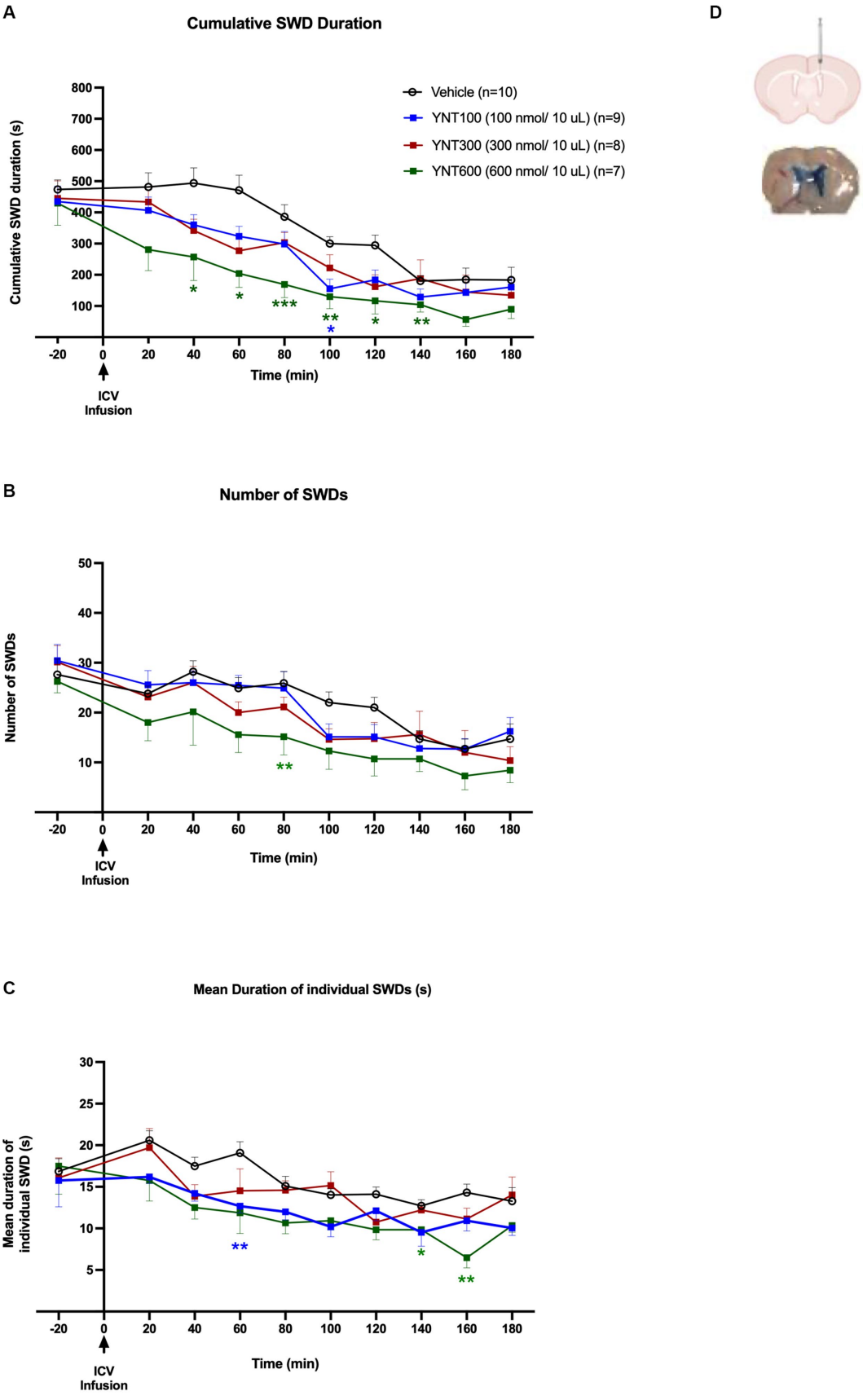

FIGURE 1 (Continued)

FIGURE 1 (Continued)
Effect of the ICV administration of YNT-185 on SWDs. The impact of ICV injection of 100nmol/10μL (n=9), 300nmol/10μL (n=8), or 600nmol/10μL (n=7) of YNT-185 or saline (n=11) on the cumulative seizure duration **(A)**, the number of seizures **(B)**, and the mean duration of individual seizures in adult GAERS **(C)**. 600nmol/10μL of YNT-185 induced a significant decrease in SWD duration, number and mean duration of starting within the 40min post-injection period (See Supplementary Figure S2 for representative EEG traces from 600nmol/10μL of YNT-185 and saline injected GAERS). Data expressed as mean±SEM. (*p<0.05, **p<0.01, *** p<0.001). Inset figure shows the traces of methylene blue determining the sites of ICV injection **(D)**.

densities of the protein bands were analyzed by Image Lab software (Bio-Rad, USA).

Data analysis

Statistical analysis was performed using the GraphPad Prism version 9.0.1 program. The effect of YNT-185 on SWDs: (1) The cumulative seizure duration (2) the number of seizures and (3) the duration of individual seizures were compared by two-way analysis of (Two factors: "Treatment and Time") variance (ANOVA) using Tukey's multiple comparison test. The relative expression of OX2R protein bands were quantified by ImageLab software. Unpaired t test was used to compare the ratio of OX2R to actin levels in the brain tissues. For statistical analysis of the percentage of SWS in the 600 nmol YNT-185 injection and control groups compared to their baseline EEG values, a repeated-measures analysis of variance (ANOVA) design with two factors, "time" and "treatment," followed by the Bonferroni test, was used. For the comparison of spectral characteristics of the 600 nmol YNT-185 injection group, a repeated-measures ANOVA design with two factors, "treatment" and "frequency bands" was applied to the mean powers in the four frequency bands. Data were presented as mean ± S.E.M. *$p < 0.05$ is considered significant.

Results

Effect of intracerebroventricular (ICV) microinjections of YNT-185 on SWDs

In the first group of the experiments, we investigated the effect of ICV injection of 100 nmol/10 μL ($n = 9$), 300 nmol/10 μL ($n = 8$), or 600 nmol/10 μL ($n = 7$) of YNT-185 or saline ($n = 11$) on absence seizures in GAERS (Figures 1A–C). ICV injection of YNT-185 markedly reduced cumulative SWD duration in adult GAERS compared to saline injected vehicle group [$F(3, 30) = 14.07$; $p < 0.0001$]. Tukey's multiple comparison tests revealed that 600 nmol/10 μL of YNT-185 induced a significant decrease in SWD duration starting from the 40 min post-injection until the 140th min post-injection period ($p < 0.001$; Figure 1A). Representative EEG traces from 600 nmol/10 μL of YNT-185 and saline-injected GAERS clearly demonstrate the YNT-185 effect on SWDs (Supplementary Figure S2). 100 nmol/10 μL of YNT-185 induced a significant decrease in the duration of SWDs at 100 min post-injection ($p = 0.01$; Figure 1A). ICV injection of YNT-185 produced a significant effect also on SWD number [$F(3, 30) = 3.29$; $p = 0.03$]. 600 nmol/10 μL of YNT-185 significantly decreased the number of SWDs at 80 min post-injection period (Figure 1B; $p < 0.01$). The mean duration of each SWD was also affected by the ICV injection of YNT-185 [$F(3, 30) = 8.656$; $p = 0.0003$]. 100 nmol/10 μL of YNT-185 significantly decreased the mean duration of SWDs at 60 min post-injection period ($p < 0.01$); this effect was observed at 140–160 min of post-injection period for 600 nmol/10 of YNT-185 injected group (Figure 1C). Interestingly, the dose of 300 nmol did not produce any statistically significant effect on cumulative SWD duration, number of SWDs, and mean duration of each SWD (Figures 1A–C). These results suggest that the inhibitory effect of YNT-185 on SWDs may not correlated with the doses of OX2R agonist YNT-185.

Thereafter, intraparenchymal doses correspond to the doses where the most pronounced effect is observed in ICV administration. So, we administered the OX2R agonist, YNT-185 intraparenchymally at the doses (either 30 or 40 nmol/500 nL) at which its effect on SWDs was most pronounced when administered ICV (600 nmol/10 μL).

Effect of intrathalamic microinjections of YNT-185 on SWDs

In the second group, the effect of bilateral VB injection (for both complexes simultaneously) of YNT-185 on absence seizures was evaluated. GAERS received bilateral VB injections of either 30 nmol/500 nL ($n = 6$), 40 nmol/500 nL ($n = 7$) of YNT-185, or 500 nL saline (0.9% NaCl solution) ($n = 7$) (Figures 2A–C). Intrathalamic microinjections of YNT-185 slightly reduced the SWDs (both duration and number) on the EEG but this effect was not statistically different between groups ($p > 0.05$; Figures 2A–C). In the 40 nmol/500 nL YNT-185 injected group, this decrease in SWD duration was significant in the 60 min post-injection period compared to vehicle as revealed by Tukey's multiple comparison test ($p = 0.04$; Figure 2A). The cumulative duration, number, and mean duration of SWDs did not differ across groups (Figures 2A–C). The number of SWDs on the EEG was slightly reduced in the 40 nmol/500 nL YNT-185 injected group at 60 min post-injection, but this effect was not statistically different ($p > 0.05$; Figure 2B).

Effect of intracortical microinjections of YNT-185 on SWDs

In the third group, we examined the effect of bilateral S1 injection of YNT-185 on SWDs in GAERS. GAERS were administered bilateral S1 injections of 40 nmol/500 nL ($n = 6$) of YNT-185 or 500 nL saline (0.9% NaCl solution) ($n = 6$). There was no statistically significant effect of YNT-185 injected bilaterally into the S1 on SWDs compared to vehicle, including the cumulative SWD duration the number of SWDs, and the mean duration of SWDs on the EEG ($p > 0.05$; Figures 3A–C).

Effect of YNT-185 on slow-wave sleep and spectral characteristics of background EEG

To determine whether YNT-185 affects sleep states in GAERS, we examined the spectral characteristics of EEG recorded from the 600 nmol ICV YNT-185 group, where YNT-185 strongly suppressed

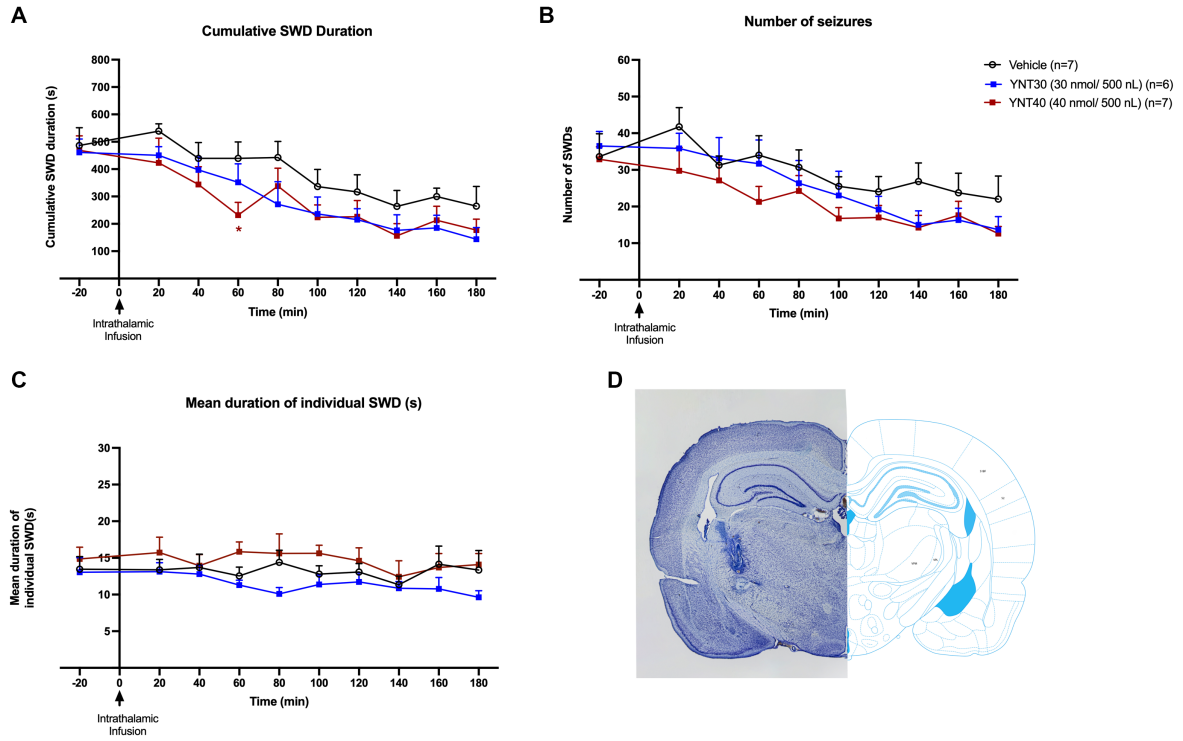

FIGURE 2
Effect of bilateral VB administration of YNT-185 on SWDs. The impact of YNT-185 injection into the bilateral VB injections of either 30 nmol/500 nL ($n = 6$), 40 nmol/500 nL ($n = 8$) of YNT-185, or 500 nL saline (0.9% NaCl solution) ($n = 7$) on the cumulative seizure duration **(A)**, the number of seizures **(B)**, and the mean duration of individual seizures **(C)**. Intrathalamic microinjections of YNT-185 did not produced any statistically significant effect on SWDs ($p > 0.05$). Data expressed as mean ± SEM. Inset figure shows the traces of bilateral guide cannula traces placed over the VB on thionine stained coronal sections **(D)**.

the SWDs. We scored slow-wave sleep (SWS), characterized by the occurrence of high amplitude delta waves in the EEG. The percentage of SWS during the post-injection period in the YNT-185 group was higher than those in baseline EEG recordings [Treatment effect: $F(1, 12) = 8.509$, $p = 0.0129$; Figure 4A]. The post-hoc Bonferroni test showed that this difference was due to a higher percentage of SWS during the 1-2 h post-injection periods ($p < 0.01$). The saline injection administered to the vehicle group did not result in any alterations in the percentage of SWS when compared to that observed in its baseline EEG recordings [Treatment effect: $F(1, 16) = 0.002$, $p = 0.96$; Figure 4B]. The spectral characteristics of EEG recorded from the 600 nmol ICV YNT-185 group, in which YNT-185 strongly suppresses SWDs, showed a significant treatment effect on the EEG band powers [$F(1, 12) = 5.135$; $p = 0.0427$] during the 1–2 h post-injection period (Figures 4E,F). Post-hoc Bonferroni test revealed that this difference was due to higher power in the delta band following YNT-185 injection ($p < 0.01$). No difference was observed in terms of band powers during 0–1 h or 2–3 post-injection periods [Treatment effect: $F(1, 12) = 0.0505$, $p = 0.8260$; $F(1, 12) = 1.928$, $p = 0.1902$, respectively; Figures 4C,D,G,H].

OX2R protein levels in the cortex and thalamus

The cortex and thalamus tissues of male adults (3 months old) and age-matched Wistar rats were dissected and then the protein levels of OX2R were evaluated by western blot analysis in the cortex and thalamus of GAERS and Wistar rats. According to human protein atlas data, the cerebellum has the highest OX2R level.[1] Therefore we used the cerebellum as positive control (Figures 5A,B). We demonstrated that the OX2R protein levels in GAERS were significantly lower than in Wistar rats in the cortex ($p = 0.048$; Figure 5A) and thalamus ($p = 0.012$; Figure 5B).

Discussion

The present study demonstrates that ICV microinjection OX2R agonist YNT-185 significantly reduces the incidence of SWDs in GAERS. In contrast, intrathalamic and intracortical administration of YNT-185 did not produce a significant effect on SWDs, whereas the dose range for parenchymal injection has been selected in accordance with the ICV administration. Further, the highest dose of YNT-185 administrated into the lateral ventricle resulted in a significant increase in the percentage of SWS and 1–4 Hz delta frequency band on the EEG during the 1–2 h post-injection period in which YNT-185 significantly suppressed absence seizures (SWDs). These findings imply that the effect of YNT-185 on SWDs could be related to its modulation of wake/

1 https://www.proteinatlas.org/ENSG00000137252-HCRTR2/tissue

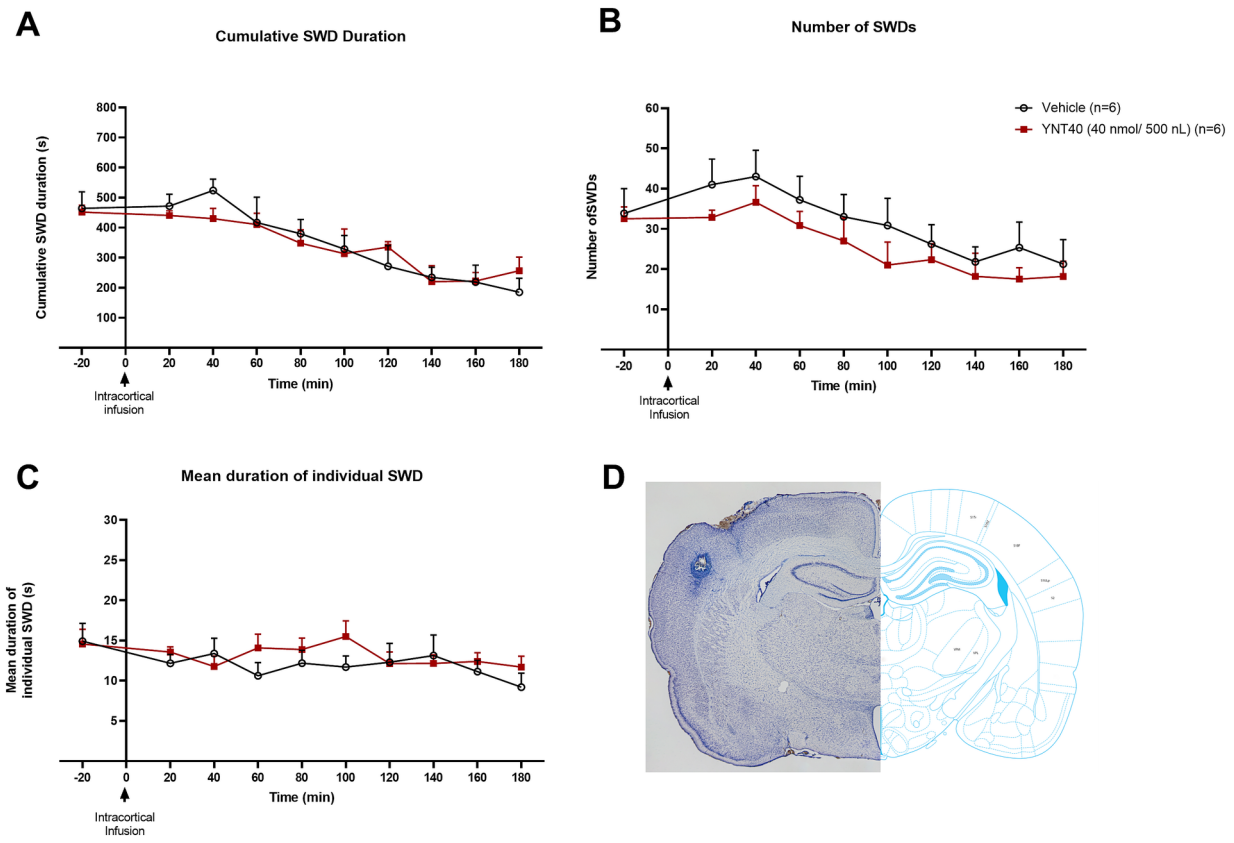

FIGURE 3
Effect of bilateral S1 administration of YNT-185 on SWDs. The impact of YNT-185 injection into the bilateral S1 injections of 40nmol/500nL (n=6) of YNT-185 or 500nL saline (0.9% NaCl solution) (n=6) on the cumulative seizure duration **(A)**, the number of seizures **(B)**, and the mean duration of individual seizures **(C)**. There was no statistically significant effect of YNT-185 injected bilaterally into the S1 on SWDs compared to vehicle (p>0.05). Data expressed as mean±SEM. Inset figure shows the traces of bilateral guide cannula traces placed over the S1 on thionine stained coronal sections **(D)**.

sleep states. In addition, OX2R expressions in the cortex and thalamus of adult GAERS were significantly lower with respect to Wistar rats. The results suggest that OX2R signaling can be related to the occurrence of SWDs and might play a role in the pathophysiology of absence epilepsy.

There is limited research on the involvement of orexinergic signaling in genetic generalized epilepsies. OX1R protein levels were reduced in the thalamus and somatosensory cortex of adult WAG/Rij rats compared to non-epileptic controls, whereas these differences were not seen in 25 days-old WAG/Rij rats those SWDs were not observed yet (15). These findings lead to the hypothesis that the age-dependent development of SWDs was associated with a down-regulation of orexin protein level in the thalamocortical network and orexin agonists can reduce the incidence of SWDs. Supporting that, our results confirmed that ICV microinjection of OX2R agonist YNT-185 reduced the incidence of SWDs in adult GAERS with reduced OX2R protein levels in the cortex and thalamus. In all, it seems that the thalamocortical circuit underlying the generation of SWDs is characterized by a dysregulation of orexins and/or orexin receptors in genetic absence epilepsy rat models and contributes to the pathogenesis of absence epilepsy. As with OX1R in WAG/Rij rats, it is important to investigate whether or not OX2R expression in GAERS is age-dependent (15). Therefore, to gain a better understanding of the relationship between orexinergic signaling and the development of SWD, age-related changes in OX2R expression in GAERS need to be demonstrated.

Research from animal models of epilepsy indicates that orexins show a proconvulsive effect and are deleterious to the pathophysiology of epilepsy. As a result, blocking orexin receptors and/or downregulation of orexin levels can attenuate seizure activity in various epilepsy models (9, 10, 20, 21). However, a few studies on animals have indicated the opposite: orexins were found to reduce epileptic activity *in-vitro* (22) and have a beneficial effect in reducing the learning and memory impairments in PTZ-kindled epilepsy rats (23). As presented here, orexin agonists might have also a beneficial effect in alleviating absence seizures. Consequently, the goal of future research should be to identify the causes of these discrepancies in orexin effects in different epilepsy models.

Absence seizures, sleep, and orexin signaling

The main function of orexinergic signaling is to regulate sleep–wake states (24) and its deficiency is associated with narcolepsy (25, 26). Consistently, OX2R agonist YNT-185 ameliorates narcolepsy

10.3389/fneur.2023.1282494

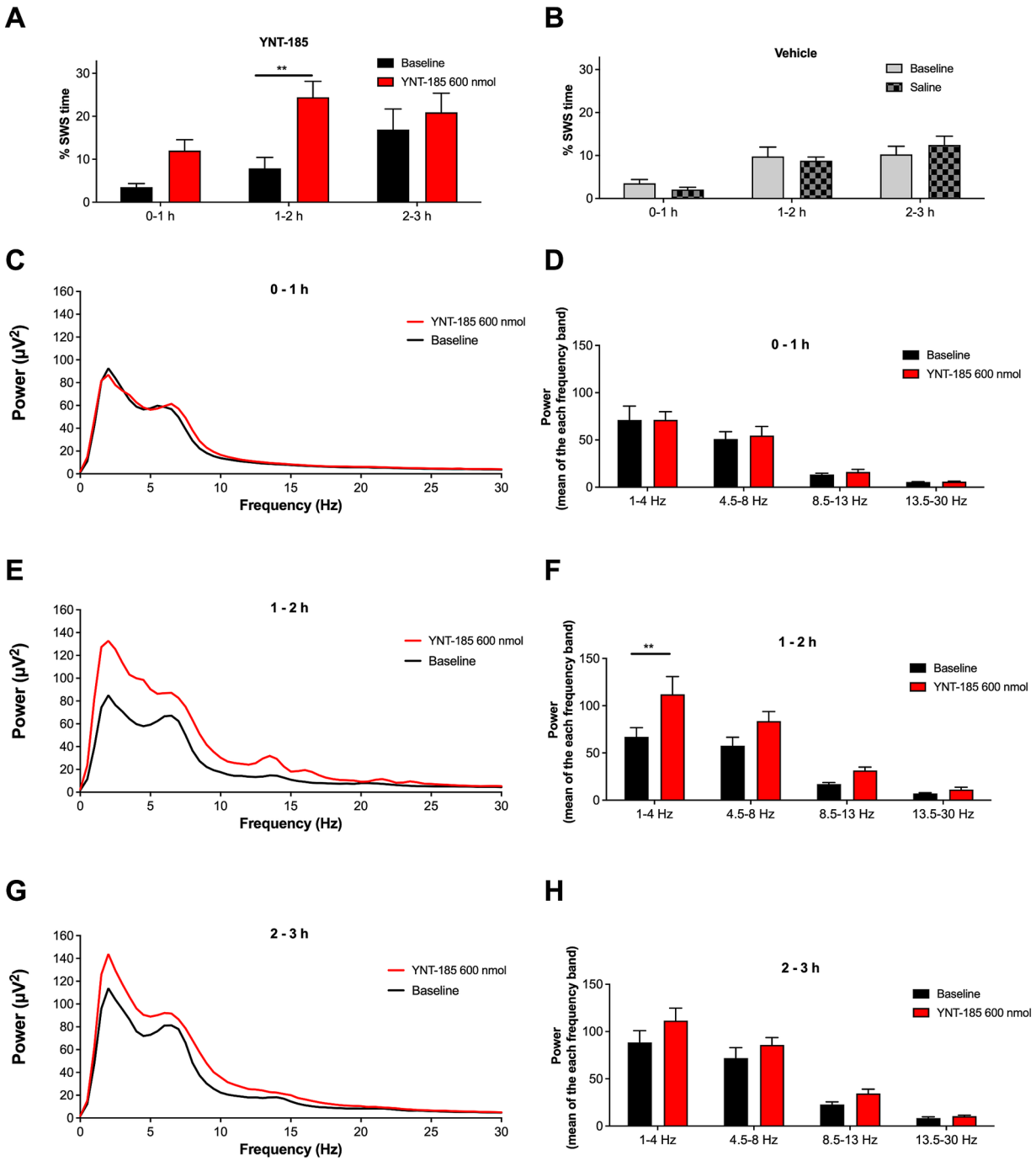

FIGURE 4
Effect of YNT-185 on percentage of slow-wave sleep and spectral characteristics of background EEG. Rats administered with 600 nmol of YNT-185 showed a significant increase in the time spent in SWS during the 1–2 h post-injection period compared to their baseline EEG recordings **(A)**. The saline injection in vehicle group did not affect the percentage of SWS when compared to that in their baseline EEG recordings **(B)**. The absolute power spectra of the EEG obtained 0-to 1 h, 1-to 2 h and 2- to 3 h post injection period in 600 nmol ICV YNT-185 group **(C,E,G)**. The mean power for delta, theta, alpha, and beta bands during 0-to 1 h, 1-to 2 h and 2- to 3 h post injection period **(D,F,H)**. Repeated measures analysis of variance test revealed significant effect of the treatment on the delta band power of the EEG frequency spectrum. Data expressed as mean ± S.E.M. $^{**}p < 0.01$. 600 nmol ICV YNT-185 ($n = 7$ rats); vehicle ($n = 10$ rats).

symptoms and markedly increases wakefulness time in mice in a mouse model of narcolepsy (27). In mice, activation of orexin neurons causes a significant increase in wakefulness and a decrease in sleep time, including both REM and NREM sleep (28). The relationship between sleep and absence epilepsy has been widely investigated. It has been shown that a well-documented relationship exists between SWDs and the vigilance level (29, 30). When emerging from wakefulness, absence seizures usually occur during the transition

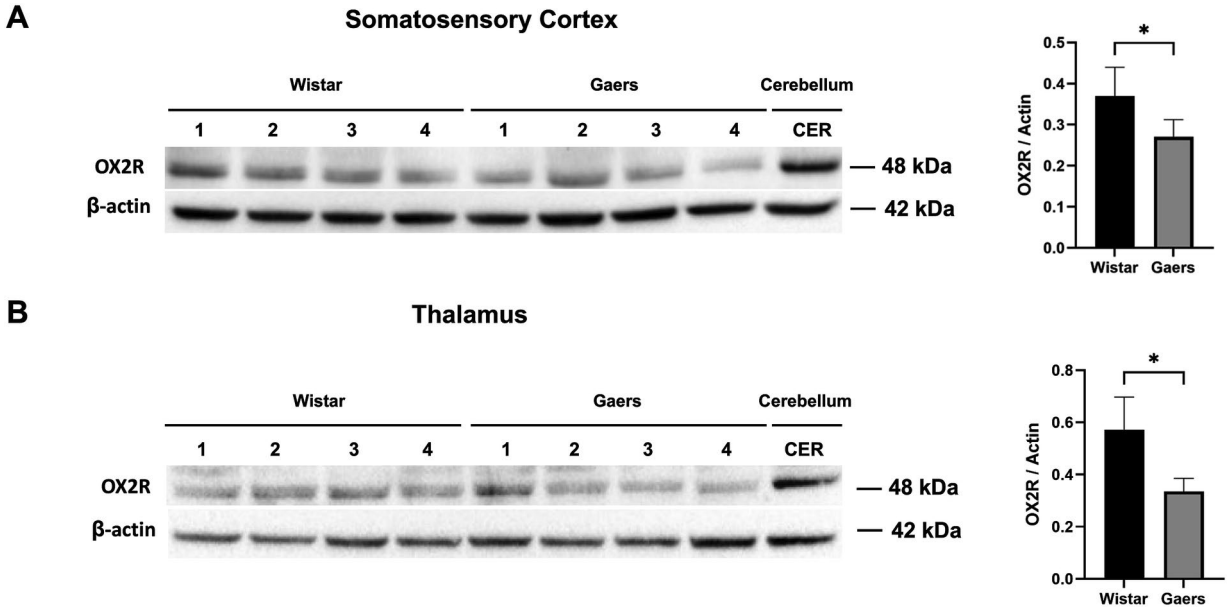

FIGURE 5
Western blot analysis of OX2R protein levels. Western blot analysis of OX2R expression in somatosensory cortex **(A)** and thalamus **(B)** of adult naïve GAERS and Wistar rats. Relative expression of OX2R protein bands in were quantified by ImageLab software. Bar graphs on the right show that OX2R protein levels in GAERS ($n = 4$) was significantly lower than Wistar rats ($n = 4$) in cortex and thalamus. Actin was used for internal loading control. The ratio of OX2R to actin levels was represented as bar graphs. Data expressed as mean ± S.E.M. (*$p < 0.05$, unpaired t test).

between wakefulness and sleep, less often during high arousal states such as physical and engaging mental activity (31). SWDs are absent during deep slow-wave sleep and REM sleep in both people with genetic generalized epilepsy and in the genetic models (32, 33). Supporting this evidence, our results indicated a significant increase in the percentage of SWS and 1–4 Hz delta frequency band on the EEG. These findings imply that the anti-absence effect of YNT-185 observed in GAERS might be related to its regulatory effect on sleep–wake states. It is also important to note here that, in rodent models of genetic absence epilepsy there is a natural course of SWDs being a relatively higher number at the beginning of the light phase of the 12:12 light–dark and decreases over time (31). This phenomenon was also noted here, where a tendency to decrease SWDs over time was seen in all experimental groups including vehicle. In further studies, the possible reasons for this pattern and the effect of orexinergic ligands on sleep–wake states in genetic generalized epilepsies need to be clarified.

In contrast to ICV results, intrathalamic and intracortical microinjections of YNT-185 did not produce such a significant effect on SWDs. The dose of 600 nmol of ICV YNT-185 on SWDs in GAERS produced the most pronounced effect whereas the lower doses of 100 and 300 nmol did not lead to any significant effect on SWDs, suggesting that the inhibitory effect of YNT-185 on SWDs may not be positively correlated with its concentration. A better elucidation of YNT-185's impact on target brain regions especially to comprehend the YNT-185 concentrations in cerebrospinal fluid, receptor binding profile, and efficacy is needed in further *in vitro* studies. Moreover, the involvement of other brain regions in which the OX2Rs are highly expressed such as the hypothalamus needs to be explored in terms of YNT-185 efficacy on SWDs.

Limited studies have reported the excitatory actions of orexins on non-specific thalamic nuclei namely some intralaminar and midline thalamic nuclei but do not alter the membrane properties of neurons in primary sensory ("first-order") or higher-order thalamic nuclei including VB (34, 35). Excitatory action of orexins is likely mediated via direct OX2R activation that has a greater expression in the thalamus compared to OX1R or indirectly by activating wake-promoting pathways projecting to the thalamus (34–36). In this study, the microinjections were administrated into the VB complex of the thalamus, which may be the reason that no significant effect on SWDs was observed. Another reason could be the reduced OX2R expression observed in the cortex and thalamus of adult GAERS. On the other hand, the intralaminar nuclei which are likely mediated via OX2R activation have also been implicated to play a role in the SWDs in animal models of absence epilepsy (37, 38). Thus, it appears that neuronal activity within the thalamocortical circuitry is differentially excited by orexins. Further pharmacological experiments on genetic models investigating the modulatory role of orexin in different non-specific thalamic nuclei may elucidate the structures underlying the absence seizure modulatory effect of orexin signaling.

The somatosensory cortex (S1) extends widely from anterior to posterior. It is most probable that the intracortical injection in our study only targets one place per hemisphere, or a small percentage of the entire S1 as observed in Figure 3. For that reason, YNT's impact on SWDs might be lessened. As a result, the observations in our study however cannot rule out the idea that OX2R in S1 regulates absence seizures. Deep cortical layers of S1 critically involved in the generation and maintenance of SWDs have been found to be sensitive to orexin (34, 39) and selectively projecting to the thalamus. In order to better understand the function of orexinergic activity in S1, it is important

to explore the possibility of using pharmacological and genetic manipulations of deep cortical layers to modify the absence phenotype. These manipulations should be tested in absence epilepsy models.

Interaction of hypothalamic orexin signaling and thalamocortical circuitry

We still need to understand whether this modulatory effect of orexin signaling mediation is on the cortical or subcortical level. Since orexin neurons are localized in the lateral hypothalamus and have extensive intracortical and thalamic projections in the rodent brain, the possible interaction of hypothalamic orexin signaling and thalamocortical circuitry involving essentially the cortex and thalamus that correlate with spindles, delta waves, and SWDs (40) needs to be addressed here. Thalamocortical cell firing is largely controlled by the thalamic reticular nucleus (TRN), which is a thin sheet of GABAergic cells exerting a strong inhibition control over thalamocortical relay cells (41). The neuronal activity of TRN cells is also directly modulated by extra-thalamic GABA inputs, and sleep–wake neuromodulators including orexin (41, 42). GABAergic neurons in the lateral hypothalamus (LH), a brain area consisting of neurochemically heterogeneous neuronal populations implicated in the modulation of arousal, selectively inhibit TRN neurons and promote wakefulness (43). The LH also receives prominent cortical projections from the medial prefrontal and orbitofrontal cortices (44, 45). SWDs have been recorded in the lateral hypothalamus of Wistar rats (46) and the hypothalamic activation during stage 2 kindling in the genetic absence epilepsy rat model (GAERS) was significantly higher compared to non-epileptic control rats (47). Supporting these findings, single unit recordings from the LH during spontaneous SWDs in freely moving GAERS rats showed that the neuronal activity in the LH is decreased and correlated during SWDs (48). These results clearly implicate that the hypothalamic signaling and thalamocortical circuitry interact and modulate each other on the level of arousal and absence seizures.

Conclusion

Present results revealing a suppressive effect of OX2R agonist on SWDs and an increase in sleep activity together with a significantly reduced expression of OXR2 in the thalamus and cortex in GAERS provide direct evidence about the involvement of orexin signaling as a potential player in the pathophysiology of absence epilepsy. However, the inhibitory effect of YNT-185 on SWDs seems not to be correlated with the doses of YNT-185. The findings contribute to a better knowledge of the effectiveness of orexin neuropeptides in GAERS absence seizures, which could be targeted by therapeutic intervention for absence epilepsy.

Data availability statement

The raw data supporting the conclusions of this article will be made available by the authors, without undue reservation.

Ethics statement

The experiments were performed in Acibadem Mehmet Ali Aydinlar University, Laboratory Animal Application and Research Center (ACU-DEHAM, HDK-2022/36). The study was conducted in accordance with the local legislation and institutional requirements.

Author contributions

AT: Writing – review & editing, Data curation, Methodology, Software. NM: Data curation, Methodology, Writing – review & editing. EE: Data curation, Methodology, Writing – review & editing. ÖS: Data curation, Methodology, Writing – review & editing. MÇ: Data curation, Methodology, Writing – review & editing. DÖ-A: Data curation, Methodology, Writing – review & editing. ÖA: Data curation, Methodology, Writing – review & editing. ZM: Writing – review & editing, Conceptualization. NÇ: Conceptualization, Formal analysis, Funding acquisition, Investigation, Project administration, Supervision, Writing – original draft, Writing – review & editing. FO: Conceptualization, Funding acquisition, Investigation, Project administration, Supervision, Writing – original draft, Writing – review & editing, Resources, Visualization.

Funding

The author(s) declare financial support was received for the research, authorship, and/or publication of this article. This study was supported by European Commission Horizon Europe Programme under the call HORIZON-WIDERA-2021-ACCESS-03 (grant number 101078981 – GEMSTONE) and Acibadem University Scientific Research Projects Commission (ABAPKO; 2022/02-26).

Conflict of interest

The authors declare that the research was conducted in the absence of any commercial or financial relationships that could be construed as a potential conflict of interest.

The author(s) declared that they were an editorial board member of Frontiers, at the time of submission. This had no impact on the peer review process and the final decision.

Publisher's note

Supplementary material

The Supplementary material for this article can be found online at: https://www.frontiersin.org/articles/10.3389/fneur.2023.1282494/full#supplementary-material

References

1. Dyer CJ, Touchette KJ, Carroll JA, Allee GL, Matteri RL. Cloning of porcine prepro-orexin cDNA and effects of an intramuscular injection of synthetic porcine orexin-B on feed intake in young pigs. *Domest Anim Endocrinol*. (1999) 16:145–8. doi: 10.1016/S0739-7240(99)00011-9

2. Sakurai T, Amemiya A, Ishii M, Matsuzaki I, Chemelli RM, Tanaka H, et al. Orexins and orexin receptors: a family of hypothalamic neuropeptides and G protein-coupled receptors that regulate feeding behavior. *Cells*. (1998) 92:573–85. doi: 10.1016/S0092-8674(00)80949-6

3. Sakurai T. Orexins and orexin receptors: implication in feeding behavior. *Regul Pept*. (1999) 85:25–30. doi: 10.1016/S0167-0115(99)00076-2

4. Sartin JL, Dyer C, Matteri R, Buxton D, Buonomo F, Shores M, et al. Effect of intracerebroventricular orexin-B on food intake in sheep. *J Anim Sci*. (2001) 79:1573–7. doi: 10.2527/2001.7961573x

5. van den Pol AN, Gao XB, Obrietan K, Kilduff TS, Belousov AB. Presynaptic and postsynaptic actions and modulation of neuroendocrine neurons by a new hypothalamic peptide, hypocretin/orexin. *J Neurosci*. (1998) 18:7962–71.

6. Chemelli RM, Willie JT, Sinton CM, Elmquist JK, Scammell T, Lee C, et al. Narcolepsy in orexin knockout mice: molecular genetics of sleep regulation. *Cells*. (1999) 98:437–51. doi: 10.1016/S0092-8674(00)81973-X

7. Scammell TE. Narcolepsy. *N Engl J Med*. (2015) 373:2654–62. doi: 10.1056/NEJMra1500587

8. Kortunay S, Erken HA, Erken G, Genç O, Şahiner M, Turgut S, et al. Orexins increase penicillin-induced epileptic activity. *Peptides*. (2012) 34:419–22. doi: 10.1016/j.peptides.2012.02.013

9. Roundtree HM, Simeone TA, Johnson C, Matthews SA, Samson KK, Simeone KA. Orexin receptor antagonism improves sleep and reduces seizures in Kcna1-null mice. *Sleep*. (2016) 39:357–68. doi: 10.5665/sleep.5444

10. Berteotti C, Calvello C, Liguori C. The role of the orexin system in the bidirectional relation between sleep and epilepsy: new chances for patients with epilepsy by the antagonism to orexin receptors? *Epilepsia*. (2023) 64:1991–2005. doi: 10.1111/epi.17661

11. Jallon P, Loiseau P, Loiseau J. Newly diagnosed unprovoked epileptic seizures: presentation at diagnosis in CAROLE study. Coordination active du reseau Observatoire longitudinal de l' Epilepsie. *Epilepsia*. (2001) 42:464–75. doi: 10.1046/j.1528-1157.2001.31400.x

12. Matricardi S, Verrotti A, Chiarelli F, Cerminara C, Curatolo P. Current advances in childhood absence epilepsy. *Pediatr Neurol*. (2014) 50:205–12. doi: 10.1016/j.pediatrneurol.2013.10.009

13. Crunelli V, Lőrincz ML, McCafferty C, Lambert RC, Leresche N, Di Giovanni G, et al. Clinical and experimental insight into pathophysiology, comorbidity and therapy of absence seizures. *Brain*. (2020) 143:2341–68. doi: 10.1093/brain/awaa072

14. Depaulis A, Charpier S. Pathophysiology of absence epilepsy: insights from genetic models. *Neurosci Lett*. (2018) 667:53–65. doi: 10.1016/j.neulet.2017.02.035

15. Celli R, Luijtelaar GV. The orexin system: a potential player in the pathophysiology of absence epilepsy. *Curr Neuropharmacol*. (2022) 20:1254–60. doi: 10.2174/1570159X19666211215122833

16. Marescaux C, Vergnes M, Micheletti G, Depaulis A, Reis J, Rumbach L, et al. A genetic form of petit mal absence in Wistar rats. *Rev Neurol*. (1984) 140:63–6.

17. Paxinos G, Watson C. *The rat brain in stereotaxic coordinates. 4th* ed. San Diego, CA: Academic Press (1998).

18. Akman O, Briggs SW, Mowrey WB, Moshé SL, Galanopoulou AS. Antiepileptogenic effects of rapamycin in a model of infantile spasms due to structural lesions. *Epilepsia*. (2021) 62:1985–99. doi: 10.1111/epi.16975

19. Yavuz M, Aydın B, Çarçak N, Akman Ö, Raci Yananlı H, Onat F. Atipamezole, a specific α 2A antagonist, suppresses spike-and-wave discharges and alters ca 2^{+}/calmodulin-dependent protein kinase II in the thalamus of genetic absence epilepsy rats. *Epilepsia*. (2020) 61:2825–35. doi: 10.1111/epi.16728

20. Kordi Jaz E, Moghimi A, Fereidoni M, Asadi S, Shamsizadeh A, Roohbakhsh A. SB-334867, an orexin receptor 1 antagonist, decreased seizure and anxiety in pentylenetetrazol-kindled rats. *Fundam Clin Pharmacol*. (2017) 31:201–7. doi: 10.1111/fcp.12249

21. Xue T, Wang S, Chen S, Wang H, Liu C, Shi L, et al. Subthalamic nucleus stimulation attenuates motor seizures via modulating the nigral orexin pathway. *Front Neurosci*. (2023) 5:1157060. doi: 10.3389/fnins.2023.1157060

22. Doreulee N, Alania M, Vashalomidze G, Skhirtladze E, Kapanadze T. Orexinergic system and pathophysiology of epilepsy. *Georgian Med News*. (2010) 188:74–9.

23. Zhao X, Xue Zhang R, Tang S, Yan Ren Y, Xia Yang W, Min Liu X, et al. Orexin-A-induced ERK1/2 activation reverses impaired spatial learning and memory in pentylenetetrazol-kindled rats via OX1R-mediated hippocampal neurogenesis. *Peptides*. (2014) 54:140–7. doi: 10.1016/j.peptides.2013.11.019

24. Adamantidis AR, Zhang F, Aravanis AM, Deisseroth K, De Lecea L. Neural substrates of awakening probed with optogenetic control of hypocretin neurons. *Nature*. (2007) 450:420–4. doi: 10.1038/nature06310

25. Bassetti CL, Adamantidis A, Burdakov D, Han F, Gay S, Kallweit U, et al. Narcolepsy—clinical spectrum, aetiopathophysiology, diagnosis and treatment. *Nat Rev Neurol*. (2019) 15:519–39. doi: 10.1038/s41582-019-0226-9

26. Nepovimova E, Janockova J, Misik J, Kubik S, Stuchlik A, Vales K, et al. Orexin supplementation in narcolepsy treatment: a review. *Med Res Rev*. (2019) 39:961–75. doi: 10.1002/med.21550

27. Irukayama-Tomobe Y, Ogawa Y, Tominaga H, Ishikawa Y, Hosokawa N, Ambai S, et al. Nonpeptide orexin type-2 receptor agonist ameliorates narcolepsy-cataplexy symptoms in mouse models. *Proc Natl Acad Sci*. (2017) 114:5731–6. doi: 10.1073/pnas.1700499114

28. Sasaki K, Suzuki M, Mieda M, Tsujino N, Roth B, Sakurai T. Pharmacogenetic modulation of orexin neurons alters sleep/wakefulness states in mice. *PLoS One*. (2011) 6:e20360. doi: 10.1371/journal.pone.0020360

29. Maganti R, Sheth RD, Hermann BP, Weber S, Gidal BE, Fine J. Sleep architecture in children with idiopathic generalized epilepsy. *Epilepsia*. (2005) 46:104–9. doi: 10.1111/j.0013-9580.2005.06804.x

30. Steriade M, Amzica F. Sleep oscillations developing into seizures in corticothalamic systems. *Epilepsia*. (2003) 44:9–20. doi: 10.1111/j.0013-9580.2003.12006.x

31. Smyk MK, Van Luijtelaar G. Circadian rhythms and epilepsy: a suitable case for absence epilepsy. *Front Neurol*. (2020) 11:245. doi: 10.3389/fneur.2020.00245

32. Halász P, Terzano MG, Parrino L. Spike-wave discharge and the microstructure of sleep-wake continuum in idiopathic generalised epilepsy. *Neurophysiologie Clinique*. (2002) 32:38–53. doi: 10.1016/S0987-7053(01)00290-8

33. Van Luijtelaar ELJM, Van der Werf SJ, Vossen JMH, Coenen AML. Arousal, performance and absence seizures in rats. *Electroencephalogr Clin Neurophysiol*. (1991) 79:430–4. doi: 10.1016/0013-4694(91)90208-L

34. Bayer L, Eggermann E, Saint-Mleux B, Machard D, Jones BE, Mühlethaler M, et al. Selective action of orexin (hypocretin) on nonspecific thalamocortical projection neurons. *J Neurosci*. (2002) 22:7835–9. doi: 10.1523/JNEUROSCI.22-18-07835.2002

35. Govindaiah G, Cox CL. Metabotropic glutamate receptors differentially regulate GABAergic inhibition in thalamus. *J Neurosci*. (2006) 26:13443–53. doi: 10.1523/JNEUROSCI.3578-06.2006

36. Marcus JN, Aschkenasi CJ, Lee CE, Chemelli RM, Saper CB, Yanagisawa M, et al. Differential expression of orexin receptors 1 and 2 in the rat brain. *J Comp Neurol*. (2001) 435:6–25. doi: 10.1002/cne.1190

37. Banerjee PK, Snead OC III. Thalamic mediodorsal and intralaminar nuclear lesions disrupt the generation of experimentally induced generalized absence-like seizures in rats. *Epilepsy Res*. (1994) 17:193–205. doi: 10.1016/0920-1211(94)90050-7

38. Seidenbecher T, Pape HC. Contribution of intralaminar thalamic nuclei to spike-and-wave-discharges during spontaneous seizures in a genetic rat model of absence epilepsy. *Eur J Neurosci*. (2001) 13:1537–46. doi: 10.1046/j.0953-816x.2001.01537.x

39. Hoerder-Suabedissen A, Hayashi S, Upton L, Nolan Z, Casas-Torremocha D, et al. Subset of cortical layer 6b neurons selectively innervates higher order thalamic nuclei in mice. *Cereb Cortex*. (2018) 28:1882–97. doi: 10.1093/cercor/bhy036

40. Steriade M. The corticothalamic system in sleep. *Front Biosci Landmark*. (2003) 8:d878–99. doi: 10.2741/1043

41. Cox CL, Huguenard JR, Prince DA. Peptidergic modulation of intrathalamic circuit activity in vitro: actions of cholecystokinin. *J Neurosci*. (1997) 17:70–82. doi: 10.1523/JNEUROSCI.17-01-00070.1997

42. Brill J, Kwakye G, Huguenard JR. NPY signaling through Y1 receptors modulates thalamic oscillations. *Peptides*. (2007) 28:250–6. doi: 10.1016/j.peptides.2006.08.043

43. Herrera CG, Cadavieco MC, Jego S, Ponomarenko A, Korotkova T, Adamantidis A. Hypothalamic feedforward inhibition of thalamocortical network controls arousal and consciousness. *Nat Neurosci*. (2016) 19:290–8. doi: 10.1038/nn.4209

44. Floyd NS, Price JL, Ferry AT, Keay KA, Bandler R. Orbitomedial prefrontal cortical projections to hypothalamus in the rat. *J Comp Neurol*. (2001) 432:307–28. doi: 10.1002/cne.1105

45. Gabbott PL, Warner TA, Jays PR, Salway P, Busby SJ. Prefrontal cortex in the rat: projections to subcortical autonomic, motor, and limbic centers. *J Comp Neurol*. (2005) 492:145–77. doi: 10.1002/cne.20738

46. Vergnes M, Marescaux C, Depaulis A. Mapping of spontaneous spike and wave discharges in Wistar rats with genetic generalized non-convulsive epilepsy. *Brain Res*. (1990) 523:87–91. doi: 10.1016/0006-8993(90)91638-W

47. Çarçak N, Ferrandon A, Koning E, Aker RG, Özdemir O, Onat FY, et al. Effect of stage 2 kindling on local cerebral blood flow rates in rats with genetic absence epilepsy. *Epilepsia*. (2009) 50:33–43. doi: 10.1111/j.1528-1167.2008.01712.x

48. Sere P, Zsigri N, Raffai T, Furdan S, Győri F, Crunelli V, et al. Activity of the lateral hypothalamus during genetically determined absence seizures. *Int J Mol Sci*. (2021) 22:9466. doi: 10.3390/ijms22179466

frontiers | Frontiers in Neurology

TYPE Original Research
PUBLISHED 11 December 2023
DOI 10.3389/fneur.2023.1231736

OPEN ACCESS

EDITED BY
Gilles van Luijtelaar,
Radboud University, Netherlands

REVIEWED BY
Enes Akyuz,
University of Wisconsin-Madison, United States
Amir Shmuel,
McGill University, Canada

*CORRESPONDENCE
Filiz Onat
✉ filiz.onat@acibadem.edu.tr

RECEIVED 30 May 2023
ACCEPTED 13 November 2023
PUBLISHED 11 December 2023

CITATION
Yavuz M, İyiköşker P, Mutlu N, Kiliçparlar S, Şalci ÖH, Dolu G, Kaymakçilar EN, Akkol S and Onat F (2023) Dexmedetomidine, an alpha 2A receptor agonist, triggers seizures unilaterally in GAERS during the pre-epileptic phase: does the onset of spike-and-wave discharges occur in a focal manner? *Front. Neurol.* 14:1231736. doi: 10.3389/fneur.2023.1231736

Dexmedetomidine, an alpha 2A receptor agonist, triggers seizures unilaterally in GAERS during the pre-epileptic phase: does the onset of spike-and-wave discharges occur in a focal manner?

Melis Yavuz[1], Pelin İyiköşker[2], Nursima Mutlu[3], Serra Kiliçparlar[2], Öykü Hazal Şalci[2], Gökçen Dolu[2], Elif Nur Kaymakçilar[2], Serdar Akkol[4] and Filiz Onat[5,6]*

[1]Department of Pharmacology, Faculty of Pharmacy, Acibadem Mehmet Ali Aydinlar University, Istanbul, Türkiye, [2]Faculty of Pharmacy, Acibadem Mehmet Ali Aydinlar University, Istanbul, Türkiye, [3]Department of Biotechnology and Genetics, Institute of Science, Istanbul University, Istanbul, Türkiye, [4]Department of Neurology, University of Alabama at Birmingham, Birmingham, AL, United States, [5]Department of Medical Pharmacology, School of Medicine, Acibadem Mehmet Ali Aydinlar University, Istanbul, Türkiye, [6]Institute of Neurosciences, Acibadem Mehmet Ali Aydinlar University, Istanbul, Türkiye

Introduction: The genetic absence epilepsy rat from Strasbourg (GAERS) is a rat model for infantile absence epilepsy with spike-and-wave discharges (SWDs). This study aimed to investigate the potential of alpha 2A agonism to induce seizures during the pre-epileptic period in GAERS rats.

Methods: Stereotaxic surgery was performed on male pups and adult GAERS rats to implant recording electrodes in the frontoparietal cortices (right/left) under anesthesia (PN23–26). Following the recovery period, pup GAERS rats were subjected to electroencephalography (EEG) recordings for 2 h. Before the injections, pup epileptiform activity was examined using baseline EEG data. Dexmedetomidine was acutely administered at 0.6 mg/kg to pup GAERS rats 2–3 days after the surgery and once during the post-natal (PN) days 25–29. Epileptiform activities before injections triggered unilateral SWDs and induced sleep durations, and power spectral density was evaluated based on EEG traces.

Results: The most prominent finding of this study is that unilateral SWD-like activities were induced in 47% of the animals with the intraperitoneal dexmedetomidine injection. The baseline EEGs of pup GAERS rats had no SWDs as expected since they are in the pre-epileptic period but showed low-amplitude non-rhythmic epileptiform activity. There was no difference in the duration of epileptiform activities between the basal EEG groups and DEX-injected unilateral SWD-like-exhibiting and non-SWD-like activities groups; however, the sleep duration of the unilateral SWD-like-exhibiting group was shorter. Power spectrum density (PSD) results revealed that the 1.75-Hz power in the left hemisphere peaks significantly higher than in the right.

Discussion: As anticipated, pup GAERS rats in the pre-epileptic stage showed no SWDs. Nevertheless, they exhibited sporadic epileptiform activities. Specifically, dexmedetomidine induced SWD-like activities solely within the left hemisphere.

These observations imply that absence seizures might originate unilaterally in the left cortex due to α_{2A}AR agonism. Additional research is necessary to explore the precise cortical focal point of this activity.

KEYWORDS

GAERS, spike-and-wave discharges, unilateral seizures, α_{2A}AR, pre-epileptic, dexmedetomidine, pups, epileptiform

Introduction

Absence seizures are the most common type of primary generalized epileptic seizures, and they are distinguished by the presence of spike-and-wave discharges (SWDs) in the electroencephalogram (EEG). These discharges are believed to be caused by cortico-thalamocortical mechanisms. Genetic animal models have played a crucial role in elucidating the underlying causes of absence seizures (1).

Idiopathic, non-convulsive, and generalized absence seizures are the three types of seizures (2). The EEG shows bilaterally coordinated and symmetrical SWDs at 3 Hz during absence seizures (3). Gibbs et al. (4) found the association between behavioral unconsciousness and the presence of 3–4 Hz spike-and-slow wave complexes on the EEG in 1935. When depth electrodes were placed into the thalamus of a patient with absence epilepsy, bilateral and synchronous SWDs were seen (5).

In the domain of absence epilepsy research, two commonly used rat models for studying absence epilepsy are the rats of Strasbourg origin [genetic absence epilepsy rat from Strasbourg (GAERS)] and Rijswijk origin (WAG/Rij). The GAERS rats from Strasbourg are a useful model in which behavioral components accompany SWDs, similar to seizures observed in childhood absence epilepsy (6). Absence epileptic seizures do not appear immediately after birth in GAERS rats but emerge after a latent period. These seizures typically arise between 40 and 120 days, with a peak at ∼60 days, when the first SWDs appear on the EEG, making GAERS rats an established model for studying absence epilepsy. As the rats aged, the frequency, and length of these discharges increased. We also observed in the EEGs previously that SWDs do not appear in GAERS rats until the 30th day after birth (7). This reflects that the pre-epileptic period, a silent phase of epileptogenesis, is anticipated to unfold (8), and our understanding of this crucial developmental stage is still limited.

The role of alpha 2A adrenergic receptors (α_{2A}AR), a specific subtype of α_2AR known to be involved in the generation and sustainability of SWDs, has been extensively investigated (9–12). In rats, a decrease in noradrenergic and dopaminergic activity has been shown to promote the occurrence of absence-like seizures (13). A previous study has shown that activating α_{2A}AR receptors with the antagonist atipamezole efficiently decreased SWDs in adult GAERS rats (14) but activating α_{2A}AR with agonist dexmedetomidine established a model of status epilepticus similar to prolonged absence seizures (15). In this study, dexmedetomidine also induced a state of switch from status to sleep and back from sleep to status (15). These findings help to show them as key players in the involvement of SWDs.

The generation of SWDs has long been debated, with two main theories emerging. Among these, the cortical theory has garnered a larger following. The somatosensory cortex has received much attention in this area and has been established as a key player in SWD generation through numerous studies (16, 17). Bancaud et al. (18) remarkable research on human patients provided direct evidence that initiating a focal discharge in the frontal cortex later propagates to the cortico-cortical pathways.

Further evidence of cortical involvement, particularly in the frontal and parietal regions, comes from EEG/fMRI data of patients with Rolandic epilepsy, where thalamic signals were found to follow cortical signals with higher amplitude (19). These findings are confirmed by neuropathological discoveries that confirm the cortical influence on SWDs. In addition, recent studies address that dexmedetomidine may facilitate seizure expression with peripheral somatosensory stimulation in rats, and interestingly, these seizures are focal initially (20, 21). These studies mention the high-frequency oscillations (ripples and fast ripples) preceded by the induction of these seizures. In this study, we aimed to investigate the SWDs before they were fully expressed in the GAERS model. Specifically, our objective is to determine whether α_{2A}AR stimulation could induce SWD activity. We aimed to understand better the early stages of SWD and the potential role of α_{2A}AR in SWD initiation.

Methods

Animals and experimental groups

The study was performed at Acibadem Mehmet Ali Aydinlar University Medical Experimental Application and Research Center (DEHAM) and was approved by the Acibadem University Experimental Animals Local Ethics Committee under decision number ACUHAYDEK2020/51.

The GAERS rats were bred and housed in a controlled environment in the animal care and production area. The room was set to a 12-h light/12-h dark cycle, and the temperature was 24 ± 2°C. The rats had unrestricted access to standard rat chow and drinking water. To preserve the GAERS strain's specific absence of epilepsy characteristics, inbreeding practices were used from the GAERS strain with 7- to 11-Hz spontaneous SWDs (1). The animals were housed in pairs in cages before the surgical procedures. However, after the completion of the stereotaxic surgeries, each

cage accommodated only one animal to ensure proper post-surgery care and monitoring.

Male GAERS offspring rats (PN 23–26) obtained from Acibadem University DEHAM, still in their epileptogenesis period and weighed between 25 and 45 g, did not yet express SWDs. The animals were implanted with electrodes on the PN 23-26 and EEGs were performed on the PN 25–29. The offspring rats were connected to the EEG and their postnatal days were between PN23 and PN26, their EEGs were recorded once after 2–3 days after the surgery and once. The SWD expressions were confirmed as none by the 20-min baseline EEG. The waiting period after stereotaxic surgery was a minimum of 2 days.

Stereotaxic surgery

Stereotaxic surgery was performed under ketamine/chlorobutanol (100 mg/kg, VetaKetam; Oruç Özel Vet. Hiz. Hay. Ve Gida San. Tic. LLC.) and xylazine (10 mg/kg; Rompun, 2%; Bayer HealthCare, LLC) anesthesia, both of which were administered intraperitoneally (*i.p.*) to all experimental group rats. The heads of the animals were first placed in the stereotaxy device after the ear bars were fixed in the anterior chamber of the stereotaxy device (Stoelting Model 51600, Stoelting Co., Illinois). Four stainless steel screws with insulated wires were implanted bilaterally to the right and left frontal bones over the cortex rat brain atlas (22) according to the coordinates provided by reference to the bregma point and adapted to the pup animals (right/left frontal; AP: +2.2, ML: ±1.5; parietal AP: −2.9, ML: ±1.5). The opposite ends of the cables, which had previously been attached to pins, were soldered to the tiny connections generated by cutting the male VGA connectors into four threads with multiwire conductor cables using phosphoric acid and a soldering device instrument. Dental acrylic was used to cover and secure the electrodes and cables to the skull. Following the surgery, a 0.9% isotonic sodium chloride solution was injected subcutaneously to supply any possible fluid loss in the animal.

EEG recordings and analysis

After the electrodes were placed by stereotaxic surgery, the animals were allowed to rest for 2 days. The animals' basal activity was then recorded to analyze the epileptiform activities and freezing behaviors. The signals from the electrodes were transferred to ML 136 bioamplifier (ADInstruments) for EEG recording using the EEG recording wire. The amplifier signals were sent to the computer using the Powerlab system (PowerLab8S ADI Instruments, Oxfordshire, UK). The frequency filter is used in the 1- to 40-Hz band. EEG recordings on the computer were analyzed with the LabChart 8.0 program. Epileptiform activity analysis was performed by manually selecting the EEG activity occurring in both cortices of the animals between the basal EEG from groups, DEX injected-unilateral SWD-like-exhibiting and non-SWD-like activities groups over the duration of 1 sec to improve the accuracy of power spectral analysis (below) by increasing sampled length of time. Sleep time was also monitored during the EEG and video recordings.

Dexmedetomidine injections

Following the recording of basal activity, 0.6 mg/kg dexmedetomidine was injected *i.p.* acutely into the animals. After the injection of dexmedetomidine, the EEG was recorded for two more hours, and a power spectrum density (PSD) analysis was performed.

PSD analysis

The SWD and SWD-like EEG data were preprocessed using Fieldtrip (23) and custom MATLAB scripts (R2022a, MathWorks, Natick, Massachusetts). SWD activity was obtained and is shown as an example (24). Figure 2 shows the EEG data after bandpass filtering (with zero-phase, third-order, Butterworth filter using bandpass function in MATLAB, between 1 and 40 Hz). Multitaper spectral decomposition was used at 0.25 Hz frequency steps with discrete prolate spheroidal sequences and 1 Hz multitapers. PSD was the amplitude of the time-frequency decomposition calculated for each frequency.

Statistical analysis

All statistical analyses were performed with GraphPad Prism version 9.5.0 (GraphPad Software, San Diego, USA). Descriptive statistics were used to examine the total, mean duration, and number of SWD-like activities and the percentage of animals in which this activity was triggered (the unilateral SWD-like-exhibiting group). The unpaired Student's *t*-test was used to compare the mean duration of epileptiform activities and sleep ($p < 0.05$ and $p < 0.01$).

Results

Proportion of animals with unilateral SWDs and the total, mean duration, and number of SWD-like activities

The baseline EEGs of pup GAERS rats did not show SWD as expected but showed low-amplitude non-rhythmic epileptiform activity. A 0.6-mg/kg dexmedetomidine injection generated unilateral SWD-like activity in 47% of the rats (Figure 1A).

The descriptive statistics of unilateral SWD-like activities in the left cortex of animals that were triggered were analyzed (the unilateral SWD-like-exhibiting group). All SWD-like activities between the animals ($n = 8$) were 297.0 ± 175.3 s up to 3 h. The mean duration of each SWD-like activity among animals exhibiting unilateral SWD-like activities was 34.9 ± 16.9 s. The number of each SWD-like activity between the animals was 8.3 ± 2.4 (Figure 1B).

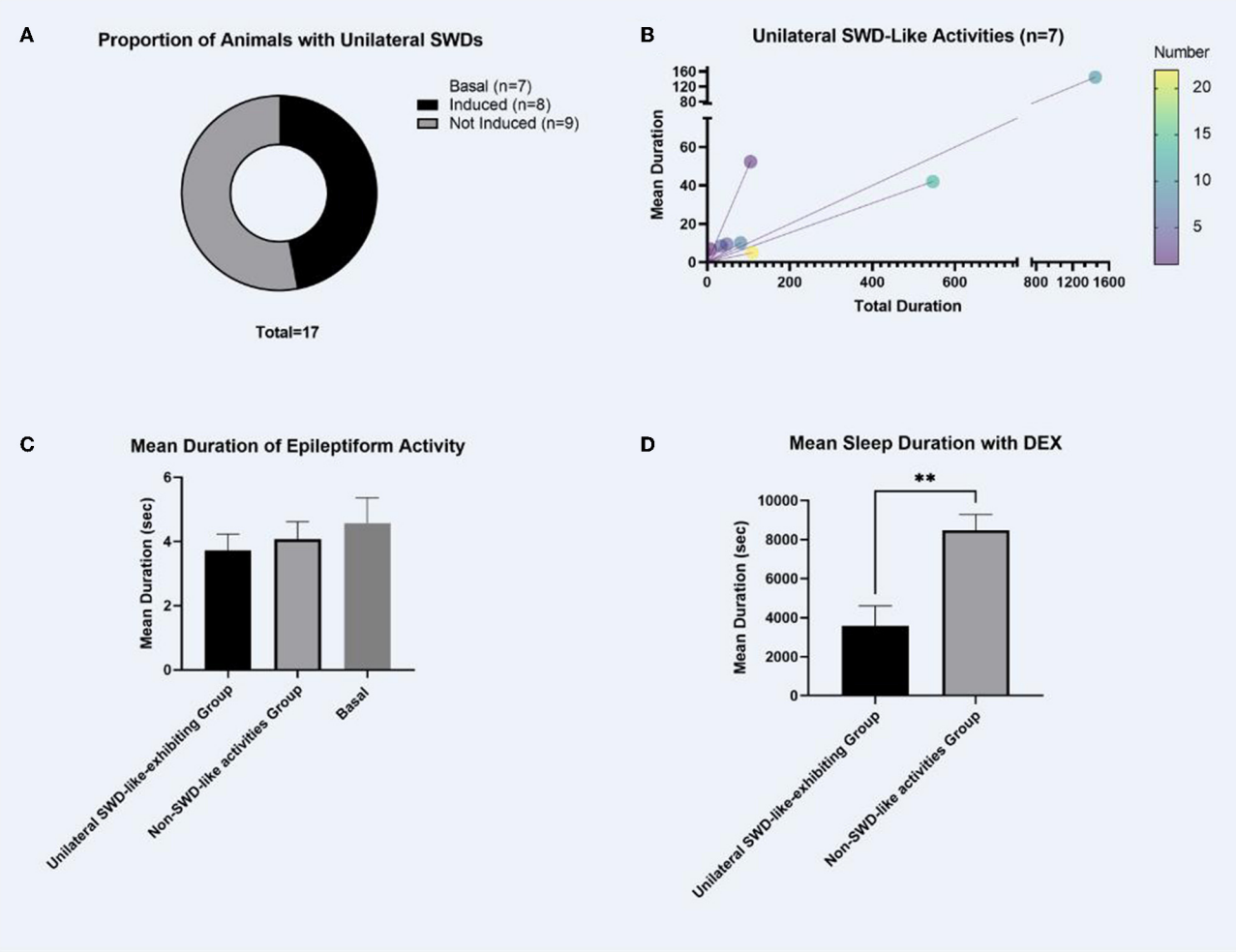

FIGURE 1
The proportion of animals with unilateral SWDs, the total mean duration of SWD-like activities, the mean duration of epileptiform activities, and the sleep duration following dexmedetomidine injections. **(A)** As expected, the baseline EEGs of pup GAERS rats did not show matured SWDs; it showed low amplitude non-rhythmic epileptiform activity. Mature SWDs occur after post-natal 30 in adult GAERS. Following a 0.6-mg/kg dexmedetomidine injection, unilateral SWD-like activity was observed in 47% (8/17) of the rats, as illustrated in **(A)**. **(B)** Characteristics of Unilateral SWD-like Activity. Unilateral SWD-like activities were analyzed within the group of animals exhibiting this response shown in **(A)** ($n = 8$). **(C)** Duration of Epileptiform Activities. Comparison of the duration of epileptiform activity between the "unilateral SWD-like-exhibiting group" and the "non-SWD-like activities group" revealed no significant difference in the **(C)**. **(D)** Sleep Duration Following Dexmedetomidine Injections. In the "unilateral SWD-like-exhibiting group," the mean sleep duration was significantly shorter compared to the "non-SWD-like activities group." No sleep activity was observed on the baseline EEG data as expected. The data were given as mean ± *SEM*. $^{**}p < 0.01$ (significant difference).

Mean duration of epileptiform activities and the sleep duration following dexmedetomidine injections

There was no significant difference in the length of epileptiform activity between "the unilateral SWD-like-exhibiting group" and "the non-SWD-like activities group" (Figure 1C). However, in the unilateral SWD-like-exhibiting group, mean sleep duration was considerably shorter than the non-SWD-like activities group ($t_{(df)} = 3.812$, $p = 0.003$, $p < 0.01$, Figure 1D).

PSD analysis of SWD-like activity

As shown in Figure 2, SWD-like activity is qualitatively similar to mature SWD activity, which classically indicates 6-Hz activity. However, SWD-like activity appears slower and peaks at 1.5–1.75 Hz. This activity developed only in the left hemispheres of 47% of the animals injected with the 0.6 mg/kg dexmedetomidine. Furthermore, the PSD results revealed that the 1.75 Hz power in the left hemisphere peaks significantly higher than that of the right hemisphere.

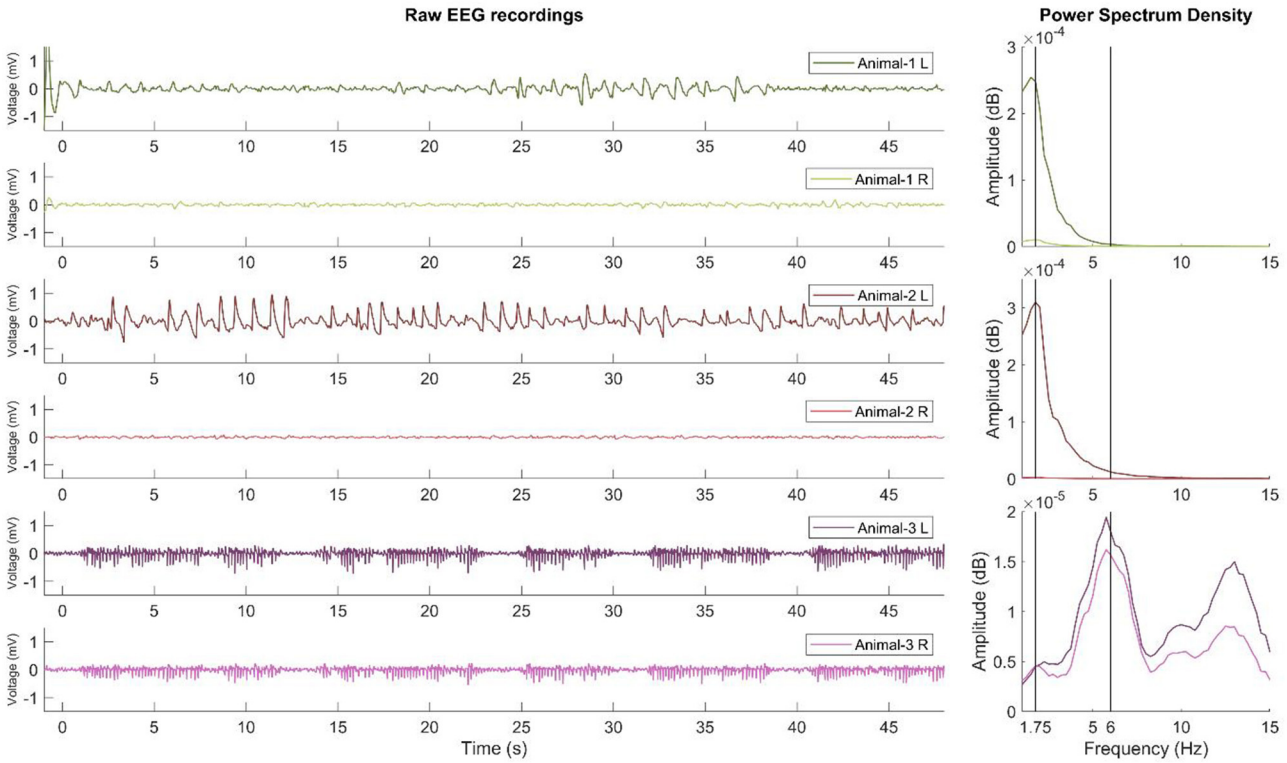

FIGURE 2
Raw recordings and PSD results of SWD and SWD-like activity. The left side of the figure shows the EEG recordings (filtered in 1–40 Hz) of two examples of SWD-like activity developed in the left hemisphere and one example of mature SWD activity recorded previously. Each subsequent two rows belong to the same animal. The right side of the figure shows the PSD results. As shown for the first two animals, SWD-like activity peaks at approximately 1.5–1.75 Hz, but for the third animal, the SWD activity peaks at 6 Hz and is similar on both hemispheres. L, left hemisphere; R, right hemisphere.

Discussion

Generalized SWDs are known to be the basic building blocks of the EEG of absence epilepsy when manifested bilaterally and synchronously (25). Several genetic and pharmacological animal models have been constructed to understand the fundamental etiological factors behind epilepsies better and identify potential therapeutic targets for anti-epileptic medicines (26). GAERS, as an absence epilepsy model, provides a valuable model to examine the underlying epileptogenesis process in the pre-epileptic stage of the first 30 days of life in this animal model. This process is important for investigating potential anti-epileptogenic and anti-seizure treatment approaches and their use in creating new animal models.

Spike-and-wave discharges are high amplitude, synchronous, and, most significantly, bilateral. Previous studies were performed with unilateral cortical resection, but no change was reported. In contrast, SWDs were no longer noticeable after bilateral resection. These results suggest that SWDs are completely abolished after bilateral removal of the focal region, most likely by interfering with an intracortical columnar circuit (27), which also supports the cortical focus, whereas only inhibition of the local cortical network removed all seizures. Another unilateral onset is that SWDs have induced fluid percussion injury in rats, and it serves as a model for complex partial seizures in human post-traumatic epilepsy (28). In this model, anti-absence ethosuximide has been shown to suppress both unilateral or bilateral SWDs, whereas carbamazepine had no effect (28). Some drugs, such as potassium chloride, block SWDs somewhat in the ipsilateral cortex and thalamus (29). Furthermore, bilateral or unilateral SWDs have been observed to alternate between hemispheres after corpus callosum excision, implying that the corpus callosum is related to SWD generalization (30). Landau–Kleffner syndrome, commonly known as electrical status epilepticus of sleep, has focal SWDs (31). However, no report has shown unilateral induction of SWD-like activities with pharmacological or chemical agents.

In addition to the induction of unilateral seizures with dexmedetomidine, this study questions the focal origin hypothesis of absence seizures, specifically SWDs. Despite the absence of SWD activity observed in the baseline EEG of the pup GAERS, which is expected to be in their epileptogenesis period (before PN30), a dose of 0.6 mg/kg dexmedetomidine selectively induced unilateral SWD-like events in the left cortex of half of the animals. Animals that exhibited unilateral SWD-like activities accounted for 47% of the total sample. Unilateral expression of normally generalized seizures suggests a focal start. Some studies with dexmedetomidine also induced focal seizures suggest the activation of α_{2A}AR may start the SWDs. In addition to these results, dexmedetomidine-inducing focal seizures in a periphery reflex model (20, 21) draw attention to α_{2A}AR-mediated seizure initiation mechanisms.

Dexmedetomidine closely resembles and facilitates natural non-REM sleep (32) and therefore improves sleep in patients receiving dexmedetomidine anesthesia in comparison to other anesthetics after surgery by altering sleep structure (33, 34). Dexmedetomidine also modulates the release of inhibitory compounds such as γ-aminobutyric acid and galanin due to reduced control over the ventrolateral preoptic nucleus, further inhibiting the locus ceruleus and tuberomamillary nucleus by the inhibition and disinhibition of the locus ceruleus and ventral lateral preoptic nucleus (35). The α_{2A}AR agonist effect of dexmedetomidine on NREM sleep might be influenced by postsynaptic α_{2A}AR (36). Meanwhile, changes in high-frequency oscillations in the thalamus and neocortex have also been observed during dexmedetomidine anesthesia (37). In a genetic model of absence epilepsy, alterations in sleep characteristics were identified in WAG/Rij rats encompassing extended transitions from wakefulness to sleep, prolonged intermediate sleep stages, more frequent subsequent arousals, and a reduced proportion of REM sleep (38–40). That also points out the positive relationship between absence seizures and the increase of NREM activity as it is already known both rhythms of SWDs and NREM activities are synchronized in the thalamocortical circuitry (41, 42). The focal point pertains to the plausible role of dexmedetomidine in potentially inducing the transition of slow wave and delta oscillations, thereby precipitating SWDs.

A recent study on the mesoscale modeling of SWDs highlights and sheds light on the initiation, maintenance, and termination of SWDs by integrating pyramidal cells (43) and interneurons in the cortex (44, 45) as well as the ventroposterior medial nucleus of the thalamus, reticular thalamic nucleus (RTN), and nervus trigeminus (46). In this model, SWD might be initiated by one of the three mechanisms: an increase in intracortical excitability, external driving from the nervus trigeminus to the thalamic ventroposterior medial nucleus, or low-frequency harmonic stimulation of the cortex. While the maintenance was caused by increased coupling from RTN nodes to both pyramidal nodes and cortical interneurons (46), the termination was driven by increased coupling from rostral RTN to the brain or high-frequency electrical stimulation. We first demonstrated that SWD-like activity might be induced unilaterally using the α_{2A}AR agonist dexmedetomidine. Though it appears to be the start of SWD-like activity in the left cortex, our previous study with a status epilepticus model found that dexmedetomidine generated sustained SWDs in adult rats, which is more consistent with the maintenance of SWD activity.

Our previous study (15) introduced this absence status epilepticus model with the induction of dexmedetomidine in adult GAERS. Recent reports on dexmedetomidine increasing the duration of SWD activity (15) provide evidence that dexmedetomidine influences SWD duration. For instance, Sitnikova et al. (47, 48) provided preliminary results of dexmedetomidine increasing mean duration of SWDs in another model of genetic absence epilepsy Wistar Albino Glaxo/Rijswijk (WAG/Rij), and dexmedetomidine does not shorten the SWDs unlike other anesthetics (49).

The mean sleep duration differed significantly between animals that exhibited unilateral SWD-like activities or not in this study as well. This difference can potentially be attributed to two distinct factors. First, anesthesia-induced sleep may interfere with the initiation of unilateral activities. Because our EEG recordings were obtained 2 h after injection, some animals may not fully emerge from the anesthesia during this timeframe. Second, given the metabolic differences among the animals, mainly as they are still in the pup stage, it is conceivable that the dosage of dexmedetomidine administered may have exceeded the specific activation threshold of α_{2A}AR. These factors may have contributed to the observed difference in sleep duration between the animals.

Another issue on dexmedetomidine as addressed by many studies is the possible induction of respiratory or cardiovascular system-related adverse effects. Recent studies point out a either positive influence or no influence on the respiratory parameters (50–53). Conversely, a significant reduction in heart rate and instances of bradycardia have been reported as some of the cardiovascular effects (51). Yet, the relationship between them is yet to be investigated in terms of the sleep and SWD-related mechanisms.

As a result, it remains unclear whether the induction of unilateral SWD-like events reflects the initiation or maintenance phase of SWDs. In any case, α_{2A}AR appears to be a strong candidate for further investigation as the primary mechanism behind the initiation or maintenance of SWDs as well as the modulation of switch mechanisms between sleep and SWDs. Further research into the exact cortical process and the role of α_{2A}AR would be valuable.

Data availability statement

The raw data supporting the conclusions of this article will be made available by the authors, without undue reservation.

Ethics statement

The animal study was approved by Acibadem University Experimental Animals Local Ethics Committee under decision number ACUHAYDEK2020/51. The study was conducted in accordance with the local legislation and institutional requirements.

Author contributions

MY and FO conceptualized and designed the study. MY organized the database, performed the statistical analysis, and wrote the first draft of the manuscript. SA performed the analysis and wrote the Results section of the PSD section of the manuscript. Pİ, NM, GD, ÖŞ, SK, and EK contributed to the EEG data acquisition. MY and FO contributed to the manuscript's revision and read and approved the submitted version. All authors approved the final version of the manuscript.

Funding

The study was funded by the ABAPKO (Grant 2022/02-20) and Europe Commission

[GEMSTONE Horizon Europe grant number 101078981].

Conflict of interest

The authors declare that the research was conducted in the absence of any commercial or financial relationships that could be construed as a potential conflict of interest.

Publisher's note

References

1. Marescaux C, Vergnes M, Depaulis A. Genetic absence epilepsy in rats from strasbourg–a review. *J Neural Transm Suppl.* (1992) 35:37–69. doi: 10.1007/978-3-7091-9206-1_4

2. Panayiotopoulos CP, Chroni E, Daskalopoulos C, Baker A, Rowlinson S, Walsh P. Typical absence seizures in adults: clinical, EEG, video-EEG findings and diagnostic/syndromic considerations. *J Neurol Neurosurg Psychiatry.* (1992) 55:1002–8. doi: 10.1136/jnnp.55.11.1002

3. Blumenfeld H. Consciousness and epilepsy: why are patients with absence seizures absent? *Prog Brain Res.* (2005) 150:271–86. doi: 10.1016/S0079-6123(05)50020-7

4. Gibbs FA, Davis H, Lennox WG. The electro-encephalogram in epilepsy and in conditions of impaired consciousness. *Arch Neurol Psychiatry.* (1935) 34:1133–48. doi: 10.1001/archneurpsyc.1935.02250240002001

5. Williams D. A study of thalamic and cortical rhythms in petit mal. *Brain.* (1953) 76:50–69. doi: 10.1093/brain/76.1.50

6. Danober L, Deransart C, Depaulis A, Vergnes M, Marescaux C. Pathophysiological mechanisms of genetic absence epilepsy in the rat. *Prog Neurobiol.* (1998) 55:27–57. doi: 10.1016/S0301-0082(97)00091-9

7. Yavuz M, Albayrak N, Özgür M, Gülçebi Idriz Oglu M, Çavdar S, Onat F. The effect of prenatal and postnatal caffeine exposure on pentylentetrazole induced seizures in the non-epileptic and epileptic offsprings. *Neurosci Lett.* (2019) 713:134504. doi: 10.1016/j.neulet.2019.134504

8. Komoltsev IG, Frankevich SO, Shirobokova NI, Volkova AA, Levshina IP, Novikova MR, et al. Differential early effects of traumatic brain injury on spike-wave discharges in Sprague-Dawley rats. *Neurosci Res.* (2021) 166:42–54. doi: 10.1016/j.neures.2020.05.005

9. King GA, Burnham WM. Alpha 2-adrenergic antagonists suppress epileptiform EEG activity in a petit mal seizure model. *Life Sci.* (1982) 30:293–8. doi: 10.1016/0024-3205(82)90511-2

10. McCallum JB, Boban N, Hogan Q, Schmeling WT, Kampine JP, Bosnjak ZJ. The mechanism of alpha2-adrenergic inhibition of sympathetic ganglionic transmission. *Anesth Analg.* (1998) 87:503–10. doi: 10.1213/00000539-199809000-00001

11. Sitnikova E, van Luijtelaar G. Reduction of adrenergic neurotransmission with clonidine aggravates spike-wave seizures and alters activity in the cortex and the thalamus in WAG/Rij rats. *Brain Res Bull.* (2005) 64:533–40. doi: 10.1016/j.brainresbull.2004.11.004

12. Micheletti G, Warter JM, Marescaux C, Depaulis A, Tranchant C, Rumbach L, et al. Effects of drugs affecting noradrenergic neurotransmission in rats with spontaneous petit mal-like seizures. *Eur J Pharmacol.* (1987) 135:397–402. doi: 10.1016/0014-2999(87)90690-X

13. Vergnes M, Marescaux C, Depaulis A, Micheletti G, Warter JM. Ontogeny of spontaneous petit mal-like seizures in Wistar rats. *Brain Res.* (1986) 395:85–7. doi: 10.1016/S0006-8993(86)80011-7

14. Yavuz M, Aydin B, Carcak N, Akman O, Raci Yananli H, Onat F. Atipamezole, a specific alpha2A antagonist, suppresses spike-and-wave discharges and alters Ca(2(+))/calmodulin-dependent protein kinase II in the thalamus of genetic absence epilepsy rats. *Epilepsia.* (2020) 61:2825–35. doi: 10.1111/epi.16728

15. Yavuz M, Akkol S, Onat F. Alpha-2a adrenergic receptor (α2AR) activation in genetic absence epilepsy: an absence status model? *Authorea.* (2022). doi: 10.22541/au.167042890.02021046/v1

16. Meeren HKM, Pijn JPM, van Luijtelaar ELJM, Coenen AML, Lopes da Silva FH. Cortical focus drives widespread corticothalamic networks during spontaneous absence seizures in rats. *J Neurosci.* (2002) 22:1480–95. doi: 10.1523/JNEUROSCI.22-04-01480.2002

17. Meeren H, van Luijtelaar G, Lopes da Silva F, Coenen A. Evolving concepts on the pathophysiology of absence seizures: the cortical focus theory. *Arch Neurol.* (2005) 62:371–6. doi: 10.1001/archneur.62.3.371

18. Bancaud J, Talairach J, Morel P, Bresson M, Bonis A, Geier S, et al. "Generalized" epileptic seizures elicited by electrical stimulation of the frontal lobe in man. *Electroencephalogr Clin Neurophysiol.* (1974) 37:275–82.

19. Szaflarski JP, DiFrancesco M, Hirschauer T, Banks C, Privitera MD, Gotman J, et al. Cortical and subcortical contributions to absence seizure onset examined with EEG/fMRI. *Epilepsy Behav.* (2010) 18:404–13. doi: 10.1016/j.yebeh.2010.05.009

20. Bortel A, Yao ZS, Shmuel A. A rat model of somatosensory-evoked reflex seizures induced by peripheral stimulation. *Epilepsy Res.* (2019) 157:106209. doi: 10.1016/j.eplepsyres.2019.106209

21. Bortel A, Pilgram R, Yao ZS, Shmuel A. Dexmedetomidine - commonly used in functional imaging studies - increases susceptibility to seizures in rats but not in wild type mice. *Front Neurosci.* (2020) 14:832. doi: 10.3389/fnins.2020.00832

22. Paxinos G, Watson C. *The Rat Brain in Stereotaxic Coordinates–The New Coronal Set, 5th Edn.* Burlington, NJ: Elsevier Academic Press (2004).

23. Oostenveld R, Fries P, Maris E, Schoffelen JM. FieldTrip: open source software for advanced analysis of MEG, EEG, and invasive electrophysiological data. *Comput Intell Neurosci.* (2011) 2011:156869. doi: 10.1155/2011/156869

24. Guyenet PG, Stornetta RL, Abbott SBG, Depuy SD, Kanbar R. The retrotrapezoid nucleus and breathing. *Adv Exp Med Biol.* (2012) 758:115–22. doi: 10.1007/978-94-007-4584-1_16

25. Antwi P, Atac E, Ryu JH, Arencibia CA, Tomatsu S, Saleem N, et al. Driving status of patients with generalized spike-wave on EEG but no clinical seizures. *Epilepsy Behav.* (2019) 92:5–13. doi: 10.1016/j.yebeh.2018.11.031

26. Cortez MA, Kostopoulos GK, Snead OC 3rd. Acute and chronic pharmacological models of generalized absence seizures. *J Neurosci Methods.* (2016) 260:175–84. doi: 10.1016/j.jneumeth.2015.08.034

27. Scicchitano F, van Rijn CM, van Luijtelaar G. Unilateral and bilateral cortical resection: effects on spike-wave discharges in a genetic absence epilepsy model. *PLoS ONE.* (2015) 10:e0133594. doi: 10.1371/journal.pone.0133594

28. Tatum S, Smith ZZ, Taylor JA, Poulsen DJ, Dudek FE, Barth DS. Sensitivity of unilateral- versus bilateral-onset spike-wave discharges to ethosuximide and carbamazepine in the fluid percussion injury rat model of traumatic brain injury. *J Neurophysiol.* (2021) 125:2166–77. doi: 10.1152/jn.00098.2021

29. Vergnes M, Marescaux C. Cortical and thalamic lesions in rats with genetic absence epilepsy. *J Neural Transm Suppl.* (1992) 35:71–83. doi: 10.1007/978-3-7091-9206-1_5

30. Vergnes M, Marescaux C, Lannes B, Depaulis A, Micheletti G, Warter JM. Interhemispheric desynchronization of spontaneous spike-wave discharges by corpus callosum transection in rats with petit mal-like epilepsy. *Epilepsy Res.* (1989) 4:8–13. doi: 10.1016/0920-1211(89)90052-1

31. McVicar KA, Shinnar S. Landau-Kleffner syndrome, electrical status epilepticus in slow wave sleep, and language regression in children. *Ment Retard Dev Disabil Res Rev.* (2004) 10:144–9. doi: 10.1002/mrdd.20028

32. Feng ZX, Dong H, Qu WM, Zhang W. Oral delivered dexmedetomidine promotes and consolidates non-rapid eye movement sleep via sleep-wake regulation systems in mice. *Front Pharmacol.* (2018) 9:1196. doi: 10.3389/fphar.2018.01196

33. Huang X, Lin D, Sun Y, Wu A, Wei C. Effect of dexmedetomidine on postoperative sleep quality: a systematic review. *Drug Des Devel Ther.* (2021) 15:2161–70. doi: 10.2147/DDDT.S304162

34. Song B, Li Y, Teng X, Li X, Yang Y, Zhu J. The effect of intraoperative use of dexmedetomidine during the daytime operation vs the nighttime operation on postoperative sleep quality and pain under general anesthesia. *Nat Sci Sleep.* (2019) 11:207–15. doi: 10.2147/NSS.S225041

35. Cheng J, Wu F, Zhang M, Ding D, Fan S, Chen G, et al. The interaction between the ventrolateral preoptic nucleus and the tuberomammillary

nucleus in regulating the sleep-wakefulness cycle. *Front Neurosci.* (2020) 14:615854. doi: 10.3389/fnins.2020.615854

36. Seidel WF, Maze M, Dement WC, Edgar DM. Alpha-2 adrenergic modulation of sleep: time-of-day-dependent pharmacodynamic profiles of dexmedetomidine and clonidine in the rat. *J Pharmacol Exp Ther.* (1995) 275:263–73.

37. Baker R, Gent TC, Yang Q, Parker S, Vyssotski AL, Wisden W, et al. Altered activity in the central medial thalamus precedes changes in the neocortex during transitions into both sleep and propofol anesthesia. *J Neurosci.* (2014) 34:13326–35. doi: 10.1523/JNEUROSCI.1519-14.2014

38. Gandolfo G, Romettino S, Gottesmann C, Van Luijtelaar G, Coenen A. Genetically epileptic rats show a pronounced intermediate stage of sleep. *Physiol Behav.* (1990) 47:213–5. doi: 10.1016/0031-9384(90)90063-A

39. Coenen AM, Van Luijtelaar EL. Genetic animal models for absence epilepsy: a review of the WAG/Rij strain of rats. *Behav Genet.* (2003) 33:635–55. doi: 10.1023/A:1026179013847

40. van Luijtelaar G, Bikbaev A. Midfrequency cortico-thalamic oscillations and the sleep cycle: genetic, time of day and age effects. *Epilepsy Res.* (2007) 73:259–65. doi: 10.1016/j.eplepsyres.2006.11.002

41. Huguenard JR, McCormick DA. Thalamic synchrony and dynamic regulation of global forebrain oscillations. *Trends Neurosci.* (2007) 30:350–6. doi: 10.1016/j.tins.2007.05.007

42. Crunelli V, Leresche N. Childhood absence epilepsy: genes, channels, neurons and networks. *Nat Rev Neurosci.* (2002) 3:371–82. doi: 10.1038/nrn811

43. van Luijtelaar G, Sitnikova E. Global and focal aspects of absence epilepsy: the contribution of genetic models. *Neurosci Biobehav Rev.* (2006) 30:983–1003. doi: 10.1016/j.neubiorev.2006.03.002

44. Polack P-O, Guillemain I, Hu E, Deransart C, Depaulis A, Charpier S. Deep layer somatosensory cortical neurons initiate spike-and-wave discharges in a genetic model of absence seizures. *J Neurosci.* (2007) 27:6590–9. doi: 10.1523/JNEUROSCI.0753-07.2007

45. Abbasova KR, Chepurnov SA, Chepurnova NE, van Luijtelaar G. The role of perioral afferentation in the occurrenceof spike-wave discharges in the WAG/Rij modelof absence epilepsy. *Brain Res.* (2010) 1366:257–62. doi: 10.1016/j.brainres.2010.10.007

46. Medvedeva TM, Sysoeva MV, Lüttjohann A, van Luijtelaar G, Sysoev IV. Dynamical mesoscale model of absence seizures in genetic models. *PLoS ONE.* (2020) 15:e0239125. doi: 10.1371/journal.pone.0239125

47. Sitnikova E, Pupikina M, Rutskova E. Alpha2 adrenergic modulation of spike-wave epilepsy: experimental study of pro-epileptic and sedative effects of dexmedetomidine. *Int J Mol Sci.* (2023) 24:9445. doi: 10.3390/ijms24119445

48. Sitnikova E, Rutskova E, Smirnov K. Alpha2-adrenergic receptors as a pharmacological target for spike-wave epilepsy. *Int J Mol Sci.* (2023) 24:1477. doi: 10.3390/ijms24021477

49. Al-Gailani L, Al-Kaleel A, Arslan G, Ayyildiz M, Agar E. The effect of general anesthetics on genetic absence epilepsy in WAG/Rij rats. *Neurol Res.* (2022) 44:995–1005. doi: 10.1080/01616412.2022.2095706

50. Hell J, Venn RM, Cusack R, Rhodes A, Grounds RM. Respiratory effects of dexmedetomidine in the ICU. *Critical Care.* (2000) 4:P193. doi: 10.1186/cc913

51. Boff GA, de Lima CM, Nobre MO, Gehrcke MI. Hemodynamic and respiratory changes from a continuous infusion of dexmedetomidine in general anesthesia in dogs: a systematic review and meta-analysis. *Res Soc Dev.* (2022) 11:e39611729980. doi: 10.33448/rsd-v11i7.29980

52. Carollo DS, Nossaman BD, Ramadhyani U. Dexmedetomidine: a review of clinical applications. *Curr Opin Anesthesiol.* (2008) 21:457–61. doi: 10.1097/ACO.0b013e328305e3ef

53. Venn RM, Hell J, Grounds RM. Respiratory effects of dexmedetomidine in the surgical patient requiring intensive care. *Crit Care.* (2000) 4:302–8. doi: 10.1186/cc712

Frontiers in Neurology

Explores neurological illness to improve patient care

The third most-cited clinical neurology journal explores the diagnosis, causes, treatment, and public health aspects of neurological illnesses. Its ultimate aim is to inform improvements in patient care.

Discover the latest Research Topics

See more →

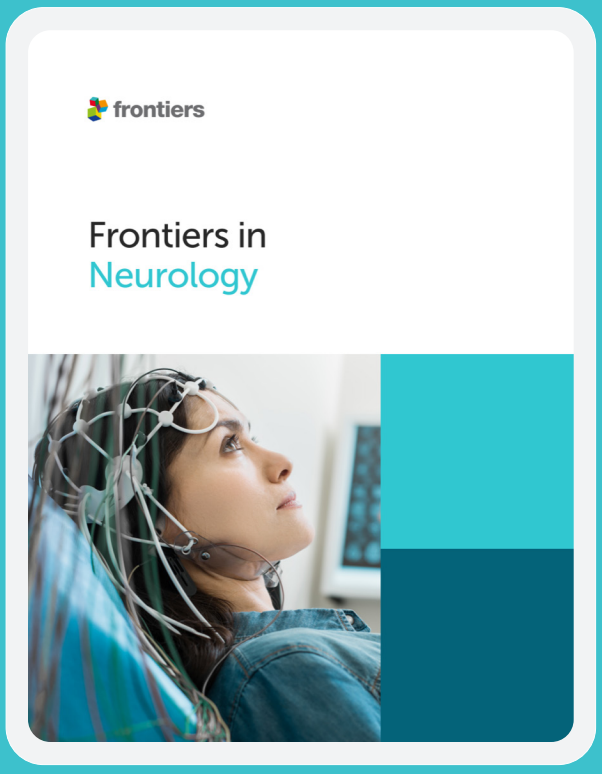

Frontiers

Avenue du Tribunal-Fédéral 34
1005 Lausanne, Switzerland
frontiersin.org

Contact us

+41 (0)21 510 17 00
frontiersin.org/about/contact